DISSERTATION

STRATEGIES FOR TARGETING CANCER: SMALL MOLECULES, EPIGENETICS AND DRUG DESIGN

Submitted by

Kelly N. Hassell

Graduate Degree Program in Cell and Molecular Biology

In partial fulfillment of the requirements

For the Degree of Doctor of Philosophy

Colorado State University

Fort Collins, Colorado

Summer 2020

Doctoral Committee:

Advisor: Debbie C. Crans
Co-advisor: Mark A. Brown

Deborah Roess
Carmen Menoni

ABSTRACT

STRATEGIES FOR TARGETING CANCER: SMALL MOLECULES, EPIGENETICS AND DRUG DESIGN

Cancer has plagued our human population since its early characterizations as abnormal cells and tissues in the mid-1900s. Initial treatment models included surgical removal of cancerous tissues. In the late 1960s, surgical removal and localized radiation were the only available options for treatment until the development of chemotherapeutics. These chemical cocktail treatments, designed to kill cancer cells, started in the late-1900s and even today remain a major line of defense in fighting this disease. The goal of the research described in this dissertation was to investigate current methodologies and techniques used to treat cancer; treatments utilizing chemotherapeutics, small molecule interactions, metallocage drug delivery, epigenetics and protein activity inhibition.

The first part of my research focused on the significance of Cisplatin as a chemotherapeutic. My findings indicate the unexpected speciation of platinum in the human body as a revelation to be utilized in novel drug design. In my reverse micelle study, the hydrolysis of the Schiff-base compound was observed to be dependent on the size of reverse micelles; resulting in partial phase selectivity. The reverse micelle model provided ample support for engineering various types of liposomal delivery options for insoluble compounds like Cisplatin. My metallocage research explored the idea of utilizing

a self-assembling Cisplatin protective capsule with fluorophores, equipped to monitor real-time cancer cell death as well as drug delivery. My findings support the efficacy of metallocages for delivery of cancer therapeutics and the necessity for continued methodology development for clinical applications.

The second part of my research focused on the use of epigenetics for gene expression regulation and protein activity inhibition. My findings reported the most recent status of drugs developed using histone deacetylases (HDAC) and histone deacetylases inhibitors (HDACi) for targeting specific cancers. And in my final chapter of SET-domain proteins, my research focused on comparing the methyltransferase activity inhibition of SMYD3 in two different cancer cells lines. The data showed the A549 lung cell line is slightly more sensitive to the SMYD3 activity inhibitor.

This dissertation describes work that has increased our collective understanding of cancer therapeutics. Furthermore, it vastly supports future cancer treatment investigations utilizing both small molecules and bioinformatics.

ACKNOWLEDGMENTS

There are several people that have greatly assisted me in my academic pursuit of my PhD. At times, the support I received seemed like an endless bounty. I'd like to thank Dr. Debbie C. Crans for their continued support and advice; Drs. Deborah Roess & Carmen Menoni for their time. And I'd like to thank Dr. Mark Brown for his steady guidance, empathy and ultimately his financial support that was crucial to the completion of this chapter in my life.

With regard to chapter 1, I would like to acknowledge my contributing authors Kaitlin Doucette and Dr. Debbie C. Crans, as well as the National Science Foundation (NSF) for my GAANN (Graduate Assistance in Areas of National Need) fellowship.

For chapter 2, I would like to acknowledge the initial data generated by Dr. Khurram S. Munawar and his funding awarded from the Higher Education Commission of Pakistan to him and his advisor Saqib Ali. In addition, coauthors on this work include Mary Fisher and Drs. Myles Sedgwick and Debbie C. Crans for their dedication to the completion of this research project. Dr. Debbie C. Crans also provided partial funding through the Alfred Cope Foundation and I would also thank NSF for my GAANN fellowship.

Specifically, with chapter 3 I would like to thank Dr. Christopher Allen ASCP(SCYM)$_{CM}$ for his help in method development, optimization and sample analysis and Dr. Marcela Henao-Tamayo for her expertise and continued support. I am grateful

for Dr. Marie Légaré and her staff for providing cell culture basic materials and the laboratory space to conduct this mini-research project. And I'd like to thank Dr. Angela Casini, Dept. of Medicinal Chemistry at Cardiff University for the donation of the 2A Pd-cages. And Drs. Deborah Roess and Carol Wilusz for their time and helpful edits that were necessary for this chapter.

I would like to thank Dr. Mark A. Brown for the encouragement and financial support to push chapter 4 from review to publication. And for chapter 5, I would like to acknowledge my contributing authors Dillon K. Jarrell, Drs. Debbie C. Crans, Shari Lanning and Mark A. Brown for their hard work and dedication to the completion of this publication. Both chapters 4 and 5 would not have been possible without the continued support and funding provided by Dr. Mark A. Brown.

Most that truly know me are aware that this journey has been full of tumultuous turns and unfortunate realities. Yet, despite this unforgettable experience; completion has been achieved. And to all that have helped me along this journey, thank you for not quitting on me during my darkest of days.

PREFACE

This dissertation thesis was submitted for the degree of Doctor of Philosophy in Cellular and Molecular Biology at the Colorado State University in Fort Collins, CO. The literature reviews and research presented in this document was conducted under the supervision of Dr. Debbie C. Crans in the Chemistry Department, Colorado State University and Dr. Mark A. Brown in the Clinical Sciences Department, Colorado State University, between January 2015 and May 2020.

This dissertation thesis is to the best of my knowledge, original work with the exceptions where acknowledgments and references have been made to previous work. Neither this, nor any similar dissertation thesis has been submitted to any other college or university.

Parts of this dissertation thesis has been published as the following:

Doucette, KA; Hassell, KN; Crans, DC. Selective speciation improves efficacy and lowers toxicity of platinum anticancer and vanadium antidiabetic drugs. *Journal of Inorganic Biochemistry* 2016, (165)56–70. https://doi.org/10.1016/j.jinorgbio.2016.09.013.

Hassell, K. N.; Histone Deacetylases and Their Inhibitors in Cancer Epigenetics. *Diseases* 2019, *7* (4), 57. https://doi.org/10.3390/diseases7040057.

Jarrell, D. K.; Hassell, K. N.; Crans, D. C.; Lanning, S.; Brown, M. A. Characterizing the Role of SMYD2 in Mammalian Embryogenesis—Future Directions. *Veterinary Sciences* **2020**, *7* (2), 63. https://doi.org/10.3390/vetsci7020063.

Kelly N Hassell
Summer 2020

TABLE OF CONTENTS

INTRODUCTION

The purpose of this dissertation is to present my research in support of the significant impact I have made in my field of study. The chapters that congeal this document have been carefully chosen and refined for the review and approval process by my doctoral committee. The five chapters that make up this dissertation have an overarching theme of small molecules in cancer therapeutics. Each of the chapters investigates alternative methods to curing some types of cancers.[1-3]

In chapter 1, the foundation and urgency for developing alternative delivery methods for the highly toxic chemotherapy drug cisplatin is explain in great detail. The proclamation of the nuances of change in the platinum coordination chemistry upon intravenous delivery to humans as essentially altered the pharmacological logical and approach of this routine drug delivery technique.[3-9]

Chapter 2 represents the liposomal approach and the future possibilities of encapsulating highly toxic and/or hydrophobic molecules for drug delivery in humans. Reverse micelles function nanoparticle with the ability to encapsulate cisplatin molecules. Nanoparticle therapeutic delivery systems specifically engineered to encapsulate drugs a with protective coating can be utilized for the administering of cisplatin to patients.[10-12] Micellular nanoparticles have a nonpolar and/or polar core that can be used to regulate cisplatin's polarity.[13-15] This chapter is a model for utilizing a multitude of different types of polymeric micelle structures for safer drug deliveries of small toxic molecules. Polymeric micellular structures are currently in clinical trials for treating some types of cancers; non-small cell lung carcinoma.[16-21]

My findings of chapter 3 represent the initial stages of method and technique development for a clinical application with the capability of monitoring the death of cancer cell in real-time via analysis by fluorescent cytometry. Measuring and tracking the fluorescent intensity and detection of localization for the metallocages upon drug delivery and degradation in the human body has the potential to greatly impact current nest practices in chemotherapeutics. The fluorescent characteristics of some metallocages can be paired with the high throughput diagnostic capabilities of flow cytometry.[22]

To complement the model systems approach, studies were undertaken in biological systems and two approaches are described in chapters 4 and 5. The field of epigenetics dives into the possibilities of regulating and manipulating the core components of the histone functions.[23-25] The information in chapter 4 was designed to help the uninformed reader prepare for the transition to a more biological and cellular approach to killing cancer cells. Magnanimously, the utilization of histone deacetylases and their inhibitors brokers a new path in engineering site-specific based drugs with the current technology of bioinformatics combined with cheminformatics.[26-28]

Finally, the research presented in chapter 5 represents one singular approach to killing cancer cells with a proprietarily designed protein activity inhibitor. The family of SET-domain proteins function as a prime example of the impact epigenetics has on the regulation to cellular functions.[29-31] SMYD2 and SMYD3 are the proteins in chapter 5 that were investigated from historical and current research perspectives. The preliminary data collected in this research indicates that there is cell death due to the impact of the drug via cellular and nuclear pathways.

The work presented in this dissertation depicts several years and attempts to achieve one goal; and my attempts to develop a novel technique and methodology that could impact the cancer research fields of clinical oncology. As one continues to read the dissertation, one must continuously consider the what-ifs without detracting from the relevancy and validity of research presented.

REFERENCES

(1) Chen, H.; Wang, X.; Gou, S. A Cisplatin-Based Platinum(IV) Prodrug Containing a Glutathione S-Transferase Inhibitor to Reverse Cisplatin-Resistance in Non-Small Cell Lung Cancer. *Journal of Inorganic Biochemistry* **2019**, *193*, 133–142. https://doi.org/10.1016/j.jinorgbio.2019.01.014.

(2) El-Deiry, W. S.; Goldberg, R. M.; Lenz, H.; Shields, A. F.; Gibney, G. T.; Tan, A. R.; Brown, J.; Eisenberg, B.; Heath, E. I.; Phuphanich, S.; Kim, E.; Brenner, A. J.; Marshall, J. L. The Current State of Molecular Testing in the Treatment of Patients with Solid Tumors, 2019. *CA: A Cancer Journal for Clinicians* **2019**. https://doi.org/10.3322/caac.21560.

(3) Doucette, KA; Hassell, KN; Crans, DC. Selective speciation improves efficacy and lowers toxicity of platinum anticancer and vanadium antidiabetic drugs. *Journal of Inorganic Biochemistry* **2016**, (165)56–70. https://doi.org/10.1016/j.jinorgbio.2016.09.013.

(4) Galluzzi, L.; Senovilla, L.; Vitale, I.; Michels, J.; Martins, I.; Kepp, O.; Castedo, M.; Kroemer, G. Molecular Mechanisms of Cisplatin Resistance. *Oncogene* **2011**, *31*, 1869.

(4) Hait, W. N. Targeted Cancer Therapeutics. *Cancer Research* **2009**, *69* (4), 1263–1267. https://doi.org/10.1158/0008-5472.CAN-08-3836.

(5) Harper, B. W.; Krause-Heuer, A. M.; Grant, M. P.; Manohar, M.; Garbutcheon-Singh, K. B.; Aldrich-Wright, J. R. Advances in Platinum Chemotherapeutics. *Chemistry - A European Journal* **2010**, *16* (24), 7064–7077. https://doi.org/10.1002/chem.201000148.

(6) Rosenblum, D.; Joshi, N.; Tao, W.; Karp, J. M.; Peer, D. Progress and Challenges towards Targeted Delivery of Cancer Therapeutics. *Nature Communications* **2018**, *9* (1). https://doi.org/10.1038/s41467-018-03705-y.

(7) Sparreboom, A.; Verweij, J. Advances in Cancer Therapeutics. *Clinical Pharmacology & Therapeutics* **2009**, *85* (2), 113–117. https://doi.org/10.1038/clpt.2008.259.

(8) Todd, R. C.; Lippard, S. J. Inhibition of Transcription by Platinum Antitumor Compounds. *Metallomics* **2009**, *1* (4), 280. https://doi.org/10.1039/b907567d.

(9) Ding, Y.; Zhai, K.; Pei, P.; Lin, Y.; Ma, Y.; Zhu, H.; Shao, M.; Yang, X.; Tao, W. Encapsulation of Cisplatin in a Pegylated Calcium Phosphate Nanoparticle (CPNP) for Enhanced Cytotoxicity to Cancerous Cells. *Journal of Colloid and Interface Science* **2017**, *493*, 181–189. https://doi.org/10.1016/j.jcis.2017.01.032.

(10) Barry, N. P. E.; Sadler, P. J. Challenges for Metals in Medicine: How Nanotechnology May Help To Shape the Future. *ACS Nano* **2013**, *7* (7), 5654–5659. https://doi.org/10.1021/nn403220e.

(11) Mochida, Y.; Cabral, H.; Kataoka, K. Polymeric Micelles for Targeted Tumor Therapy of Platinum Anticancer Drugs. *Expert Opinion on Drug Delivery* **2017**, *14* (12), 1423–1438. https://doi.org/10.1080/17425247.2017.1307338.

(12) Shahin, M.; Safaei-Nikouei, N.; Lavasanifar, A. Polymeric Micelles for PH-Responsive Delivery of Cisplatin. *Journal of Drug Targeting* **2014**, *22* (7), 629–637. https://doi.org/10.3109/1061186X.2014.921925.

(13) Shi, C.; Yu, H.; Sun, D.; Ma, L.; Tang, Z.; Xiao, Q.; Chen, X. Cisplatin-Loaded Polymeric Nanoparticles: Characterization and Potential Exploitation for the Treatment of Non-Small Cell Lung Carcinoma. *Acta Biomaterialia* **2015**, *18*, 68–76. https://doi.org/10.1016/j.actbio.2015.02.009.

(14) Yokoyama, M.; Okano, T.; Sakurai, Y.; Suwa, S.; Kataoka, K. Introduction of Cisplatin into Polymeric Micelle. *Journal of Controlled Release* **1996**, *39* (2–3), 351–356. https://doi.org/10.1016/0168-3659(95)00165-4.

(15) Cabral, H.; Kataoka, K. Progress of Drug-Loaded Polymeric Micelles into Clinical Studies. *Journal of Controlled Release* **2014**, *190*, 465–476. https://doi.org/10.1016/j.jconrel.2014.06.042.

(16) Han, Y.; Yin, W.; Li, J.; Zhao, H.; Zha, Z.; Ke, W.; Wang, Y.; He, C.; Ge, Z. Intracellular Glutathione-Depleting Polymeric Micelles for Cisplatin Prodrug Delivery to Overcome Cisplatin Resistance of Cancers. *Journal of Controlled Release* **2018**, *273*, 30–39. https://doi.org/10.1016/j.jconrel.2018.01.019.

(17) Kim, J.; Pramanick, S.; Lee, D.; Park, H.; Kim, W. J. Polymeric Biomaterials for the Delivery of Platinum-Based Anticancer Drugs. *Biomaterials Science* **2015**, *3* (7), 1002–1017. https://doi.org/10.1039/C5BM00039D.

(18) Li, J.; Li, Z.; Li, M.; Zhang, H.; Xie, Z. Synergistic Effect and Drug-Resistance Relief of Paclitaxel and Cisplatin Caused by Co-Delivery Using Polymeric Micelles. *Journal of Applied Polymer Science* **2015**, *132* (6), n/a-n/a. https://doi.org/10.1002/app.41440.

(19) Wan, X.; Min, Y.; Bludau, H.; Keith, A.; Sheiko, S. S.; Jordan, R.; Wang, A. Z.; Sokolsky-Papkov, M.; Kabanov, A. V. Drug Combination Synergy in Worm-like Polymeric Micelles Improves Treatment Outcome for Small Cell and Non-Small Cell Lung Cancer. *ACS Nano* **2018**, *12* (3), 2426–2439. https://doi.org/10.1021/acsnano.7b07878.

(20) Wang, R.; Hu, X.; Xiao, H.; Xie, Z.; Huang, Y.; Jing, X. Polymeric Dinulcear Platinum(Ii) Complex Micelles for Enhanced Antitumor Activity. *Journal of Materials Chemistry B* **2013**, *1* (6), 744. https://doi.org/10.1039/c2tb00240j.

(21) Zhuang, W.; Ma, B.; Liu, G.; Chen, X.; Wang, Y. A Fully Absorbable Biomimetic Polymeric Micelle Loaded with Cisplatin as Drug Carrier for Cancer Therapy. *Regenerative Biomaterials* **2018**, *5* (1), 1–8. https://doi.org/10.1093/rb/rbx012.

(22) Henry, C. M.; Hollville, E.; Martin, S. J. Measuring Apoptosis by Microscopy and Flow Cytometry. *Methods* **2013**, *61* (2), 90–97. https://doi.org/10.1016/j.ymeth.2013.01.008.

(23) Sippl, W.; Jung, M. *Epigenetic Drug Discovery*; **2019**.

(24) Nebbioso, A.; Tambaro, F. P.; Dell'Aversana, C.; Altucci, L. Cancer Epigenetics: Moving Forward. *PLOS Genetics* **2018**, *14* (6), e1007362. https://doi.org/10.1371/journal.pgen.1007362.

(25) Arnold, K.; Bordoli, L.; Kopp, J.; Schwede, T. The SWISS-MODEL Workspace: A Web-Based Environment for Protein Structure Homology Modelling. *Bioinformatics* **2006**, *22* (2), 195–201. https://doi.org/10.1093/bioinformatics/bti770.

(26) Yang, F.; Zhao, N.; Ge, D.; Chen, Y. Next-Generation of Selective Histone Deacetylase Inhibitors. *RSC Advances* **2019**, *9* (34), 19571–19583. https://doi.org/10.1039/C9RA02985K.

(27) Dawson, M. A.; Kouzarides, T. Cancer Epigenetics: From Mechanism to Therapy. *Cell* **2012**, *150* (1), 12–27. https://doi.org/10.1016/j.cell.2012.06.013.

(28) Hassell. Histone Deacetylases and Their Inhibitors in Cancer Epigenetics. *Diseases* **2019**, *7* (4), 57. https://doi.org/10.3390/diseases7040057.

(29) Brown, M. A.; Foreman, K.; Harriss, J.; Das, C.; Zhu, L.; Edwards, M.; Shaaban, S.; Tucker, H. C-Terminal Domain of SMYD3 Serves as a Unique HSP90-Regulated Motif in Oncogenesis. *Oncotarget* **2015**, *6* (6). https://doi.org/10.18632/oncotarget.2970.

(30) Brown, M. A.; Edwards, M. A.; Alshiraihi, I.; Geng, H.; Dekker, J. D.; Tucker, H. O. The Lysine Methyltransferase SMYD2 Is Required for Normal Lymphocyte Development and Survival of Hematopoietic Leukemias. *Genes & Immunity* **2020**. https://doi.org/10.1038/s41435-020-0094-8.

(31) Jarrell, D. K.; Hassell, K. N.; Crans, D. C.; Lanning, S.; Brown, M. A. Characterizing the Role of SMYD2 in Mammalian Embryogenesis—Future Directions. *Veterinary Sciences* **2020**, *7* (2), 63. https://doi.org/10.3390/vetsci7020063.

CHAPTER 1 – LITERATURE REVIEW[1]

1.1 Overview of Cancer Therapeutics

Since the early characterizations and diagnosis of cancers, doctors and research scientists have been searching for the cure that effectively kills toxic cells while keeping the patient healthy. Several therapeutic methods have developed and evolved throughout the past fifty years. Despite the strides made in chemotherapeutics, our current state-of-the-art methods that utilizes cisplatin, requires patients to be subjected to costly pre- and post-administration hospital stays. The monitoring of toxicity levels in the patients is mandatory due to the large amounts of excessive cisplatin concentrations intravenously administered; targeting both cancer and healthy cells. Some research suggests that the ineffectiveness of chemotherapy agents has led to several failed attempts to halt the metastasis of some cancers. The current therapy model for the intravenous delivery of the anticancer agent cisplatin utilizes multiple cellular membrane transporters for entering and exiting cancer cells. Due to the systemic, non-targeted delivery of cisplatin, patients experience side-effects that are directly linked to the excessively high dosage requirements which eventually accumulate, and trigger cisplatin resistance. Drug resistance is a cell's natural defense mechanism developed over time to protect itself from toxins and various types of environmental stress, all of which are intended to trigger

[1] Doucette, KA; Hassell, KN; Crans, DC. Selective speciation improves efficacy and lowers toxicity of platinum anticancer and vanadium antidiabetic drugs. *Journal of Inorganic Biochemistry* 2016, (165)56–70. https://doi.org/10.1016/j.jinorgbio.2016.09.013.

apoptosis. If successfully delivered to a cell, cisplatin binds to the damaged DNA in the nucleus of the cancer cell and induces apoptosis.

1.2 Speciation Chemistry

Speciation chemistry is a branch of chemistry that was historically developed in northern Europe and for decades had a home in the area of solution chemistry.[2-5] Because there are several discipline and area specific definitions for speciation[6-9], recent recommendations have been carried out within the International Union of Pure and Applied Chemistry (IUPAC) establishing a commission that developed several recommendations for the scientific community on the definition of speciation. In addition to the classical areas of solution chemistry[2], bioinorganic chemistry and Vanadium chemistry have also embraced the principles of speciation and as a result[2,5,8] have used these for development within these disciplines. Speciation studies have been done for a number of metals ions and systems[9-12] using a range of analytical methods for analysis.[8,11,13-16] The availability of improved and high-resolution analytical methods along with powerful tools for data analysis have revolutionized for scientists the ability to measure different species under biological conditions[7,12-13,16] and environmental conditions.[9-11] However, regardless of the improved analytical methods available, the coordination chemistry of the target element dictates the processing and the potential of what can be observed. Such considerations are at the essence of chemical speciation[17-18] and the focus for what can be observed. The classical solution chemistry definition of speciation was illustrated in figure 1.1 as equations (1) and (2).[17]

Equation (1) shows H_+, a metal ion (M), and a ligand (L) forming a complex with the stoichiometry defined by p, q, and r respectively in an equilibrium reaction. The formation constant of the complex β(p, q, r) is shown in equation (2), in which the concentration of the complex is divided by the multiplied concentrations of the individual constituents of H_+, M and L raised to their respective powers, p, q, and r.[4] The quotients values for p, q, and r are determined by a titration followed by the evaluation of the constants of the entire system using computations in an iterative process.[2,17] These potentiometric studies are most effective when an entire pH range is considered. Because hydrolysis reactions do not involve L, these complexes will be described as (p,q,0),where p and q are the coefficients for H_+ and the metal respectively, and the formation constant is defined by the concentration for the respective precursors.[17] Such speciation studies result in a series of constants that represent the system and allow for prediction of species distribution. Several important limitations with the classical speciation approach include the types of reactions and specific species.[17] Only reactions with changes in H_+ give observable changes and indicate differences in the speciation. In addition, the hydration number (i.e. the number of water molecules in the formula) in a complex cannot be measured because such addition does not add or take away a proton and thus is not detected. Furthermore, since this definition of speciation focuses on composition, it is important to recognize that stereochemistry has not been taken applied. Stated differently, the classical definition of each species focuses on the atom composition rather than where the atoms are localized in space. There are differences in both the composition; speciation, as well as orientation in space are explained in detail in this literature review.

1.2.1 *Significance of Platinum(II) Drugs*

The most common platinum (Pt) drugs and the three that are currently food and drug administration (FDA) approved for clinical use in the US are Pt(II) drugs (cisplatin, carboplatin and oxaliplatin), figure 1.2.[19-21] They are believed to follow the same general mode of action, in which the drug chelates DNA and results in cellular apoptosis.[22-26] The generally accepted mechanism shown in figure 1.3 suggests that the neutral form (deprotonated hydrolysis product) of the cisplatin is the form that is traversing the nuclear membrane after having been formed in the cytoplasm; this mechanism is not accepted uniformly. This is due to the positively charged Pt compound that undergoes Coulombic attraction to the cell membrane and therefore are formed prior to the formation of its neutral species. Hydrolysis is likely to follow the steps shown in figure 1.4. This schematically underlines the fact that cisplatin by hydrolysis forms charged species, but that upon deprotonation the hydrolysis products can be neutral or have one positive charge.[27-26] Several aspects of the species in this scheme and the speciation is presented in greater detail below. Pt can also exist in oxidation state IV, and such Pt-compounds are even more inert than Pt(II) compounds. In general Pt(IV) compounds believed to undergo reduction forming Pt(II) complexes upon reaching the tumor, and their mode of action proceeds according to the mechanism for the other Pt(II) complexes.[27-28] Most of the reported processing of Pt(II) drugs generally involves hydrolytic reactions, thus keeping the Pt in oxidation state II, diagramed in figure 1.4. Characterization of the chemical and biological processing of cisplatin and other Pt(II) compounds has been investigated using several analytical approaches including HPLC-ICP-MS, XAS, XANES, LC and potentiometry.[29-34] The fact that the Pt(II) compounds undergo slow ligand

exchange reactions allows the isolation and characterization of the different species using a wide range of analytical methods.[35-38] In the following, the fundamental speciation of the Pt systems, including the different processes that cisplatin and other Pt-drugs undergo under physiological conditions, is explained in great detail. In addition to cisplatin the two other main FDA-approved Pt-drugs, carboplatin and oxaliplatin, shown in figure 1.2, were both developed to improve the properties of cisplatin so that it would be a more efficacious and less toxic drug to a wider range of cancers.[39-40] Specifically, carboplatin was developed to be more water soluble and have less nephrotoxic effects for treatment of a wide range of cancers, and oxaliplatin was developed similarly; used for treatment of colorectal cancers.[41-42]

1.3 The Proposed Mechanism of Action for Platinum(II) Complexes

Pt(II) compounds react upon entering cells[18,22] and it is important to understand the products that it forms in a biological matrix. Cisplatin is administered intravenously and the focus here is therefore on the speciation that takes place as the Pt-drug is about to enter the cellular target. The more extensive processing leading to the ultimate speciation that occurs in the various different biological matrices including the GI tract, blood, cell media and cells are beyond the coverage in this review and the readers are referred elsewhere.[43] The specific reactions in the cytoplasm which we describe here will impact the mechanism of action of cisplatin and the other Pt(II) anticancer drugs. Generally it is expected that upon entrance through the cellular membrane into the cytoplasm, that the two chloride ligands are replaced by aqua ligands, shown in figure 1.4[26,44-45] which, because they are positively charged, can deprotonate to form the neutral

dihydroxy substituted Pt complex in both figures 1.3 and 1.4. Aqua ligands that are bound to the Pt complex before they are deprotonated are acidic, with pKa values in the range of 5–8.[46] Monoaquated cisplatin has a pKa of 6.6, while diaquated cisplatin (both chloride ligands replaced with aqua ligands) has a pKa of 5.5. Cisplatin with an aqua and hydroxide ligand replacing the chloride ligands has a pKa of 7.3.[46] Which species enter the cell of the species shown in figure 1.3. Many are convinced that it is the diaquated Pt-compound that enters the cell[24,47], but a number of researchers believe that it is the monoaqua derivative that penetrates the nucleus [24] and reacts with DNA. Strong arguments favor each position. The neutral diaquated Pt-compound, because of the neutral charge would seem to readily traverse the membranes and is the final hydrolysis product illustrated in figure 1.3. However, the positively charged mono or diaquated Pt derivatives are readily attracted to the membrane interface, and since more of this compound has been observed in speciation studies, this possibility seems like a viable alternative. Whether it is a monochlorido or a dihydroxido Pt complex that reacts with DNA, such a species will result in coordination of the two guanosine moieties on one DNA strand to the Pt atom, which will induce a 35–40 degree bend in the DNA, which will induce cellular apoptosis, as shown in figure 1.3.[18,26-27,45,48] Cisplatin and oxaliplatin are found to form about 60–65% intra-strand adducts between two adjacent guanine bases (PtGG), 25–30% intra-strand adducts between adjacent adenine and guanine bases (PtAG), and 5–10% intra-strand adducts of the type PtGNG, where N is any of the four bases, and 1–3% inter-strand adducts (G-Pt-G).[25,34] These types of experiments distinguishing between these possibilities are nontrivial and would be very valuable for the community. When used as an anticancer agent, the toxic nature of cisplatin does

require that patients are carefully monitored when drug is administered. The cisplatin is administered by intravenous injection, and generally requires that the patient is checked in at an appropriate treatment facility for a couple of days.[47] The aquation and hydrolysis of cisplatin is decreased by administering the drug in saline solution because the higher concentration of Cl^- thermodynamically stabilizes the chloride complex, cisplatin, with respect to the aqua complexes and reduces hydrolysis.[50-51] Even after administration, cisplatin is reported to be relatively stable within the blood stream and extracellular fluid. These observations have supported the slow ligand exchange, allowing for use of analytical techniques that involve isolation of the compounds using HPLC and LC based methods.[52-53]

1.3.1 *The Speciation of Tetrachloridoplatinate(II) and Final Conversion to Cisplatin*

Due to the nature of hydrolysis and aquation of the chloride ligands, the substitution reaction, that is, aquation of the Pt(II)Cl bond becomes more significant. The preparation of cisplatin presented has the objective of giving the one a sense of the chemistry involved in preparing this compound, and thus indirectly the first reactions taking place upon cellular uptake. Because the ligand exchange to Pt(II) is slow, it is possible to isolate both the cis and trans forms of the compound with the formula $[PtCl_2(NH_3)_2]$.[22] The preparation of cisplatin begins with potassium tetrachloridoplatinate(II), which is originally formed from treatment of Pt with Cl_2 at high temperatures (350°C). Treatment of tetrachloridoplatinate(II) $[PtCl_4]^{2-}$ with KI results in tetraiodidoplatinate(II) ($[PtI_4]^{2-}$), which is treated with two equivalents of ammonia to form the yellow solid cis-diamminediiodidoplatinum(II) (cis-$[PtI_2(NH_3)_2]$).[54] Treatment of this

product with two equivalents of AgNO3 results in the formation of cis-diamminediaquaplatinum(II) (cis-[Pt(H2O)2(NH3)2]$^{2+}$).[55] The final product is formed after reacting this compound with excess potassium chloride (KCl) resulting in cisplatin (cis-[PtCl2(NH3)2]$^{2-}$).[55] It is interesting to note that these last two steps are the reverse reaction that takes place intracellularly upon uptake of the Pt-compound. Furthermore, the fact is that cisplatin is used and not the diaquated compound (cis-[Pt(H2O)2(NH3)2]$^{2-}$) because of the more favorable drug uptake properties.

The speciation of tetrachloridoplatinate(II) was reported in aqueous solution at basic pH and in acidic solution.[56-58] These studies are important because this compound can be viewed as a reference compound to which the reactivity of Pt-based antitumoral drug compounds can be compared. The major species present in aqueous solutions is the original tetrachloridoplatinate(II) species, however, several additional hydrolysis products were also observed in figure 1.4. The speciation of this compound was determined as a function of the chloride concentration at acidic pH and the equilibrium concentrations are shown in figure 1.4.[57-58] In the presence of higher Cl^- concentrations less of the aquation product was found and the kinetics of the hydrolysis reactions were determined. The first and second aquation steps were found to be sufficiently different for each of the products to have a definite lifetime. The first aquation step, or replacement of one of the chloride ligands for an aqua ligand, was found to have a first order rate constant of $3.69 \times 10^5\ s^{-1}$. Furthermore, this study reported a $\log\beta = 29.9 + 1.0$ for the double substituted product at high pH levels. This value measured for the stability of $[Pt(OH)3]^-$ compares relatively well with a theoretically estimated value of 28.3.[59] These results suggest that the predominant form of Pt in aqueous solution near neutral pH is not likely

to be the charged monoaqua or diaqua species, but instead the Pt-species containing two chloride ligands and two ammine ligands.[33,58] Indeed, some studies suggest, because in part that the predominant form is the monoaqua species, that the species causing the biological activity may be the monoaqua species instead of the diaqua species that is generally depicted in many reviews.[60-62] Arguments have been made that a neutral species is best at penetration of the cell membrane, though it is well known that positively charged compounds readily penetrate cellular membranes.[63]

1.3.2 *Speciation of Cisplatin in Aqueous Solution and in the Presence of Metabolites*

Aqueous solutions of cisplatin slowly convert to form both the monoaqua and diaqua forms (cis-[PtCl(H2O)(NH3)2]$_{+}$ and cis-[Pt(H2O)2(NH3)2]$_{2+}$) that after deprotonation, produce OH-analogs (cis-[PtCl(HO)(NH3)2] and cis-[Pt(HO)2(NH3)2]), illustrated in figure 1.5.[33,50] These reactions lead to a derivative that can react and form adducts with the DNA. The production of these hydrolysis products was investigated by monitoring the reaction for days to assure that equilibrium was established.[64] The changes in cisplatin concentration (that is measuring the decay, disappearance, or hydrolysis) were monitored for 50h and the results are shown in figure 1.6. Despite the slow reactions, it was found that the reaction rates are sensitive to the surrounding environment. For example, in the presence of high concentrations of Cl^-, the rate of the first and second aquation steps will decrease by 10–20%. The first order rate constants k1 of cisplatin aquation for three different chloride concentrations were $1.79 \times 10^{-5}\ s^{-1}$ (0mg/L Cl^-), $1.68 \times 10^{-5}\ s^{-1}$ (50mg/L Cl^-), and $2.06 \times 10^{-5}\ s^{-1}$ (100mg/L Cl^-). For cisplatin second order reverse reaction, rate constants of $k{-}1 = 6.5 \times 10^{-3}\ M^{-1}\ s^{-1}$, $5.8 \times 10^{-3}\ M^{-1}$

s^{-1} and $4.1 \times 10^{-3}\ M^{-1}\ s^{-1}$ were measured.[18,33] Although the changes in the reaction kinetics are modest, the data in figure 1.6 show that there are some accumulation of unknown Pt species after about 24h in solution. Importantly, this data was used to justify the fact that cisplatin is administered in salt solutions in order to improve the speciation of cisplatin and its efficacy.[65] Since the speciation of cisplatin changes in the presence of the Cl^- anion, it follows that it will also change significantly if other, more nucleophilic metabolites, including protein or DNA that are present in solution or in the cell. As a late third row transition metal, Pt prefers soft ligands both in terms of thermodynamics and kinetics. That is, sulfur ligands are preferred over nitrogen, which again are preferred over oxygen ligands. Many studies have been done illustrating the reactivity of Pt(II) compounds, and the following example describes a case study. The reactions of cisplatin with S-based ligands have been investigated and in the case of methionine were also monitored at high (150mM) and low (1.5mM) chloride concentrations (using HPLC-ICP-DRCMS). The first order rate constant of cisplatin substitution in the presence of methionine at low chloride concentration was $k1 = 2.28 \times 10^{-4}\ s^{-1}$, which is one order of magnitude higher than the rate constant observed for cisplatin aquation in water containing the equal amount of chloride and no methionine. At high chloride concentration, the first order rate constant of cisplatin aquation was $k1 = 1.41 \times 10^{-4}\ s^{-1}$ in the presence of methionine and thus faster than the rate constant in water.[37] These results demonstrate that the environment is important, and that cisplatin hydrolyzes faster in the presence of metabolites. Therefore, subtle changes in the reactivity and properties of the drug upon administration are likely. The cytoplasm contains metabolites including phosphate, citrate, glucose, amino acids as well as cellular components such as

glutathione and ascorbate that maintain the redox environment of the cell.[66-68] Reduced drug accumulation of cisplatin has been reported in drug-resistant cell lines.[69-72] This reduced drug accumulation could be explained by a number of different mechanisms including reduced drug uptake from the culture media due to alterations in some specific membrane transporters, enhanced drug efflux, or changes in the metabolite concentrations in the resistant cell lines[72-73] or a combination of these factors. Once formed, the Pt-DNA adducts can be repaired by specific enzymes that recognize the DNA damage.[74-75] Another limiting factor is that once incorporated into the cells, the drug can be inactivated by binding to different biomolecules present within the cell cytosol such as glutathione and other sulfur containing proteins.[44,76] Due to the high affinity of Pt for sulfur ligands, glutathione is likely to react with cisplatin.[18,77-78] Glutathione adducts are reported upon administration of cisplatin, and once formed, are exported out of the cell. This is consistent with reduced drug accumulation in cisplatin-resistant cell lines.[79-80] In contrast, studies done with carboplatin and glutathione have indicated that reactions between carboplatin and thiols such as glutathione are very slow, with only small amounts of Pt-thiolato complexes being detectable via ^{15}N NMR spectroscopy and HPLC in mice treated with ^{15}N carboplatin. This difference in reactivity with thiols between carboplatin and cisplatin may account for the decreased nephrotoxicity observed with carboplatin.[81] However, it is important to recognize that the identification of one pathway to reduce cisplatin accumulation does not preclude activity of other mechanisms.

Studies with amino acids and other metabolites are of interest because stability of the complexes is important with regard to understanding potential reactions that take place in the cytoplasm.[82-83] As shown in table 1.1, the stability of Pt complexes with

peptides and the amino acid guanidinoacetic acid (GAA) with both chloride, ammine and hydroxide ligands demonstrate that the cisplatin complex has comparable stability with most except a few complexes.[84] It also shows that cisplatin complexing with guanidinoacetic acid in the place of its chloride ligands has a higher formation constant than does cisplatin itself, as do several other similar studied Pt complexes. Increased stability of these complexes can have a profound effect on the ability of these compounds to react with DNA. This study investigated the reaction with the unusual amino acid guanidinoacetic acid because it is found at high concentrations in the kidney and liver, and thus complexes formed with it may have significance with regards to toxicity and development of resistance.[84-85] Since cisplatin accumulates in the kidney and the liver, the dramatic reduction in the levels of this amino acid is observed upon administration of cisplatin in urinary tract cancer patients. Guanidinoacetic acid is significantly involved in renal metabolism, since it is mainly synthesized in the kidneys and subsequently excreted in urine or methylated for creatine production.[84] The comparable stability of cisplatin in the presence of a sea of alternative nucleophiles including GAA thus explains why the original compound remains intact as long as it does.

In addition to cellular metabolites having the potential to inactivate these anticancer Pt complexes, other components in the administration liquid could potentially react similarly. This is an important fact, dimethyl sulfoxide (DMSO) can be used by clinicians to solubilize Pt drugs and it was recently reported that this practice has the potential to inactivate cisplatin and other anticancer Pt complexes.[19] DMSO is commonly used as a solvent for solubilizing small molecules at high concentrations in biological studies. Clinical Pt compounds are commonly dissolved in DMSO for biologic experiments as

well.[19,86] This is very important, because DMSO is nucleophilic, and will coordinate with the platinum, displacing its chloride ligands and thus changing the structure and reactivity of the anticancer agent by changing the speciation.[87] This change in the structure of the Pt compound has been reported to dramatically inhibit the cytotoxicity and ability to initiate apoptosis of Pt drugs.[19] This recent report further underlines how necessary it is to take into consideration the administration fluid by the Pt drug so that the efficacy of the drug is not decreased during drug administration.[19]

1.4 Cisplatin Uptake Mechanism

The toxic nature of cisplatin requires that patients are carefully hydrated and monitored prior, during and following the drug administration.[47,88] The common mode of administration of Pt-based drugs is by intravenous injection, and generally requires that a patient is checked in one additional day pre- and post-treatment at an appropriate outpatient facility.[89] It is the perception that cisplatin and other Pt-based anticancer drugs, as neutrally charged molecules, will enter the cell.[20,24] However, a reasonable potential exists that positively charged drugs enter as well[90-94] (or that a mechanism involving an initial pre-complex forms). This point is particularly important because only a small fraction of the administered Pt-drug will reach the nuclear DNA and produce the critical cytotoxic regions.[18,90,95]

The many possible uptake pathways that are open to the Pt-drug are illustrated in figure 1.7. Such pathways include the copper influx transporter 1 and other transporters (Ctr1, ATP7A and ATP7B)[94], polyorganic specific cation transporters such as OCT1–3[92-93,96] as well as a sodium dependent process that has yet to be fully characterized with

regard to its role and interaction.[91,97] Melanosomes provide another method for the transport of Pt drugs through cells.[98] Finally, endocytosis and passive diffusion are common mechanisms for Pt based drug entry to the cell. In contrast, reactions of the Pt drug with glutathione can lead to their exportation via the multidrug resistant protein transporters, MRP 1–5.[99] Protein systems are recognized as a principal contributor to the reduction in efficacy of Pt-drugs and the development of resistance, in addition to the transporters described above. The efficiency of the drugs in reaching and reacting with the DNA is dependent on its ability to produce active hydrolysis products once inside the cell and whether or not these hydrolysis products are inactivated by binding to serum proteins[100-102] and other proteins. Proteins such as human serum albumin (HSA) and γ-globulin, which make up about 80% of total plasma proteins, have been studied to explore how they bind and to determine how much Pt they bind.[18,102] Such studies with serum proteins have indicated that after administration, the largest percentage of the Pt drugs are bound to extra and intracellular proteins, with as much as 80–85% of Pt compound being bound after a 5h incubation period.[18,101,103-105] In studies with HSA it was found that as a result of Pt-binding, disulfide bonds may break, and this is possibly accompanied by intramolecular cross-linking of the protein which may result in the partial unfolding of HSA at high drug concentrations.[106-105] Such changes may lead to a change in the protein's biological activity, as disulfide bonds play an important role in maintaining the shape of the protein, which may contribute to the observed toxicity of Pt-compounds.[105] More studies with HSA indicate that there is no saturation of the albumin with cisplatin, but rather that the bound metal complex is influenced by the ratio between the drug and the protein, initial concentration of the protein, incubation time, and nature of the incubation

medium.[102] A 14-day incubation of HSA with cisplatin in a 60-fold drug excess yielded as much as 20 Pt atoms bound to each protein. Generally, shorter incubation periods and lower cisplatin/albumin ratios lead to lower fractions of bound Pt to protein.[102] More comprehensive coverage of the reactions with HSA, transferrin, γ-globulin and transporters with the Pt drugs have been published.[3,72,96,99,100-101,107]

1.5 Alternative Drug Delivery Methods

1.5.1 *Different Approaches to Cisplatin Formulation and Delivery*

Both liposomal delivery and using inert Pt(IV) coordinated-molecules maximize clinical efficacy of cisplatin by considering speciation. These approaches account for the impact of the cellular environment on cisplatin in different ways. Cisplatin was the first Pt-based drug and remains an important anticancer drug as it is often the first drug of choice used singularly or in combination with other compounds.[18,20-21,26-27,47,62,108-109] Two recent examples of Pt-based drugs[110-114], which were developed using fundamentally different approaches to treatment and delivery as investigated in this manuscript are described below. There are associated differences between them, resulting in placing these drugs in different speciation spaces; one in which the cisplatin is wrapped in a liposome and a second one in which the Pt oxidation state is IV in place of II.

1.5.2 *Lipoplatin – Changes in Speciation Decrease Toxicity of Cisplatin and Increase Efficacy*

Lipoplatin, also known as liposomal cisplatin, utilizes a liposomal delivery system for the intracellular deposit of cisplatin, figure 1.8.[114] Lipoplatin was developed in an effort to circumnavigate the high nephrotoxicity levels patients experienced when using cisplatin

as a primary line of treatment.[81] The lower toxicity presumably arises in part because of reduced glutathione or metallothionein mediated detoxification levels when treating some types of cancers. By targeting cisplatin resistant cell lines and specific cancerous organelles, the liposomal preparation permits the drug to enter the system through the vascular network tissue of the malignant tumor. The lipids in the Lipoplatin capsule emulate the cellular membrane of the tumor cells they are targeted to, and consist of soy phosphatidyl choline, cholesterol, dipalmitoyl phosphatidyl glycerol (DPPG), and methoxyl-polyethylene glyceroldiesteroyl phosphatidylethanolamine. This membrane composition allows for fusion with the phospholipid cellular membrane[115] of the targeted tumor and is found to rapidly enter the targeted cell via endocytosis and direct fusion of the lipoplatin nanoparticles of the membrane due to the presence of fusogenic lipid DPPG on its shell.[112] Through direct fusion of nanoparticles that penetrate the leaky cell membranes of malignant tumors, illustrated in figure 1.8, lipoplatin represents a promising strategy to combat the cells resistant to Pt(II)-compounds.[111-113] Once inside the cell, the cisplatin is released, hydrolyzed as detailed in figures 1.3 and 1.4, and exhibits its anticancer activity by forming the cytotoxic intra-strand DNA adducts. By utilizing this nanoparticle (110nm) administration, cisplatin derived drugs exhibit increased specificity to the targeted cancer tumor[115-117] presumably because the method of liposomal uptake circumvents other methods of Pt resistance, such as up or down regulation of metal ion transporters.[118] In addition to preventing the decrease in cytotoxic Pt concentrations, the pharmacokinetic studies with lipoplatin indicated that this delivery method has resulted in a decrease in the distribution volume, shortened the half-life of the speciation allow administration of a systemic lower dose resulting in overall lower toxicity.

1.5.3 *Satraplatin – Pt(IV)-Compound Modified with a Speciation Profile*

In addition to the Pt(II) based drugs, researchers have found that Pt(IV) compounds also exhibit desirable anticancer properties.[110] Satraplatin (trans, cis, cis diacetatoamminedichlorido(cyclohexylamine)platinum(IV), JM216), was one of the most successful orally active Pt(IV) antitumor drugs, illustrated in figure 1.9.[124-125] Satraplatin has a six-coordinate Pt(IV) with two ammine and two chloride ligands in the plane and two additional axial acetate groups, making this compound more lipophilic. Once in the bloodstream and intracellular matrix, the Satraplatin compound is metabolized. The Pt(IV) is reduced to Pt(II) in cells[126] and the Pt(IV) loses its acetato groups, forming a structure analogous to cisplatin (except for the replacement of one of the ammine groups with a cyclohexylammine group. This cisplatin-analog metabolite, referred to as JM 118 cis-amminedichlorido(cyclohexylamine)platinum(II) then follows a mechanism of action similar to that of cisplatin in that it enters the nucleus where it binds to DNA to form inter- and intra-strand cross-links, distorting the DNA. Satraplatin was an orally active anticancer agent. Exhaustive consideration of speciation for this compound would include examination of biological environments including the GI tract. Since this topic is beyond this manuscript, we would like to direct readers to elsewhere for information on such speciation as well for speciation in vivo.[127] We have hypothesized that the speciation of this drug is contributing to the improved efficacy of this compound. Satraplatin is low molecular weight, neutral, and kinetically inert in acidic media. The lower reactivity of the Pt(IV) compound allows oral administration because degradation in the gastric environment is not as problematic as with the Pt(II) compounds. Satraplatin is unstable in light and alkaline media, however, considering the oral administration its stability in acidic

environments is much more important. Indeed, the half-life of reduction of Satraplatin with 5mM ascorbate is around 50 minutes, leaving adequate time for gastrointestinal absorption as parent Pt(IV) complex and allowing it to be administered orally.[128] The asymmetrical stable ligands, the ammine and cyclohexylammine, of Satraplatin alter its DNA adduct profile such that inhibition of DNA synthesis is increased and likelihood of being recognized by DNA-mismatch repair is decreased[129-130], which contributes to the ability of Satraplatin to overcome cisplatin resistance. In addition to increased efficacy as a result of its DNA binding and inhibition properties, Satraplatin represents a distinct class of Pt compounds that act very differently in uptake and during cellular processing than the Pt(II) compounds as a result of its increased lipophilicity and asymmetrical stable ligands. The effectiveness of Satraplatin is related to the reduction of the Pt(IV) compound as it reaches the tumor sites and its ability to survive the uptake and the processing before entering the nucleus and reaching DNA.[124-125] Therefore, being hydrolytically inert, and considering the slow hydrolyzation of the Pt ligands, it is more likely to reach tumor DNA without reacting with other metabolites;[131-132] Pt drugs have increased plasma clearance in comparison to cisplatin.[112]

These studies have shown that lipoplatin reached a higher plasma concentration while decreasing nephrotoxic side effects.[114] The direct consequences of these improved properties indicate that lipoplatin can be administered using an outpatient treatment facility[115], which is contrary to the intravenous treatment of cisplatin that requires constant monitoring and thus pre and post-administration overnight hospital stay.[114] Lipoplatin has been tested in clinical trial studies as both a primary course of action and secondary line of treatment for malignant tumors.[114] Previous studies have indicated that lipoplatin could

be successful as a secondary line of treatment for patients that had developed cisplatin resistance during the course of chemotherapy.[119] In clinical trials, drugs administered in concert with Lipoplatin include gemcitabine, used for treatment of pancreatic cancers[120], and Paclitaxel, used as an anti-microtubule agent given to treat Kaposi sarcomas.[121] Phase II clinical trials with lipoplatin administered in concert with gemcitabine as treatment for pancreatic cancer patients was also reported.[122] Additionally, phase III clinical trials that have utilized lipoplatin in combination with gemcitabine or paclitaxel for patients with non-small cell lung cancer were also reported.[123]

Combined, these studies demonstrate that the subtle change in the speciation chemistry of cisplatin has a profound effect on the efficacy and toxicity of the drug. Although the fundamental mechanism of action remains the same, the changes in the stability and although the intravenous injection cisplatin tends to be stable, there is the potential that in addition to reacting in the more reducing cellular environment in tumors that the Pt(IV)-drugs react and form the toxic Pt(II) prematurely before reaching the tumor. It is possible that in red blood cells (RBC) the reducing environment is responsible for forming the reactive Pt(II) form of the metal drug. Studies done with V(V) indicate that in the blood, the oxidation state of the metal is reduced to V(IV)[133] and similarly was observed in cell culture.[134] Such reaction may be occurring at least partly with Pt(IV) drugs as well, particularly in the reducing environments of the RBC before the drugs reach the tumor site. This possibility should be investigated in studies with Pt(IV) drugs. Related to Satraplatin is Mitaplatin illustrated in figure 1.10. Other examples of Pt(IV)-based drugs have been investigated including mitaplatin combining the cisplatin structure with two dichloroacetato groups in the axial positions.[110] Upon uptake in the tumor cells, this

compound decomposes to form cisplatin by losing the two equivalents of dichloroacetate.[135-136] Dichloroacetate inhibits pyruvate dehydrogenase kinase (PDK) which is involved in glucose metabolism and found in excess in cancer cells. Inhibition of PDK blocks the proliferation and survival of cancerous cells.[137] By inhibiting the phosphorylation of pyruvate dehydrogenase in the mitochondria, it primes the mitochondria of cancer cell for apoptosis, induced by the additional platinum to the nuclear DNA.[110] Although the design of this compound with cisplatin as a “Holy Grail” is conceptually interesting: mitaplatin was not found to be any more effective than cisplatin in animal and human studies[138]. Therefore, mitaplatin did not have successful clinical phase I trials, leaving the satraplatin model to be the better Pt(IV)-compound.[139] Satraplatin had shown success in Phase I, II, and III clinical trials and then failed. Satraplatin was given in concert with other anticancer agents, such as docetaxel for the treatment of prostate cancer, paclitaxel in the treatment of non-small cell lung cancer, and capecitabine for treatment of advanced solid tumors.[139] Positive results in clinical trials caused GPC biotech to file for the accelerated approval of Satraplatin. This application was rejected because Satraplatin did not show convincing enough benefit in terms of overall survival, and concerns were raised that only 51% of patients in the trial had received prior docetaxel.[139] Recently, clinical trials with this drug have continued. Experiments were reported in which Satraplatin was reformulated by encapsulation in cyclodextrin. This modification increased the solubility of Satraplatin, making it more suitable for medical treatments, while enhancing its stability in cellular environments by protecting against undesirable hydrolytic decomposition.[140] Clinical trial studies utilizing cisplatin-based compounds as recent as 2019 and early 2020 have published data in

support of the significant impact in preventing the metastatic spread in previously treatment resistant triple-negative breast cancer patients.[141]

1.6 Conclusion

In this chapter, we have described the fundamental speciation reactions, the role and the importance of speciation with regards to the activity of Platinum based drugs; one of the most effective anticancer drugs. The problems associated with Pt treatment include high toxicity, lowered specificity and developing resistance that can be combated by developing new and improved strategies and systems. Pt(II) and Pt(IV) both undergo slow ligand exchange reactions, which is why isolation of a range of species is possible. The inherent stability of the Pt compounds can readily be illustrated by description of the aquation and hydrolysis of the parent tetrachloridoplatinate(II) $[PtCl4]^{2-}$, as well as cisplatin. Most of the administered cisplatin obtained from tissue samples from subjects treated with Pt-compounds is in the form of the parent drug. Only a small percentage is present as the monoaquated form and even less as the diaquated form. Some investigators favor the interpretation that the diaquated product of cisplatin reacts with DNA because these complexes are neutral, however, very little of this compound forms, so it is possible that the monoaquated hydrolysis product is a compound that reacts directly with DNA and is responsible for most of the Pt bound to DNA. This would imply a different mechanism of action than what is generally believed.

As illustrated with the case of lipoplatin, satraplatin and mitaplatin, speciation can be used to improve efficacy of cisplatin usage. Lipoplatin can be prepared by enclosing cisplatin in a liposome and this modification of the cisplatin results in decreased toxicity.

The lower toxicity of Lipoplatin is presumably because of the improved uptake and targeting and decreased systemic concentration of the drug. The practical consequence of the lower toxicity of the drug is that lipoplatin administration can be done in an outpatient manner, rather than requiring a hospital stay as in the case of cisplatin. Consideration of Pt chemistry also allows the administration of the inert nontoxic Pt(IV) compound, Satraplatin, and the selectivity for tumor tissues even though it is administered orally. Importantly, both Lipoplatin and Satraplatin have potential as a second line of treatment of tumors that have developed cisplatin resistance. In summary, we urge that as the community moves forward in development of new drugs, it will consider speciation chemistry as one of the key strategies that will be considered in the future development of anticancer drugs. Take into consideration the information summarized in table 1.2. Indeed, minor reformulations or reconsiderations of Pt-based drug speciation can improve Pt′s significance in targeted cancer treatment methodology; especially individualized medicine. The data presented here utilizing liposomes (as nanoparticles) for Pt prodrug entry has promise as a low cytotoxic method for patients, as well as more cost effective for both the provider and insured.

1.7 Figures

$$pH^+ + qM + rL \rightleftharpoons (H^+)_p(M)_q(L)_r \quad (1)$$

$$\beta(p,q,r) = \frac{\left[(H^+)_p(M)_q(L)_r\right]}{[H^+]^p[M]^q[L]^r} \quad (2)$$

Figure 1.1 Equations 1 and 2: Equation (1) shows H_+, a metal ion (M), and a ligand (L) forming a complex with the stoichiometry defined by p, q, and r respectively in an equilibrium reaction. The formation constant of the complex β(p, q, r) is shown in equation (2), in which the concentration of the complex is divided by the multiplied concentrations of the individual constituents of H_+, M and L raised to their respective powers, p, q, and r.[4] The quotients values for p, q, and r are determined by a titration followed by the evaluation of the constants of the entire system using computations in an iterative process.[2,17] These potentiometric studies are most effective when an entire pH range is considered. Because hydrolysis reactions do not involve L, these complexes will be described as (p,q,0),where p and q are the coefficients for H_+ and the metal respectively, and the formation constant is defined by the concentration for the respective precursors.[17]

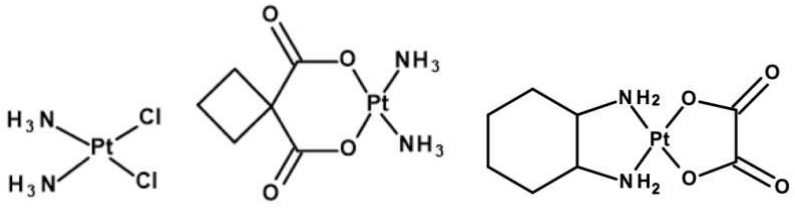

Figure 1.2 (from left to right): cisplatin, carboplatin, and oxaliplatin. The platinum chemotherapeutics approved by the FDA used in the clinical treatment of human beings in the United States. Developed to improve the properties of cisplatin, to be more efficacious and less toxic drug various cancers.[39-40] Carboplatin was developed to be more water soluble and have less nephrotoxic. Oxaliplatin was developed similarly; used for treatment of colorectal cancers.[41-42]

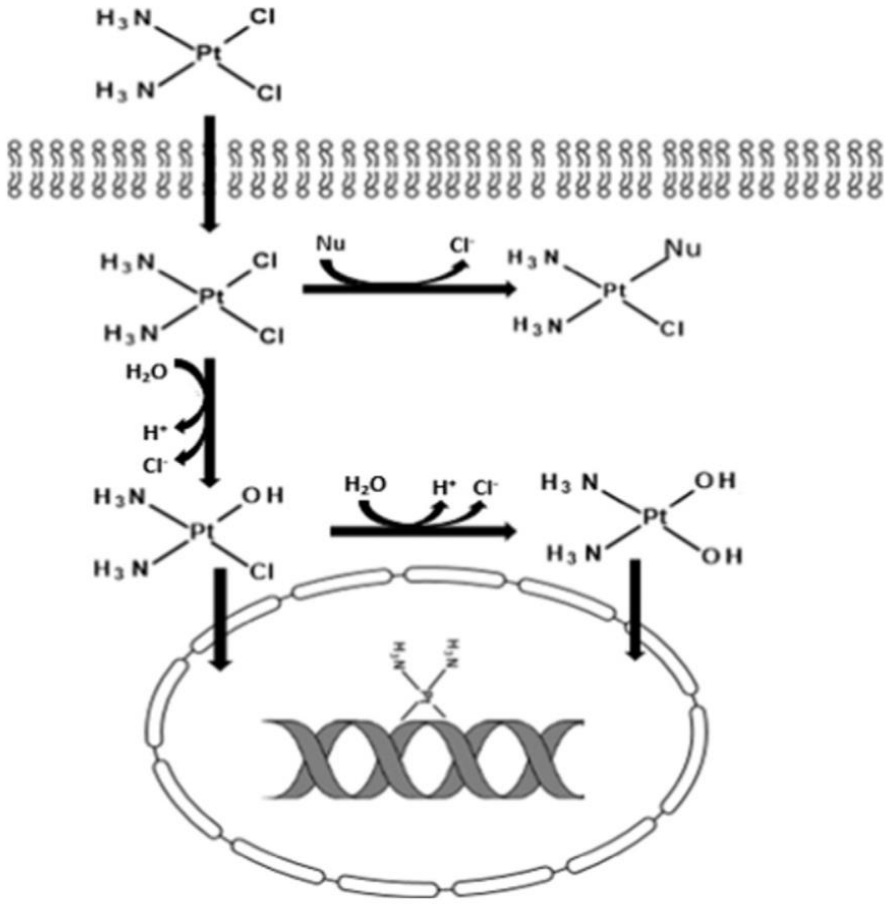

Figure 1.3 Proposed cellular uptake mechanism of cisplatin. Hydrolysis of one or two chloride ligands after cell membrane penetration and potential deprotonation before nuclear uptake. The neutral form of the deprotonated hydrolysis product transverses the nuclear membrane after formation in the cytosol. Modified from[49, 141].

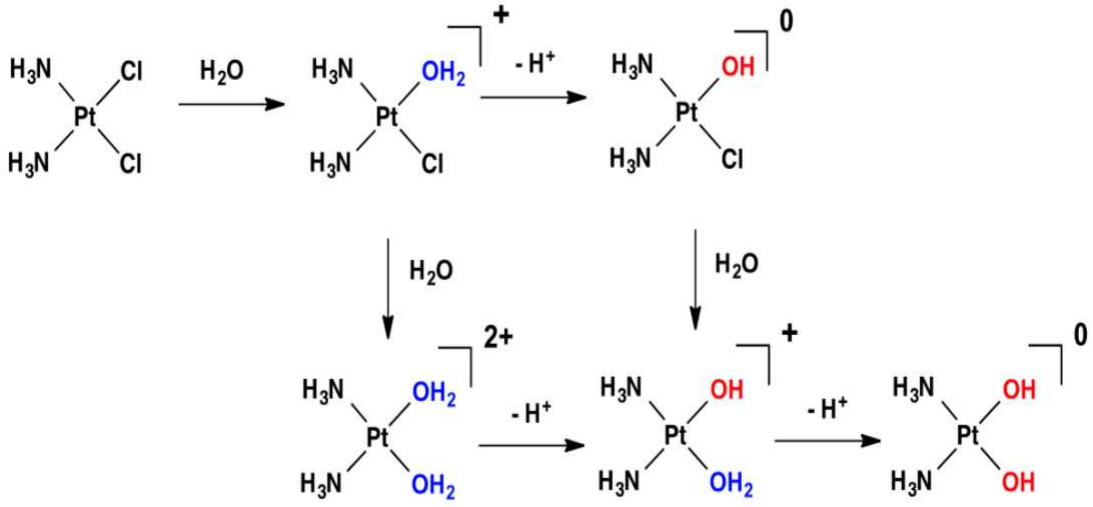

Figure 1.4 Schematic illustration of the aquation reaction followed by deprotonation. Aqua ligands that are bound to the Pt complex before they are deprotonated are acidic, with pKa values in the range of 5–8. Monoaquated cisplatin has a pKa of 6.6, while diaquated cisplatin (both chlorides replaced with aqua ligands) has a pKa of 5.5. Cisplatin with an aqua and hydroxide ligand (replacing the chloride ligands) has a pKa of 7.3.[46] Permission from Ref.141

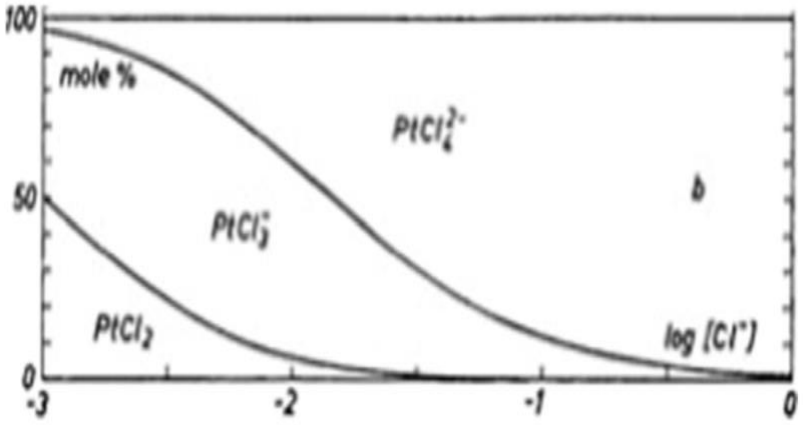

Figure 1.5 Speciation of $PtCl_4]^{2-}$. Measured at acidic pH and shown as a function of Cl^- concentration. Adapted from Ref. 58,141 with permission. In this speciation diagram, (x-axis; electronegativity, y-axis; concentration) the most major species in aqueous solution shown is the original tetrachlorideplatinate(II). The speciation of which has been determined to be a function of equilibrium and chloride concentrations at low pH levels.

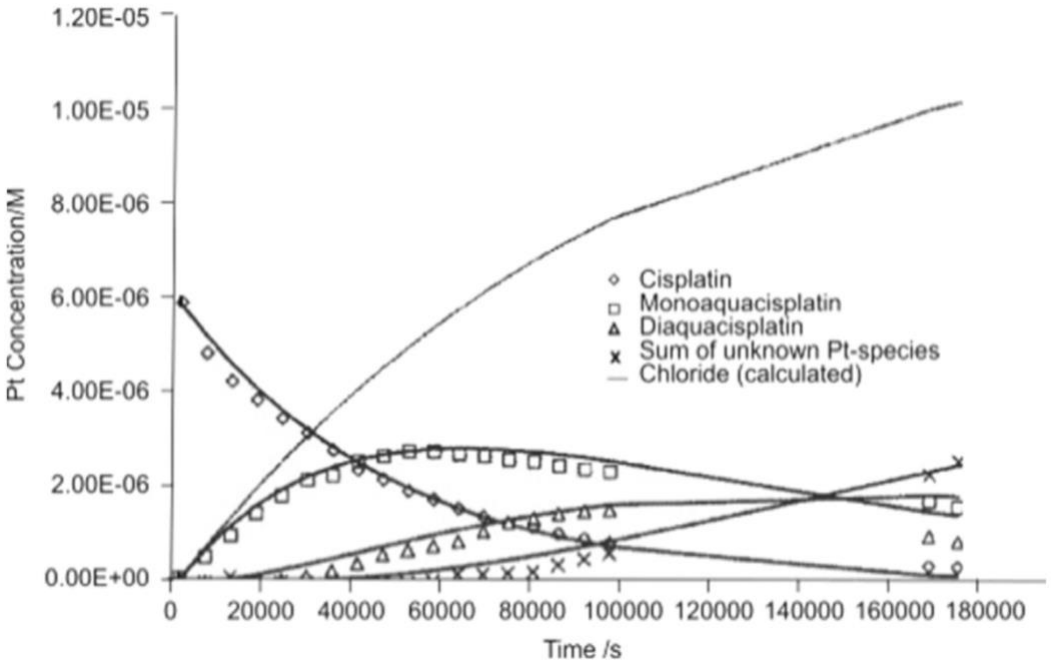

Figure 1.6 Cisplatin decay at 0mM Cl- concentration. This cisplatin decay graph illustrates the significant changes in potential cisplatin concentration for over 50h. These data were initially used to for the justification of the administration of cisplatin intravenously in salt solution for increased efficacy. Adapted from Ref. 33, 18, 141 with permission.

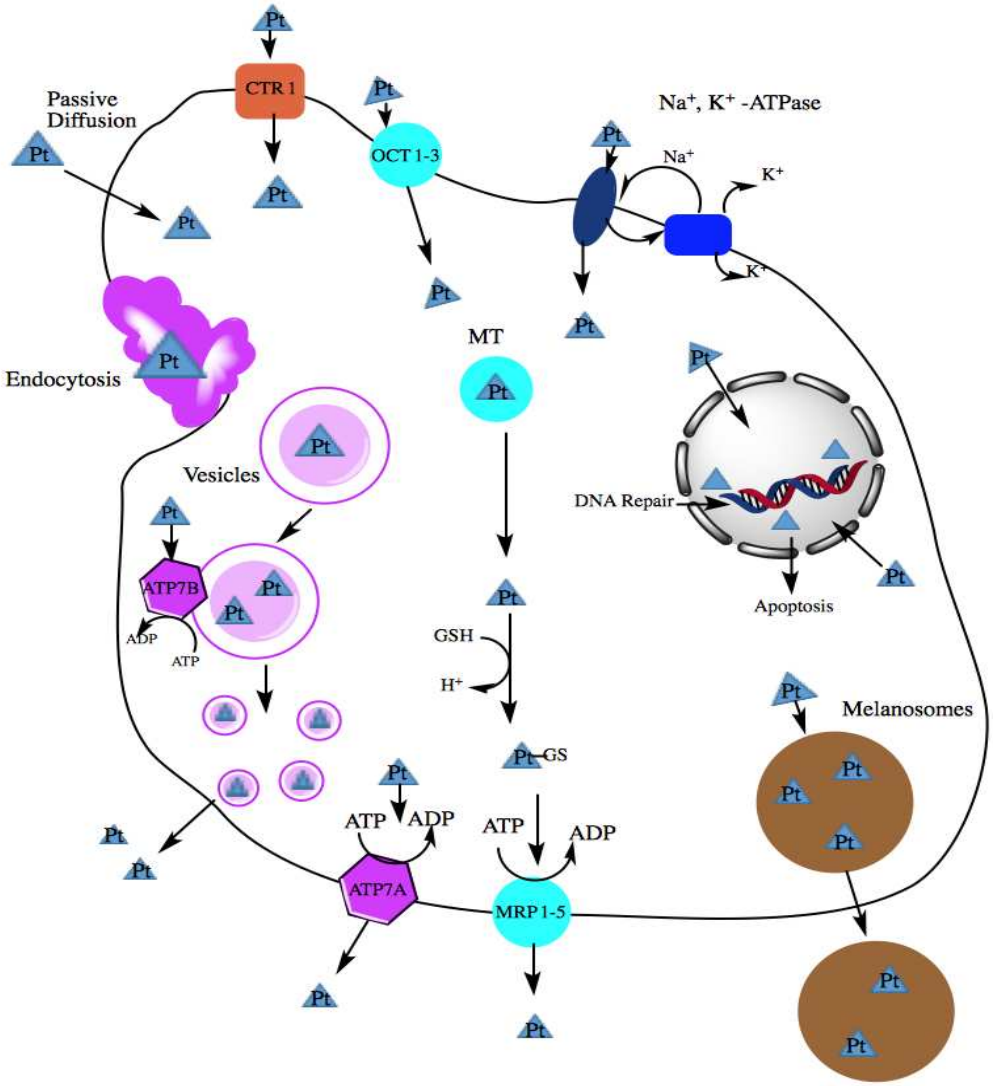

Figure 1.7 The proposed cisplatin influx and efflux pathways. Permission by Ref 141. The possible uptake pathways that are open to the Pt-drug include the copper influx transporter 1 and other transporters (Ctr1, ATP7A and ATP7B)[94], polyorganic specific cation transporters such as OCT1–3[92-93,96] as well as a sodium/potassium-dependent process that has yet to be fully characterized with regard to its role and interaction.[91,97] Melanosomes provide another method for the transport of Pt drugs through cells.[98] Endocytosis and passive diffusion are common mechanisms for Pt based drug entry to the cell. In contrast, reactions of the Pt drug with glutathione can lead to their exportation via the multidrug resistant protein transporters, MRP 1–5.[99]

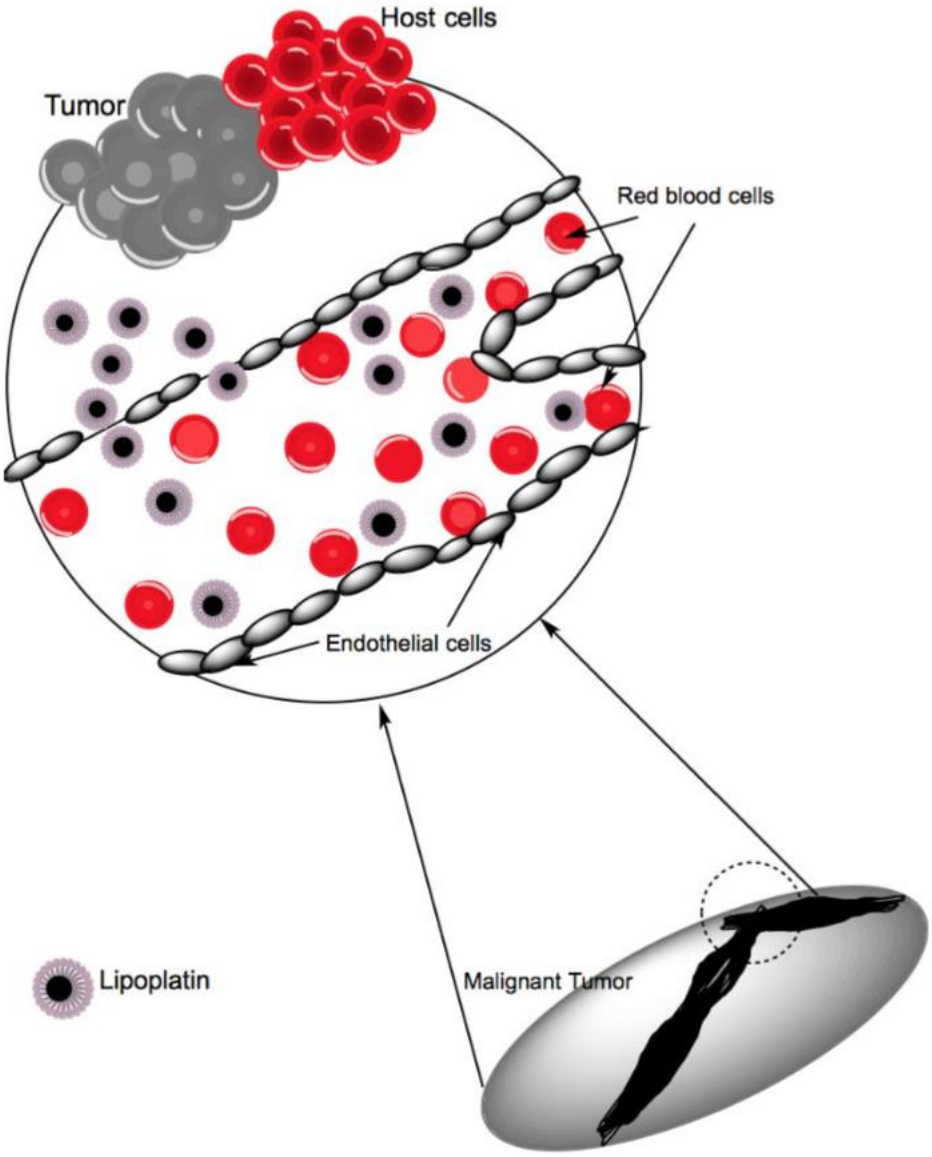

Figure 1.8 Proposed administration of Lipoplatin. Lipoplatin injected directly into malignant tumor, enter the blood via vascular tissue network (top). Lipoplatin fused with the phospholipid cellular membrane cisplatin intercellular delivery (bottom). Adapted with modification from [112, 141].

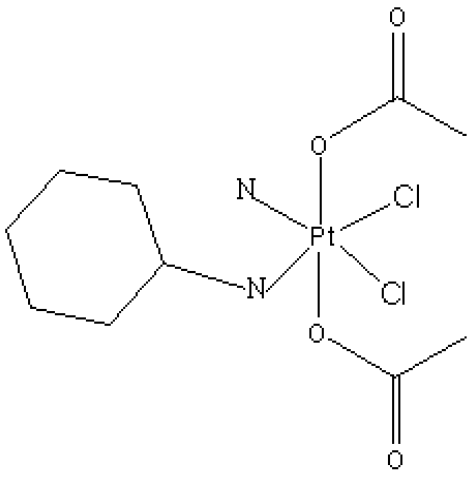

Satraplatin

Figure 1.9 Chemical structure of Satraplatin. Satraplatin (trans, cis, cis diacetatoamminedichlorido(cyclohexylamine)platinum(IV), or JM216),[124-125] has a six-coordinate Pt(IV) with two ammine and two chloride ligands in the plane and two additional axial acetate groups for lipophilic properties. In the bloodstream and intracellular matrix, Satraplatin is metabolized as Pt(IV) is reduced to Pt(II) in cells[126] and the Pt(IV) loses its acetato groups, forming a structural analog to cisplatin, or JM 118 (cis-amminedichlorido(cyclohexylamine)platinum(II)). It then follows a mechanism of action similar to that of cisplatin; enters the nucleus where it binds to DNA to form inter and intra-strand crosslinks to distort the DNA.

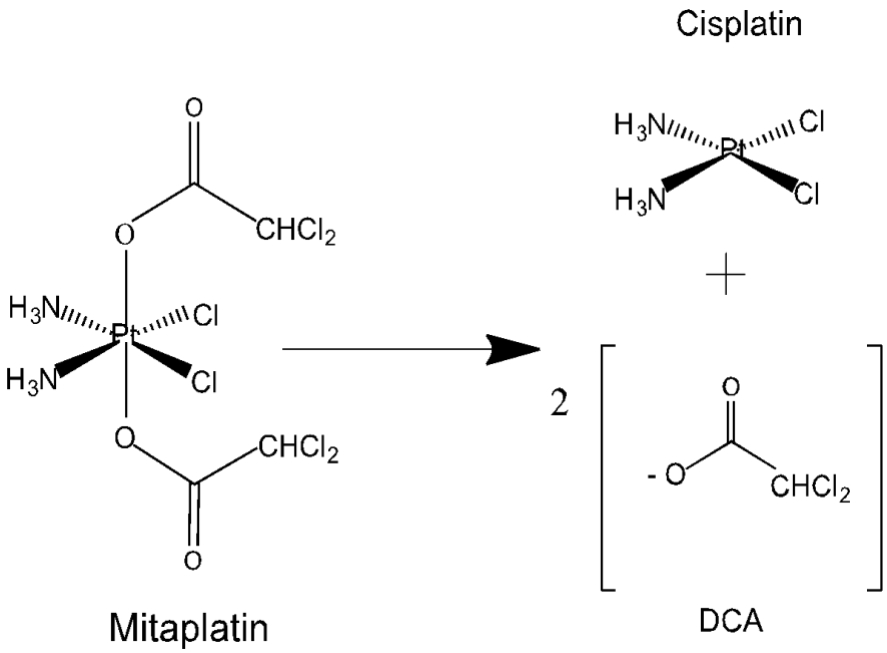

Figure 1.10 Chemical structural of Mitaplatin. Decomposition of mitaplatin in which one molecule degrading yields two equivalent molecules of dichloroacetate and one cisplatin molecule. It then follows a mechanism of action similar to that of cisplatin; enters the nucleus where it binds to DNA to form inter and intra-strand crosslinks to distort the DNA.

1.8 Tables

Table 1.1 Formation constants of Pt-complexes with neutrally charged guanidinoacetic acid (GAA), chloride, ammine, and hydroxide substituents.

Table 1.1 shows cisplatin complexing with guanidinoacetic acid in the place of its chloride ligands has a higher formation constant than does cisplatin itself, as do several other similar studied Pt complexes. Increased stability of these complexes can have a profound effect on the ability of these compounds to react with DNA. Adapted from Ref. 84,141

Species	Log β	Species	Log β
$[HGAA]^{+}$	10.97 (0.01)/10.84[a]/10.85[b]	$[Pt_2(OH)_2(GAA)_2]^{2+}$	6.98 (0.03)
$[PtCl_4]^{2-}$	16.27 (0.05)	$[Pt(Cl)_2GAA]$	18.36 (0.02)
$[PtCl_2(OH)]^{2-}$	4.52 (0.03)	*cis*-$[Pt(NH_3)_2Cl_2]$	22.99 (0.01)
$[PtCl_3(OH)_3]^{2-}$	(−)22.24 (0.02)	$[Pt(OH)_2(NH_3)_2]$	(−) 6.11 (0.03)
$[Pt_2Cl_4(OH)_2]^{2-}$	6.37 (0.05)	$[Pt(NH_3)_2GuAA]^{2+}$	22.09 (0.07)[c]
$[PtGAA]^{2+}$	12.1 (0.02)	$[Pt(OH)(NH_3)_2GAA]^{+}$	12.99 (0.02)
$[PtGAA_2]^{2+}$	15.99 (0.01)	$[Pt_2(OH)_2(NH_3)_4]^{2+}$	14.60 (0.01)
$[Pt(HGAA)_2]^{4+}$	36.11 (0.01)	$[Pt(NH_3)_2(HGuAA)_2]^{4+}$	48.20 (0.05)
$[Pt(OH)_2(GAA)_2]$	(−) 4.83 (0.02)	$[Pt(NH_3)_2(HGuAA)GuAA]^{3+}$	39.46 (0.04)

Table 1.2 Summary of Pt(II) and Pt(IV) Anticancer Drugs

Table 1.2 compares and summarizes the advantages and disadvantages of Pt(II) and Pt(IV) anticancer drugs as featured in the above text from the presented literature review.

Classification	Drug/compound	Advantages	Disadvantages
Pt(II):	Cisplatin	broad spectrum antimicrobial, high antitumoral activity	semi-soluble in water, nephrotoxicity, drug resistance, acute vomiting, intravenous adminstration
	Carboplatin	good anticancer tumor activity, no nephrotoxicity	Myelosuppression, platelet disorder, drug resistance, intravenous administration, peripheral neurotoxicity
	Oxaliplatin	no drug resistance, good anticancer tumor activity, low side effects	neurotoxicity, digestive tract toxicity, intravenous administration
	Lipoplatin	low toxicity, no drug resistance, liposomal drug delivery, good anticancer activity	direct tumor injection administration, excretion process not well known
Pt(IV):	Satraplatin	no resistance, low side effects, oral administration	dose-limiting myelosuppression and vomiting
	Mtaplatin	okay anticancer activity; not better than cisplatin alone	high side effects; unsuccessful clinical trials

REFERENCES

(1) Crans, D. C.; Ehde, P. M.; Shin, P. K.; Pettersson, L. Structural and Kinetic Characterization of Simple Complexes as Models for Vanadate-Protein Interactions. *Journal of the American Chemical Society* **1991**, *113* (10), 3728–3736. https://doi.org/10.1021/ja00010a015.

(2) Rehder, D. The (Biological) Speciation of Vanadate(V) as Revealed by 51V NMR: A Tribute on Lage Pettersson and His Work. *Journal of Inorganic Biochemistry* **2015**, *147*, 25–31. https://doi.org/10.1016/j.jinorgbio.2014.12.014.

(3) Templeton, D. M.; Ariese, F.; Cornelis, R.; Danielsson, L.-G.; Muntau, H.; van Leeuwen, H. P.; Lobinski, R. Guidelines for Terms Related to Chemical Speciation and Fractionation of Elements. Definitions, Structural Aspects, and Methodological Approaches (IUPAC Recommendations 2000). *Pure and Applied Chemistry* **2000**, *72* (8), 1453–1470. https://doi.org/10.1351/pac200072081453.

(4) Kiss, T.; Jakusch, T.; Hollender, D.; Dörnyei, Á.; Enyedy, É. A.; Pessoa, J. C.; Sakurai, H.; Sanz-Medel, A. Biospeciation of Antidiabetic VO(IV) Complexes. *Coordination Chemistry Reviews* **2008**, *252* (10–11), 1153–1162. https://doi.org/10.1016/j.ccr.2007.09.011.

(5) Schluter, D. Ecology and the Origin of Species. *Trends in Ecology & Evolution* **2001**, *16* (7), 372–380. https://doi.org/10.1016/S0169-5347(01)02198-X.

(6) Powell, K. J.; Brown, P. L.; Byrne, R. H.; Gajda, T.; Hefter, G.; Sjöberg, S.; Wanner, H. Chemical Speciation of Environmentally Significant Metals with Inorganic Ligands Part 2: The Cu2+-OH-, Cl-, CO32-, SO42-, and PO43- Systems (IUPAC Technical Report). *Pure and Applied Chemistry* **2007**, *79* (5), 895–950. https://doi.org/10.1351/pac200779050895.

(7) Szpunar, J. Advances in Analytical Methodology for Bioinorganic Speciation Analysis: Metallomics, Metalloproteomics and Heteroatom-Tagged Proteomics and Metabolomics. *The Analyst* **2005**, *130* (4), 442. https://doi.org/10.1039/b418265k.

(8) Nurchi, V. M.; Crisponi, G.; Villaescusa, I. Chemical Equilibria in Wastewaters during Toxic Metal Ion Removal by Agricultural Biomass. *Coordination Chemistry Reviews* **2010**, *254* (17–18), 2181–2192 https://doi.org/10.1016/j.ccr.2010.05.022.

(9) Pereira, C. D.; Techy, J. G.; Ganzarolli, E. M.; Quináia, S. P. Chromium Fractionation and Speciation in Natural Waters. *Journal of Environmental Monitoring* **2012**, *14* (6), 1559. https://doi.org/10.1039/c2em10949b.

(10) Kondo, Y.; Takeda, S.; Furuya, K. Distinct Trends in Dissolved Fe Speciation between Shallow and Deep Waters in the Pacific Ocean. *Marine Chemistry* **2012,** *134–135*, 18–28. https://doi.org/10.1016/j.marchem.2012.03.002.

(11) McNaughton, R. L.; Reddi, A. R.; Clement, M. H. S.; Sharma, A.; Barnese, K.; Rosenfeld, L.; Gralla, E. B.; Valentine, J. S.; Culotta, V. C.; Hoffman, B. M. Probing in Vivo Mn2+ Speciation and Oxidative Stress Resistance in Yeast Cells with Electron-Nuclear Double Resonance Spectroscopy. *Proceedings of the National Academy of Sciences* **2010**, *107* (35), 15335–15339. https://doi.org/10.1073/pnas.1009648107.

(12) Lobinski, R.; Becker, J. S.; Haraguchi, H.; Sarkar, B. Metallomics: Guidelines for Terminology and Critical Evaluation of Analytical Chemistry Approaches (IUPAC Technical Report). *Pure and Applied Chemistry* **2010**, *82* (2), 493–504. https://doi.org/10.1351/PAC-REP-09-03-04.

(13) May, P. M.; Rowland, D.; Königsberger, E.; Hefter, G. JESS, a Joint Expert Speciation System IV: A Large Database of Aqueous Solution Physicochemical

Properties with an Automatic Means of Achieving Thermodynamic Consistency. *Talanta* **2010**, *81* (1–2), 142–148. https://doi.org/10.1016/j.talanta.2009.11.049.

(14) Crisponi, G.; Dean, A.; Di Marco, V.; Lachowicz, J. I.; Nurchi, V. M.; Remelli, M.; Tapparo, A. Different Approaches to the Study of Chelating Agents for Iron and Aluminium Overload Pathologies. *Analytical and Bioanalytical Chemistry* **2013**, *405* (2–3), 585–601. https://doi.org/10.1007/s00216-012-6468-7.

(15) Kiss, T.; Odani, A. Demonstration of the Importance of Metal Ion Speciation in Bioactive Systems. *Bulletin of the Chemical Society of Japan* **2007**, *80* (9), 1691–1702. https://doi.org/10.1246/bcsj.80.1691.

(16) Crans, D. C.; Woll, K. A.; Prusinskas, K.; Johnson, M. D.; Norkus, E. Metal Speciation in Health and Medicine Represented by Iron and Vanadium. *Inorganic Chemistry* **2013**, *52* (21), 12262–12275. https://doi.org/10.1021/ic4007873.

(17) Michalke, B. Platinum Speciation Used for Elucidating Activation or Inhibition of Pt-Containing Anti-Cancer Drugs. *Journal of Trace Elements in Medicine and Biology* **2010**, *24* (2), 69–77. https://doi.org/10.1016/j.jtemb.2010.01.006.

(18) Hall, M. D.; Telma, K. A.; Chang, K. E.; Lee, T. D.; Madigan, J. P.; Lloyd, J. R.; Goldlust, I. S.; Hoeschele, J. D.; Gottesman, M. M. Say No to DMSO: Dimethylsulfoxide Inactivates Cisplatin, Carboplatin, and Other Platinum Complexes. *Cancer Research* **2014**, *74* (14), 3913–3922. https://doi.org/10.1158/0008-5472.CAN-14-0247.

(19) Farrell, N. Nonclassical Platinum Antitumor Agents: Perspectives for Design and Development of New Drugs Complementary to Cisplatin. *Cancer Investigation* **1993**, *11* (5), 578–589. https://doi.org/10.3109/07357909309011676.

(20) Romero-Canelón, I.; Sadler, P. J. Systems Approach to Metal-Based Pharmacology. *Proceedings of the National Academy of Sciences* **2015**, *112* (14), 4187–4188. https://doi.org/10.1073/pnas.1503858112.

(21) Reedijk, J.; Lohman, P. H. M. Cisplatin: Synthesis, Antitumour Activity and Mechanism of Action. *Pharmaceutisch Weekblad* **1985**, *7* (5), 173–180. https://doi.org/10.1007/BF02307573.

(22) Boulikas, T.; Vougiouka, M. Cisplatin and Platinum Drugs at the Molecular Level. (Review). *Oncol. Rep.* **2003**, *10* (6), 1663–1682.

(23) Wang, D.; Lippard, S. J. Cellular Processing of Platinum Anticancer Drugs. *Nature Reviews Drug Discovery* **2005**, *4* (4), 307–320. https://doi.org/10.1038/nrd1691.

(24) Bernges, F.; Holler, E. The Reaction of Platinum(II) Complexes with DNA. Kinetics of Intrastrand Crosslink Formation *in Vitro*. *Nucleic Acids Research* **1991**, *19* (7), 1483–1489. https://doi.org/10.1093/nar/19.7.1483.

(25) Reedijk, J. The Mechanism of Action of Platinum Antitumor Drugs. *Pure and Applied Chemistry* **1987**, *59* (2), 181–192. https://doi.org/10.1351/pac198759020181.

(26) Sadler, P. J.; Guo, Z. Metal Complexes in Medicine: Design and Mechanism of Action. *Pure and Applied Chemistry* **1998**, *70* (4), 863–871. https://doi.org/10.1351/pac199870040863.

(27) Wexselblatt, E.; Gibson, D. What Do We Know about the Reduction of Pt(IV) pro-Drugs? *Journal of Inorganic Biochemistry* **2012**, *117*, 220–229. https://doi.org/10.1016/j.jinorgbio.2012.06.013.

(28) Hann, S.; Zenker, A.; Galanski, M.; Bereuter, T. L.; Stingeder, G.; Keppler, B. K. HPIC-UV-ICP-SFMS Study of the Interaction of Cisplatin with Guanosine Monophosphate. *Fresenius' Journal of Analytical Chemistry* **2001**, *370* (5), 581–586. https://doi.org/10.1007/s002160100740.

(29) Vasilchenko, D.; Tkachev, S.; Baidina, I.; Korenev, S. Speciation of Platinum(IV) in Nitric Acid Solutions. *Inorganic Chemistry* **2013**, *52* (18), 10532–10541. https://doi.org/10.1021/ic401499j.

(30) Wang, Y.; Wang, H.; Li, H.; Sun, H. Metallomic and Metalloproteomic Strategies in Elucidating the Molecular Mechanisms of Metallodrugs. *Dalton Transactions* **2015**, *44* (2), 437–447. https://doi.org/10.1039/C4DT02814G.

(31) Strange, R. W.; Feiters, M. C. Biological X-Ray Absorption Spectroscopy (BioXAS): A Valuable Tool for the Study of Trace Elements in the Life Sciences. *Current Opinion in Structural Biology* **2008**, *18* (5), 609–616. https://doi.org/10.1016/j.sbi.2008.06.002.

(32) Hann, S.; Koellensperger, G.; Stefánka, Zs.; Stingeder, G.; Fürhacker, M.; Buchberger, W.; Mader, R. M. Application of HPLC-ICP-MS to Speciation of Cisplatin and Its Degradation Products in Water Containing Different Chloride Concentrations and in Human Urine. *J. Anal. At. Spectrom.* **2003**, *18* (11), 1391–1395. https://doi.org/10.1039/B309028K.

(33) Zayed, A.; Jones, G. D. D.; Reid, H. J.; Shoeib, T.; Taylor, S. E.; Thomas, A. L.; Wood, J. P.; Sharp, B. L. Speciation of Oxaliplatin Adducts with DNA Nucleotides. *Metallomics* **2011**, *3* (10), 991. https://doi.org/10.1039/c1mt00041a.

(34) Yang, Z.; Hou, X.; Jones, B. T. Determination of Platinum in Clinical Samples. *Applied Spectroscopy Reviews* **2002**, *37* (1), 57–88. https://doi.org/10.1081/ASR-120004747.

(35) Gil, S.; Carmona, A.; Martínez-Criado, G.; León, A.; Prezado, Y.; Sabés, M. Analysis of Platinum and Trace Metals in Treated Glioma Rat Cells by X-Ray Fluorescence Emission. *Biological Trace Element Research* **2015**, *163* (1–2), 177–183. https://doi.org/10.1007/s12011-014-0097-2.

(36) Stefánka, Z.; Hann, S.; Koellensperger, G.; Stingeder, G. Investigation of the Reaction of Cisplatin with Methionine in Aqueous Media Using HPLC-ICP-DRCMS. *J. Anal. At. Spectrom.* **2004**, *19* (7), 894–898. https://doi.org/10.1039/B402028F.

(37) Robillard, M. S.; Bacac, M.; van den Elst, H.; Flamigni, A.; van der Marel, G. A.; van Boom, J. H.; Reedijk, J. Automated Parallel Solid-Phase Synthesis and Anticancer Screening of a Library of Peptide-Tethered Platinum(II) Complexes. *Journal of Combinatorial Chemistry* **2003**, *5* (6), 821–825. https://doi.org/10.1021/cc030011z.

(38) Perego, P.; Robert, J. Oxaliplatin in the Era of Personalized Medicine: From Mechanistic Studies to Clinical Efficacy. *Cancer Chemotherapy and Pharmacology* **2016**, *77* (1), 5–18. https://doi.org/10.1007/s00280-015-2901-x.

(39) Calvert, A. H.; Newell, D. R.; Gumbrell, L. A.; O'Reilly, S.; Burnell, M.; Boxall, F. E.; Siddik, Z. H.; Judson, I. R.; Gore, M. E.; Wiltshaw, E. Carboplatin Dosage: Prospective Evaluation of a Simple Formula Based on Renal Function. *Journal of Clinical Oncology* **1989**, *7* (11), 1748–1756. https://doi.org/10.1200/JCO.1989.7.11.1748.

(40) Zaniboni, A.; Meriggi, F. The Emerging Role of Oxaliplatin in the Treatment of Gastric Cancer. *Journal of Chemotherapy* **2005**, *17* (6), 656–662. https://doi.org/10.1179/joc.2005.17.6.656.

(41) Harrap, K. R. Preclinical Studies Identifying Carboplatin as a Viable Cisplatin Alternative. *Cancer Treatment Reviews* **1985**, *12*, 21–33. https://doi.org/10.1016/0305-7372(85)90015-5.

(42) Levina, A.; McLeod, A. I.; Kremer, L. E.; Aitken, J. B.; Glover, C. J.; Johannessen, B.; Lay, P. A. Reactivity–Activity Relationships of Oral Anti-Diabetic Vanadium Complexes in Gastrointestinal Media: An X-Ray Absorption Spectroscopic Study. *Metallomics* **2014**, *6* (10), 1880–1888. https://doi.org/10.1039/C4MT00146J.

(43) Siddik, Z. H. Cisplatin: Mode of Cytotoxic Action and Molecular Basis of Resistance. *Oncogene* **2003**, *22* (47), 7265–7279. https://doi.org/10.1038/sj.onc.1206933.

(44) Fuertes, M.; Castilla, J.; Alonso, C.; Pérez, J. Cisplatin Biochemical Mechanism of Action: From Cytotoxicity to Induction of Cell Death Through Interconnections Between Apoptotic and Necrotic Pathways. *Current Medicinal Chemistry* **2003**, *10* (3), 257–266. https://doi.org/10.2174/0929867033368484.

(45) *Biological Inorganic Chemistry: Structure and Reactivity*; Bertini, I., Ed.; University Science Books: Sausalito, Calif, **2007**.

(46) Barefoot, R. R. Speciation of Platinum Compounds: A Review of Recent Applications in Studies of Platinum Anticancer Drugs. *Journal of Chromatography B: Biomedical Sciences and Applications* **2001**, *751* (2), 205–211. https://doi.org/10.1016/S0378-4347(00)00498-9.

(47) Todd, R. C.; Lippard, S. J. Inhibition of Transcription by Platinum Antitumor Compounds. *Metallomics* **2009**, *1* (4), 280. https://doi.org/10.1039/b907567d.

(48) Sundquist, W. I.; Lippard, S. J. The Coordination Chemistry of Platinum Anticancer Drugs and Related Compounds with DNA. *Coordination Chemistry Reviews* **1990**, *100*, 293–322. https://doi.org/10.1016/0010-8545(90)85013-I.

(49) Nagai, N.; Okuda, R.; Kinoshita, M.; Ogata, H. Decomposition Kinetics of Cisplatin in Human Biological Fluids. *Journal of Pharmacy and Pharmacology* **1996**, *48* (9), 918–924. https://doi.org/10.1111/j.2042-7158.1996.tb06002.x.

(50) Hann, S.; Koellensperger, G.; Stefánka, Zs.; Stingeder, G.; Fürhacker, M.; Buchberger, W.; Mader, R. M. Application of HPLC-ICP-MS to Speciation of Cisplatin and Its Degradation Products in Water Containing Different Chloride Concentrations and in Human Urine. *J. Anal. At. Spectrom.* **2003**, *18* (11), 1391–1395. https://doi.org/10.1039/B309028K.

(51) van der Vijgh, W. J. F. Clinical Pharmacokinetics of Carboplatin: *Clinical Pharmacokinetics* **1991**, *21* (4), 242–261. https://doi.org/10.2165/00003088-199121040-00002.

(52) Eastman, A. The Formation, Isolation and Characterization of DNA Adducts Produced by Anticancer Platinum Complexes. *Pharmacology & Therapeutics* **1987**, *34* (2), 155–166. https://doi.org/10.1016/0163-7258(87)90009-X.

(53) Cleare, M. J.; Hoeschele, J. D. Studies on the Antitumor Activity of Group VIII Transition Metal Complexes. Part I. Platinum (II) Complexes. *Bioinorganic Chemistry* **1973**, *2* (3), 187–210. https://doi.org/10.1016/S0006-3061(00)80249-5.

(54) Alderden, R. A.; Hall, M. D.; Hambley, T. W. The Discovery and Development of Cisplatin. *Journal of Chemical Education* **2006**, *83* (5), 728. https://doi.org/10.1021/ed083p728.

(55) Wood, S. A. Experimental Determination of the Hydrolysis Constants of Pt2+ and Pd2+ at 25°C from the Solubility of Pt and Pd in Aqueous Hydroxide Solutions. *Geochimica et Cosmochimica Acta* **1991**, *55* (7), 1759–1767. https://doi.org/10.1016/0016-7037(91)90021-V.

(56) Elding, L. I. Preparation and Properties of the Tetra-Aquaplatinum(II) Ion in Perchloric Acid Solution. *Inorganica Chimica Acta* **1976**, *20*, 65–69. https://doi.org/10.1016/S0020-1693(00)94092-1.

(57) Elding, L. I.; Leden, I.; Sunner, S.; Frank, V.; Brunvoll, J.; Bunnenberg, E.; Djerassi, C.; Records, R. On the Stepwise Dissociation of the Tetrachloridoplatinate(II) Ion in Aqueous Solution. I. Equilibria at 25 Degrees C. *Acta Chemica Scandinavica* **1966**, *20*, 706–715. https://doi.org/10.3891/acta.chem.scand.20-0706.

(58) Wood, S. A.; Mountain, B. W.; Fenlon, B. J. Thermodynamic Constraints on the Solubility of Platinum and Palladium in Hydrothermal Solutions; Reassessment of Hydroxide, Bisulfide, and Ammonia Complexing. *Economic Geology* **1989**, *84* (7), 2020–2028. https://doi.org/10.2113/gsecongeo.84.7.2020.

(59) Lepre, C. A.; Lippard, S. J. Interaction of Platinum Antitumor Compounds with DNA. In *Nucleic Acids and Molecular Biology 4*; Eckstein, F., Lilley, D. M. J., Eds.; Springer Berlin Heidelberg: Berlin, Heidelberg, **1990**; Vol. 4, pp 9–38. https://doi.org/10.1007/978-3-642-84150-7_2.

(60) Dasari, S.; Bernard Tchounwou, P. Cisplatin in Cancer Therapy: Molecular Mechanisms of Action. *European Journal of Pharmacology* **2014**, *740*, 364–378. https://doi.org/10.1016/j.ejphar.2014.07.025.

(61) Muggia, F.; Farrell, N. Platinum Coordination Compounds in CancerChemotherapy. *Critical Reviews in Oncology/Hematology* **2005**, *53* (1), 1–2. https://doi.org/10.1016/j.critrevonc.2004.11.007.

(62) Vaara, M. Agents That Increase the Permeability of the Outer Membrane. *Microbiol. Rev.* **1992**, *56* (3), 395–411.

(63) Hohmann, H.; Hellquist, B.; van Eldik, R. Effect of Steric Hindrance on Kinetic and Equilibrium Data for Substitution Reactions of Diaqua(N-Substituted Ethylenediamine)Palladium(II) with Chloride in Aqueous Solution. *Inorganica Chimica Acta* **1991**, *188* (1), 25–32. https://doi.org/10.1016/S0020-1693(00)80912-3.

(64) Berners-Price, S. J.; Sadler, P. J. Coordination Chemistry of Metallodrugs: Insights into Biological Speciation from NMR Spectroscopy. *Coordination Chemistry Reviews* **1996**, *151*, 1–40. https://doi.org/10.1016/S0010-8545(96)90191-5.

(65) Gutscher, M.; Pauleau, A. L.; Marty, L.; Brach, T.; Wabnitz, G. H.; Samstag, Y.; Meyer, A. J.; Dick, T. P. Real-Time Imaging of the Intracellular Glutathione Redox Potential. *Nature Methods* **2008**, *5*, 553.

(66) Simpson, D. P. Citrate Excretion: A Window on Renal Metabolism. *American Journal of Physiology-Renal Physiology* **1983**, *244* (3), F223–F234. https://doi.org/10.1152/ajprenal.1983.244.3.F223.

(67) Rolland, F.; Winderickx, J.; Thevelein, J. M. Glucose-Sensing Mechanisms in Eukaryotic Cells. *Trends in Biochemical Sciences* **2001**, *26* (5), 310–317. https://doi.org/10.1016/S0968-0004(01)01805-9.

(68) Corte-Rodríguez, M.; Espina, M.; Sierra, L. M.; Blanco, E.; Ames, T.; Montes-Bayón, M.; Sanz-Medel, A. Quantitative Evaluation of Cellular Uptake, DNA Incorporation and Adduct Formation in Cisplatin Sensitive and Resistant Cell Lines: Comparison of Different Pt-Containing Drugs. *Biochemical Pharmacology* **2015**, *98* (1), 69–77. https://doi.org/10.1016/j.bcp.2015.08.112.

(69) Giaccone, G. Clinical Perspectives on Platinum Resistance: *Drugs* **2000**, *59* (Supplement 4), 9–17. https://doi.org/10.2165/00003495-200059004-00002.

(70) Zhou, D.; Cong, Y.; Qi, Y.; He, S.; Xiong, H.; Wu, Y.; Xie, Z.; Chen, X.; Jing, X.; Huang, Y. Overcoming Tumor Resistance to Cisplatin through Micelle-Mediated Combination Chemotherapy. *Biomaterials Science* **2015**, *3* (1), 182–191. https://doi.org/10.1039/C4BM00305E.

(71) Gottesman, M. M.; Lavi, O.; Hall, M. D.; Gillet, J. P. Toward a Better Understanding of the Complexity of Cancer Drug Resistance. *Annual Review of Pharmacology and Toxicology* **2016**, *56* (1), 85–102. https://doi.org/10.1146/annurev-pharmtox-010715-103111.

(72) Galluzzi, L.; Senovilla, L.; Vitale, I.; Michels, J.; Martins, I.; Kepp, O.; Castedo, M.; Kroemer, G. Molecular Mechanisms of Cisplatin Resistance. *Oncogene* **2011**, *31*, 1869.

(73) Sawant, A.; Kothandapani, A.; Zhitkovich, A.; Sobol, R. W.; Patrick, S. M. Role of Mismatch Repair Proteins in the Processing of Cisplatin Interstrand Cross-Links. *DNA Repair* **2015**, *35*, 126–136. https://doi.org/10.1016/j.dnarep.2015.10.003.

(74) Martin, L. P.; Hamilton, T. C.; Schilder, R. J. Platinum Resistance: The Role of DNA Repair Pathways. *Clinical Cancer Research* **2008**, *14* (5), 1291–1295. https://doi.org/10.1158/1078-0432.CCR-07-2238.

(75) *Cisplatin: Chemistry and Biochemistry of a Leading Anticancer Drug*; Lippert, B., Ed.; Verlag Helvetica Chimica Acta ; Wiley-VCH: Zürich : Weinheim ; New York, **1999**.

(76) Lempers, E. L. M.; Reedijk, J. Reversibility of Binding of Cisplatin-Methionine in Proteins by Diethyldithiocarbamate or Thiourea: A Study with Model Adducts. *Inorganic Chemistry* **1990**, *29* (2), 217–222. https://doi.org/10.1021/ic00327a014.

(77) Goto, S.; Iida, T.; Cho, S.; Oka, M.; Kohno, S.; Kondo, T. Overexpression of Glutathione S-Transferase π Enhances the Adduct Formation of Cisplatin with Glutathione in Human Cancer Cells. *Free Radical Research* **1999**, *31* (6), 549–558. https://doi.org/10.1080/10715769900301121.

(78) Godwin, A. K.; Meister, A.; O'Dwyer, P. J.; Huang, C. S.; Hamilton, T. C.; Anderson, M. E. High Resistance to Cisplatin in Human Ovarian Cancer Cell Lines Is Associated with Marked Increase of Glutathione Synthesis. *Proceedings of the National Academy of Sciences* **1992**, *89* (7), 3070–3074. https://doi.org/10.1073/pnas.89.7.3070.

(79) Pratibha, R.; Sameer, R.; Rataboli, P. V.; Bhiwgade, D. A.; Dhume, C. Y. Enzymatic Studies of Cisplatin Induced Oxidative Stress in Hepatic Tissue of Rats. *European Journal of Pharmacology* **2006**, *532* (3), 290–293. https://doi.org/10.1016/j.ejphar.2006.01.007.

(80) Barnham, K. J.; Djuran, M. I.; Murdoch, P. del S.; Ranford, J. D.; Sadler, P. J. Ring-Opened Adducts of the Anticancer Drug Carboplatin with Sulfur Amino Acids. *Inorganic Chemistry* **1996,** *35* (4), 1065–1072. https://doi.org/10.1021/ic950973d.

(81) dos Santos, N. A. G.; Carvalho Rodrigues, M. A.; Martins, N. M.; dos Santos, A. C. Cisplatin-Induced Nephrotoxicity and Targets of Nephroprotection: An Update. *Archives of Toxicology* **2012**, *86* (8), 1233–1250. https://doi.org/10.1007/s00204-012-0821-7.

(82) Daley-Yates, P. T.; McBrien, D. C. H. Cisplatin Metabolites in Plasma, a Study of Their Pharmacokinetics and Importance in the Nephrotoxic and Antitumour Activity of Cisplatin. *Biochemical Pharmacology* **1984**, *33* (19), 3063–3070. https://doi.org/10.1016/0006-2952(84)90610-5.

(83) Miranda, J. L.; Moura, L. C.; San Gil, R. A. S.; Cruz, M. T. M.; Silva, A. C. O.; Barbosa, Á. A. Experimental and Theoretical Studies on the Complexes between

Cisplatin and Guanidinoacetic Acid. *Polyhedron* **2015**, *102*, 313–320. https://doi.org/10.1016/j.poly.2015.09.061.

(84) Marescau, B.; Deshmukh, D. R.; Kockx, M.; Possemiers, I.; Qureshi, I. A.; Wiechert, P.; De Deyn, P. P. Guanidino Compounds in Serum, Urine, Liver, Kidney, and Brain of Man and Some Ureotelic Animals. *Metabolism* **1992**, *41* (5), 526–532. https://doi.org/10.1016/0026-0495(92)90213-T.

(85) Peaston, A.; Maddison, J. Treatment of Superficial Tumours on Horses with Dimethyl Sulfoxide and Cisplatin. *Australian Veterinary Journal* **1995**, *72* (2), 76–77. https://doi.org/10.1111/j.1751-0813.1995.tb15343.x.

(86) Kerrison, S. J. S.; Sadler, P. J. Solvolysis of Cis-[Pt(NH $_3$) $_2$ Cl $_2$] in Dimethyl Sulphoxide and Reactions of Glycine with [PtCl $_3$ (Me $_2$ SO)] $^-$ as Probed by ^{195}Pt Nuclear Magnetic Resonance Shifts and ^{195}Pt ^{15}N Coupling Constants. *J. Chem. Soc., Chem. Commun.* **1977**, No. 23, 861–863. https://doi.org/10.1039/C39770000861.

(87) Madias, N. E.; Harrington, J. T. Platinum Nephrotoxicity. *The American Journal of Medicine* **1978**, *65* (2), 307–314. https://doi.org/10.1016/0002-9343(78)90825-2.

(88) Zhou, H.; Wang, G.; Lu, Y.; Pan, Z. Bio-Inspired Cisplatin Nanocarriers for Osteosarcoma Treatment. *Biomaterials Science* **2016,** *4* (8), 1212–1218. https://doi.org/10.1039/C6BM00331A.

(89) Calderone, V.; Casini, A.; Mangani, S.; Messori, L.; Orioli, P. L. Structural Investigation of Cisplatin–Protein Interactions: Selective Platination of His19 in a Cuprozinc Superoxide Dismutase. *Angewandte Chemie International Edition* **2006,** *45* (8), 1267–1269. https://doi.org/10.1002/anie.200502599.

(90) Kasahara, K.; Fujimura, M.; Bando, T.; Shibata, K.; Shirasaki, H.; Matsuda, T. Modulation of Sensitivity to Cis-Diamminedichloroplatinum (II) by Thromboxane A2 Receptor Antagonists in Non-Small-Cell Lung Cancer Cell Lines. *British Journal of Cancer* **1996**, *74* (10), 1553–1558. https://doi.org/10.1038/bjc.1996.588.

(91) Lovejoy, K. S.; Todd, R. C.; Zhang, S.; McCormick, M. S.; D'Aquino, J. A.; Reardon, J. T.; Sancar, A.; Giacomini, K. M.; Lippard, S. J. *Cis* -Diammine(Pyridine)Chloroplatinum(II), a Monofunctional Platinum(II) Antitumor Agent: Uptake, Structure, Function, and Prospects. *Proceedings of the National Academy of Sciences* **2008**, *105* (26), 8902–8907. https://doi.org/10.1073/pnas.0803441105.

(92) Zhang, S.; Lovejoy, K. S.; Shima, J. E.; Lagpacan, L. L.; Shu, Y.; Lapuk, A.; Chen, Y.; Komori, T.; Gray, J. W.; Chen, X.; Lippard, S. J.; Giacomini, K. M. Organic Cation Transporters Are Determinants of Oxaliplatin Cytotoxicity. *Cancer Research* **2006**, *66* (17), 8847–8857. https://doi.org/10.1158/0008-5472.CAN-06-0769.

(93) Ishida, S.; Lee, J.; Thiele, D. J.; Herskowitz, I. Uptake of the Anticancer Drug Cisplatin Mediated by the Copper Transporter Ctr1 in Yeast and Mammals. *Proceedings of the National Academy of Sciences* **2002**, *99* (22), 14298–14302. https://doi.org/10.1073/pnas.162491399.

(94) Esteban-Fernández, D.; Montes-Bayón, M.; Blanco González, E.; Gómez Gómez, M. M.; Palacios, M. A.; Sanz-Medel, A. Atomic (HPLC-ICP-MS) and Molecular Mass Spectrometry (ESI-Q-TOF) to Study Cis-Platin Interactions with Serum Proteins. *J. Anal. At. Spectrom.* **2008**, *23* (3), 378–384. https://doi.org/10.1039/B711922D.

(95) Jonker, J. W. Pharmacological and Physiological Functions of the Polyspecific Organic Cation Transporters: OCT1, 2, and 3 (SLC22A1-3). *Journal of Pharmacology and Experimental Therapeutics* **2003**, *308* (1), 2–9. https://doi.org/10.1124/jpet.103.053298.

(96) Cheng, P. W.; Liu, S. H.; Hsu, C. J.; Lin-Shiau, S. Y. Correlation of Increased Activities of Na+, K+ ATPase and Ca2+ ATPase with the Reversal of Cisplatin Ototoxicity Induced by d-Methionine in Guinea Pigs. *Hearing Research* **2005**, *205* (1–2), 102–109. https://doi.org/10.1016/j.heares.2005.03.008.

(97) Chen, K. G.; Leapman, R. D.; Zhang, G.; Lai, B.; Valencia, J. C.; Cardarelli, C. O.; Vieira, W. D.; Hearing, V. J.; Gottesman, M. M. Influence of Melanosome Dynamics on Melanoma Drug Sensitivity. *JNCI: Journal of the National Cancer Institute* **2009**, *101* (18), 1259–1271. https://doi.org/10.1093/jnci/djp259.

(98) Gradhand, U.; Kim, R. B. Pharmacogenomics of MRP Transporters (ABCC1-5) and BCRP (ABCG2). *Drug Metabolism Reviews* **2008**, *40* (2), 317–354. https://doi.org/10.1080/03602530801952617.

(99) Pinato, O.; Musetti, C.; Farrell, N. P.; Sissi, C. Platinum-Based Drugs and Proteins: Reactivity and Relevance to DNA Adduct Formation. *Journal of Inorganic Biochemistry* **2013,** *122*, 27–37. https://doi.org/10.1016/j.jinorgbio.2013.01.007.

(100) Reedijk, J. Why Does Cisplatin Reach Guanine-N7 with Competing S-Donor Ligands Available in the Cell? *Chemical Reviews* **1999**, *99* (9), 2499–2510. https://doi.org/10.1021/cr980422f.

(101) Timerbaev, A. R.; Aleksenko, S. S.; Polec-Pawlak, K.; Ruzik, R.; Semenova, O.; Hartinger, C. G.; Oszwaldowski, S.; Galanski, M.; Jarosz, M.; Keppler, B. K. Platinum Metallodrug-Protein Binding Studies by Capillary Electrophoresis-Inductively Coupled Plasma-Mass Spectrometry: Characterization of Interactions between Pt(II) Complexes and Human Serum Albumin. *Electrophoresis* **2004**, *25* (13), 1988–1995. https://doi.org/10.1002/elps.200305984.

(102) Hahn, M.; Kleine, M.; Sheldrick, W. S. Interaction of Cisplatin with Methionine- and Histidine-Containing Peptides: Competition between Backbone Binding, Macrochelation and Peptide Cleavage. *JBIC Journal of Biological Inorganic Chemistry* **2001**, *6* (5–6), 556–566. https://doi.org/10.1007/s007750100232.

(103) Da Silva, V. J.; Costa, L. A. S.; Dos Santos, H. F. Ab Initio Reaction Path for Cisplatin Interaction WithL-Cysteine AndL-Methionine. *International Journal of Quantum Chemistry* **2008**, *108* (2), 401–414. https://doi.org/10.1002/qua.21494.

(104) Neault, J. F.; Tajmir-Riahi, H. A. Interaction of Cisplatin with Human Serum Albumin. Drug Binding Mode and Protein Secondary Structure. *Biochimica et Biophysica Acta (BBA) - Protein Structure and Molecular Enzymology* **1998**, *1384* (1), 153–159. https://doi.org/10.1016/S0167-4838(98)00011-9.

(105) Kragh-Hansen, U.; Chuang, V. T. G.; Otagiri, M. Practical Aspects of the Ligand-Binding and Enzymatic Properties of Human Serum Albumin. *Biological & Pharmaceutical Bulletin* **2002**, *25* (6), 695–704. https://doi.org/10.1248/bpb.25.695.

(106) Hagrman, D. Kinetic Study on the Reaction of Cisplatin with Metallothionein. *Drug Metabolism and Disposition* **2003**, *31* (7), 916–923. https://doi.org/10.1124/dmd.31.7.916.

(107) Guo, Z.; Sadler, P. J. Metals in Medicine. *Angewandte Chemie International Edition* **1999**, *38* (11), 1512–1531. https://doi.org/10.1002/(SICI)1521-3773(19990601)38:11<1512::AID-ANIE1512>3.0.CO;2-Y.

(108) Jamieson, E. R.; Lippard, S. J. Structure, Recognition, and Processing of Cisplatin−DNA Adducts. *Chemical Reviews* **1999**, *99* (9), 2467–2498. https://doi.org/10.1021/cr980421n.

(109) Johnstone, T. C.; Kulak, N.; Pridgen, E. M.; Farokhzad, O. C.; Langer, R.; Lippard, S. J. Nanoparticle Encapsulation of Mitaplatin and the Effect Thereof on *In Vivo* Properties. *ACS Nano* **2013**, *7* (7), 5675–5683. https://doi.org/10.1021/nn401905g.

(110) Mylonakis, N.; Athanasiou, A.; Ziras, N.; Angel, J.; Rapti, A.; Lampaki, S.; Politis, N.; Karanikas, C.; Kosmas, C. Phase II Study of Liposomal Cisplatin (Lipoplatin™) plus Gemcitabine versus Cisplatin plus Gemcitabine as First Line Treatment in Inoperable (Stage IIIB/IV) Non-Small Cell Lung Cancer. *Lung Cancer* **2010**, *68* (2), 240–247. https://doi.org/10.1016/j.lungcan.2009.06.017.

(111) Stathopoulos, G. P.; Boulikas, T.; Vougiouka, M.; Deliconstantinos, G.; Rigatos, S.; Darli, E.; Viliotou, V.; Stathopoulos, J. G. Pharmacokinetics and Adverse Reactions of a New Liposomal Cisplatin (Lipoplatin): Phase I Study. *Oncol. Rep.* **2005**, *13* (4), 589–595.

(112) Fantini, M.; Gianni, L.; Santelmo, C.; Drudi, F.; Castellani, C.; Affatato, A.; Nicolini, M.; Ravaioli, A. Lipoplatin Treatment in Lung and Breast Cancer. *Chemother Res Pract* 2011, **2011**, 125192. https://doi.org/10.1155/2011/125192.

(113) Boulikas, T. Clinical Overview on Lipoplatin ™ : A Successful Liposomal Formulation of Cisplatin. *Expert Opinion on Investigational Drugs* **2009**, *18* (8), 1197–1218. https://doi.org/10.1517/13543780903114168.

(114) Stathopoulos, G. P.; Boulikas, T. Lipoplatin Formulation Review Article. *Journal of Drug Delivery* 2012, **2012**, 1–10. https://doi.org/10.1155/2012/581363.

(115) Arany, I.; Safirstein, R. L. Cisplatin Nephrotoxicity. *Seminars in Nephrology* **2003**, *23* (5), 460–464. https://doi.org/10.1016/S0270-9295(03)00089-5.

(116) Sorenson, C. M.; Eastman, A. Mechanism of Cis-Diamminedichloroplatinum(II)-Induced Cytotoxicity: Role of G2 Arrest and DNA Double-Strand Breaks. *Cancer Res.* **1988**, *48* (16), 4484–4488.

(117) Harrington, K. J. Liposomal Cancer Chemotherapy: Current Clinical Applications and Future Prospects. *Expert Opinion on Investigational Drugs* **2001**, *10* (6), 1045–1061. https://doi.org/10.1517/13543784.10.6.1045.

(118) Karpathiou, G.; Argiana, E.; Koutsopoulos, A.; Froudarakis, M. E. Response of a Patient with Pleural and Peritoneal Mesothelioma after Second-Line Chemotherapy with Lipoplatin and Gemcitabine. *Oncology* **2007**, *73* (5–6), 426–429. https://doi.org/10.1159/000136800.

(119) Froudarakis, M. E.; Pataka, A.; Pappas, P.; Anevlavis, S.; Argiana, E.; Nikolaidou, M.; Kouliatis, G.; Pozova, S.; Marselos, M.; Bouros, D. Phase 1 Trial of Lipoplatin and Gemcitabine as a Second-Line Chemotherapy in Patients with Nonsmall Cell Lung Carcinoma. *Cancer* **2008**, *113* (10), 2752–2760. https://doi.org/10.1002/cncr.23921.

(120) Boulikas, T. Low Toxicity and Anticancer Activity of a Novel Liposomal Cisplatin (Lipoplatin) in Mouse Xenografts. *Oncol. Rep.* **2004**, *12* (1), 3–12.

(121) Kamel, D.; Gray, C.; Walia, J. S.; Kumar, V. PARP Inhibitor Drugs in the Treatment of Breast, Ovarian, Prostate and Pancreatic Cancers: An Update of Clinical Trials. *Current Drug Targets* **2018**, *19* (1). https://doi.org/10.2174/1389450118666170711151518.

(122) Li, J.; Li, Z.; Li, M.; Zhang, H.; Xie, Z. Synergistic Effect and Drug-Resistance Relief of Paclitaxel and Cisplatin Caused by Co-Delivery Using Polymeric Micelles. *Journal of Applied Polymer Science* **2015,** *132* (6). https://doi.org/10.1002/app.41440.

(123) Bhargava, A.; Vaishampayan, U. N. Satraplatin: Leading the New Generation of Oral Platinum Agents. *Expert Opinion on Investigational Drugs* **2009**, *18* (11), 1787–1797. https://doi.org/10.1517/13543780903362437.

(124) Choy, H. Satraplatin: An Orally Available Platinum Analog for the Treatment of Cancer. *Expert Review of Anticancer Therapy* **2006**, *6* (7), 973–982. https://doi.org/10.1586/14737140.6.7.973.

(125) Hall, M. D.; Daly, H. L.; Zhang, J. Z.; Zhang, M.; Alderden, R. A.; Pursche, D.; Foran, G. J.; Hambley, T. W. Quantitative Measurement of the Reduction of Platinum(Iv) Complexes Using X-Ray Absorption near-Edge Spectroscopy (XANES). *Metallomics* **2012**, *4* (6), 568. https://doi.org/10.1039/c2mt20053h.

(126) Hall, M. D.; Hambley, T. W. Platinum(IV) Antitumour Compounds: Their Bioinorganic Chemistry. *Coordination Chemistry Reviews* **2002**, *232* (1–2), 49–67. https://doi.org/10.1016/S0010-8545(02)00026-7.

(127) Kelland, L. R. An Update on Satraplatin: The First Orally Available Platinum Anticancer Drug. *Expert Opinion on Investigational Drugs* **2000**, *9* (6), 1373–1382. https://doi.org/10.1517/13543784.9.6.1373.

(128) Fink, D.; Nebel, S.; Aebi, S.; Zheng, H.; Cenni, B.; Nehmé, A.; Christen, R. D.; Howell, S. B. The Role of DNA Mismatch Repair in Platinum Drug Resistance. *Cancer Res.* **1996**, *56* (21), 4881–4886.

(129) Vaisman, A.; Lim, S. E.; Patrick, S. M.; Copeland, W. C.; Hinkle, D. C.; Turchi, J. J.; Chaney, S. G. Effect of DNA Polymerases and High Mobility Group Protein 1 on the Carrier Ligand Specificity for Translesion Synthesis Past Platinum−DNA Adducts. *Biochemistry* **1999**, *38* (34), 11026–11039. https://doi.org/10.1021/bi9909187.

(130) Gramatica, P.; Papa, E.; Luini, M.; Monti, E.; Gariboldi, M. B.; Ravera, M.; Gabano, E.; Gaviglio, L.; Osella, D. Antiproliferative Pt(IV) Complexes: Synthesis, Biological Activity, and Quantitative Structure–Activity Relationship Modeling. *JBIC Journal of Biological Inorganic Chemistry* **2010**, *15* (7), 1157–1169. https://doi.org/10.1007/s00775-010-0676-4.

(131) Platts, J. A.; Ermondi, G.; Caron, G.; Ravera, M.; Gabano, E.; Gaviglio, L.; Pelosi, G.; Osella, D. Molecular and Statistical Modeling of Reduction Peak Potential and Lipophilicity of Platinum(IV) Complexes. *JBIC Journal of Biological Inorganic Chemistry* **2011**, *16* (3), 361–372. https://doi.org/10.1007/s00775-010-0731-1.

(132) Levina, A.; McLeod, A. I.; Gasparini, S. J.; Nguyen, A.; De Silva, W. G. M.; Aitken, J. B.; Harris, H. H.; Glover, C.; Johannessen, B.; Lay, P. A. Reactivity and Speciation of Anti-Diabetic Vanadium Complexes in Whole Blood and Its Components: The Important Role of Red Blood Cells. *Inorganic Chemistry* **2015**, *54* (16), 7753–7766. https://doi.org/10.1021/acs.inorgchem.5b00665.

(133) Garner, M.; Reglinski, J.; Smith, W. E.; McMurray, J.; Abdullah, I.; Wilson, R. A1 H Spin Echo and 51V NMR Study of the Interaction of Vanadate with Intact Erythrocytes. *JBIC Journal of Biological Inorganic Chemistry* **1997**, *2* (2), 235–241. https://doi.org/10.1007/s007750050129.

(134) Coghlan, A. Bitter Pill for Cancer's Sweet Tooth. *New Scientist* **2010**, *206* (2760), 6–7. https://doi.org/10.1016/S0262-4079(10)61171-2.

(135) Griffith, D.; Morgan, M. P.; Marmion, C. J. A Novel Anti-Cancer Bifunctional Platinum Drug Candidate with Dual DNA Binding and Histone Deacetylase Inhibitory Activity. *Chemical Communications* **2009**, No. 44, 6735. https://doi.org/10.1039/b916715c.

(136) Zhang, W.; Zhang, S. L.; Hu, X.; Tam, K. Y. Targeting Tumor Metabolism for Cancer Treatment: Is Pyruvate Dehydrogenase Kinases (PDKs) a Viable Anticancer Target? *International Journal of Biological Sciences* **2015**, *11* (12), 1390–1400. https://doi.org/10.7150/ijbs.13325.

(137) Gibson, D. Platinum(iv) Anticancer Prodrugs – Hypotheses and Facts. *Dalton Transactions* **2016**, *45* (33), 12983–12991. https://doi.org/10.1039/C6DT01414C.

(138) Wheate, N. J.; Walker, S.; Craig, G. E.; Oun, R. The Status of Platinum Anticancer Drugs in the Clinic and in Clinical Trials. *Dalton Transactions* **2010**, *39* (35), 8113. https://doi.org/10.1039/c0dt00292e.

(139) Zhang, J. Q.; Li, K.; Jiang, K. M.; Cong, Y. W.; Pu, S. P.; Xie, X. G.; Jin, Y.; Lin, J. Development of an Oral Satraplatin Pharmaceutical Formulation by Encapsulation with Cyclodextrin. *RSC Advances* **2016**, *6* (21), 17074–17082. https://doi.org/10.1039/C5RA27182G.

(140) Ma, X.; Rong, S.; Zhang, Y.; Jia, L. Current Perspectives on Genotype Classification and Individualized Drug Targeting in Triple-Negative Breast Cancer. *Tropical Journal of Pharmaceutical Research* **2018**, *17* (2), 359. https://doi.org/10.4314/tjpr.v17i2.23.

(141) Doucette, KA; Hassell, KN; Crans, DC. Selective speciation improves efficacy and lowers toxicity of platinum anticancer and vanadium antidiabetic drugs. *Journal of Inorganic Biochemistry* **2016**, (165)56–70. https://doi.org/10.1016/j.jinorgbio.2016.09.013.

CHAPTER 2 – SCHIFF-BASES IN REVERSE MICELLES; PACKAGING SMALL INSOLUBLE MOLECULES FOR DRUG DELIVERY

2.1 Significance of Work/Specific Aims

This chapter investigates the use of the sodium bis(2-ethylhexyl) sulfosuccinate (AOT)/isooctane reverse micellar system for stabilizing two water-insoluble Schiff-bases as a potential model for liposomal Cisplatin drug delivery. The aim of the study was to utilize two known compounds: 3- trifluoromethylamine-5-chlorosalicyl aldehyde (3TF-Cl) and 3-trifluoromethylamine salicylaldehyde (3TF-S), to analyze their interaction within the interface of a reverse micelle. This interaction is dependent on the size of reverse micelle but not the AOT overall concentration, therefore making the system dependent on the concentration of reverse micelles. We hypothesized that the interaction between the 3TF-Cl and 3TF-S molecules are resulting from their association with the hydrophobic AOT interface near the organic solvent layers of the reverse micelle system. Both compounds, 3TF-Cl and 3TF-S are insoluble in water but react with water to reform the aldehyde and the amine.

2.2 Introduction

Despite the hydrolytic instability of Schiff-base compounds, they are still an integral component in biology with several medicinal applications and over 500 publications and 11,000 plus citations per year, according to Web of Science statistics. Schiff-bases are organic molecules formed by the condensation reaction between an amine and an aldehyde/ketone[1-3] and as such are susceptible to hydrolytic attack; examples of the two

Schiff-bases investigated in this work are shown in figure 2.1. Regardless of this phenomenon, they continue to be used in catalysis, such as Jacobsen's catalyst and other asymmetric catalysts developed by Dr. Noyori, which resulted in a Nobel prize awarded in 2001.[4] In biology, the Schiff base is an important key enzyme intermediate involved in carbohydrate metabolism[5] and in the formation of condensation products with the pyridoxal phosphate (PLP) cofactor.[3] Other important roles of Schiff-bases are uses as diagnostic tools[4,6-7] metal Schiff-base complexes are used as medicines[8-12] and others can be found in the functions of cornea with rhodopsin.[5,13-15] Fundamentally, the condensation products are hydrophobic molecules and sensitive to hydrolysis. Since many of the applications of these Schiff-bases involve aqueous solvents, the hydrolytic instability becomes an additional variable.[5,9,15-19] In the following chapter, we explored the possibility that placing a Schiff-base in a heterogeneous environment will increase its stability. Meaning, its reactivity with water and the hydrolysis of Schiff-bases are decreased, and simultaneously the hydrophobic properties of the heterogeneous environment favors solubility.[20-21]

Reactions in confinement can exhibit advantages over reactions in bulk because of reactant proximity and changes in reactivity.[22-23] Design of such a system can be challenging, and often relies on serendipitous solubility and proximity of components involved in the intended reaction. Most organic reactions involve compounds that are hydrophobic and reflect the solubility that is conducive to traditional organic solvents. As a result, reverse micelles (RMs) have been explored with reactions that involve hydrophilic compounds, thus far. Studies of systems with multiple hydrophobic compounds have generally not been done, and very little information is available on the

association of and the impact of organic compounds on reverse micelles.[13,20-21] In the following study, we investigated the location and reactivity of organic compounds in a suspension of AOT/isooctane reverse micelles.[21,24] We hypothesized that a Schiff-base change occurs between the primary hydrogen and amine group; perhaps rotating up and outward of its initial plane, reversing its hydrolytic properties.

Microemulsions are complex solutions containing ternary or higher order structures that display a single phase. They can contain various types of structures including discrete spherical droplets, interconnected bicontinuous water channels, and liquid crystals. Reverse micelles (RMs) of sodium bis(2-ethylhexyl) sulfosuccinate (AOT) in nonpolar organic solvent (figure 2.2a) can solubilize water into organized structures containing a water pool surrounded by the surfactant polar head groups.[25-27] The AOT-RM system is composed of a negatively charged head group and two tail groups with a positive counter ion, such as sodium shown in the figure 2.2b. The AOT ion interacts with the water pool, probe molecules present in the water and the surfactant molecule itself. On varying the amount of water ($[H_2O]/[AOT] = w_0$), one can vary the size of water pool.[20,27-29]

The two water insoluble compounds shown in figure 2.1 were used to test the hydrophobic interactions between AOT/isooctane in reverse micelles. These two Schiff-base compounds have closely related structural properties and characteristics but differ in their substitution patterns, polarity, and stability in reverse micelles. Both Schiff-base compounds were synthesized by a fluoro-aromatic amine condensing with an aldehyde compounds.[29,36-40] In this study, we hypothesized that the polar environment of the interface between reverse micelles and the organic solvent region may be a desirable

environment for hydrophobic molecules such as Schiff-bases. The differences in hydrolytic properties may be observed with a simple change in the molecular structure of the Schiff-bases.

2.3 Materials and Methods

NaAOT (Sodium bis(2-ethylhexyl)sulfosuccinate) stocks were purified by the method described previously.[28] 10g NaAOT dissolved in 150mL methanol and 15g charcoal. Water contents per AOT molecules were determined by ^{1}H NMR spectroscopy by using *d6*-DMSO, measuring around 0.3 water molecules per molecule of AOT.[28-29, 32]

Synthesis of 3-trifluoromethyl amine salicylaldehyde *(3TF-S)*:

To a 250mL flask 80mL methanol, equimolar 5-chlorosalicylaldehylde and 3-trifluoromethyl amine were added and the reaction was stirred until the colorless liquid changed to golden-yellow transparent solution under reflux for 3 hrs. The volume of the reaction was reduced by one-third of its original volume and left for days at room temperature. Light yellow crystals were obtained after 2-3 days. Alternatively, the methanol was removed under reduced pressure to yield a crude golden oil. This crude Schiff-base was then dissolved in 100 mL diethyl ether and washed with 100 mL saturated $NaHCO_3$. The phases were separated and the aqueous phase was extracted with diethyl ether and washed with saturated $NaHCO_3$ and brine. The solution was dried with sodium sulfate, and after removing the sodium sulfate the solution is concentrated under reduced pressure to yield 70-90% 3-trifluoromethyl amine-5-chlorosalicylaldehylde (3TF-Cl). The golden-yellow solid compound was data analyzed in isooctane. HSMS (DART) $C_{11}H_{10}ClF_4NO_2$ $[(M+H)_+]$ found 300.0405 and the was calculated for 300.0398. M.P.:

88^{o}C; IR (u/cm^{-1}): 1616 (HC=N), 1109 (C-F), ^{1}H NMR (DMSO-d$_6$, 400 MHz, δ (ppm)): 12.50 (s, -OH), 8.99 (s, HC=N), 7.78-7.79 (m, H2, H14), 7.68-7.71 (m, H4, H5, H6), 7.03 (d, H11, J [^{1}H-^{1}H] = 8.8 Hz), 7.45 (dd, H12, J [^{1}H-^{1}H] = 8.8, 2.8 Hz); ^{13}C NMR (DMSO-d$_6$, 101 MHz, δ (ppm)): 149.6 (C1), 123.7 (C2), 123.8 (q, C, ^{1}J [^{19}F-^{13}C] = 3.75 Hz), 134.5 (C4), 131.8 (C5), 130.1 (C6), 118.2 (q, C7, ^{1}J [^{19}F-^{13}C] = 3.75 Hz), 163.9 (C8), 119.6 (C9), 159.7 (C10), 119.0 (C11), 133.6 (C12), 131.5 (C13), 132.3 (C14).

3-trifluoromethyl amine salicylaldehyde (3TF-S) was similarly prepared as described previously above. The yellowish solid compound was analyzed in isooctane. HSMS (DART) found 266.0756 and calculated for $C_{14}H_8O_2F_3$ [$(M+H)^+$] 266.0549. M.P.: 85^{o}C; IR (u/cm^{-1}): 1618 (HC=N), 1109 (C-F), ^{1}H NMR (DMSO-d$_6$, 400 MHz, δ (ppm)): 12.86 (s, -OH), 8.66 (s, HC=N), 7.54-7.58 (m, H2, H4, H14), 7.41-7.50 (m, H5, H6, H13), 7.07 (dd, H11, J [^{1}H-^{1}H] = 5.7, 1.2 Hz), 6.70 (dt, H12, J [^{1}H-^{1}H] = 7.5, 1.2 Hz); ^{13}C NMR (DMSO-d$_6$, 101 MHz, δ (ppm)): 149.2 (C1), 119.3 (C2), 123.4 (q, C3, ^{2}J [^{19}F-^{13}C] = 3.75 Hz), 130.0 (C4), 132.1 (C5), 131.7 (C6), 118.0 (q, C7, ^{1}J [^{19}F-^{13}C] = 3.75 Hz), 164.2 (C8), 118.9 (C9), 161.1 (C10), 117.4 (C11), 133.8 (C12), 124.6 (C13), 132.1 (C14). HSMS (DART) calculated for $C_{14}H_8O_2F_3$ [$(M+H)^+$] 266.0549, found 266.0756.

Reverse Micelle preparation:

The microemulsions were prepared by dissolving AOT in isooctane to get the 0.20M, 0.50M and 0.75M stock solutions. The reverse micelles (RMs) are prepared by adding a known amount of D_2O to generate the desired size in isooctane (size is proportional to w_0 = [H_2O]/[AOT]). The reverse micelles containing probe molecules are prepared by using AOT in isooctane and to make up an equivalent 10mM probe in the water pool. Specifically, microemulsion samples are prepared by adding 3mL AOT-

Isooctane/D_2O and Schiff-base compound to 5mL vials which were vortexed to dissolve the Schiff-base.

NMR spectroscopy:

^1H NMR was used to characterize the interaction of probe molecules with the reverse micelle interface using parameters reported previously. Position of ^1H NMR peaks are references against the isooctane signal and reported against 3-(trimethylsilyl)propanesulfonic acid, sodium salt (DSS). The ^{19}F NMR spectra were recorded using isooctane for the reference as described previously.[12]

Dynamic Light Scattering (DLS):

DLS data was collected to confirm the formation of the reverse micelles in the absence and presence of the Schiff-base compound probes. The reserve micelles containing 3TF-Cl or 3TF-S were found to have experimentally indistinguishable sizes compared to reverse micelles containing only D_2O. Both reverse micelles containing Schiff-base (3TF-Cl or 3TF-S) were sizes similarly to those described in recently publications.[33]

Direct Analysis in Real Time (DART):

High resolution mass spectrometry experiments were conducted by Direct Analysis in Real Time (DART) on an Agilent 6220 TOF-LCMS interfaced to an Agilent 1200 with a DART source. Direct analysis in real time allows for mass spectral identification based on time of flight mass spectrometry (TOF-MS).[34] Data collected provides selectivity and accurate element composition assignments further supporting the completed synthesis of the compounds and their relative isotopes.

2.4 Results

Schiff-bases are known to be very sensitive to hydrolysis, but their structures are very attractive ligands for metal ions, making them interesting vehicles for this study. The condensation product abbreviated 3TS-S was synthesized from 3-trifluoromethylamine (3TF) and salicylaldehyde (S). The condensation product abbreviated 3TF-Cl was synthesized from 3-trifluoromethylamine (3TF) and 5-chlorosalicyl aldehyde (Cl) for comparison with 3TF-S. Because of the insolubility of these compounds in water, the Schiff-bases were solubilized in AOT/isooctane reverse micelles allowing for the exploration of the hydrolysis activity of the two Schiff-bases with the expectation that the 3TF-S would be more stable than the 3TF-Cl because of the electron withdrawing effects of the chlorine (Cl) atom.

Initially, $_1$H NMR experiments were conducted to characterize the conditions used to best monitor the changes in the AOT/isooctane reverse micelles. Specifically, 3TF-Cl was added directly to AOT/isooctane/D_2O systems with the AOT concentrations 0.20M, 0.50M and 0.75M with w_0 8 and w_0 20. Similar chemical shifts were found for the probes within this series of samples, suggesting that it does not make a difference what AOT concentration is used. The data shown displayed a change in environment for the compound in going from pure isooctane to RMs suspensions, but that the concentration of AOT did not significantly influence the chemical shifts. As a result, the rest of the experiments in this chapter were done at 0.50M AOT. (*data not shown*)

The $_1$H NMR spectra show significant shifts between the isooctane spectrum with the OH signal at about 12.5ppm and at the CH=N signal at about 9.5ppm. These shifts suggest that the 3TF-Cl was associated with the interface. Minor changes are also

apparent for the aromatic protons in the region 6.5ppm through 8ppm. The changes in the signal suggest that the environment for a portion of the molecule of 3TF-Cl change significantly once the RMs are formed in the isooctane solution. There is a small but distinct upfield shift in the signal as the water pool increases suggesting a small but significant change in the nanosized structure that forms as the RMs size change. A similar pattern is observed with the CH=N proton. The shift from isooctane to RMs is about 0.1ppm downfield, but the upfield shift as the RMs size increases is much smaller suggesting that the changes in location of 3TF-Cl is minor once the RMs have been prepared.

In figure 2.3, the signal at ~12.5ppm for the OH-group decreases as the w_0 size increases. As the w_0 increase more D_2O is present allowing more opportunities for exchange. The signal at 12.7ppm decreases and disappears with increasing w_0 and a new signal at 9.8ppm emerges at w_0 12 and above. We have interpreted the results to mean that the phenyl-OH exchange with the D_2O pool is slow when the D_2O pool is closely associated with the interface. However, as the water volume increases and more D_2O is available, the signal is lost. The fact that this OH proton can be observed initially shows that the exchange with the water pool is slow when the water is associated with the interface. Such exchange would only be possible if 1) the phenol-OH is placed in or near the water pool and the D_2O can reach it or 2) if the phenol-OH is placed up in the hydrophobic interface and the D_2O traversed up reaching the 3TF-Cl, or 3) that the 3TF-Cl traversed from the interface and reached the D_2O in the water pool.

The spectra recorded in isooctane are shown for comparison. To examine the time dependence of the OH-exchange, ^1H NMR spectra were recorded at w_0 1, 8, 16, and 30

for 4 hrs. A new signal emerges near 10ppm in w_0 16 and 30 samples after about 3 hours for w_0 16 and after 45min for w_0 30. This signal was attributed to the hydrolysis of 3TF-Cl. In figure 2.4, the spectra obtained as the system is monitored as a function of time at different sizes of the RMs are shown. When the RMs is small (w_0 0 and 8), there is little change in the ^{1}H NMR spectra up to 5 hours, and no signal is observed near 10ppm. As the size of the RMs increase (to w_0 16) the ^{1}H NMR spectra (shown in figure 2.4) demonstrated that hydrolysis is not observed until 5 hours of treatment. Finally, as the w_0 increase to 30 the NMR signal near 10ppm emerges already after ~30-45min. These results show that 3TF-Cl is very sensitive to D_2O, and already at 30min in large reverse micelles, observable amounts of hydrolysis product formed. These results demonstrated that the hydrolysis does take place, but only when the RMs is large. To further investigate this phenomenon, an additional water insoluble Schiff-base was examined.

^{1}H NMR Spectra of 3TF-S in AOT/isooctane RMs. 3TF-S was added directly to AOT/isooctane/D_2O systems with varying w_0 size and vortexed. Once the solutions were transparent the ^{1}H NMR spectra was recorded. The partial spectra are shown in figure 2.5. The phenyl-OH signal in isooctane shifts downfield in the presence of AOT RMs suggesting some level of interaction as observed for 3TF-Cl, and the shift remains the same as the RMs size increase. A similar pattern was observed for the CH=N proton at about 8.5ppm. Interestingly, the phenyl-OH does not exchange quickly, and the phenol-OH signal remains significant even when 3TF-S resides in large RMs (w_0 30). As seen in figure 2.5, a signal near 10ppm appears at w_0 8 RMs. This signal is attributed to the hydrolysis product, salicylic aldehyde. The corresponding signals for the protons on the aromatic ring also are consistent with formation of this hydrolysis product. The hydrolysis

of the 3TF-S compound was observed at a much smaller RMs size than for the 3TF-Cl, showing that the former was more readily hydrolyzed. ^{19}F NMR spectra were recorded of the 3TF-Cl at w_0 10 and 20 RMs. In these samples, no difference was observed for the ^{1}H NMR shift. The ^{19}F NMR spectrum does change when comparing a w_0 10 to a w_0 20 RM sample. The observed change is indicative that there are some environmental changes for the CF_3 group in the 3TF-Cl molecule. (*data not shown*)

2.5 Discussion

AOT/isooctane RMs are used in many different applications and as such serves to stabilize, activate and solubilize.[5,19,33] As a result, these systems are used for many practical purposes and understanding the characteristics of the properties of such systems is important. Indeed, much has been done to investigate these systems, probing how RMs respond to additives.[22,29,35] Specifically, several systems have been characterized, investigating the nature of the water pool by investigating its acidity and how the water pool support chemical reactions.[18,36] More importantly, spectroscopy was used to characterize the location of molecules.[35,37] In this study, we investigated the location of a molecule that is readily soluble in the organic solvent. The past systems, researchers have investigated are generally somewhat water soluble, and thus these molecules generally partition near the interface or in the water pool.[19,32] Recently my research group found a system that was not soluble in water, but readily soluble in the AOT/isooctane RMs.[30] This finding was particularly surprising, because the systems came about by replacement of the cation, and although this replacement represented

only a total of 0.01% of cations in this system, the solubility of the compound was more than doubled.

In the case of the two Schiff-bases investigated here, there was very little if any water solubility. This is evident by the color of the solution and by the UV-vis spectroscopy documenting that no absorption from the compound was observed. However, they dissolved in the AOT/isooctane/D_2O-RMs. The compounds both showed a significant change in environment when placed in AOT RMs as observed by changes in the ^1H NMR chemical shifts in RMs or in pure isooctane. This observation would suggest that these compounds associate with the RMs regardless of their solubility in isooctane. Although some research supports the association slightly varies with w_0 size, these Schiff-bases remain associated with the RMs regardless of the size of the water pool. This association is important, because it provides a method by which a water insoluble compound would be placed in proximity to a water source. Because of the limitations in solubility, exploring differences in the concentrations of the compounds varied and were not investigated. However, in this study of the changing w_0 size, we found that the population of the Schiff-base in the interface, shifted. The average occupation number of the system, which were found to range from 0.790 to 1.111 probe per micelle at w_0 16 to w_0 18 RM's, respectively.[6,16,18]

These studies surprisingly demonstrate that an organic molecule soluble in the organic solvent associate with the RMs is pertinent. Such association is important to the subsequent reactivity, and more about such association is desirable because such solubility can be useful for future applications. The properties of Schiff-bases vary. Some are poorly soluble in organic solvents and a survey of related structures were not highly

soluble in AOT-reverse micelles. These properties are likely originating from the molecules that are polar and semi-hydrophobic. The rate by which these Schiff-bases hydrolyze is effectively monitoring the interaction between the water and the Schiff-base.[19,32,35]

The hydrolysis of 3TF-Cl and 3TF-S were greater in larger RMs. Because of the electronic withdrawing nature of chlorine, and thus making the amine more reactive, 3TF-Cl was expected to be the least stable Schiff-base of the two. As seen in figure 2.5, a signal near 10ppm appears at w_0 8 for 3TF-S much sooner than for the 3TF-Cl. This observation documents that in the AOT/isooctane RMs 3TF-S is more readily hydrolyzed than 3TF-Cl. Considering the fact, that these two compounds are insoluble in water, hydrolysis in water cannot be conducted. The changes in the structural data presume that it is associating with the interface of the RM. Therefore, the fact that the hydrolysis does not take place in small RMs is presumably not related to the size of the water pool but the number of water molecules that are partitioning at the interface. Considering that the 3TF-Cl was expected to be more hydrolytically active, the reversal of the compound's hydrolytic activity is significantly important.

2.6 Conclusion

This research demonstrated that the hydrolysis of Schiff-bases is dependent on their molecular environment. Although, electronic properties of substituents change the reactivity of the Schiff-bases, some patterns can be reversed by their environment. The environmental changes can be induced by changes in the size of the reverse micelle and the origin of this change may be due to the difference in the bulk water and interfacial

bound water; which changes with the size of the water pool. Alternatively, changes in the packing of the surfactant may impact environmental changes. In summary, the size of the molecules and their conformation will be important for the detailed structural and physical organization of this nanosized system which will determine the reactivity of Schiff-bases.

Much like the characteristics of the Schiff-base compounds used in this model study, cisplatin could be encapsulated within a reverse micelle for liposomal drug delivery. A reverse micelle or a similar micelle structure has the potential to be optimized as a safe delivery vehicle for insoluble compounds that are prone to hydrolysis such as that like the chemotherapeutic Cisplatin. In future studies, a proprietary micelle model designed to encapsulate the highly toxic Cisplatin drug should be used for intravenous delivery in the treatment of some types of cancers. It is my expectation that the engineered micelle will mimic the natural properties of a healthy human cell, as it fuses to the cancer cells during drug delivery.

Contributions: The original data collection and HNMR spectra were generated by Drs. Khurram Munawar and Myles Sedgwick with Mrs. Mary Fisher. Analysis and concept application were competed by Drs. Kelly N. Hassell and Debbie C. Crans.

2.7 Figures

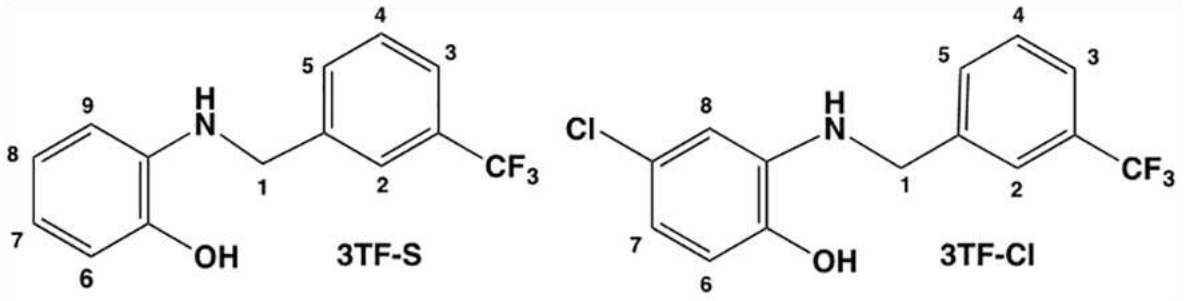

Figure 2.1 Structures of two Schiff-base compounds. 3-trifluoromethyl amine salicylaldehyde (3TF-S) and 3-trifluoromethyl amine-5-chlorosalicylaldehylde (3TF-Cl) Two water insoluble compounds; (*left*) 3-trifluoromethyl amine salicylaldehyde (3TF-S), (*right*) 3-trifluoromethyl amine-5-chlorosalicylaldehylde (3TF-Cl) used as probes to analyze interactions between reverse micelles and the organic solvent region.

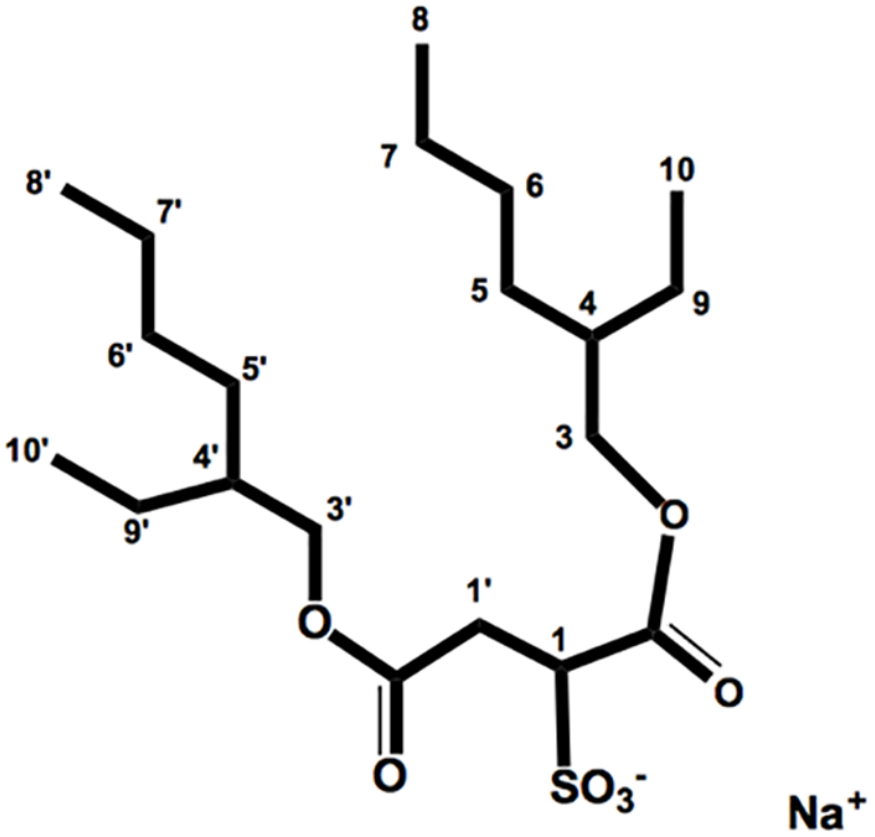

Figure 2.2a bis(2-ethylhexyl)sulfosuccinate (AOT) Structure. Compound used to make the reverse micelle system. Molecular arrangement drives the formation of the water pool and non-polar region of AOT micellular system. Modified from Ref. 8,30

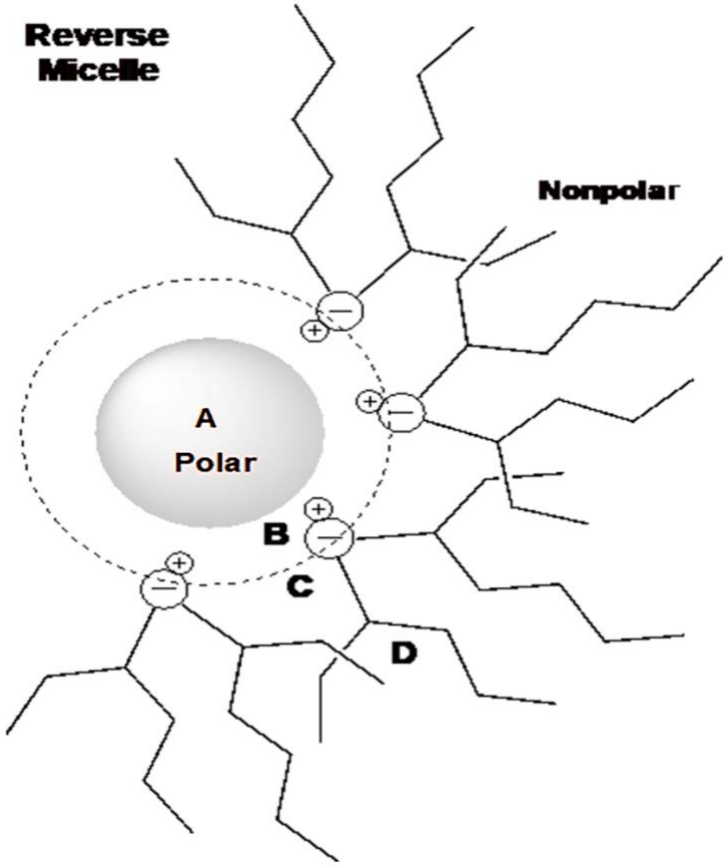

Figure 2.2b Reverse Micelle Structure. A pH-dependent gradient exists along the edges of the water pool in area A and B. A-D regions **a:** water pool **b:** surfactant interface **c:** AOT tails **d:** non-aqueous organic solvent region. Modified from Ref. 8,30

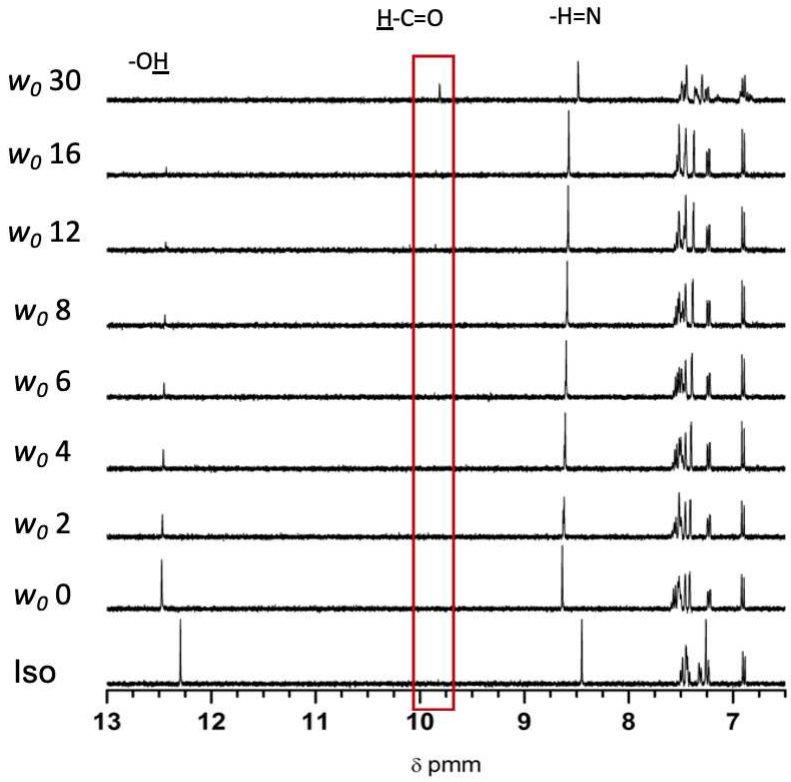

Figure 2.3 $_1$H NMR spectra recorded the 3TF-Cl Schiff-base in 0.2 AOT/isooctane/D_2O-RMs of varying in sizes (w_0 0 to w_0 30) compared to spectra recorded in isooctane (control). The signal at ~12.5ppm for the OH-group decreases as the w_0 size increases. As the w_0 increase more D_2O is present allowing more opportunities for exchange. The signal at 12.7ppm decreases and disappears with increasing w_0 and a new signal at 9.8ppm emerges at w_0 12 size and larger, indicating the phenyl-OH exchange with the D2O pool is slow when the D2O pool is closely associated with the interface.

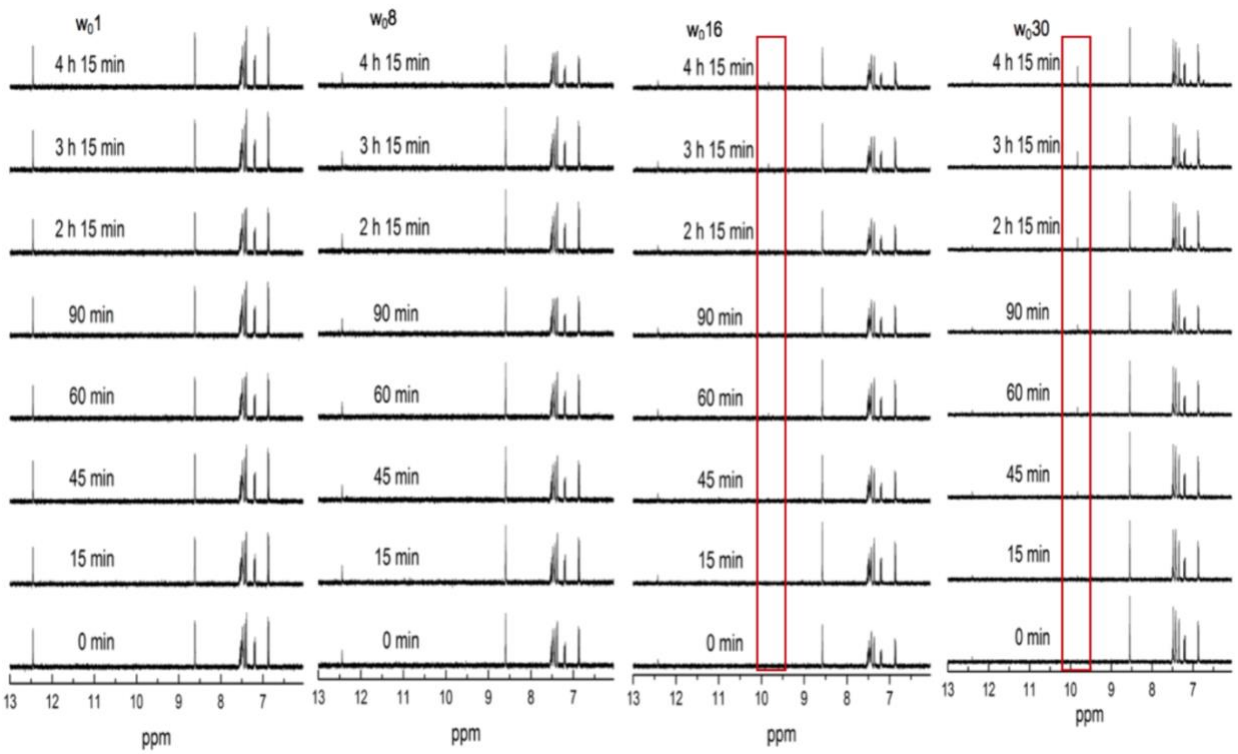

Figure 2.4 $_1$H NMR spectra were recorded of the 3TF-Cl Schiff-base with *w0* at 0, 8, 16 and 30 as a function of time. $_1$H NMR spectra were recorded at *w0* at 1, 8, 16, and 30 for 4hrs. A new signal emerges near 10ppm in *w0* 16 and 30 samples after about 3hrs for *w0* 16 and after 45min for *w0* 30. This signal was attributed to the hydrolysis of 3TF-Cl.

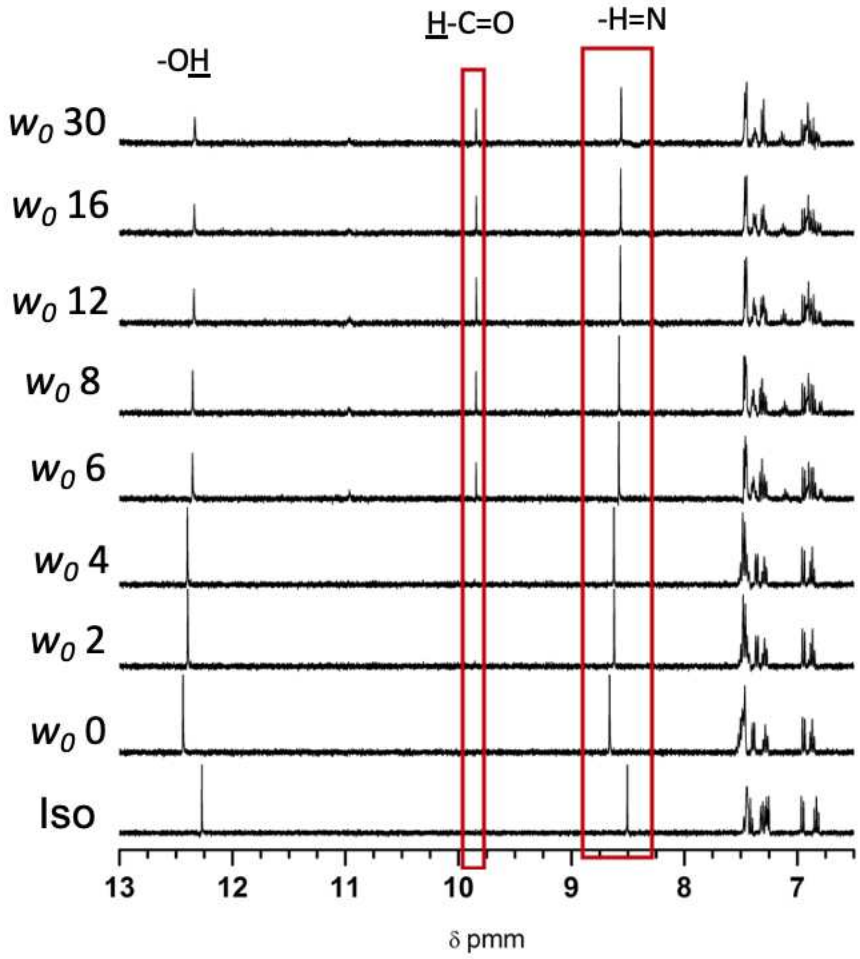

Figure 2.5 $_1$H NMR spectra were recorded of the 3TF-S Schiff base in 0.2M AOT/isooctane/D_2O-RMs with w_0 varying in size from 0 through 30. Spectra are compared to that recorded in isooctane (control). The phenyl-OH signal in isooctane shifts downfield in the presence of AOT RMs suggesting some level of interaction as observed for 3TF-Cl, and the shift remains the same as the RMs size increase. Similar patterns were observed for the CH=N proton at about 8.5ppm. The phenyl-OH does not exchange rapidly and the phenol-OH signal remains significant even in when 3TF-S resides in large RMs (w_0 30) at the signal near 10ppm appears at w_0 8.

REFERENCES

(1) Chen, G.; Liang, G.; Wang, Y.; Deng, P.; Zhou, H. A Homodinuclear Cobalt Complex for the Catalytic Asymmetric Michael Reaction of β-Ketoesters to Nitroolefins. *Org. Biomol. Chem.* **2018**, *16* (20), 3841–3850. https://doi.org/10.1039/C8OB00773J.

(2) Correa, N. M.; Pires, P. A. R.; Silber, J. J.; El Seoud, O. A. Real Structure of Formamide Entrapped by AOT Nonaqueous Reverse Micelles: FT-IR and 1H NMR Studies. *J. Phys. Chem. B* **2005**, *109* (44), 21209–21219. https://doi.org/10.1021/jp053425m.

(3) Castro, M. E.; Percino, M. J.; Cerón, M.; Soriano, G.; Chapela, V. M. Theoretical Inhibition Efficiency Study of Schiff Base (E)-2-(2-Hydroxybenzylideneamino)Phenylarsonic Acid and Its Isomers. *Int J Electrochem Sci* **2014**, *9*, 14.

(4) Noyori, R. Asymmetric Catalysis: Science and Opportunities (Nobel Lecture 2001). *Adv. Synth. Catal.* **2003**, *345* (12), 15–32. https://doi.org/10.1002/adsc.200390002.

(5) Correia, I.; Pessoa, J. C.; Duarte, M. T.; da Piedade, M. F. M.; Jackush, T.; Kiss, T.; Castro, M. M. C. A.; Geraldes, C. F. G. C.; Avecilla, F. Vanadium(IV AndV) Complexes of Schiff-bases and Reduced Schiff-bases Derived from the Reaction of Aromatico-Hydroxyaldehydes and Diamines: Synthesis, Characterisation and Solution Studies. *Eur. J. Inorg. Chem.* **2005**, *2005* (4), 732–744. https://doi.org/10.1002/ejic.200400481.

(6) Brasen, C.; Esser, D.; Rauch, B.; Siebers, B. Carbohydrate Metabolism in Archaea: Current Insights into Unusual Enzymes and Pathways and Their Regulation. *Microbiol. Mol. Biol. Rev.* **2014**, *78* (1), 89–175. https://doi.org/10.1128/MMBR.00041-13.

(7) Caulkins, B. G.; Bastin, B.; Yang, C.; Neubauer, T. J.; Young, R. P.; Hilario, E.; Huang, Y. M.; Chang, C. A.; Fan, L.; Dunn, M. F.; Marsella, M. J.; Mueller, L. J. Protonation States of the Tryptophan Synthase Internal Aldimine Active Site from Solid-State NMR Spectroscopy: Direct Observation of the Protonated Schiff Base

Linkage to Pyridoxal-5′-Phosphate. *J. Am. Chem. Soc.* **2014**, *136* (37), 12824–12827. https://doi.org/10.1021/ja506267d.

(8) Maiti, J.; Sarkar, Y.; Parui, P. P.; Chakraborty, S.; Biswas, S.; Das, R. Photophysical Study of a Charge Transfer Oxazole Dye in Micelles: Role of Surfactant Headgroups. *J. Lumin.* **2015**, *163*, 21–27. https://doi.org/10.1016/j.jlumin.2015.02.054.

(9) Majumder, R.; Sarkar, Y.; Das, S.; Jewrajka, S. K.; Ray, A.; Parui, P. P. A Ratiometric Solvent Polarity Sensing Schiff Base Molecule for Estimating the Interfacial Polarity of Versatile Amphiphilic Self-Assemblies. *The Analyst* **2016**, *141* (11), 3246–3250. https://doi.org/10.1039/C6AN00582A.

(10) Maurya, M. R.; Uprety, B.; Avecilla, F.; Adão, P.; Costa Pessoa, J. Vanadium(v) Complexes of a Tripodal Ligand, Their Characterisation and Biological Implications. *Dalton Trans.* **2015**, *44* (40), 17736–17755. https://doi.org/10.1039/C5DT02716K.

(11) Liu, X.; Manzur, C.; Novoa, N.; Celedón, S.; Carrillo, D.; Hamon, J. R. Multidentate Unsymmetrically-Substituted Schiff-bases and Their Metal Complexes: Synthesis, Functional Materials Properties, and Applications to Catalysis. *Coord. Chem. Rev.* **2018**, *357*, 144–172. https://doi.org/10.1016/j.ccr.2017.11.030.

(12) Hong, Z.; Liu, L.; Sugiyama, M.; Fu, Y.; Wong, C. H. Concise Synthesis of Iminocyclitols via Petasis-Type Aminocyclization. *J. Am. Chem. Soc.* **2009**, *131* (24), 8352–8353. https://doi.org/10.1021/ja901656e.

(13) Pessoa, J. C.; Etcheverry, S.; Gambino, D. Vanadium Compounds in Medicine. *Coord. Chem. Rev.* **2015**, *301–302*, 24–48. https://doi.org/10.1016/j.ccr.2014.12.002.

(14) Piechnick, R.; Heck, M.; Sommer, M. E. Alkylated Hydroxylamine Derivatives Eliminate Peripheral Retinylidene Schiff-bases but Cannot Enter the Retinal Binding Pocket of Light-Activated Rhodopsin. *Biochemistry* **2011**, *50* (33), 7168–7176. https://doi.org/10.1021/bi200675y.

(15) Reiff, C.; Owczarek-Lipska, M.; Spital, G.; Röger, C.; Hinz, H.; Jüschke, C.; Thiele, H.; Altmüller, J.; Nürnberg, P.; Da Costa, R.; Neidhardt, J. The Mutation p.E113K

in the Schiff Base Counterion of Rhodopsin Is Associated with Two Distinct Retinal Phenotypes within the Same Family. *Sci. Rep.* **2016**, *6* (1). https://doi.org/10.1038/srep36208.

(16) Baruah, B.; Roden, J. M.; Sedgwick, M.; Correa, N. M.; Crans, D. C.; Levinger, N. E. When Is Water Not Water? Exploring Water Confined in Large Reverse Micelles Using a Highly Charged Inorganic Molecular Probe. *J. Am. Chem. Soc.* **2006**, *128* (39), 12758–12765. https://doi.org/10.1021/ja0624319.

(17) Palazzo, G.; Lopez, F.; Giustini, M.; Colafemmina, G.; Ceglie, A. Role of the Cosurfactant in the CTAB/Water/ *n*- Pentanol/ *n*- Hexane Water-in-Oil Microemulsion. 1. Pentanol Effect on the Microstructure. *J. Phys. Chem. B* **2003**, *107* (8), 1924–1931. https://doi.org/10.1021/jp026430o.

(18) Correa, N. M.; Zorzan, D. H.; D'Anteo, L.; Lasta, E.; Chiarini, M.; Cerichelli, G. Reverse Micellar Aggregates: Effect on Ketone Reduction. 2. Surfactant Role. *J. Org. Chem.* **2004**, *69* (24), 8231–8238. https://doi.org/10.1021/jo049172v.

(19) Stahla, M. L.; Baruah, B.; James, D. M.; Johnson, M. D.; Levinger, N. E.; Crans, D. C. ^{1}H NMR Studies of Aerosol-OT Reverse Micelles with Alkali and Magnesium Counterions: Preparation and Analysis of MAOTs. *Langmuir* **2008**, *24* (12), 6027–6035. https://doi.org/10.1021/la8002965.

(20) Riter, R. E.; Willard, D. M.; Levinger, N. E. Water Immobilization at Surfactant Interfaces in Reverse Micelles. *J. Phys. Chem. B* **1998**, *102* (15), 2705–2714. https://doi.org/10.1021/jp973330n.

(21) Falcone, R. D.; Correa, N. M.; Biasutti, M. A.; Silber, J. J. Properties of AOT Aqueous and Nonaqueous Microemulsions Sensed by Optical Molecular Probes. *Langmuir* **2000**, *16* (7), 3070–3076. https://doi.org/10.1021/la9909446.

(22) Angelico, R.; Amin, S.; Monduzzi, M.; Murgia, S.; Olsson, U.; Palazzo, G. Impact of Branching on the Viscoelasticity of Wormlike Reverse Micelles. *Soft Matter* **2012**, *8* (42), 10941. https://doi.org/10.1039/c2sm26528a.

(23) Sripradite, J.; Miller, S. A.; Johnson, M. D.; Tongraar, A.; Crans, D. C. How Interfaces Affect the Acidity of the Anilinium Ion. *Chem. Eur. J.* **2016**, *22* (11), 3873–3880. https://doi.org/10.1002/chem.201504804.

(24) Baruah, B.; Swafford, L. A.; Crans, D. C.; Levinger, N. E. Do Probe Molecules Influence Water in Confinement? *J. Phys. Chem. B* **2008**, *112* (33), 10158–10164. https://doi.org/10.1021/jp800390t.

(25) Blach, D.; Correa, N. M.; Silber, J. J.; Falcone, R. D. Interfacial Water with Special Electron Donor Properties: Effect of Water Surfactant Interaction in Confined Reversed Micellar Environments and Its Influence on the Coordination Chemistry of a Copper Complex. *J. Colloid Interface Sci.* **2011**, *355* (1), 124–130. https://doi.org/10.1016/j.jcis.2010.11.067.

(26) Ghosh, S. Comparative Studies on Brij Reverse Micelles Prepared in Benzene/Surfactant/Ethylammonium Nitrate Systems: Effect of Head Group Size and Polarity of the Hydrocarbon Chain. *J. Colloid Interface Sci.* **2011**, *360* (2), 672–680. https://doi.org/10.1016/j.jcis.2011.05.006.

(27) Cordes, E. H.; Jencks, W. P. On the Mechanism of Schiff Base Formation and Hydrolysis. *J. Am. Chem. Soc.* **1962**, *84* (5), 832–837. https://doi.org/10.1021/ja00864a031.

(28) Nave, S.; Paul, A.; Eastoe, J.; Pitt, A. R.; Heenan, R. K. What Is So Special about Aerosol-OT? Part IV. Phenyl-Tipped Surfactants. *Langmuir* **2005**, *21* (22), 10021–10027. https://doi.org/10.1021/la050767a.

(29) Sedgwick, M. A.; Trujillo, A. M.; Hendricks, N.; Levinger, N. E.; Crans, D. C. Coexisting Aggregates in Mixed Aerosol OT and Cholesterol Microemulsions. *Langmuir* **2011**, *27* (3), 948–954. https://doi.org/10.1021/la103875w.

(30) Sánchez-Lombardo, I.; Baruah, B.; Alvarez, S.; Werst, K. R.; Segaline, N. A.; Levinger, N. E.; Crans, D. C. Size and Shape Trump Charge in Interactions of Oxovanadates with Self-Assembled Interfaces: Application of Continuous Shape Measure Analysis to the Decavanadate Anion. *New J. Chem.* **2016**, *40* (2), 962–975. https://doi.org/10.1039/C5NJ01788B.

(31) Zulauf, Martin.; Eicke, H. Friedrich. Inverted Micelles and Microemulsions in the Ternary System Water/Aerosol-OT/Isooctane as Studied by Photon Correlation Spectroscopy. *J. Phys. Chem.* **1979**, *83* (4), 480–486. https://doi.org/10.1021/j100467a011.

(32) Luna, M. A.; Correa, N. M.; Silber, J. J.; Falcone, R. D.; Moyano, F. Properties of AOT Reverse Micelle Interfaces with Different Polar Solvents: Properties of AOT Reverse Micelle Interfaces. *J. Phys. Org. Chem.* **2016**, *29* (11), 580–585. https://doi.org/10.1002/poc.3535.

(33) Rahdar, A.; Almasi-Kashi, M. Dynamic Light Scattering of Nano-Gels of Xanthan Gum Biopolymer in Colloidal Dispersion. *J. Adv. Res.* **2016**, *7* (5), 635–641. https://doi.org/10.1016/j.jare.2016.06.009.

(34) Munawar, K. S.; Ali, S.; Tahir, M. N.; Khalid, N.; Abbas, Q.; Qureshi, I. Z.; Shahzadi, S. Investigation of Derivatized Schiff Base Ligands of 1,2,4-Triazole Amine and Their Oxovanadium(IV) Complexes: Synthesis, Structure, DNA Binding, Alkaline Phosphatase Inhibition, Biological Screening, and Insulin Mimetic Properties. *Russ. J. Gen. Chem.* **2015**, *85* (9), 2183–2197. https://doi.org/10.1134/S1070363215090248.

(35) Bru, R.; Sánchez-Ferrer, A.; García-Carmona, F. Kinetic Models in Reverse Micelles. *Biochem. J.* **1995**, *310* (3), 721–739. https://doi.org/10.1042/bj3100721.

(36) Quintana, S. S.; Falcone, R. D.; Silber, J. J.; Correa, N. M. Comparison between Two Anionic Reverse Micelle Interfaces: The Role of Water-Surfactant Interactions in Interfacial Properties. *ChemPhysChem* **2012**, *13* (1), 115–123. https://doi.org/10.1002/cphc.201100638.

(37) Gaidamauskas, E.; Cleaver, D. P.; Chatterjee, P. B.; Crans, D. C. Effect of Micellar and Reverse Micellar Interface on Solute Location: 2,6-Pyridinedicarboxylate in CTAB Micelles and CTAB and AOT Reverse Micelles. *Langmuir* **2010**, *26* (16), 13153–13161. https://doi.org/10.1021/la101579f.

CHAPTER 3 – TRACKING CAGES; A PRELIMINARY STUDY OF PALLADIUM METALLOCAGES IN HELA CELLS VIA FLOW CYTOMETRY

3.1 Significance of Work

Understanding Pd-cage cellular uptake will assist in understanding of the mechanism of action utilized by various metallocages during drug delivery and perhaps lead to more specific pharmacological therapeutics for treating cancer. This feasibility study for delivering encapsulated cisplatin via Palladium metallocages (Pd-cages) which have been characterized and are autofluorescent. The focus of this project was to determine the cytotoxicity and structural stability of Pd-cages in treatment of HeLa cells. I used flow cytometry to analyze association of Pd-cages with HeLa cells at various concentrations over a 72-hour time course. The data represents the investigation of Pd-cages in HeLa cells using flow cytometry methodology to analyze. Demonstrating the use of this technique for potential application within the clinical science fields. This study provides evidence that supports the association of Pd-cages is most apparent within the first 24 hours of incubation. Furthermore, HeLa cell survival decreases as a function of time with increased concentrations.

3.2 Introduction

Our current state-of-the-art method of chemotherapy requires patients being treated with cisplatin to have a pre and post-administration hospital stay. The monitoring of toxicity levels in the patients is mandatory due to the large amounts of cisplatin intravenously administered; targeting cancer and healthy cells. Some research suggests that the ineffectiveness of chemotherapy agents lead to failed attempts to halt the

metastasis of cancer.[1-5] Pd-cages offer unique characteristics that enables its tracking during and after drug delivery while monitoring structural stability, degradation via flow cytometry. In this mini-project, I investigated the feasibility of utilizing Pd-cages to delivery cisplatin to HeLa cells using flow cytometry to track Pd-cage association with cells and monitor cancer cell death. The main focus of this mini-research study was to explore the tracking abilities of Pd-cages using flow cytometry, a real-time clinical diagnostic instrument.

The most common current therapy model for the intravenous delivery of the anticancer agent cisplatin has multiple cellular membrane transporters used to entry of cisplatin into cancer cells.[6-8] Due to the systemic, non-targeted delivery of cisplatin, patients experience side effects that are directly linked to high dosage requirements of which eventually accumulate in cells and trigger cisplatin resistance.[9-12] Cells naturally have a defense mechanism that has developed over time to protect them from toxins and other various types environmental stressors, all of which are intended to trigger apoptosis; also known as drug resistance. See Chapter 1.2 to 1.4 for more details on cisplatin mechanism of action and cellular uptake in cells.

Cisplatin resistance can result from the epigenetic changes at the molecular and cellular levels caused by the accumulation of platinum throughout the body from efflux of each cancer cell.[13-15] In figure 3.1, the various cisplatin uptake pathways along the mammalian cell membrane are illustrated. This efflux leads to the lack of intended accumulation in targeted cancer cells. Cisplatin can utilize multiple mechanisms in addition to endocytosis and passive diffusion to cross the cell's membrane. The copper influx transporter 1 (Ctr1), ATP7A, ATP7B, polyorganic cation transporters (OCT1-3),

sodium-potassium pumps and melanosomes all play a significant role in allowing the efflux of cisplatin.[16-19] In addition, the cisplatin molecule combines with a glutathione-S-transferase complex, is tagged for export and then moved through the multidrug resistant protein transporters (MRP 1-5).[17,20-22] Traditionally, anticancer agents are able electrostatically bind to the minor DNA grooves, causing additional damage to the cell that triggers an apoptotic response.[23-24]

3.3 Research Overview

Coordination complexes are designed to interact with biomolecules and can function as anticancer agents for drug delivery. Metallocages with motifs of metal to ligand (MxLx) are coordination complexes of M2L4, that self-assemble to encapsulate small molecules to create a cavity within a ligand frame.[25] Palladium metallocages ($C_{80}H_{52}Pd_2B_4F_{16}N_{12}$, 1741.41 g/mol) offer unique physical characteristics allowing for the encapsulation of two cisplatin molecules within a caged-complex and a fluorophore tag that can be used for tracking and diagnostics. The fluorescent properties of the metallocages become excited during the chemical bonding and formation of the exo-functionalized bipyridyl ligand attachments shown in figure 3.2. This structure of a synthesized Pd-cage modified to represent the Pt(II) molecules encapsulated. The coordination chemistry between square planar Pd(II) or platinum(II) cations and pyridyl ligands have been a reproducible model for supramolecular self-assemblies with encapsulated molecules.[26-28]

This drug delivery method has the potential to treat a variety of cancers and foster a new approach toward drug discovery in nanomedicines.[29] Specifically, it could be used

in types of cancers in which patients can be treated with localized drug agents, possibly alleviating the textbook side effects of intravenously delivered cisplatin. Based on the published literature from the Casini group at Cardiff University illustrated by figure 3.2; an exo-functionalized Pd2L4 metallocage using bis(pyridyl) ligands and square planar coordinated palladium(II) ions has been synthesized by metal mediated self-assembly intracellularly.[28,30-33]

In this research study, HeLa cells were treated with concentrations of empty Pd-cages ranging between 1.0µM to 50.0µM to analyze Pd-cage effects on cell viability. The auto-fluorescent characteristics of the self-assembled Pd-cages with a diagnostic fluorophore panel was used to investigate, track and monitor for potential use in cisplatin drug delivery. Flow cytometry analysis in real-time enables the potential application for high-throughput method development in clinical sciences. Improving chemotherapy treatments hinge on researching and developing new methods to circumnavigate the resistance mechanisms of cisplatin and other platinum-based drugs. Methods utilizing a more targeted drug delivery system for cisplatin have yet to be developed and fully explored and understood.

3.4 Materials and Methods

Palladium Metallocages (Pd-cages):

Pd-cages were synthesized by the Casini lab at Cardiff University as previous described.[28,30,32] Small aliquots were prepared prior to experimentation; one-hour incubation in dimethyl sulfoxide (DMSO) solution before dosing the HeLa cells. The

structural identification and confirmation was verified using mass spectroscopy, IR spectroscopy and ^{1}HNMR techniques[28] (data not shown).

Cell Culture Preparations:

For this mini-project HeLa cells were donated by a fellow graduate student who had previous maintained this culture in phenol red MEM growth media. After two cell culture passes, the HeLa cell were maintained in phenol red-free MEM growth media supplemented by 10% fetal bovine serum (FBS), 10mM penicillin-streptomycin, 2mM L-glutamine and 1mM sodium pyruvate and incubated at 37°C with 5% CO2. Upon harvest, the cells were manually counted using a hemocytometer, and stained with Trypan blue® to visually analyze morphology and viability. At 1 x 105 cells/well, a 12-well plate was seeded to ensure that the cells did not exceed 70-80% confluency during the 72-hour data acquisition. For flow cytometry, SYTOX-7AAD™, a cell membrane impermeable fluorescent dye was added 45mins prior to data collection to detect the live/dead cell populations.

For this project, impermeable cell membrane fluorescent dyes were used to indicate degradation of their lipid bilayers which identified cells as non-viable. SYTOX AADvanced Ready Flow Reagent (SYTOX-7AAD™; cat. # R37173) was manufactured by ThermoFisher and donated by Dr. Chris Allen from the CSU Flow Cytometry Core. Table 3.1 details the two-color fluorescent dye panel excitation and emission detection wavelengths used in this analysis.

Sample preparation:

In part 1, HeLa cells were incubated with 0.0-50.0µM Pd-cages for 24 hours. In part 2, 1.0µM Pd-cage was incubated with HeLa cells for 0-72 hours prior to flow

cytometry analysis. Maintaining sterile cell culture techniques, treated HeLa cells were transferred in 2.0mL aliquots to 5.0mL polypropylene round bottom tubes (Falcon/Corning #352002) for flow cytometric analysis. Before analysis, 2-3 drops of SYTOX-7AAD™ stain (ThermoFisher) was added to each sample for the live/dead cell count detection.

Flow cytometry analysis:

HeLa cells were interrogated using a CyAn ADP flow cytometer (S/N 509, Dako Cytomation) equipped with 405nm (25mW semiconductor), 488nm (20mW semiconductor) and 635 nm (25mW semiconductor) lasers. This instrument has 2 scatter and 9 fluorescence parameters. Fluorescent excitation was achieved using a 488nm (blue) laser. Fluorescent emission was collected using a FL1 (PE-Cy5, 680/30 bandpass filter) collection channels. Data were acquired using Summit Software v4.3 (Dako Cytomation) and post-acquisition analyses were performed using FlowJo Software v10.6.1 (BD BioSciences).

3.5 Results & Discussion

This flow cytometry study was conducted in two parts; dose response and time-course analysis. Part 1 investigates the cytotoxicity of 2A Pd-cages in HeLa cells at concentrations ranging from 0.0µM to 50.0µM. Gating was used to discriminate between the % live and % dead in the intact HeLa cell population. Part 2 investigates the cytotoxicity of 1.0µM Pd-cages incubated in HeLa cells for 0-72 hours. Gating was used to discriminate between the % live and % dead in the intact HeLa cell population.

3.5.1 Analysis of % Live vs. % Dead in HeLa Cells Treated with 0.0µM to 50.0µM Dose Pd-Cages After 24 Hours

To evaluate the cytotoxic effects of the empty Pd-cages on HeLa cells, bivariate gating was applied to discriminate between the % live and % dead (see figure 3.3A-F) in the HeLa cell population. In figure 3.3, bivariate gated histograms with ancestral density-dot plots display the cytotoxic effects of the increasing concentrations of empty Pd-cages on HeLa cells after 24 hours of incubation. Figure 3.4, the graph represents the data collected in figure 3.3. The evidence supports the increasing dose of Pd-cages in concentrations ranging from 0.0µM to 50.0µM have a detrimental effect on the survival of HeLa cells. Higher concentrations of Pd-cages effectively kill more HeLa cells. The 0.50µM to 50.0µM concentrations shows as a direct correlation with the increased detection of the % of dead cells and decreased detections of % live HeLa cells.

3.5.2 Analysis of % Live vs. % Dead of Pd-Cages at 1.0µM in HeLa Cells after 0-72 Hours Incubation

To investigate the cytotoxic effects of the 1.0µM dosage of the Pd-cage on the population HeLa cells, the dot-plots with adjunct histograms were gated to discriminate between the two over time (see figure 3.5A-E). The graph in figures 3.6A and 3.6B, represent the data collected in the density-dot plots, of which illustrate an inverse change in both populations (% live and % dead) from 0-72 hours, as well as with the positive and negative controls.

In figure 3.5A-E, bivariate gated histograms with ancestral density dot-plots display the cytotoxic effects of Pd-cages at 1.0µM in HeLa cells from 0-72 hours. As time

increases, the cytotoxicity of empty Pd-cages on HeLa cells also increases. The graph in figure 3.6A & 3.6B, represent time points ranging from to 0-72 hours for Pd-cages at 1.0µM. As the % live decreases, the % dead increases over time. Therefore, the most effective time to dose is within the first 24-48 hours as seen in figure 3.6A. In comparison to the controls in figure 3.6B, the inverse relationship between the (-) control and the (+) control exists and sets the standard for correlation with figure 3.6A.

3.6 Conclusion

This chapter demonstrated techniques that have the potential to provide alternative methods to track Pd-cages or fluorescent metallocages of any composition in real-time with the potential for high throughout impact in the fields of clinical oncology and diagnostics. Overall, this research study has provided evidence of some efficacy and cytotoxicity data on the effect of empty 2A Pd-cages have on killing HeLa cells. Utilizing flow cytometry analysis for the cellular uptake of Pd-cage has provided significant evidence in support of my initial hypothesis; empty Pd-cages can effectively be used at lower concentration ranging between 1.0µM to 10.0µM. Pd-cages seem to be most effective if administered for up to 24-48 hours as reflected by the incubation times in HeLa cells. While this mini-study was carried out using one sample vial per sample, a 96-well plate could be utilized in future studies to maximize the tracking and monitoring of Pd-cages.

With regards to the flow cytometry future studies, slight adjustments could be made for more conclusive data collection. For example, the establishing of tradition controls for figure 3.3 and 3.5 should have been accomplished by running an untreated population of

just HeLa cells and a vial of Pd-cages as blanks at time point zero for a strong baseline analysis. As for the lack of statistical analysis, there were thousands of individual cells analyzed in this preliminary study, but at maximum with two runs collected per sample which makes this more qualitative, than quantitative. Initially when performing this experimentation for my flow cytometry course, neither my instructor nor I were thinking about the publication of this material. If given the opportunity and financial means to continue this mini-project, I would repeat experiments with three replicates and dial down voltage intensity on the forward scatter to prevent the appearance of skewed data. This minor adjustment would allow for a full spectrum analysis of the sample. And during experimentation, the degraded Pd-cages became sticking and difficult to remove from the flow cytometer. To reduce this residual accumulation from self-assembling of ligands potentially forming dimers and/or trimers, I would add additional wash steps to methodology to ensure complete removal of unwanted Pd-cages for analysis.

Note: Due to the current COVID-19 global pandemic, I do not have access to the CSU flow cytometry core facility as this mini-project has not been identified as critical research.

3.7 Figures and Tables

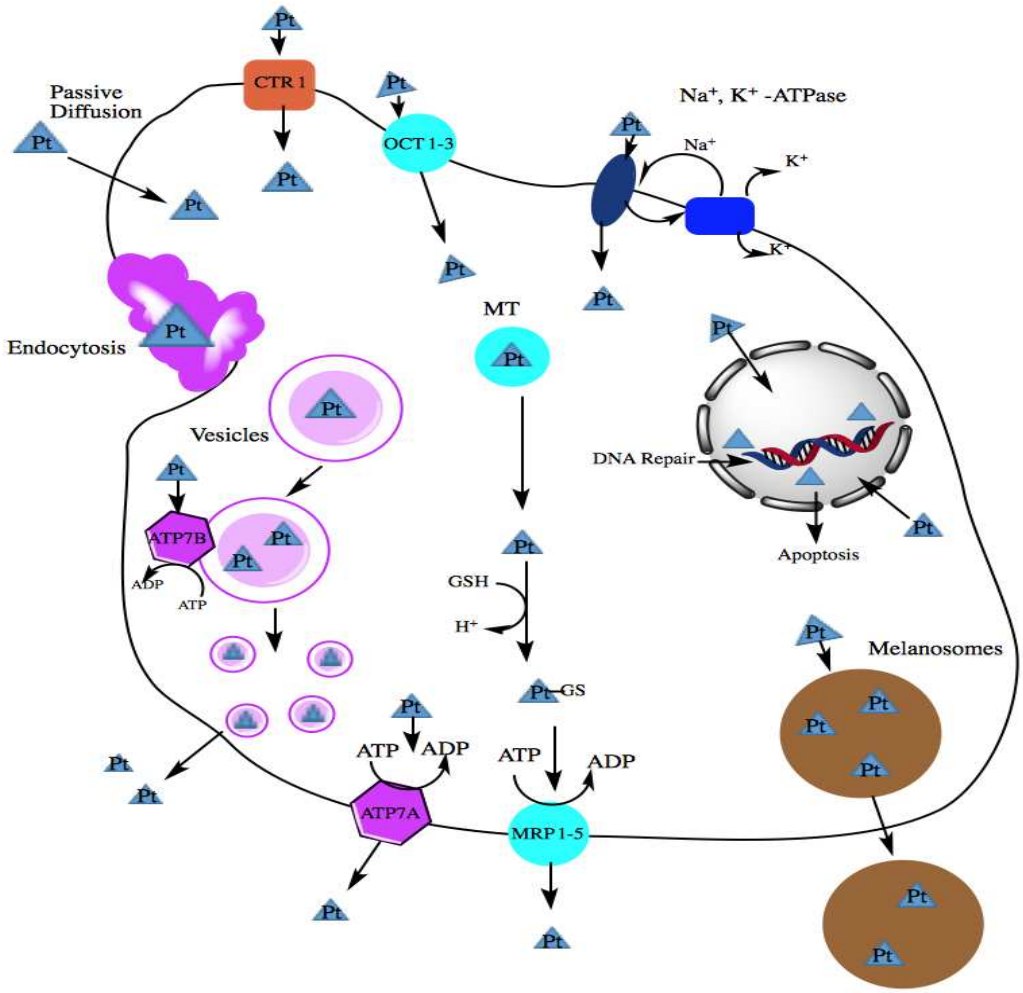

Figure 3.1 Cisplatin (Pt) efflux in animal cells. Uptake pathways for cisplatin (Pt) in mammalian cells. In addition to endocytosis and passive diffusion, cisplatin utilizes multiple pathways for entering cancer cells such as copper influx transporter 1 (Ctr1), ATP7A, ATP7B, polyorganic cation transporters (OCT1-3), sodium-potassium pumps and melanosomes. When cisplatin (Pt) combines with glutathione-S-transferase, the molecule is tagged for export through the multidrug resistant protein transporters (MRP 1-5). Permission from Ref. 23

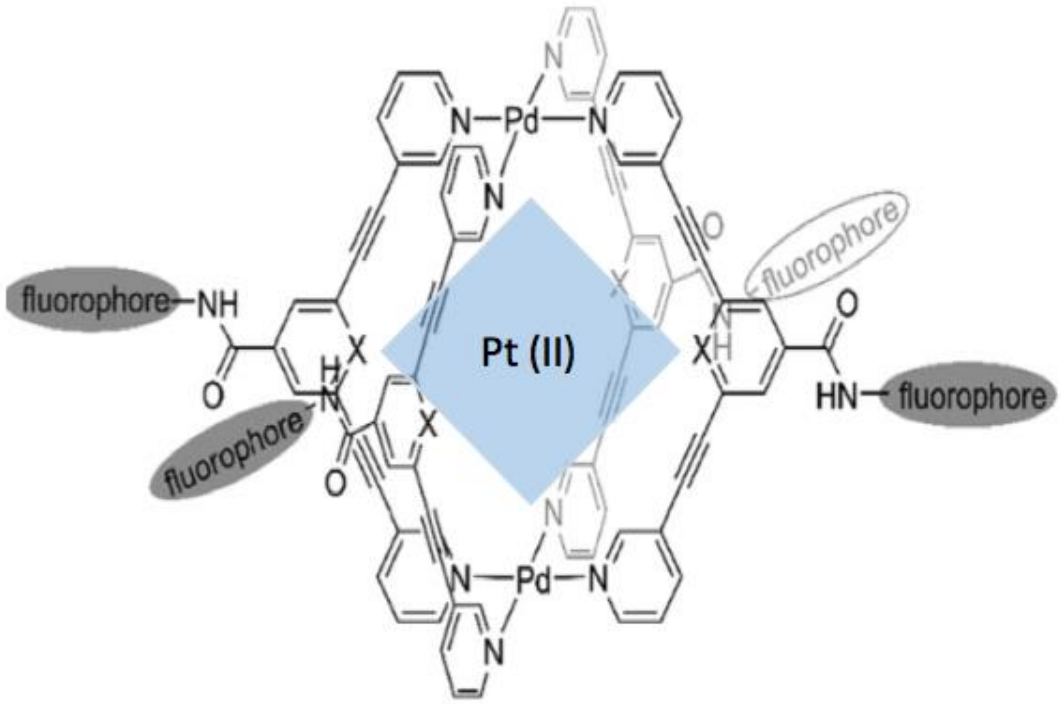

Figure 3.2 Palladium metallocage structure encapsulating Pt(II). Self-assembled Pd_2L_4 cage structure coupled with fluorophores and an exo-positioned carboxy group on the outer shell. One molecule of Pt(II) encapsulated in the center of the self-assembled Pd-cage. Modified from Ref. 28

Table 3.1 Fluorescent dye

Fluorescent dye panel excitation and emission detection wavelengths used in flow cytometry analysis.

	Fluorescent dyes/filters	Excitation (nm)	Emission (max) (nm)
HeLa cells	SYTOX-7AAD™	488	647

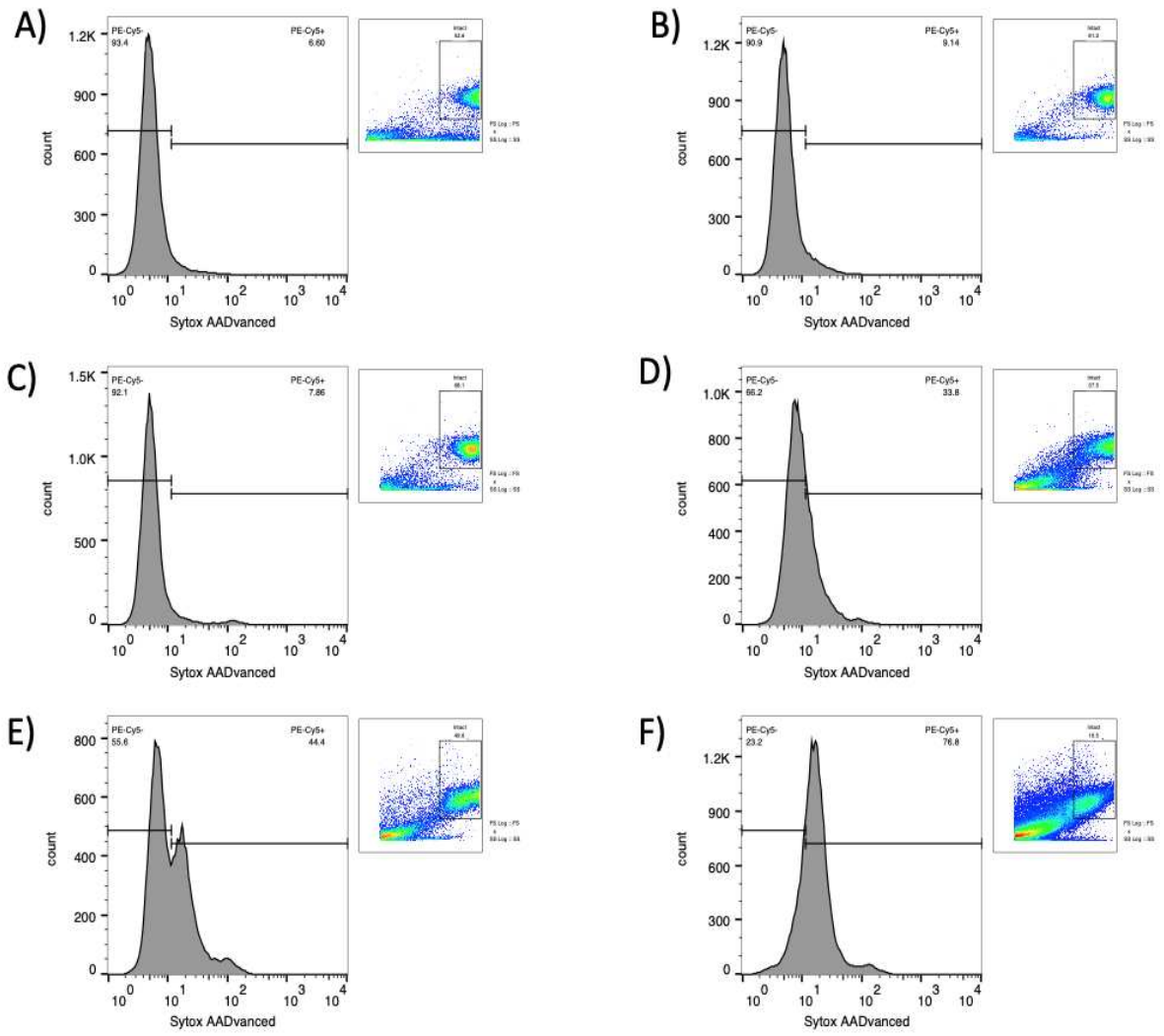

Figure 3.3(A-F) Gated histograms of flow cytometry % Live vs.% Dead for Pd-cages from 0.0µM to 50.0µM in HeLa cells after 24 hours incubation. The X-axis (SYTOX-AADvanced) represents the log values of the live/dead cell count detected by PE-Cy5. The Y-axis represents the total number of cells counted. PE-Cy5- represents the live cell population and PE-Cy5+ represents the dead. Each of the above gates were established and applied to discriminate between live intact in HeLa cells with incorporated Pd-cages dead HeLa cells from 0.50µM to 50.0µM concentrations of Pd-cages. A) 0.0µM, histogram, 93.4% of the cell were live and 6.60% of the cells were dead. B) 0.50µM histogram, 90.9% of the cells were live and 9.14% of the cells were dead. C) 1.0µM live cells at 92.1% and dead cells at 7.86%. D) 10.0µM 66.2% live and 33.8% dead cells. E) 20.0µM 55.6% live and 44.4% dead cells. F) 50.0µM with 23.3% live and 76.8% dead cells.

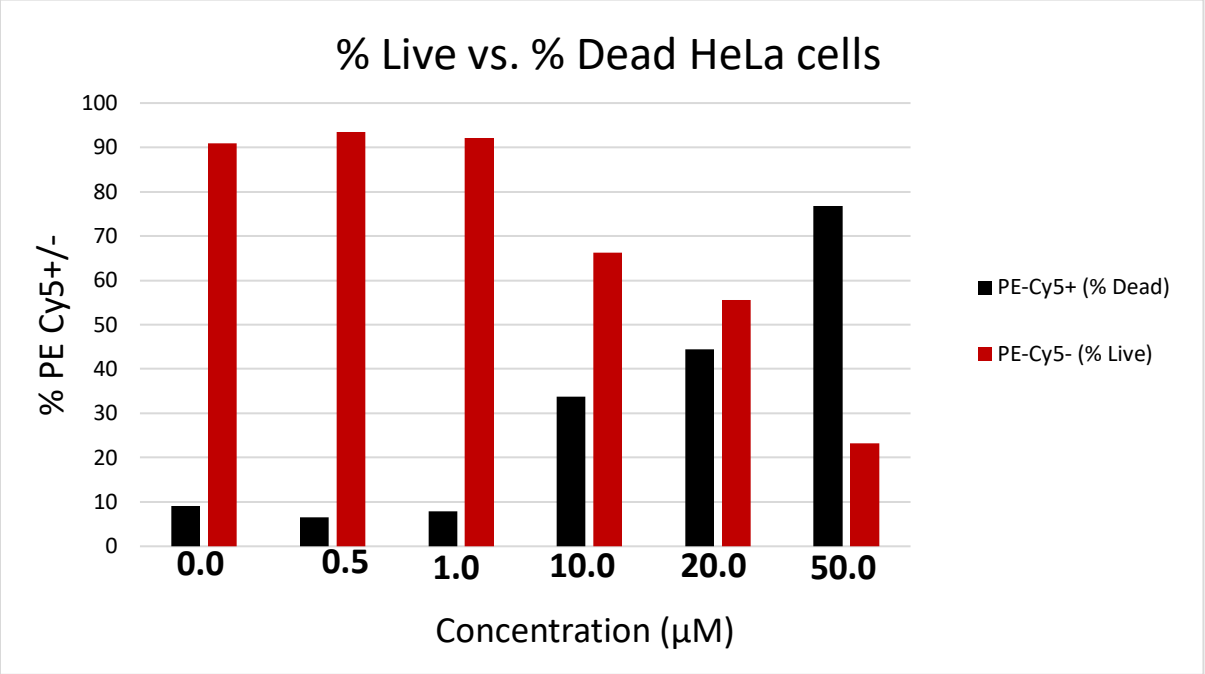

Figure 3.4 % Live vs.% Dead for Pd-cages from 0.0µM to 50.0µM in HeLa cells after 24 hours incubation. X-axis = Pd-cage concentrations [µM],Y-axis = % PE Cy5 +/- detection. Red = live intact HeLa with incorporated Pd-cages. Black = dead HeLa cells. At 0.0µM, 93.4% of the cell were live and 6.60% of the cells were dead. At 0.50µM, 90.9% of the cells were live and 9.14% of the cells were dead. At 1.0µM live cells at 92.1% and dead cells at 7.86%. At 10.0µM 66.2% live and 33.8% dead cells. At 20.0µM 55.6% live and 44.4% dead cells. At 50.0µM with 23.3% live and 76.8% dead cells.

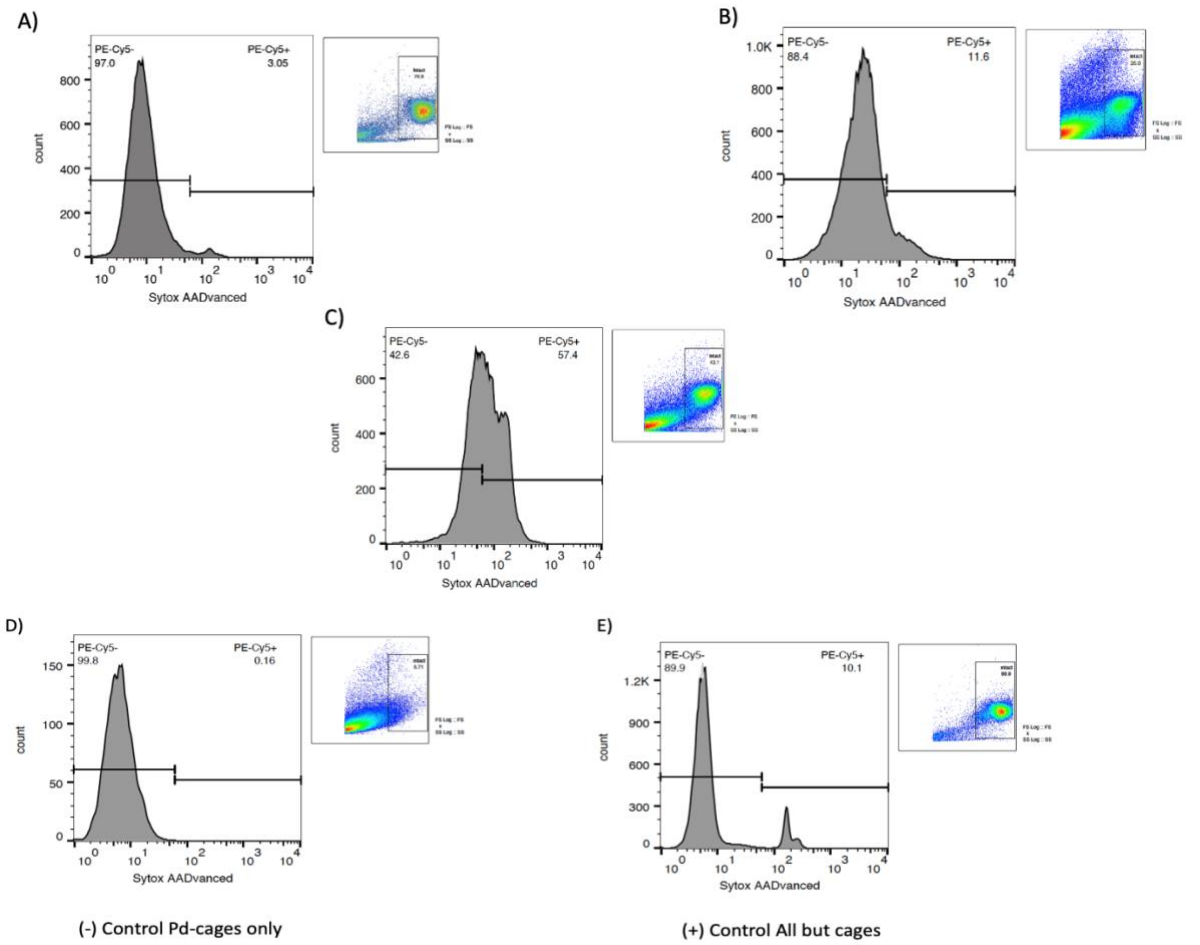

Figure 3.5(A-E) Gated histograms of flow cytometry % Live vs. % Dead analysis of Pd-cages [1.0µM] in HeLa cells from 0-72hours. The X-axis (SYTOX AADvanced) represents the log values of the % live vs. % dead cell count detected by PE-Cy5+/-. The Y-axis represents the total number of cells counted. PE-Cy5- represents the live cell population and PE-Cy5+ represents the dead. Each of the above gates were established and applied to discriminate between the live/dead HeLa cells with incorporated Pd-cages. A) at 24h, 97.0% of the cell were live and 3.05% of the cells were dead. B) at 48h, 88.4% of the cells were live and 11.6% of the cells were dead. C) at 72h, live cells at 42.6% and dead cells at 57.4%. Two controls are at 0h; D) - control the live cells represent 99.8% and dead are 0.16% of the population. E) + control, the 89.9% represents the live and 10.1% are the dead cells in the sample.

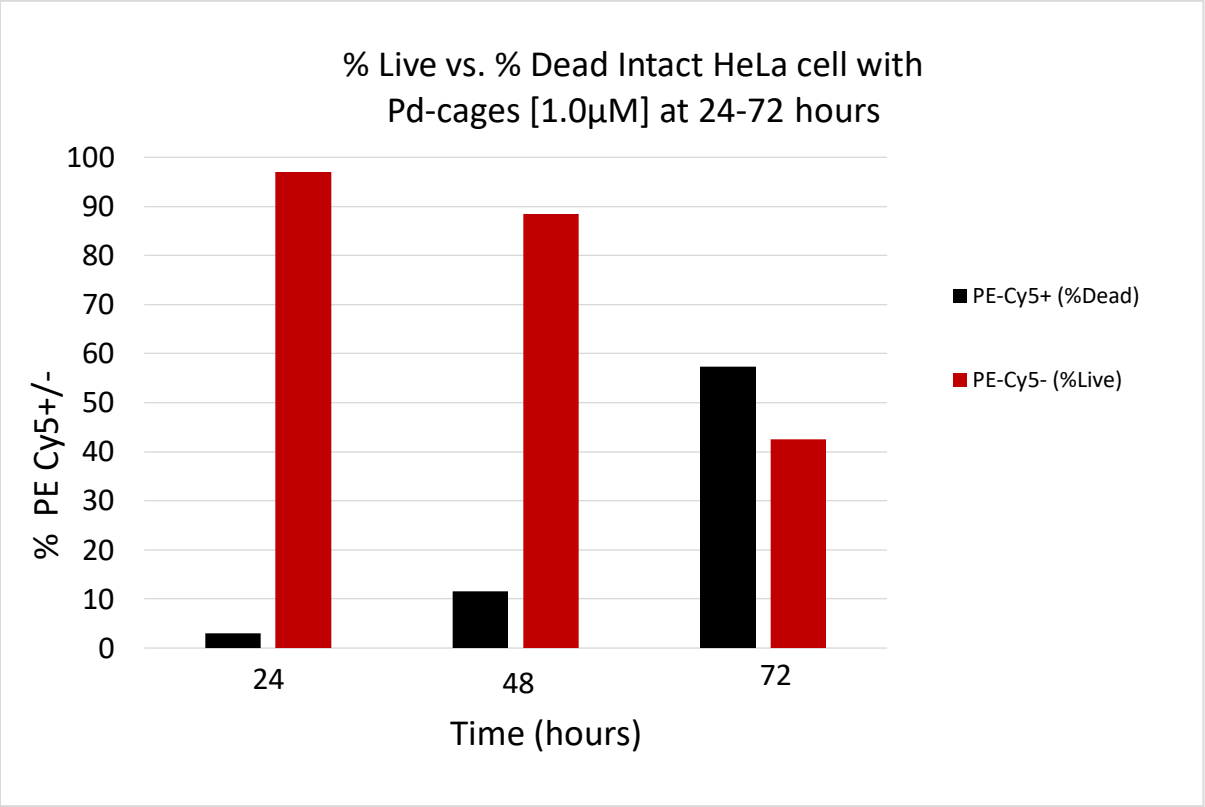

Figure 3.6A % Live vs. % Dead intact HeLa cells with incorporated Pd-cages at 1.0µM from 24-72 hours. X-axis = Time (hours),Y-axis = % PE Cy5 +/- detection. Red = live intact HeLa with incorporated Pd-cages. Black = dead HeLa cells. At 24h, 97.0% of the cell were live and 3.05% of the cells were dead. At 48h, 88.4% of the cells were live and 11.6% of the cells were dead. At 72h, live cells at 42.6% and dead cells at 57.4%.

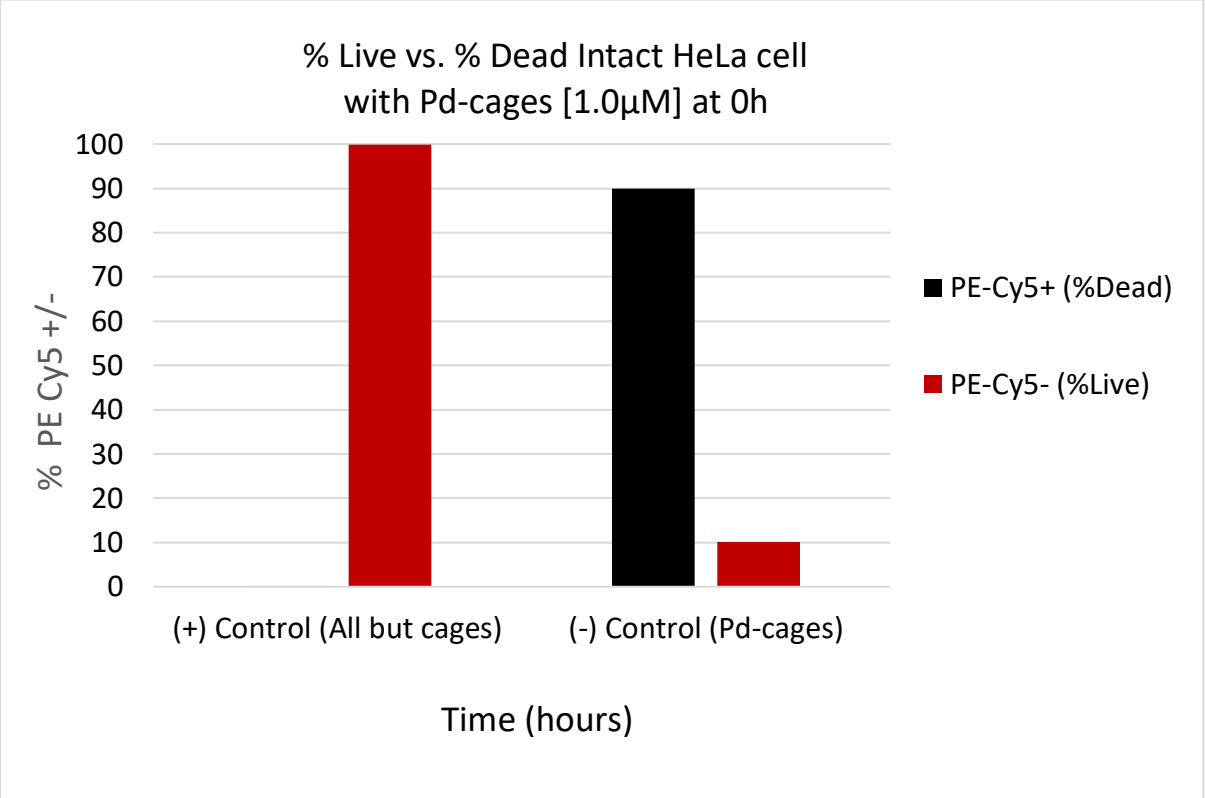

Figure 3.6B % Live vs. % Dead controls at 0h. X-axis = Time (hours),Y-axis = % PE Cy5 +/- detection. Red = live intact HeLa with incorporated Pd-cages. Black = dead HeLa cells. At 0h, (+) control all but cages; 89.9% of the sample fluoresced as live and 10.1% as dead. (-) control Pd-cages only; 99.8% of the sample fluoresced as live and 0.16% as dead.

REFERENCES

(1) Puckett, C. A.; Barton, J. K. Methods to Explore Cellular Uptake of Ruthenium Complexes. *Journal of the American Chemical Society* **2007**, 129 (1), 46–47. https://doi.org/10.1021/ja0677564.

(2) Longley, D.; Johnston, P. Molecular Mechanisms of Drug Resistance. *The Journal of Pathology* **2005**, 205 (2), 275–292. https://doi.org/10.1002/path.1706.

(3) Pitto-Barry, A.; Barry, N. P. E.; Zava, O.; Deschenaux, R.; Dyson, P. J.; Therrien, B. Double Targeting of Tumours with Pyrenyl-Modified Dendrimers Encapsulated in an Arene-Ruthenium Metallaprism. *Chemistry - A European Journal* **2011**, 17 (6), 1966–1971. https://doi.org/10.1002/chem.201002634.

(4) Vajpayee, V.; Yang, Y. J.; Kang, S. C.; Kim, H.; Kim, I. S.; Wang, M.; Stang, P. J.; Chi, K. W. Hexanuclear Self-Assembled Arene-Ruthenium Nano-Prismatic Cages: Potential Anticancer Agents. *Chemical Communications* **2011**, 47 (18), 5184. https://doi.org/10.1039/c1cc10167f.

(5) Fahmy; Brüßler; Alawak; El-Sayed; Bakowsky; Shoeib. Chemotherapy Based on Supramolecular Chemistry: A Promising Strategy in Cancer Therapy. *Pharmaceutics* **2019**, 11 (6), 292. https://doi.org/10.3390/pharmaceutics11060292.

(6) Ishida, S.; Lee, J.; Thiele, D. J.; Herskowitz, I. Uptake of the Anticancer Drug Cisplatin Mediated by the Copper Transporter Ctr1 in Yeast and Mammals. *Proceedings of the National Academy of Sciences* **2002**, 99 (22), 14298–14302. https://doi.org/10.1073/pnas.162491399.

(7) Florea, A. M.; Büsselberg, D. Cisplatin as an Anti-Tumor Drug: Cellular Mechanisms of Activity, Drug Resistance and Induced Side Effects. *Cancers* **2011**, 3 (1), 1351–1371. https://doi.org/10.3390/cancers3011351.

(8) Xu, X.; Ho, W.; Zhang, X.; Bertrand, N.; Farokhzad, O. Cancer Nanomedicine: From Targeted Delivery to Combination Therapy. *Trends in Molecular Medicine* **2015**, 21 (4), 223–232. https://doi.org/10.1016/j.molmed.2015.01.001.

(9) Zava, O.; Mattsson, J.; Therrien, B.; Dyson, P. J. Evidence for Drug Release from a Metalla-Cage Delivery Vector Following Cellular Internalisation. *Chemistry - A European Journal* **2010**, 16 (5), 1428–1431. https://doi.org/10.1002/chem.200903216.

(10) Zhang, C. X.; Lippard, S. J. New Metal Complexes as Potential Therapeutics. *Current Opinion in Chemical Biology* **2003**, 7 (4), 481–489. https://doi.org/10.1016/S1367-5931(03)00081-4.

(11) Zheng, Y. R.; Suntharalingam, K.; Johnstone, T. C.; Lippard, S. J. Encapsulation of Pt(IV) Prodrugs within a Pt(II) Cage for Drug Delivery. *Chemical Science* **2015**, 6 (2), 1189–1193. https://doi.org/10.1039/C4SC01892C.

(12) Makovec, T. Cisplatin and beyond: Molecular Mechanisms of Action and Drug Resistance Development in Cancer Chemotherapy. *Radiology and Oncology* **2019**, 53 (2), 148–158. https://doi.org/10.2478/raon-2019-0018.

(13) Shen, D. W.; Pouliot, L. M.; Hall, M. D.; Gottesman, M. M. Cisplatin Resistance: A Cellular Self-Defense Mechanism Resulting from Multiple Epigenetic and Genetic Changes. *Pharmacological Reviews* **2012**, 64 (3), 706–721. https://doi.org/10.1124/pr.111.005637.

(14) Ramachandran, S.; Quist, A. P.; Kumar, S.; Lal, R. Cisplatin Nanoliposomes for Cancer Therapy: AFM and Fluorescence Imaging of Cisplatin Encapsulation, Stability, Cellular Uptake, and Toxicity. *Langmuir* **2006**, 22 (19), 8156–8162. https://doi.org/10.1021/la0607499.

(15) Martinho, N.; Santos, T. C. B.; Florindo, H. F.; Silva, L. C. Cisplatin-Membrane Interactions and Their Influence on Platinum Complexes Activity and Toxicity. *Frontiers in Physiology*, **2019**, 9. https://doi.org/10.3389/fphys.2018.01898.

(16) Kalayda, G. V.; Wagner, C. H.; Buß, I.; Reedijk, J.; Jaehde, U. Altered Localisation of the Copper Efflux Transporters ATP7A and ATP7B Associated with Cisplatin Resistance in Human Ovarian Carcinoma Cells. *BMC Cancer* **2008**, 8 (1). https://doi.org/10.1186/1471-2407-8-175.

(17) Howell, S. B.; Safaei, R.; Larson, C. A.; Sailor, M. J. Copper Transporters and the Cellular Pharmacology of the Platinum-Containing Cancer Drugs. *Molecular Pharmacology* **2010**, 77 (6), 887–894. https://doi.org/10.1124/mol.109.063172.

(18) Kilari, D. Role of Copper Transporters in Platinum Resistance. *World Journal of Clinical Oncology* **2016**, 7 (1), 106. https://doi.org/10.5306/wjco.v7.i1.106.

(19) Zisowsky, J.; Koegel, S.; Leyers, S.; Devarakonda, K.; Kassack, M. U.; Osmak, M.; Jaehde, U. Relevance of Drug Uptake and Efflux for Cisplatin Sensitivity of Tumor Cells. *Biochemical Pharmacology* **2007**, 73 (2), 298–307. https://doi.org/10.1016/j.bcp.2006.10.003.

(20) Barry, N. P. E.; Zava, O.; Dyson, P. J.; Therrien, B. Excellent Correlation between Drug Release and Portal Size in Metalla-Cage Drug-Delivery Systems. *Chemistry - A European Journal* **2011**, 17 (35), 9669–9677. https://doi.org/10.1002/chem.201003530.

(21) Blair, B. G.; Larson, C. A.; Adams, P. L.; Abada, P. B.; Pesce, C. E.; Safaei, R.; Howell, S. B. Copper Transporter 2 Regulates Endocytosis and Controls Tumor Growth and Sensitivity to Cisplatin In Vivo. *Molecular Pharmacology* **2011**, 79 (1), 157–166. https://doi.org/10.1124/mol.110.068411.

(22) Holzer, A. K.; Manorek, G. H.; Howell, S. B. Contribution of the Major Copper Influx Transporter CTR1 to the Cellular Accumulation of Cisplatin, Carboplatin, and Oxaliplatin. *Molecular Pharmacology* **2006**, 70 (4), 1390–1394. https://doi.org/10.1124/mol.106.022624.

(23) Doucette, K. A.; Hassell, K. N.; Crans, D. C. Selective Speciation Improves Efficacy and Lowers Toxicity of Platinum Anticancer and Vanadium Antidiabetic Drugs. *Journal of Inorganic Biochemistry* **2016**, 165, 56–70. https://doi.org/10.1016/j.jinorgbio.2016.09.013.

(24) Wang, Z.; Zhu, G. DNA Damage Repair Pathways and Repair of Cisplatin-Induced DNA Damage. In Reference Module in Chemistry, Molecular Sciences and Chemical Engineering; *Elsevier* **2018**. https://doi.org/10.1016/B978-0-12-409547-2.14251-9.

(25) Ndagi, U.; Mhlongo, N.; Soliman, M. Metal Complexes in Cancer Therapy; an Update from Drug Design Perspective. *Drug Design, Development and Therapy* **2017**, Volume11, 599–616. https://doi.org/10.2147/DDDT.S119488.

(26) Rebolledo, A. P.; Vieites, M.; Gambino, D.; Piro, O. E.; Castellano, E. E.; Zani, C. L.; Souza-Fagundes, E. M.; Teixeira, L. R.; Batista, A. A.; Beraldo, H. Palladium(II) Complexes of 2-Benzoylpyridine-Derived Thiosemicarbazones: Spectral Characterization, Structural Studies and Cytotoxic Activity. *Journal of Inorganic Biochemistry* **2005**, 99 (3), 698–706. https://doi.org/10.1016/j.jinorgbio.2004.11.022.

(27) Kaiser, F.; Schmidt, A.; Heydenreuter, W.; Altmann, P. J.; Casini, A.; Sieber, S. A.; Kühn, F. E. Self-Assembled Palladium and Platinum Coordination Cages: Photophysical Studies and Anticancer Activity: Self-Assembled Palladium and Platinum Coordination Cages: Photophysical Studies and Anticancer Activity. *European Journal of Inorganic Chemistry* **2016** (33), 5189–5196. https://doi.org/10.1002/ejic.201600811.

(28) Schmidt, A.; Hollering, M.; Drees, M.; Casini, A.; Kühn, F. E. Supramolecular Exo-Functionalized Palladium Cages: Fluorescent Properties and Biological Activity. *Dalton Transactions* **2016**, 45 (20), 8556–8565. https://doi.org/10.1039/C6DT00654J.

(29) Ahmedova, A.; Momekova, D.; Yamashina, M.; Shestakova, P.; Momekov, G.; Akita, M.; Yoshizawa, M. Anticancer Potencies of Pt II and Pd II Linked M 2 L 4 Coordination Capsules with Improved Selectivity. *Chemistry - An Asian Journal* **2016**, 11 (4), 474–477. https://doi.org/10.1002/asia.201501238.

(30) Schmidt, A.; Hollering, M.; Han, J.; Casini, A.; Kühn, F. E. Self-Assembly of Highly Luminescent Heteronuclear Coordination Cages. *Dalton Transactions* **2016**, 45 (31), 12297–12300. https://doi.org/10.1039/C6DT02708C.

(31) Chen, L.; Chen, Q.; Wu, M.; Jiang, F.; Hong, M. Controllable Coordination-Driven Self-Assembly: From Discrete Metallocages to Infinite Cage-Based Frameworks. *Accounts of Chemical Research* **2015**, 48 (2), 201–210. https://doi.org/10.1021/ar5003076.

(32) Schmidt, A.; Casini, A.; Kühn, F. E. Self-Assembled M2L4 Coordination Cages: Synthesis and Potential Applications. *Coordination Chemistry Reviews* **2014**, 275, 19–36. https://doi.org/10.1016/j.ccr.2014.03.037.

(33) Schmitt, F.; Freudenreich, J.; Barry, N. P. E.; Juillerat-Jeanneret, L.; Süss-Fink, G.; Therrien, B. Organometallic Cages as Vehicles for Intracellular Release of Photosensitizers. *Journal of the American Chemical Society* **2012**, 134 (2), 754–757. https://doi.org/10.1021/ja207784t.

CHAPTER 4 – LITERATURE REVIEW: HISTONE DEACETYLASES AND THEIR INHIBITORS IN CANCER EPIGENETICS[2]

4.1 Significance of Work

Understanding the functional roles of histone deacetylases (HDAC) and histone deacetylase inhibitors (HDACi) is essential to utilizing epigenetics in the war on cancer. Their roles in epigenetics has significantly altered the development of anticancer drugs used to treat the most rare, persistent forms of cancer. During transcription, HDAC and HDACi are used to regulate the genetic mutations found in cancerous cells by removing and/or preventing the removal of the acetyl group on specific histones. This activity determines the relaxed or condensed conformation of the nucleosome, changing the accessibility zones for transcription factors. These modifications lead to other biological processes for the cell, including cell cycle progression, proliferation, and differentiation. Each HDAC and HDACi class or group has a distinctive mechanism of action that can be utilized to halt the progression of cancerous cell growth. While the use of HDAC- and HDACi-derived compounds are relatively new in targeted treatments of some cancers, they have a proven efficacy when the appropriately utilized. This chapter highlights the mechanisms of action utilized by HDAC and HDACi in various cancer, their role in epigenetics, current drug manufacturers, and the impact that predicative modeling systems have on cancer therapeutic drug discovery.

[2] Hassell, K. N.; Histone Deacetylases and Their Inhibitors in Cancer Epigenetics. *Diseases* 2019, *7* (4), 57. https://doi.org/10.3390/diseases7040057.

4.2 Introduction

Epigenetics is the modification of a cell's DNA without changing its original sequence. This reprogramming can cause genes to be turned on/off depending of the intended expression for the cell. Epigenetic mechanisms allow genetically identical cells to adopt different phenotypes, regulating transcriptional availability of the genome through differential chromatin marking and packaging, in which networks of mutually reinforced or counteracting signals are created.[1] Chromatin markers can be preserved and/or changed according to environmental, developmental, or pathological needs. The genetic and epigenetic mechanisms influence each other by cooperatively enabling the initial stages of cancer cell growth.[2] The deregulation of epigenetic control in cells has been noted as a common characteristic of cancerous tumor cells. Therefore, the role of epigenetic drugs has become increasingly important in reverting the malignant phenotype. HDAC and HDACi have become more influential in epigenetics as they provide specific epi-based treatments to target specific types of cancers.[1,3,4] Acetylation neutralizes the positively charged histone lysine residue, causing a relaxed chromatin conformation which increases the accessibility of transcriptional modifiers to the gene. In the removal of an acetyl group from a histone, chromatin condensation is induced, leading to gene transcription repression.[5,6]

Recently, histone deacetylases (HDAC) and histone deacetylase inhibitors (HDACi) have been effectively used to modulate acetylation in efforts to regulate the accessibility of transcription factors to DNA coding regions. HDAC and HDACi play a major role in several biological processes, such as cell cycle progression, proliferation, and differentiation. HDAC and their inhibitors can be used to post-translationally modify

histones—the histone code that is read and recognized by other proteins to regulate gene expression. Unlike other histone code modifications, DNA methylation and phosphorylation effect protein interactions and expression level of HDAC and HDACi, which can be used to activate and/or repress overall gene expression.[7,8] Lysine acetylation is an example of a reversible transcriptional modification that is controlled by the antagonistic interactions found between histone acetylases (HATs) and HDAC.

4.3 HDAC Classifications

HDAC are known for their unique ability to catalyze the removal of acetyl groups from the amino-terminal lysine residues of histones and nonhistone proteins. The most commonly acetylated nonhistone protein is p53, a tumor suppressor. Mutations to p53 have been found in more than 50% of all types of cancers.[9] There are four main human classes for HDAC that have been grouped based on their homology to yeast proteins, enzymatic activity, and cellular localization.

4.3.1 *Class I*

Class I is found in the nucleus and includes HDAC1, 2, 3, and 8. HDAC1 and 2 are similar in their catalytic domain on the N-terminus and their interactions with other proteins in the form of a complex of which regulates their deacetylation activity. Co-Rest (Co-repressor for element-1-silencing transcription factor) is one of the known protein complexes that contain HDAC1 and 2. Co-Rest works with REST (RE-1-silencing transcription factor) to regulate neuronal cell growth.[10] The other two remaining members of class I, HDAC3 and 8, are also similar in their characterizations and can be found interacting with HDAC4, 5, and 7 within the SMRT (silence mediator for retinoid and

thyroid receptors) and N-Cor (nuclear receptor co-repressor) complex formations.[10] Class I HDACs are deregulated in cancers. Their overexpression has been found in tissues from breast, gastric pathway, pancreas, lungs, and prostate. HDAC1, 2, and 3 are commonly found in renal cancer and Hodgkin's lymphoma. The catalytic activity of HDAC1 and 2 has been used to regulate the functions of p53.[11,12] Evidence of a frame shift gene mutation distinctively characterizes HDAC2 in class I. HDAC3 has documented interaction activity with cancer-associated genes (CAGE) in testicular cancers.[13,14] HDAC8 deacetylates lysine residues of histone and nonhistone proteins, and can be found in cervical cancers, neuroblastomas, and pancreatic ductal adenocarcinomas.[15]

4.3.2 *Class II*

Class II HDACs are localized in the cell cytoplasm and nucleus, providing a distinctive characteristic that allows for shuttling between the two cellular compartments. There are two subclasses for Class II: HDAC4, 5, 7, and 9 are grouped as IIa, and class IIb includes HDAC6 and 10. Class IIa members: HDAC4, 5, and 7 share similarities, as well as the Class IIb members. HDAC9 contains splice variants and has a catalytic domain on its C-terminus. Evolutionary data supports the relationship of HDAC6 and HDAC10. HDAC6 contains two catalytic domains that work together in a tandem formation. However, the catalytic domain has been identified to resemble HDAC9. Data supports the anticancer properties of HDAC6; the deacetylation of microtubules in tumor cells suppresses angiogenesis, leading to the repression of metastasis. However, the expression of HDAC6 in tumor cells has been observed in patients with higher breast cancer survival rates.[16-17] The three nuclear export signals are significant players in the functional

characteristics of HDAC6 as a catalyzed nuclear–cytoplasmic pathway with targets unrelated to transcription.[18]

HDAC6 is highly expressed in breast cancer, is used as a late-stage cancer indicator, and is present in both the positive progesterone and α-estrogen receptors. Genes associated with the isoform HDAC6 are estrogen induced and are upregulated as late mRNA expressions in the cDNA microarray using MCF-7 cells. The mRNA expression levels analyzed via RT-PCR are higher in patients with small breast cancer tumors (<2 cm diameter). Survival rates in breast cancer patients can be linked to the increased HDAC6 protein and mRNA expression.[17,19] HDAC10 is the most recently characterized, with catalytic domain activity found primarily on its N-terminus and with the C-terminus consisting of a secondary catalytic domain known as the leucine-rich domain (LRD) region. The LRD region allows HDAC10 to act as a recruiter of acetyl groups in its interactions with other HDAC complexes, such as HDAC1, 2, 3, 4, 5, and 6. HDAC4 interacts with HDAC3 via N-CoR, has been found overexpressed in breast cancers, and is used as a cancer progression marker in esophageal carcinomas.[20] HDAC4 has catalytic activity that structurally regulates access to the Zn^{2+} binding domain.[21] HDAC5 and 9 are used as markers in medulloblastomas and rare form of breast cancer and can be used to determine the cancer patient's survival.[22] HDAC5 with lysine-specific demethylase 1 proteins (LSD1) are overexpressed in estrogen receptor-negative breast cancer.[23]

The regulation of HDAC5 has proven to be an effective form of therapeutic treatment. HDAC7 has been found overexpressed in pancreatic cancer and acute lymphoblastic leukemia and has been reported as insensitive to its previously designated HDACi,

trichostatin A(TSA).[1,21,24] HDAC10 is found in cervical cancer as a metastasis suppressor.[25]

4.3.3 *Class III*

Class III is more frequently referred to as the Sirtuins (silence mating-type information regulation-2), which are required to maintain chromatin. Seven Sirtuins have been classified and found in the cytoplasm, nucleus, and mitochondria. SIRT2 is the only one found in the cytoplasm. SIRT1, 6, and 7 are found in the nucleus and SIRT3, 4, and 5 are found in the mitochondria. Sirtuins have enzymatic NAD+ (nicotinamide adenine dinucleotide)-dependent functions that regulate transcription, metabolism, and cellular stress responses. Class III (Sirtuins) has been linked to cancer pathways due to functional involvement in controlling the cell's survival under stress conditions. SIRT1 regulates cancer cell growth and has been identified as a tumor suppressor in retinoblastoma and can be modulated in cancer by deacetylate histones.[26] SIRT1 promotes cell cycle arrest, DNA repair, and cell survival under low stress conditions. In higher stress conditions (lacking tumor suppressors and mitotic checkpoints), SIRT1 can promote tumor formation and cancerous cell growth.[27-28] SIRT2 acts as a tumor suppressor and its absence disrupts normal mitotic checkpoints at G_1, G_2, and metaphase, which causes increased tumorigenesis.[29-30] When downregulated, SIRT2 blocks cell metabolism to inhibit the metastatic spread of hepatocellular carcinoma cells.[31-32] SIRT3 has been found in transcription factor regulation of various types of breast cancers.[33] SIRT4 acts as a tumor suppressor in gastric cancers. It interacts with glutamate dehydrogenase and poly ADP-ribose polymerase I (PARP) inhibition.[34-35] SIRT5 promotes cell proliferation in

hepatocellular carcinoma.[36-37] However, SIRT6 plays a role in tumor suppression as it restricts the cancerous cell metabolism to protect the original genomics of the surrounding healthy cells, as observed in retinoblastoma.[38] SIRT7 has been found in the nucleolus, interacting with H3 histone, as well as in the activation of RNA polymerase I in its mechanistic action of tumoral growth inhibition in prostate and non-small cell lung cancer and osteosarcoma.[39-40]

4.3.4 *Class IV*

HDAC11 has been classified by itself in Class IV and it often considered a hybrid of the HDAC's in Class I and II. The catalytic domain of HDAC11 is in the N-terminus and resembles HDAC3 and 8, which validates its unique hybrid classification. The expression of HDAC11 has been found in the kidneys, brain, heart, testis, and skeletal muscles of the human body. Its major function has been in the association of oligodendrocyte development and immune system responses.[5] HDAC11 is overexpressed in Hodgkin's lymphoma and interacts with HDAC1 and 2. Small interfering RNAs (siRNAs) can selectively inhibit HDAC11 expression and induce apoptosis in human leukemia cell lines and increase necrosis.[41-42] HDAC11′s lysine defatty-acylase properties are more efficient than its deacetylase activity. Probing discoveries may lead to other class IIa HDACs with similar or shared defatty-acylase ability. HDAC11 defatty-acylates substrates with an efficiency that is more than 10,000-fold greater than its deacetylase activity. This functionality of HDAC11 resembles that of the sirtuin family; catalyzing acyl group removal. Defatty-acylase activity presents as a new classification and appears evolutionarily divergent amongst the previous grouped zinc-dependent HDACs.[41,43]

4.3.5 *Similarities in Classes I, II & IV*

HDAC Classes I, II, and IV, known as the classical HDACs, are Zn^{2+} dependent enzymes. The activities of HDACs correspond to chromatin formation, histone acetylation modulation, and the altering of transcription factors involved in the promoter regions of genes. Cancer is classified as a genetic disease that results from mutations found within the genetic code of a normal cell. Chromosomal dysfunctions occur in normal cells with regards to its ability to suppress the tumor developing genes, which causes the hyper-activation of oncogenes. The use of HDACs in targeting tumor cells is becoming the leading research method used to regulate and/or suppress the metastasis of some types of cancers. See HDAC summary table 1.1 below for Classes I-IV.

4.4 HDAC Inhibition

Just as HDAC are classified into subfamilies of multiprotein complexes, HDAC inhibitors (HDACi) have been grouped based on their ability to interfere with the function of HDAC. HDACi are cytostatic agents that modulate gene expression via indirect induction of histone acetylation. In research studies, HDACi have demonstrated interference activity within cancerous tumor cells, altering proliferation in vivo and in vitro. They act as inhibitors by inducing cell cycle arrest, differentiation, and apoptosis.[44-45] Inhibitors of HDAC may enable the re-expression of repressed regulatory genes in cancer cells and reverse their malignant phenotype. For example, sodium butyrate and trichostatin A (TSA) are known inhibitors of HDAC activity, demonstrated by the induction G_0–G_1 cell cycle arrest and apoptosis in the SW620 colonic carcinoma cell line.[46] HDACi inhibits the activity of HDAC enzymes, promoting the acetylation of histones and

nonhistone proteins. This inhibition can increase gene expression and alter DNA processing, including replication and repair. HDACi used as epigenetic regulators in cancer therapeutics have been generated from natural and synthetic resources.[47-48] Specifically, in breast cancer cells with overexpressed hormone estrogen receptor-2 (HER2), HDACi can be epigenetically dysregulated by the phosphorylation of the transcriptional protein Sp1 motif.[19,49] They are currently classified into five different groups: hydroxamates, aliphatic acids, benzamides, tetrapeptides/depsipeptides, and sirtuin inhibitors.

4.4.1 *Group 1*

Group 1, the hydroxamates, consists of trichostatin A (TSA), suberoylanilide hydroxamic acid (Vorinostat), Panabinostat, Belinostat, and abexinostat hydrochloride. Of the five members in this group Vorinostat, Panobinostat, and Belinostat are most highly developed and heavily tested. Group 1, in addition to Groups 3 and 4, has been classified as inhibitors of Class I and II HDACs due to their ability to bind the Zn^{2+} ion required for HDAC enzymatic activity.

In 2006, Vorinostat was approved by the FDA for treatment of cutaneous T-cell lymphoma. Vorinostat is a second-generation polar compound that binds to the catalytic domain on HDAC. The hydroxylamine chelates the Zn^{2+} within the catalytic pockets of HDAC to inhibit its deacetylation. Vorinostat has been clinically trialed for the treatment of other forms of cancer, such as non-Hodgkin's lymphoma, breast, and colon cancer, but did not show the same type of success as documented with cutaneous T-cell lymphomas. Vorinostat (SAHA) has been used in several clinical trials; phase III for glioblastomas,

phase II for uterine sarcomas and other solid malignant tumors.[50-51] In the phase II clinical trial for uterine sarcoma, the study investigated the efficacy of Vorinostat as a monotherapy in patients with HDAC-positive, advanced metastatic, and mixed epithelial mesenchymal tumors after receiving antiproliferative therapy.[52-53] Vorinostat has been renamed Zolinza® and is currently manufactured by Merck in capsule form for oral administration.[50]

Panobinostat is a nonselective HDACi that has completed Phase I and II clinical trials and can be used separately or in combination with other therapeutic treatments of non-Hodgkin's lymphoma, leukemia myeloblasts, acute myeloid leukemia, multiple myelomas, and other advanced solid tumors found in the lung and breast tissues.[54,55] When used in combination with other compounds, Panobinostat has the mechanistic ability to interfere with DNA methylation and tyrosine kinase inhibition.[56] Panobinostat keeps genes that suppress cell division and growth of cancerous cells active. In 2015, Panobinostat was approved by the FDA in combination with Bortezomib in treating patients with multiple myeloma. It has been renamed Farydak® and is currently manufactured by Novartis for intravenous administration.[57]

In March 2012, Belinostat was been used in various clinical trials for solid tumors and hematological cancers. Belinostat induces the accumulation of acetylated histones and proteins, thus altering the gene expression and inducing cell-cycle arrest or apoptosis of cancerous cells. When used separately, Belinostat has an antitumoral effect in the treatment of peripheral T-cell lymphoma, cutaneous T-cell lymphoma, liver cancer, and thymoma.[47] As of 2014, Belinostat was approved by the FDA for the treatment of patients with relapsed or refractory peripheral T-cell lymphoma (PTCL). It has been renamed

Beleodaq® and is currently manufactured by Topotarget Inc. for intravenous administration.[58]

4.4.2 *Group 2*

Group 2 HDACi contains an aliphatic acids group. Valproic acid (VPA) has been the most widely used and understood within group 2 HDACi. Traditionally, VPA had been used in the clinical treatment of epilepsy, bipolar disorder, schizophrenia, and in extreme cases of migraine headaches and depression. As a HDACi, it has been used in Phase I and II clinical trials to treat various types of cancers. VPA has demonstrated efficacy when used in combination with other anticancer compounds that are known for therapeutic treatment of lymphocytic leukemia, acute myeloid leukemia, melanoma, HIV infections, and autoimmune lymphoproliferative syndrome. The short-chained fatty acid structure of VPA enhances the mechanism of action in treating glioblastoma and breast cancer patients.[51,59-60]

4.4.3 *Group 3*

In Group 3, Entinostat is a synthetic derivative that inhibits Class I and II HDACs. Entinostat is a selective autophagy inducer, an orally administered drug that is in development by Syndax Pharmaceuticals with exemestane for advanced hormone receptor breast cancer.[61] Clinical research supports the activity of Entinostat as an antitumor promoter and inhibitor of HDAC activity. While it has not been approved by the FDA for monotherapeutic use, it has been approved in combination with anticancer tumor compounds.[47,61-62]

4.4.4 Group 4

Group 4, characterized by tetrapeptide structure (also called depsipeptides), consists of Apicidin and Romidepsin. This group is also known as the bicyclic peptides that inhibit Class I and II HDACs. Apicidin and Romidepsin are clinically proven to have potent cytotoxicity against malignant cancer cells in vivo and in vitro. In patients with colorectal, renal, and breast cancers, depsipeptides have been administered with short-term toxicity. For example, Romidepsin (Istodax®) is a naturally harvested product from bacteria and is currently being used in cancer treatments due to its toxicity observed in the treatment of peripheral T-cell lymphoma.[63-64] The mechanism of action utilized by Romidepsin triggers the accumulation of acetylated histones to induce apoptosis in cancer cells.[65-66] Since 2009, Romidepsin has been successfully included in over 50 interventional drug trials. As of 2011, the FDA approval for Istodax® incorporated usage in the therapeutic treatment of patients with peripheral T-cell lymphoma. Currently, Istodax® is manufactured by Celgene Corporation as injectables.[63]

4.4.5 Group 5

The sirtuin inhibitors of Group 5 include physiological inhibitors—nicotinamide, cambinol, and sirtinol derivatives—that work specifically on SIRT1 and 2. Of the seven human sirtuins, SIRT1 and 2 are upregulated in cancerous tumors and are therefore the most studied. Since SIRT1 and 2 have the ability to inactivate proteins like p53 in transcription and post-translation, developing inhibitors could provide a wealth of anticancer agents used for various treatments. For example, benzimidazole modulates antiproliferation cell activity and has proven efficacy in two different types of breast cancer

cell lines; luminal and basal A subtype.[67] The specific mechanism used by benzimidazole to inhibit SIRT1 and 2 has not been clearly defined, but these novel derivatives provide a new trajectory for developing new therapeutic drug agents to fight various types of cancers. Another inhibitor of SIRT1 and 2 activities is cambinol and its derivatives. In vitro and in vivo research studies demonstrate cambinol's antilymphoma abilities. Cambinol inhibits SIRT1 and 2 by inducing the hyperacetylation of p53.[68] Unfortunately, there are two negative outcomes in using cambinol for therapeutic treatments: its moderate level of potency and poor stability. Despite the minor drawbacks, cambinol is still a promising anticancer drug agent and has a good foundation for large scale optimization.[27,29,31,89] (See HDACi summary Table 4.2)

4.5 Advances in Studying HDAC/HDACi in Cancer

The research and development of cancer therapeutics that was once limited to time consuming wet-lab procedures has evolved to incorporate complex high throughput bioinformatics analysis. Several research groups globally have made significant contributions to our understanding of the mechanistic influence of HDAC/HDACi in various types of cancers. Researchers that have employed the use of in silico techniques utilize vast genomic databases in concert with or in lieu of wet-lab bench analysis and have revolutionized our acquisition of knowledge and understanding. In studying HDAC/HDACi compounds, utilizing the configuration of their Zn^{2+} binding domains (ZBD) further enriches our capacity to understand all possible functional interactions for designing specific drug targets. Zinc-binding domains are the key to unlock the targeted active sites within HDAC structures that can be utilized by the HDACi groups to execute

inhibition. Zinc ions and hydroxamic acid have a high affinity; both are essential to ZBD structural design in HDACs. The combination of the ligand–receptor interaction and the cap end group with the presenting residues located at the HDAC active sites are the agents of specificity for HDACi.[69] The intricacies of the cap end to linker residues in ZBD were characterized most efficiently via in silico approaches. Hsu et al. designed an amino acid sequence to use in their homology modeling of HDAC5 and 9. With access to GenBank and the SWISS-MODEL server, targeted template alignment analysis generated 3D predictive models for HDAC interactions. In simulations, protein interactions were visualized in BIOVIA DS and PyMOL software.[70-71] In one screening process, the Hsu group identified six novel nonhydroxamate inhibitors for specifically targeting class IIa HDACs. The use of bioinformatics allowed this one group to make a huge leap in their understanding of how to target the mechanism of action via localized active sites and conformational models.

4.6 Conclusion

Research studies of HDAC and HDACi have led to major advances in the therapeutic treatment of various forms of cancer. There are pitfalls associated with using traditional research methods, specifically time and processing requirements, and when using computer simulations, human error can still exist. However, the impact of vast database analysis by supercomputers and artificial intelligence is mandatory in drug discovery. In silico approaches have proven to be resourceful in gaining knowledge of cancer epigenetics. The software and hardware abilities of supercomputers can physically outperform any lab scientist. The next generation of researchers will need to have the

training and knowledge necessary to program supercomputers of tomorrow to keep up with the large datasets processed daily for therapeutics. Conceptualizing the many different mechanistic actions between HDAC and HDACi has altered the development of targeted cancer therapeutics. The sirtuins and their inhibitors appear to be the most promising in terms of pharmaceutical marketability due to their duel functionality in the regulation of the cell cycle, apoptosis, and deacetylation of p53, respectively. However, when taking into account the mechanisms that are used in manipulating a cell's genetic code, there could be several other keys to be found that can unlock the epigenetic codes of cancer. In silico approaches are a great way to explore a path of thought without enduring laborious wet bench procedures—a lifetime saving approach.

Moving forward, using bioinformatics software will greatly improve time and efficiency in studying proteins that potentially regulate HDAC and HDACi activity in cancers. Future studies should employ large information systems and mega-database resources for analysis.

4.7 Tables

Table 4.1 HDAC Summary. Table summarizes the characteristics of HDAC and their activity in some cancers.

Class:	Localization:	HDAC	Characteristics:	Activity in Cancer:	Refs.
I*	nucleus	1	N-terminus catalytic domain	Overexpressed in tissues from breast, gastric, pancreas, lungs, cervical and prostate cancers	10-12
		2			10-12
		3	Interaction with HDAC4, 5, 7 & cancer-associated genes (CAGE)		13-14
		8	Interaction with HDAC4, 5, 7		15
IIa*	cytoplasm & nucleus	4	C-terminus catalytic domain combines with HDAC3 via N-CoR, catalytic activity structurally regulates access to the Zn2+ binding domain	Suppresses p21; overexpressed in breast, colon, ovarian and gastric cancers	22
		5	Interacts with lysine-specific demethylase 1	Markers in medulloblastomas & breast cancer	24
		7	C-terminus activity; non-deacetylase dependent	Overexpression in pancreatic cancer & acute lymphoblastic leukemia	11, 22 & 25
		9	Splice variants with catalytic domain on its C-terminus	Markers in medulloblastomas	25
IIb*	cytoplasm & nucleus	6	2 tandem catalytic domains	Highly expressed in breast cancer; stage indicator	16, 20
	cytoplasm	10	Catalytic domain activity at N-terminus & C-terminus leucine rich domain (LRD)	Cervical cancer as a metastasis suppressor	21
III**	nucleus	SIRT1	Lys382 residue deacetylate of H1, H3, and H4; C-terminus p53 acetylation regulator	Tumor suppressor in retinoblastoma	27-31
		SIRT6	Glycolysis regulator in cancer cells	Tumor suppressor in retinoblastoma	
		SIRT7	Deacetylates lysine 18 residue of H3; succinyls activity	Ovarian, colorectal, osteosarcoma, prostate, hepatocellular, breast & non-small cell lung	45-51
	cytoplasm	SIRT2	Deacetylating α-tubulin	Tumor suppressor; ovarian, breast, leukemia, neuroblastoma, pancreatic & hepatocellular	32-37
	mitochondria	SIRT3	Transcription factor regulation via deacetylation	Transcription factor regulation in breast cancer	38
		SIRT4	Glutamate dehydrogenase and poly ADP-ribose polymerase (PARP) inhibition	Tumor suppressor in gastric cancers	39-41
		SIRT5	Promotes cell proliferation	Hepatocellular carcinoma	44
IV*	nucleus	11	Interacts with HDAC1 & 2; defatty-acylate substrate activity	Overexpressed in Hodgkin's lymphoma	5, 52-54
* Zn2+ dependent					
** NAD+ dependent					

Table 4.2 HDACi Summary. Table summarizes HDACi characteristics and their activity in some cancers.

Class:	HDACi	Characteristics:	Activity in Cancer:	Drug Name:	Refs.
I	hydroxamic acid (Vorinostat)	Inhibits HDAC class I & II via Zn^{2+} ion interactions	Induces apoptosis in T-cell lymphomas, thymoma & liver	Zolinza	65-70
	Panobinostat			Farydak	71-74
	Belinostat			Beleodaq	60, 75
	valproic acis (VPA)			N/A	67,76 -79
II	Entinostat	Synergistic enhancement obsevered with other anticancer compounds due to short-chained fatty acid	Lymphocytic leukemia, acute myeloid leukemia, melanoma & glioblastoma	N/A	60, 80-82
III	Apicidin	Benzamide group; inhibits HDAC class I & II; selective autophagy inducer	Antitumor promoter in hormone receptor breast cancer	N/A	83
IV	Romidepsin	Bicyclic peptides; inhibit HDAC class I & II; triggers the accumulation of acetylated histones to induce apoptosis in cancer cells	Colorectal, renal, breast cancers & T-cell lymphoma	Istodax	83-86
V	Cambinol	Inhibits SIRT1 and 2 by induced hyperacetylation of p53	Inhibits SIRT1 and 2 by inducing the hyperacetylation of p53	N/A	29, 31, 27, 88- 89

REFERENCES

(1) Benedetti, R.; Conte, M.; Altucci, L. Targeting Histone Deacetylases in Diseases: Where Are We? *Antioxidants & Redox Signaling* **2015**, *23* (1), 99–126. https://doi.org/10.1089/ars.2013.5776.

(2) Dawson, M. A.; Kouzarides, T. Cancer Epigenetics: From Mechanism to Therapy. *Cell* **2012**, *150* (1), 12–27. https://doi.org/10.1016/j.cell.2012.06.013.

(3) Bai, Y.; Li, W.; Wang, T.; Ahmad, D.; Cui, G. Research Advances in the Use of Histone Deacetylase Inhibitors for Epigenetic Targeting of Cancer. *Current Topics in Medicinal Chemistry* **2019**, *19*. https://doi.org/10.2174/1568026619666190125145110.

(4) Lin, H. Y.; Chen, C.-S.; Lin, S. P.; Weng, J. R.; Chen, C. S. Targeting Histone Deacetylase in Cancer Therapy. *Medicinal Research Reviews* **2006**, *26* (4), 397–413. https://doi.org/10.1002/med.20056.

(5) Barneda-Zahonero, B.; Parra, M. Histone Deacetylases and Cancer. *Molecular Oncology* **2012**, *6* (6), 579–589. https://doi.org/10.1016/j.molonc.2012.07.003.

(6) Ell, B.; Kang, Y. Transcriptional Control of Cancer Metastasis. *Trends in Cell Biology* **2013**, *23* (12), 603–611. https://doi.org/10.1016/j.tcb.2013.06.001.

(7) Marks, P. A.; Xu, W.-S. Histone Deacetylase Inhibitors: Potential in Cancer Therapy. *Journal of Cellular Biochemistry* **2009**, *107* (4), 600–608. https://doi.org/10.1002/jcb.22185.

(8) McClure, J. J.; Li, X.; Chou, C. J. Advances and Challenges of HDAC Inhibitors in Cancer Therapeutics. In *Advances in Cancer Research*; Elsevier, 2018; Vol. 138, pp 183–211. https://doi.org/10.1016/bs.acr.2018.02.006.

(9) Ropero, S.; Esteller, M. The Role of Histone Deacetylases (HDACs) in Human Cancer. *Molecular Oncology* **2007**, *1* (1), 19–25. https://doi.org/10.1016/j.molonc.2007.01.001.

(10) Stengel, K. R.; Hiebert, S. W. Class I HDACs Affect DNA Replication, Repair, and Chromatin Structure: Implications for Cancer Therapy. *Antioxidants & Redox Signaling* **2015**, *23* (1), 51–65. https://doi.org/10.1089/ars.2014.5915.

(11) Heideman, M. R.; Wilting, R. H.; Yanover, E.; Velds, A.; de Jong, J.; Kerkhoven, R. M.; Jacobs, H.; Wessels, L. F.; Dannenberg, J.-H. Dosage-Dependent Tumor Suppression by Histone Deacetylases 1 and 2 through Regulation of c-Myc Collaborating Genes and P53 Function. *Blood* **2013**, *121* (11), 2038–2050. https://doi.org/10.1182/blood-2012-08-450916.

(12) Li, X.; Peterson, Y. K.; Inks, E. S.; Himes, R. A.; Li, J.; Zhang, Y.; Kong, X.; Chou, C. J. Class I HDAC Inhibitors Display Different Antitumor Mechanism in Leukemia and Prostatic Cancer Cells Depending on Their P53 Status. *Journal of Medicinal Chemistry* **2018**, *61* (6), 2589–2603. https://doi.org/10.1021/acs.jmedchem.8b00136.

(13) Kwon, Y.; Kim, Y.; Jung, H.; Jeoung, D. Role of HDAC3-MiRNA-CAGE Network in Anti-Cancer Drug-Resistance. *International Journal of Molecular Sciences* **2018**, *20* (1), 51. https://doi.org/10.3390/ijms20010051.

(14) Hanigan, T. W.; Aboukhatwa, S. M.; Taha, T. Y.; Frasor, J.; Petukhov, P. A. Divergent JNK Phosphorylation of HDAC3 in Triple-Negative Breast Cancer Cells Determines HDAC Inhibitor Binding and Selectivity. *Cell Chemical Biology* **2017**, *24* (11), 1356-1367.e8. https://doi.org/10.1016/j.chembiol.2017.08.015.

(15) Vanaja, G. R.; Ramulu, H. G.; Kalle, A. M. Overexpressed HDAC8 in Cervical Cancer Cells Shows Functional Redundancy of Tubulin Deacetylation with HDAC6. *Cell Communication and Signaling* **2018**, *16* (1). https://doi.org/10.1186/s12964-018-0231-4.

(16) Riester, D.; Hildmann, C.; Schwienhorst, A. Histone Deacetylase Inhibitors—Turning Epigenic Mechanisms of Gene Regulation into Tools of Therapeutic Intervention in Malignant and Other Diseases. *Applied Microbiology and Biotechnology* **2007**, *75* (3), 499–514. https://doi.org/10.1007/s00253-007-0912-1.

(17) Zhang, T.; Li, J.; Ma, X.; Yang, Y.; Sun, W.; Jin, W.; Wang, L.; He, Y.; Yang, F.; Yi, Z.; Hua, Y.; Liu, M.; Chen, Y.; Cai, Z. Inhibition of HDACs-EphA2 Signaling Axis with WW437 Demonstrates Promising Preclinical Antitumor Activity in Breast

Cancer. *EBioMedicine* **2018**, *31*, 276–286. https://doi.org/10.1016/j.ebiom.2018.05.003.

(18) Hai, Y.; Christianson, D. W. Histone Deacetylase 6 Structure and Molecular Basis of Catalysis and Inhibition. *Nature Chemical Biology* **2016**, *12* (9), 741–747. https://doi.org/10.1038/nchembio.2134.

(19) Li, G.; Xie, Q.; Yang, Z.; Wang, L.; Zhang, X.; Zuo, B.; Zhang, S.; Yang, A.; Jia, L. Sp1-mediated Epigenetic Dysregulation Dictates HDAC Inhibitor Susceptibility of HER2-overexpressing Breast Cancer. *International Journal of Cancer* **2019**. https://doi.org/10.1002/ijc.32425.

(20) Zeng, L. S.; Yang, X. Z.; Wen, Y. F.; Mai, S. J.; Wang, M. H.; Zhang, M. Y.; Zheng, X. F. S.; Wang, H. Y. Overexpressed HDAC4 Is Associated with Poor Survival and Promotes Tumor Progression in Esophageal Carcinoma. *Aging* **2016**, *8* (6), 1236–1248. https://doi.org/10.18632/aging.100980.

(21) Bottomley, M. J.; Lo Surdo, P.; Di Giovine, P.; Cirillo, A.; Scarpelli, R.; Ferrigno, F.; Jones, P.; Neddermann, P.; De Francesco, R.; Steinkühler, C.; Gallinari, P.; Carfí, A. Structural and Functional Analysis of the Human HDAC4 Catalytic Domain Reveals a Regulatory Structural Zinc-Binding Domain. *Journal of Biological Chemistry* **2008**, *283* (39), 26694–26704. https://doi.org/10.1074/jbc.M803514200.

(22) Beetch, M.; Lubecka, K.; Shen, K.; Flower, K.; Harandi-Zadeh, S.; Suderman, M.; Flanagan, J. M.; Stefanska, B. Stilbenoid-Mediated Epigenetic Activation of Semaphorin 3A in Breast Cancer Cells Involves Changes in Dynamic Interactions of DNA with DNMT3A and NF1C Transcription Factor. *Molecular Nutrition & Food Research* **2019**, 1801386. https://doi.org/10.1002/mnfr.201801386.

(23) Cao, C.; Vasilatos, S. N.; Bhargava, R.; Fine, J. L.; Oesterreich, S.; Davidson, N. E.; Huang, Y. Functional Interaction of Histone Deacetylase 5 (HDAC5) and Lysine-Specific Demethylase 1 (LSD1) Promotes Breast Cancer Progression. *Oncogene* **2017**, *36* (1), 133–145. https://doi.org/10.1038/onc.2016.186.

(24) Pham, L.; Kaiser, B.; Romsa, A.; Schwarz, T.; Gopalakrishnan, R.; Jensen, E. D.; Mansky, K. C. HDAC3 and HDAC7 Have Opposite Effects on Osteoclast Differentiation. *J. Biol. Chem.* **2011**, *286* (14), 12056–12065. https://doi.org/10.1074/jbc.M110.216853.

(25) Song, C.; Zhu, S.; Wu, C.; Kang, J. Histone Deacetylase (HDAC) 10 Suppresses Cervical Cancer Metastasis through Inhibition of Matrix Metalloproteinase (MMP) 2 and 9 Expression. *Journal of Biological Chemistry* **2013**, *288* (39), 28021–28033. https://doi.org/10.1074/jbc.M113.498758.

(26) Farghali, H.; Kemelo, M. K.; Canová, N. K. SIRT1 Modulators in Experimentally Induced Liver Injury. *Oxidative Medicine and Cellular Longevity* **2019**, *2019*, 1–15. https://doi.org/10.1155/2019/8765954.

(27) Bosch-Presegue, L.; Vaquero, A. The Dual Role of Sirtuins in Cancer. *Genes & Cancer* **2011**, *2* (6), 648–662. https://doi.org/10.1177/1947601911417862.

(28) Dai, H.; Sinclair, D. A.; Ellis, J. L.; Steegborn, C. Sirtuin Activators and Inhibitors: Promises, Achievements, and Challenges. *Pharmacology & Therapeutics* **2018**, *188*, 140–154. https://doi.org/10.1016/j.pharmthera.2018.03.004.

(29) Chen, J.; Chan, A. W. H.; To, K. F.; Chen, W.; Zhang, Z.; Ren, J.; Song, C.; Cheung, Y. S.; Lai, P. B. S.; Cheng, S. H.; Ng, M. H. L.; Huang, A.; Ko, B. C. B. SIRT2 Overexpression in Hepatocellular Carcinoma Mediates Epithelial to Mesenchymal Transition by Protein Kinase B/Glycogen Synthase Kinase-3β/β-Catenin Signaling. *Hepatology* **2013**, *57* (6), 2287–2298. https://doi.org/10.1002/hep.26278.

(30) McGlynn, L. M.; Zino, S.; MacDonald, A. I.; Curle, J.; Reilly, J. E.; Mohammed, Z. M. A.; McMillan, D. C.; Mallon, E.; Payne, A. P.; Edwards, J.; Shiels, P. G. SIRT2: Tumour Suppressor or Tumour Promoter in Operable Breast Cancer? *European Journal of Cancer* **2014**, *50* (2), 290–301. https://doi.org/10.1016/j.ejca.2013.10.005.

(31) Huang, S.; Zhao, Z.; Tang, D.; Zhou, Q.; Li, Y.; Zhou, L.; Yin, Y.; Wang, Y.; Pan, Y.; Dorfman, R. G.; Ling, T.; Zhang, M. Downregulation of SIRT2 Inhibits Invasion of Hepatocellular Carcinoma by Inhibiting Energy Metabolism. *Translational Oncology* **2017**, *10* (6), 917–927. https://doi.org/10.1016/j.tranon.2017.09.006.

(32) Kim, H. S.; Vassilopoulos, A.; Wang, R. H.; Lahusen, T.; Xiao, Z.; Xu, X.; Li, C.; Veenstra, T. D.; Li, B.; Yu, H.; Ji, J.; Wang, X. W.; Park, S. H.; Cha, Y. I.; Gius, D.; Deng, C. X. SIRT2 Maintains Genome Integrity and Suppresses Tumorigenesis

through Regulating APC/C Activity. *Cancer Cell* **2011**, *20* (4), 487–499. https://doi.org/10.1016/j.ccr.2011.09.004.

(33) Toubai, T.; Tamaki, H.; Peltier, D. C.; Rossi, C.; Oravecz-Wilson, K.; Liu, C.; Zajac, C.; Wu, J.; Sun, Y.; Fujiwara, H.; Henig, I.; Kim, S.; Lombard, D. B.; Reddy, P. Mitochondrial Deacetylase SIRT3 Plays an Important Role in Donor T Cell Responses after Experimental Allogeneic Hematopoietic Transplantation. *The Journal of Immunology* **2018**, *201* (11), 3443–3455. https://doi.org/10.4049/jimmunol.1800148.

(34) Hu, Y.; Lin, J.; Lin, Y.; Chen, X.; Zhu, G.; Huang, G. Overexpression of SIRT4 Inhibits the Proliferation of Gastric Cancer Cells through Cell Cycle Arrest. *Oncol Lett* **2019**, *17* (2), 2171–2176. https://doi.org/10.3892/ol.2018.9877.

(35) Fu, L.; Dong, Q.; He, J.; Wang, X.; Xing, J.; Wang, E.; Qiu, X.; Li, Q. SIRT4 Inhibits Malignancy Progression of NSCLCs, through Mitochondrial Dynamics Mediated by the ERK-Drp1 Pathway. *Oncogene* **2017**, *36* (19), 2724–2736. https://doi.org/10.1038/onc.2016.425.

(36) Chang, L.; Xi, L.; Liu, Y.; Liu, R.; Wu, Z.; Jian, Z. SIRT5 Promotes Cell Proliferation and Invasion in Hepatocellular Carcinoma by Targeting E2F1. *Molecular Medicine Reports* **2017**. https://doi.org/10.3892/mmr.2017.7875.

(37) Bringman-Rodenbarger, L. R.; Guo, A. H.; Lyssiotis, C. A.; Lombard, D. B. Emerging Roles for SIRT5 in Metabolism and Cancer. *Antioxid. Redox Signal.* **2018**, *28* (8), 677–690. https://doi.org/10.1089/ars.2017.7264.

(38) Sebastián, C.; Zwaans, B. M. M.; Silberman, D. M.; Gymrek, M.; Goren, A.; Zhong, L.; Ram, O.; Truelove, J.; Guimaraes, A. R.; Toiber, D.; Cosentino, C.; Greenson, J. K.; MacDonald, A. I.; McGlynn, L.; Maxwell, F.; Edwards, J.; Giacosa, S.; Guccione, E.; Weissleder, R.; Bernstein, B. E.; Regev, A.; Shiels, P. G.; Lombard, D. B.; Mostoslavsky, R. The Histone Deacetylase SIRT6 Is a Tumor Suppressor That Controls Cancer Metabolism. *Cell* **2012**, *151* (6), 1185–1199. https://doi.org/10.1016/j.cell.2012.10.047.

(39) Blank, M. F.; Grummt, I. The Seven Faces of SIRT7. *Transcription* **2017**, *8* (2), 67–74. https://doi.org/10.1080/21541264.2016.1276658.

(40) Wei, W.; Jing, Z. X.; Ke, Z.; Yi, P. Sirtuin 7 Plays an Oncogenic Role in Human Osteosarcoma via Downregulating CDC4 Expression. *Am J Cancer Res* **2017**, *7* (9), 1788–1803.

(41) Bagchi, R. A.; Ferguson, B. S.; Stratton, M. S.; Hu, T.; Cavasin, M. A.; Sun, L.; Lin, Y.-H.; Liu, D.; Londono, P.; Song, K.; Pino, M. F.; Sparks, L. M.; Smith, S. R.; Scherer, P. E.; Collins, S.; Seto, E.; McKinsey, T. A. HDAC11 Suppresses the Thermogenic Program of Adipose Tissue via BRD2. *JCI Insight* **2018**, *3* (15). https://doi.org/10.1172/jci.insight.120159.

(42) Moreno-Yruela, C.; Galleano, I.; Madsen, A. S.; Olsen, C. A. Histone Deacetylase 11 Is an ε-N-Myristoyllysine Hydrolase. *Cell Chemical Biology* **2018**, *25* (7), 849-856.e8. https://doi.org/10.1016/j.chembiol.2018.04.007.

(43) Cao, J.; Sun, L.; Aramsangtienchai, P.; Spiegelman, N. A.; Zhang, X.; Huang, W.; Seto, E.; Lin, H. HDAC11 Regulates Type I Interferon Signaling through Defatty-Acylation of SHMT2. *Proceedings of the National Academy of Sciences* **2019**, *116* (12), 5487–5492. https://doi.org/10.1073/pnas.1815365116.

(44) Di Pompo, G.; Salerno, M.; Rotili, D.; Valente, S.; Zwergel, C.; Avnet, S.; Lattanzi, G.; Baldini, N.; Mai, A. Novel Histone Deacetylase Inhibitors Induce Growth Arrest, Apoptosis, and Differentiation in Sarcoma Cancer Stem Cells. *Journal of Medicinal Chemistry* **2015**, *58* (9), 4073–4079. https://doi.org/10.1021/acs.jmedchem.5b00126.

(45) Huang, M.; Zhang, J.; Yan, C.; Li, X.; Zhang, J.; Ling, R. Small Molecule HDAC Inhibitors: Promising Agents for Breast Cancer Treatment. *Bioorganic Chemistry* **2019**, *91*, 103184. https://doi.org/10.1016/j.bioorg.2019.103184.

(46) Janssens, N.; Janicot, M.; Perera, T. The Wnt-Dependent Signaling Pathways as Target in Oncology Drug Discovery. *Investigational New Drugs* **2006**, *24* (4), 263–280. https://doi.org/10.1007/s10637-005-5199-4.

(47) Licciardi, P.; Ververis; Hiong; Karagiannis. Histone Deacetylase Inhibitors (HDACIs): Multitargeted Anticancer Agents. *Biologics: Targets and Therapy* **2013**, 47. https://doi.org/10.2147/BTT.S29965.

(48) McDonald, A. J.; Curt, K. M.; Patel, R. P.; Kozlowski, H.; Sackett, D. L.; Robey, R. W.; Gottesman, M. M.; Bates, S. E. Targeting Mitochondrial Hexokinases Increases

Efficacy of Histone Deacetylase Inhibitors in Solid Tumor Models. *Experimental Cell Research* **2019**, *375* (2), 106–112. https://doi.org/10.1016/j.yexcr.2018.12.012.

(49) Banerjee, A.; Mahata, B.; Dhir, A.; Mandal, T. K.; Biswas, K. Elevated Histone H3 Acetylation and Loss of the Sp1–HDAC1 Complex de-Repress the GM2-Synthase Gene in Renal Cell Carcinoma. *Journal of Biological Chemistry* **2019**, *294* (3), 1005–1018. https://doi.org/10.1074/jbc.RA118.004485.

(50) Merarchi, M.; Sethi, G.; Shanmugam, M.; Fan, L.; Arfuso, F.; Ahn, K. Role of Natural Products in Modulating Histone Deacetylases in Cancer. *Molecules* **2019**, *24* (6), 1047. https://doi.org/10.3390/molecules24061047.

(51) Aztopal, N.; Erkisa, M.; Erturk, E.; Ulukaya, E.; Tokullugil, A. H.; Ari, F. Valproic Acid, a Histone Deacetylase Inhibitor, Induces Apoptosis in Breast Cancer Stem Cells. *Chemico-Biological Interactions* **2018**, *280*, 51–58. https://doi.org/10.1016/j.cbi.2017.12.003.

(52) Khan, O.; Fotheringham, S.; Wood, V.; Stimson, L.; Zhang, C.; Pezzella, F.; Duvic, M.; Kerr, D. J.; La Thangue, N. B. HR23B Is a Biomarker for Tumor Sensitivity to HDAC Inhibitor-Based Therapy. *Proceedings of the National Academy of Sciences* **2010**, *107* (14), 6532–6537. https://doi.org/10.1073/pnas.0913912107.

(53) West, A. C.; Johnstone, R. W. New and Emerging HDAC Inhibitors for Cancer Treatment. *Journal of Clinical Investigation* **2014**, *124* (1), 30–39. https://doi.org/10.1172/JCI69738.

(54) McClure, J. J.; Zhang, C.; Inks, E. S.; Peterson, Y. K.; Li, J.; Chou, C. J. Development of Allosteric Hydrazide-Containing Class I Histone Deacetylase Inhibitors for Use in Acute Myeloid Leukemia. *Journal of Medicinal Chemistry* **2016**, *59* (21), 9942–9959. https://doi.org/10.1021/acs.jmedchem.6b01385.

(55) Wieduwilt, M. J.; Pawlowska, N.; Thomas, S.; Olin, R.; Logan, A. C.; Damon, L. E.; Martin, T.; Kang, M.; Sayre, P. H.; Boyer, W.; Gaensler, K. M. L.; Anderson, K.; Munster, P. N.; Andreadis, C. Histone Deacetylase Inhibition with Panobinostat Combined with Intensive Induction Chemotherapy in Older Patients with Acute Myeloid Leukemia: Phase I Study Results. *Clinical Cancer Research* **2019**. https://doi.org/10.1158/1078-0432.CCR-19-0171.

(56) Grasso, C. S.; Tang, Y.; Truffaux, N.; Berlow, N. E.; Liu, L.; Debily, M. A.; Quist, M. J.; Davis, L. E.; Huang, E. C.; Woo, P. J.; Ponnuswami, A.; Chen, S.; Johung, T. B.; Sun, W.; Kogiso, M.; Du, Y.; Qi, L.; Huang, Y.; Hütt-Cabezas, M.; Warren, K. E.; Le Dret, L.; Meltzer, P. S.; Mao, H.; Quezado, M.; van Vuurden, D. G.; Abraham, J.; Fouladi, M.; Svalina, M. N.; Wang, N.; Hawkins, C.; Nazarian, J.; Alonso, M. M.; Raabe, E. H.; Hulleman, E.; Spellman, P. T.; Li, X. N.; Keller, C.; Pal, R.; Grill, J.; Monje, M. Functionally Defined Therapeutic Targets in Diffuse Intrinsic Pontine Glioma. *Nat. Med.* **2015**, *21* (6), 555–559. https://doi.org/10.1038/nm.3855.

(57) Schlenk, R. F.; Krauter, J.; Raffoux, E.; Kreuzer, K. A.; Schaich, M.; Noens, L.; Pabst, T.; Vusirikala, M.; Bouscary, D.; Spencer, A.; Candoni, A.; Gil, J. S.; Berkowitz, N.; Weber, H. J.; Ottmann, O. Panobinostat Monotherapy and Combination Therapy in Patients with Acute Myeloid Leukemia: Results from Two Clinical Trials. *Haematologica* **2018**, *103* (1), e25–e28. https://doi.org/10.3324/haematol.2017.172411.

(58) Plumb, J. A.; Finn, P. W.; Williams, R. J.; Bandara, M. J.; Romero, M. R.; Watkins, C. J.; La Thangue, N. B.; Brown, R. Pharmacodynamic Response and Inhibition of Growth of Human Tumor Xenografts by the Novel Histone Deacetylase Inhibitor PXD101. *Mol. Cancer Ther.* **2003**, *2* (8), 721–728.

(59) Bolden, J. E.; Shi, W.; Jankowski, K.; Kan, C. Y.; Cluse, L.; Martin, B. P.; MacKenzie, K. L.; Smyth, G. K.; Johnstone, R. W. HDAC Inhibitors Induce Tumor-Cell-Selective pro-Apoptotic Transcriptional Responses. *Cell Death & Disease* **2013**, *4* (2), e519–e519. https://doi.org/10.1038/cddis.2013.9.

(60) Makarević, J.; Rutz, J.; Juengel, E.; Maxeiner, S.; Mani, J.; Vallo, S.; Tsaur, I.; Roos, F.; Chun, F.; Blaheta, R. HDAC Inhibition Counteracts Metastatic Re-Activation of Prostate Cancer Cells Induced by Chronic MTOR Suppression. *Cells* **2018**, *7* (9), 129. https://doi.org/10.3390/cells7090129.

(61) Ferrari, P.; Nicolini, A. Overcoming Endocrine Resistance in Breast Cancer. In *Oncogenomics*; Elsevier, 2019; pp 393–422. https://doi.org/10.1016/B978-0-12-811785-9.00029-6.

(62) Chen, Y.; Wang, X.; Xiang, W.; He, L.; Tang, M.; Wang, F.; Wang, T.; Yang, Z.; Yi, Y.; Wang, H.; Niu, T.; Zheng, L.; Lei, L.; Li, X.; Song, H.; Chen, L. Development of Purine-Based Hydroxamic Acid Derivatives: Potent Histone Deacetylase Inhibitors

with Marked in Vitro and in Vivo Antitumor Activities. *Journal of Medicinal Chemistry* **2016**, *59* (11), 5488–5504. https://doi.org/10.1021/acs.jmedchem.6b00579.

(63) Barbarotta, L.; Hurley, K. Romidepsin for the Treatment of Peripheral T-Cell Lymphoma. *J Adv Pract Oncol* **2015**, *6* (1), 22–36.

(64) Foss, F. M.; Zinzani, P. L.; Vose, J. M.; Gascoyne, R. D.; Rosen, S. T.; Tobinai, K. Peripheral T-Cell Lymphoma. *Blood* **2011**, *117* (25), 6756–6767. https://doi.org/10.1182/blood-2010-05-231548.

(65) Smolewski, P.; Robak, T. The Discovery and Development of Romidepsin for the Treatment of T-Cell Lymphoma. *Expert Opinion on Drug Discovery* **2017**, 1–15. https://doi.org/10.1080/17460441.2017.1341487.

(66) Sun, W. J.; Huang, H.; He, B.; Hu, D. H.; Li, P. H.; Yu, Y. J.; Zhou, X. H.; Lv, Z.; Zhou, L.; Hu, T. Y.; Yao, Z. C.; Lu, M. D.; Shen, X.; Zheng, Z. Q. Romidepsin Induces G2/M Phase Arrest via Erk/Cdc25C/Cdc2/CyclinB Pathway and Apoptosis Induction through JNK/c-Jun/Caspase3 Pathway in Hepatocellular Carcinoma Cells. *Biochemical Pharmacology* **2017**, *127*, 90–100. https://doi.org/10.1016/j.bcp.2016.12.008.

(67) Yoon, Y. K.; Ali, M. A.; Wei, A. C.; Choon, T. S.; Osman, H.; Parang, K.; Shirazi, A. N. Synthesis and Evaluation of Novel Benzimidazole Derivatives as Sirtuin Inhibitors with Antitumor Activities. *Bioorganic & Medicinal Chemistry* **2014**, *22* (2), 703–710. https://doi.org/10.1016/j.bmc.2013.12.029.

(68) Mahajan, S. S.; Scian, M.; Sripathy, S.; Posakony, J.; Lao, U.; Loe, T. K.; Leko, V.; Thalhofer, A.; Schuler, A. D.; Bedalov, A.; Simon, J. A. Development of Pyrazolone and Isoxazol-5-One Cambinol Analogues as Sirtuin Inhibitors. *Journal of Medicinal Chemistry* **2014**, *57* (8), 3283–3294. https://doi.org/10.1021/jm4018064.

(69) Sultana, F.; Manasa, K. L.; Shaik, S. P.; Bonam, S. R.; Kamal, A. Zinc Dependent Histone Deacetylase Inhibitors in Cancer Therapeutics: Recent Update. *Current Medicinal Chemistry* **2018**, *25*. https://doi.org/10.2174/0929867325666180530094120.

(70) Monga, M.; Sausville, E. Developmental Therapeutics Program at the NCI: Molecular Target and Drug Discovery Process. *Leukemia* **2002**, *16* (4), 520–526. https://doi.org/10.1038/sj.leu.2402464.

(71) Arnold, K.; Bordoli, L.; Kopp, J.; Schwede, T. The SWISS-MODEL Workspace: A Web-Based Environment for Protein Structure Homology Modelling. *Bioinformatics* **2006**, *22* (2), 195–201. https://doi.org/10.1093/bioinformatics/bti770.

CHAPTER 5 – SET- DOMAIN PROTEINS[3]

5.1 Significance of Work

This chapter starts with a brief review of the SET- domain proteins and highlights specific characteristics of both SMYD2 and SMYD3 for potential use in the clinical management of some types of cancers. The latter part of this chapter presents preliminary research data from an investigation in which the aims were (1) to analyze the potential use of SMYD2 and SYMD3 as targets in treating cancer. (2) to evaluate the colony formation and viability of lung carcinoma cell (A549) and colorectal adenocarcinoma cells (DLD-1) after treatment with a SMYD3 inhibitor. I've hypothesized that the full-length protein sequence alignments of SMYD3 with its cofactor domains will show potential areas of significance to be utilize in its inhibitory drug design. I hypothesized that the SMYD3 inhibitor will prevent the lysine methyltransferase and show signs of an effective drug treatment for lung carcinomas and colorectal adenocarcinomas. The results of the drug inhibition assays indicate the decrease in colony formation for both A549 and DLD-1 cell lines were a result of increased SYMD3 dosage concentrations. Similarly, in the viability assays, both A549 and DLD-1 cell lines showed sensitivity to the SMYD3 inhibitor. The SMYD2 and SYMD3 data could further be used to extrapolate the essentials for constructing predictive models for additional protein interactions and active site docking regions for their respective protein structures. This chapter serves as a springboard for and supports the necessity of continued research in this area.

---

[3] Jarrell, D. K.; Hassell, K. N.; Crans, D. C.; Lanning, S.; Brown, M. A. Characterizing the Role of SMYD2 in Mammalian Embryogenesis—Future Directions. *Veterinary Sciences* **2020**, *7* (2), 63.

5.2 Introduction

The Su(var)3-9 Enhancer of Zeste and Trithorax (SET) protein domain; a posttranslational modification domain, is controlled by the enzymatic activity of specific histones. Originally isolated as the Trithorax protein from *Drosophila melanogaster*, this family of multidomain proteins has nuclear activities for which gene expression, regulation and epigenetic modifications data have been linked to the methylation of the histone lysine residues.[1-6] This activity, described as methyltransferase activity, uniquely characterizes the large and/or small subunits of the SET-domain proteins, this activity occurs due to the presence of histone lysine methyltransferases (HKMTs).[7-11] This dichotomy in localization of enzymatic activity presents challenges to studying the mechanistic behavior of this particular domain, yet also presents viable options for modifiable enzyme-substrate docking active sites utilized during drug design. The human SET protein domain has been reported as an evolutionarily conserved region responsible for activating or silencing gene expression. The methylation of histone #3 (H3) on lysine residue #4 (K4) identifies the behavior of the human SET domain proteins (SET7/9).[12-15] In plants; the methylation of lysine residue #14 without histone modification has been identified as the enzyme Rubisco (Ribulose-1,5-bisphosphate carboxylase/oxygenase) large subunit methyltransferase (LSMT).[16-19]

Structurally, the SET-domain has a tertiary confirmation of 10–12 β-strands in its core region and two outer heterologous domains that consist of a highly conserved anti-parallel β-barrel (N-terminus) and a loop or knot-like structure blocking its enzymatic active sites; C-terminus.[5,13,20-22] The catalytic region of the SET-domain protein family presents the targeted location for the development of specific chromatin modification

enzymes that can utilized in oncological therapeutics. Continued investigation of the lysine methylation activity at the C-terminus of the SET-domain can lead to advancements novel inhibitory drug discovery for the treatment some cancers.[4,23-24] The molecular mechanism of action of SET-domain proteins found in some cancers are not fully understood. Clarity could lead to the development of pharmacological treatments that are more efficient, site-specific and overall more beneficial for the individual patient; perhaps brokering individualized medicine.

5.3 Human SET- Domain Classification

The human SET protein domain has been identified via association with eight human genes families. ASH1L (absent, small, or homeotic disc1) has been identified by its substrate binding site blocked by a regulatory SET-domain loop. This loop contains the regulatory catalytic region involved in gene activation.[3,25-26] BAT8/G9a; a G-like protein encoding gene, has been associated with the repression of transcription via lysine methylation of non-histone and histone containing substrates.[27-29] EHMT1, EHMT2 (euchromatin histone-lysine *N*-methyltransferase genes 1 & 2 and EZH1, EZH2 (histone-lysine *N*-methyltransferase genes 1 & 2) are known to regulate skeletal growth and cell proliferation; specifically chondrocytes.[30-32] Very little is known about the FP13812/Q71M33-human gene, however there has been evidence to support transcription level activity similar to that of EHMT1.[33] MLL, MLL2, MLL3, MLL5 (mixed linage leukemia) located on human chromosomes 11q23, 12q13.12, 7q36.1, 7q22.1, respectively. MLL functions as an analog of *Drosophila trx* encoding for *HOX* genes.[34-36] MLL2 associates with Pax7(paired-box-transcription factor) to form the histone

methyltransferase(HMT) complex involved in H3K4 methylation.[34,37] MLL3 forms a complex with MLL4 and regulates the expression of p53 during DNA repair.[34,38] MLL5 is homologs to *Drosophila* gene CG9007 and has dual functions; indirectly regulates histone modification enzymes without the presence of methylation and promotes myogenic differentiation via Pax7, Myf5 and myogenin.[34,39-40] NSD1 (nuclear receptor-binding SET domain containing protein 1) encodes for histone methyltransferases; corepressor and coactivator. NSD1 consists of ten conserved domains and is associated with transcriptional repression.[41-43] Nuclear receptor SET-domain-3 NSD3/ Wolf-Hirschhorn syndrome candidate 1-like 1(WHSC1L1) located on the human chromosome at 8p11.23 has been reported overexpressed via upregulation in tumor cell proliferation and metastasis.[44-46] SETD1A represents a robust gene that impacts H3K4 methylation and plays a key role in mitosis. It has been evolutionarily conserved and its loss of function can lead to irregularities in proliferation.[47-50] Research evidence supports the role of SETD2 as a modulator of alternative splicing during tumorigenesis. SETD2; responsible for H3 lysine 36 trimethylation (H3K36me3) of histones has also shown data that indicates it can methylate α-tubulin at lysine 40.[51-53] SETD3 mediates the encoding for actin-specific histidine *N*-methyltransferase of which play a significant role in muscle differentiation, carcinogenesis and DNA-damaged induced apoptosis.[54-59] The overexpression of the SETD4 gene has been observed in breast carcinogenesis; human ER-negative breast cancers.[60,61] SETD5 is located on human chromosome 3p25.3 and is responsible for transcription regulation, heterochromatin formation and X-chromosome inactivation via lysine methylation.[5,20,62] SETD6 works as gene transcription repressor and cofactor in cellular processes; proliferation and signaling.[63,64] SETD7/9 encoded for histone lysine

methyltransferases that manipulate human embryonic stem cell differentiation. [65-67] SETD8 data support methyltransferase activity essential for cellular processes; DNA replication and damage repair, cell cycle regulation and transcription.[68] TAF10(TATA-box binding protein, DNMT1(DNA methyltransferase-1), ERα(estrogen receptor-alpha), NF-χB(nuclear factor kappa B, PCAF(P300/CREB binding protein-associated factor), p53 and Tat (HIV-1) all serve as nonhistone substrates for SETD8.[69-73] SETDB1 and SETDB2 both work as co-factor that encode for the methylation of H3K9 activity, of which has been observed in the suppression of transcription.[74-77] SMYD(SET/MYND domain) is a complex of SET domain that functions as the methyltransferase and the MYND domain consists of the zinc finger that allows for multiple protein interactions. The four members of this group are SMYD1, SMYD2, SMYD3, SMYD4 and SMYD5.[22,78-81] SYMD1(SET/MYND domain protein 1) modulates chromatin formation via lysine methylation for encoding cardiac and skeletal muscle cell differentiation.[82,83,84,85] SMYD2 domain encodes for H3K36 methyltransferase and interacts with histone deacetylase complexes to suppress cell proliferation.[86-90] SMYD3 plays multiple roles in gene expression and its overexpression has been observed in cancerous tissues. SYMD3 transcriptional regulates H3K4 lysine methylation as involved in cell cycle signaling and proliferation.[91-100] SMYD4 has been designated as a tumor suppressor; observed in carcinogenesis.[15,101-102] SMYD5 transcripts have been observed in early stage developmental gene expression, embryogenesis and hematopoiesis.[103-105] Suppressor of variegation 3-9 homolog 2 (SUV39H1) has been identified as a regulatory component of NF-χB pathway, heterochromatin replication, DNA repair.[106-108] SUV39H2 enzymatic activity indicates binding site modulation via lysine methyltransferase.[109-111] SUV420H1

and SUV420H2 form a complex with *S*-adenosyl-*L*-methionine (SAM) utilizing its *N*-terminal domain and Zn^{2+}-binding post-SET domain to enzymatically methylate H4K20.[14,112] WBP7(KMT2B) triggers the recruitment of nuclear factor erythroid-2 (NFE2); transcriptional activator that methylate H3K4, overexpressed in solid tumor cell lines.[113-115] Wolf-Hirschhorn syndrome candidate 1(WHSC1) functions as a peptide inhibitor. As a modulator of cell cycle signaling and proliferation, overexpression has been reported in cervical cancer tissues and cells.[27,116-119] (See Summary Table 5.1).

5.4 Research Overview

5.4.1 *MYND Family*

Of the five membered SMYD protein family, SMYD1-3 have been more fully characterized than SMYD4 and SMYD5. In figure 5.1, the MYND domain of SMYD1-3 has been aligned with two references; ETO a known SMYD3 zinc finger corepressor and ZMYND10, a known co-expressor that adds stability to the structure. The MYND family domain highlights the conserved amino acid residues that show their significance and role in the folding of the protein structure. The cysteine residues shown in dark red indicate sites for protein crosslinking; which allows for increased structural stability and rigidity for maintaining potential catalytic activity. Highlighted in blue, the lysine residues denote areas that can interact with negatively charged amino acids to build stabilizing hydrogen bonds or salt-bridges. Residues of leucine, shown in green are hydrophobic and commonly appear as alpha helix structures. Tyrosine residues (in teal) with aromatic characteristics and tryptophan (in light green) both have the potential to interact with non-protein ligands via stacking. However, tyrosine can trigger protein kinase activity via

phosphorylation. The histidine residues in pink indicate areas of proton transfer; allowing for potential metal binding sites.[120-122]

The MYND domain incorporates a zinc-finger motif that facilitates its unique protein-protein interactions; illustrated by the 3D ribbon model in figure 5.2. The three superimposed sample of SMYD3, ZMYND10 and ETO display similar curvatures and loop-like folds in the regions that contain the highly conserved cysteines (C1-6 and C8) and histidine (H7) residues. The cysteine residues mark sites for increased protein cross-linkage potential for increased structural stability. This domain maintains its rigidity, and possibly prevents access to the catalytic region; however, the histidine (H7) residue represents a key location for potentially docking metals and other interactive proteins due to the Zn^{2+} ions that help to provide support and structure. Point mutations in the cysteine residues of the MYND domain can inhibit the MYND-mediated protein interactions.

5.4.2 *SMYD2 as a Potential Target in Treating Cancer*

SMYD2 was initially characterized in cardiomyocytes[123-125], where it was shown to methylate histone H3 at K4 and at K36.[126] The bulk of research attention in SMYD2 has been due its overexpression in several cancers and its interactions with known oncogenes. Overexpression of SMYD2 has been observed in breast, pancreatic, colorectal, esophageal, blood, lung, bladder, and hepatocellular cancers (see table 5.2), and SMYD2-positive tumors are often correlated with poor patient outcomes. These studies have revealed two principal mechanisms of action in which SMYD2 has shown a contribution to carcinogenesis and cancer progression. First, aberrant histone methylation has been associated with many cancer types and results in altered

expression levels of several oncogenes. Second, in addition to histone targets, SMYD2 has been shown to directly modulate the activity of cell cycle regulators via post-translational methylation. SMYD2 represses the activity of tumor suppressers p53 (apoptosis) and RB1 (cell-cycle arrest) via mono-methylation at p53:K370 and RB1:K860 and K810.[125,127-128] Methylation of AHNAK and AHNAK2—two proteins involved in cell migration and invasion—may also contribute to the role of SMYD2 in carcinogenesis.[129] Other SMYD2 methylation targets include HSP90AB1, ERα, PARP1, PTEN, BMPR2, and β-Catenin.[130-134] The known targets of SMYD2, the tissue(s) that are involved, and the observed correlations with cancers are summarized in table 5.2.

An improved understanding of the specific mechanisms by which SMYD2 contributes to carcinogenesis is likely to reveal new targets for clinical intervention. Small molecule SMYD2 inhibitors have already been shown to be effective in vitro and are promising for the treatment of a wide range of cancers.[135] The understanding of the role of SMYD2 in cancers is certainly incomplete and requires further investigation. Its function in embryogenesis is even less understood. Further study into the normal roles of SMYD2 in development is necessary for a more-complete understanding of organ development, stem cell differentiation, epigenetics, and SMYD2-mediated pathogenic pathways.

5.4.3 *SMYD2 in the WNT Pathway and Mesendodermal Differentiation*

SMYD2 expression has been detected in tissues derived from all three germ layers, including muscle (mesoderm), liver (endoderm) and brain (ectoderm). It is predominantly expressed in the heart during development; however its role in cardiac development remains unclear. It has been demonstrated that SMYD2 forms a complex

with the cytoplasmic chaperone proteins Heat Shock Protein-90 (HSP90) and the abundant sarcomeric protein titin.[136] Research has revealed that a SMYD2 deficiency resulted in impaired titin stability and altered muscle function. Unexpectedly, however, the Nkx2.5-conditional Smyd2-knockout (cardiac-specific) in mice did not impact heart development suggesting that SMYD2 is not essential for heart development or that its role manifests prior to Nkx2.5 expression in cardiac progenitor cells. Further investigation into the latter conclusion led to studies revealing a role for SMYD2 prior to Nkx2.5 expression. SMYD2 methylates β-Catenin, which is essential for its nuclear translocation and subsequent activation of WNT signaling.[130] Activation of WNT signaling drives pluripotent stem cell commitment to mesendoderm lineages[90] and is the first step in the differentiation of human pluripotent stem cells (hPSC) to cardiomyocytes *in vitro*.[137-138] In addition to direct activation of β-Catenin, SMYD2-knockout hPSC lines demonstrated a remarkable reduction of H3K4me1 and H3K36me2 levels at the transcriptional start sites of several signature mesendoderm genes (T, EOMES, MIXL1, and GSC) during differentiation to mesoderm and endoderm.[139] Therefore, We've hypothesized that the principal role of SMYD2 in heart development occurs prior to Nkx2.5 expression, which approx. begins 3-4 days after WNT activation via β-Catenin translocation.[140]

The role of SMYD2 in the WNT signaling pathway may also explain its presence and importance in other mesendodermal tissues during development; liver, kidney, and reproductive systems. Future studies should investigate the specific roles of SMYD2 in the development of these organs using tissue-specific conditional knockout models that allow for ablation of SMYD2 expression at various timepoints during development. Finally, dysregulation of the WNT pathway has been observed in a wide range of cancers,

including colorectal, hepatocellular and breast carcinomas.[141-143] The overlap between SMYD2 and the WNT pathway, particularly given their independent associations with such a wide range of cancers, merits immediate further investigation.

5.4.4 *SMYD2 in Hematopoiesis and Leukemia*

SMYD2 overexpression has been observed in several blood cancers, including adult B-acute lymphoblastic leukemia (B-ALL), T-cell acute lymphoblastic leukemia (T-ALL), Chronic myeloid leukemia (CML), Mixed lineage leukemia rearranged adult B-acute lymphoblastic leukemia (MLLr-B-ALL), Acute myeloid leukemia (AML) and additional hematopoietic lesions, including chronic lymphatic leukemia (CLL) and Diffuse Large B-Cell Lymphoma (DLBCL).[144-146] Despite this knowledge, the role of SMYD2 in hematopoiesis was unclear prior to recent work investigating the effects of SMYD2 deletion in hematopoietic stem cells (HSCs) and their downstream progenitor pools.[147] It has been discovered that a murine HSC-specific Smyd2 conditional knockout (CKO) yielded a significant decrease in HSC numbers as well as a decrease in some, but not all, downstream myeloid and lymphoid lineages. Deeper investigation revealed that these effects are mediated at least in part by the induction of apoptosis in blood progenitor cells of Smyd2-CKO animals. Additionally, it has been found that Smyd2-CKO mice exhibited disrupted STAT3 and WNT/β-Catenin signaling in HSC lineages, agreeing with previous studies describing the interactions between SMYD2 and these two proliferation-inducing signaling pathways.[130,148]

5.4.5 *SMYD2 in the Hypothalamus and Vomeronasal Organ (VNO)*

In the initial characterization of SMYD2 in 2006 the goal was to determine which embryonic tissues expressed SMYD2 during development.[86] The whole-mount *in situ* hybridization using murine embryos analyzed at day 13.5 with a probe was specific to Smyd2. The most pronounced expression was observed in the heart. The hypothalamus and vomeronasal organ (VNO) were observed to be clear of SMYD2 expression. To my knowledge, a possible developmental role of SMYD2 in this region has never been investigated following these initial observations. We've proposed that SMYD2 plays a role in the origin and/or migration of Gonadotropin-Releasing Hormone (GnRH) neurons from the VNO, which are known to emerge from the VNO around E11 and migrate into the basal forebrain between E12-E17 in mice.[149-153,179] GnRH is released from GnRH neurons located in the hypothalamus in pulsatile fashion during adolescence and is essential for proper reproductive function. The release of GnRH represents the initial step in the hypothalamic-pituitary-gonadal signaling axis. Because of the strong SMYD2 signal in the VMO and the hypothalamus during GnRH neural migration between the two developing organs, it is plausible that SMYD2 plays a role in proper neuronal differentiation and/or networking during development. Several factors are implicated in proper GnRH neural migration, including growth factors, extracellular matrix/adhesion molecules, neurotransmitters, G-protein-coupled receptors, and transcription factors.[146] Studies that investigate the roles of histone methylation at transcriptional start sites or direct post-transcriptional methylation in the expression or activity of these factors may elucidate a role for SMYD2 in VMO and hypothalamic development. Furthermore, thorough epigenetic analysis in these regions will likely further clarify the specific mechanisms that

drive VMO development, GnRH neuron migration, and neural networking in the hypothalamus.

5.4.6 *SMYD3 as a Potential Target in Treating Cancer*

SMYD3 consists of Su(var)3–9, Enhancer of Zeste and Trithorax also known as N-terminal portion of SET domain (N-SET) that encodes for histone lysine methyltransferase activity, followed by Myeloid translocation protein 8 (see figure 5.3), Nervy, Deaf (MYND) domain; a cofactor is responsible for recruiting other proteins for various interactions. The N-SET is connected to the intermediate or linker sequence (I-SET) domain that has been identified as the Rubisco - large subunit methyltransferase (LSMT) like region; highly conserved in multiple divergent species (see figures 5.6 and 5.7). The C-SET domain incudes the catalytic SET-dependent folded segments for enzymatic activity. The post-SET functions as a critical component of the active site by supplying an aromatic residue that anchors against the conserved SET core to form a hydrophobic channel. The C-terminus has a knot-like structure blocking its enzymatic active sites.[21,67,154]

In figure 5.3, the full-length SMYD3 protein structure was illustrated using SWISS-DOCK software. From this 3D image, protein activity and potential docking sites for small molecule interactions can be predicted. The MYND domain has two Zn^{2+} ions which indicate potential docking and formidable stability in this region. While little known, Rubisco-LSMT (I-SET) serves a physical linker to between the MYND and central regions of the SYMD3 protein; connecting with the N-SET. At this point the histone lysine methyltransferase encoding region is attached to the C-SET zone, which is responsible for regulating the SMYD3 catalytic activity. Both of these regions are of major significance

in understanding how to regulate and/or potentially inhibit SMYD3 methyltransferase activity. The C-terminus blocks the access to the catalytic C-SET. Greater knowledge and understanding of how to regulate this loop structure would be beneficial in designing more effective SMYD3 inhibitors.

SMYD3 gene encodes for cell proliferation, cell cycle progression and is found overexpressed in some cancer cells; hepatocellular and colorectal. Research supports the upregulation of SMYD3 via the Ras signaling pathway and has been observed in tumorous cells; expressed as increased cell growth and proliferation. With functional methyltransferase activity mainly targeted on H3K4, its transcriptional regulation has been reported as a major component in RNA polymerase complex synthesis.[27,96,99,156-157] In addition to having non-histone targets, SMYD3 has the functional ability to trimethylate H3, H4, and H5; allowing for a broader range of effects in triggering the development of skeletal and cardiac muscle tissue as well as mediating estrogen-receptor gene expression. SMYD3 encodes a protein that consists of two dynamic components; structurally appearing and functioning like an open or closed lock. The N-terminus region structurally appears to be a lobe containing the SET, MYND and post-SET domains. The MYND domain has a zinc finger motif with a core consisting of seven histidine paired with cysteines.[91,158-159] At the C-terminus, the residues can exist in two conformational states; *holo* represents the closed hinge/clamp and *apo* represents the open hinge/clamp structure. A cofactor, *S*-Adenosyl methionine (AdoMet) or SAM functions as a key to unlock SMYD3, in its closed conformation. Once, SMYD3 is methylated, *S*-adenosyl-*L*-homocysteine (SAH) complex forms. (see figure 5.4)

In figure 5.5, the N-SET regions of human SMYD3, SET8 and SET9 have been superimposed with the N-SET regions of a plant (garden pea), two types of yeast (neurospora and pombe, and the Chlorella virus for analysis. In the four β-sheets that comprise the N-SET (figure 5.5), significant tyrosine residue shifts closer to the C-terminus of SMYD3. This distinctive localization has been identified as a key component to the catalytic activity of this evolutionarily conserved region seen in multiple divergent species.

5.5 Intermediate linker (I-SET) Domain; Rubisco LSMT- Like

Flanked between the N-SET and the C-SET, there is an intermediate linker or spacer sequence termed; I-SET. The I-SET structurally appears to be approx. one-third the size of the SMYD3, yet significant in enzymatic activity and maintaining stability in the structure between the N-SET and C-SET. The I-SET has been observed to have functions similar to the Rubisco-large subunit methyltransferase (LSMT)-like motifs found in various other species spanning different biological domains of life.[22,93,95] figures 5.6 and 5.7 are 3D ribbon models of the short and long sequenced regions of the I-SET. In the shorter sequenced region of the I-SET shown in figure 5.6 illustrate the same superimposed regions of the N-SET in figure 5.5; a plant (garden pea), two types of yeast (neurospora and pombe, and the Chlorella virus. However, shown in the Loop 1 and Helix 1 of the I-SET are the amino acids glutamate, cysteine, lysine, histidine and arginine; which designates potential methylation. These carboxyl groups and/or nitrogen side-chain atoms of glutamate, cysteine, lysine, histidine and arginine allow for the methyl group

donated from the SAM-AdoMet complex during methyltransferase activity described in figure 5.4.

In figure 5.7, the long version of the I-SET illustrates the protein sequence alignments for human SMYD3 (red) and the garden pea Rubisco-LSMT (green) as superimposed 3D ribbon structures. Flanked by the β4 of the N-SET and β1 of the C-SET, the long version of the I-SET displays with every turn the helixes and loops of this region as they align; structurally mimicking on another. This pattern indicates the potential for similar catalytic activity as functions for these specific residues with homology that supports the conservation of this region in both humans and the common pea plant.

5.5.1 *Rubisco (Ribulose-1,5-Bisphosphate Carboxylase/Oxygenase) in Multiple Species*

Multiple species have organisms that utilize Rubisco for CO_2 fixation, as a means of survival, and are structurally homologous. Phylogenetically, the Rubisco protein exists in the hierarchy of various species, from single-cells protists to multicellular eukaryotes. The Rubisco enzymes are involved in the CO_2 fixation of which is the rate limiting step of photosynthesis. Within the catalytic domain of large subunit of Rubisco are trimethylated lysine residues that carry out various posttranslational modifications similar to those found in plants and other species.[161-163] This trimethylated lysine residue motif of Rubisco-LSMT, traditionally found in plants, has also been identified in aquatic species; both of which structurally and functionally mimic the intermediate linker (I-SET) domain found in humans. In some plant species that have adapted to aquatic or extreme arid conditions, Rubisco has been an indicative phylogenetic marker of evolution. Carnivorous, Crassulacean Acid Metabolism (CAM) and C3 carbon-fixation plants are evidence that

supports the dependence on Rubisco synthesis for survival in extreme environmental conditions.[164-168] In the photosynthesis process for bacteria, plants and archaea, the Rubisco usage in the CO_2 fixation process was aided by the inorganic metal competition within the active site of the enzyme. Traces of Mg^{2+} have consistently in biochemical research analysis found to be an integral member maintaining the magnetic affinity within the substrate.[169-176]

5.6 Materials & Methods

Phylogenetic Analysis:

Protein sequences (see Supplemental figure 5.1) were collected from the National Center for Biotechnology Information Search database (NCBI) and aligned using Clustal Omega software. A phylogenetic tree was generated from the same aligned Rubisco-LSMT protein sequences to illustrate its evolutionary lineage.

SMYD3 Inhibitor:

Proprietary compound designed to target histone lysine methyltransferase activity by blocking and/or restricting the necessary conformational protein folding structure formation.

Cell Culture Preparation:

A549 lung carcinoma cells and DLD-1 colorectal adenocarcinoma cells were donated by a fellow graduate student that had previous maintained this culture in phenol-red MEM growth media and in the proper cell culture conditions at 37°C with 5% CO_2. During two cell culture passes, both cell culture lines were maintained in phenol-red MEM growth media supplemented by 10% fetal bovine serum (FBS), 10mM penicillin-

streptomycin, 2mM L-glutamine and 1mM sodium pyruvate, incubated at 37°C with 5% CO_2. Once the cultures reached 70% confluency, the A549 and DLD-1 cells were seeded separately onto 6-well plates. The culture media with concentrations of the SMYD3 inhibitor ranging from 0.0-250.0µM was to the labeled 6-well plate. The plates were transferred to incubation at 37°C with 5% CO_2 for two assays; survival rate and cell proliferation rate.

Colony Formation Assay:

This assay was conducted to test the ability of a single cell to grow into a colony that consists of at least 50 cells. Lung (A549) and colorectal cancer cells (DLD-1) were treated with various concentrations of SMYD3 inhibitor and were incubated for 2 weeks at 37°C with 5% CO_2. Upon harvest, colonies were fixed with 75% of Ethanol, stained with 10µL 0.5% of Crystal violet dye™ and counted using a stereomicroscope. Linear quadratic regression curves were generated using Graphpad™ Prism 6 software. Using regression curves, preliminary data were generated due to only two trials conducted.

Cell Viability Assay:

Lung and colorectal cancer cells were treated with various concentrations of SMYD3 inhibitor and incubated for 48h at 37°C with 5% CO_2. Upon harvest, dead cells were excluded using Trypan dye blue™. Viable cells were counted using Bio-Rad automated cell counter. Linear quadratic regression curves were generated using Graphpad™ Prism 6 software. Using regression curves, preliminary data were generated from only two trials.

5.7 Results

5.7.1 *Phylogenetic Analysis*

In figure 5.8, Model organism such as Zea *mays*, C. *elegans* and Arabidopsis *thaliana* are represented as descendants from the same evolutionary branch. However, lower hierarchy of life level organism is represented as descendants from alternate evolutionary roots. Both unicellular and multicellular organisms have protein sequence evidence that phylogenetically links various species. Ultimately meaning the Rubisco LSMT (I-SET) protein sequence has been conserved throughout evolution.

The SET-domain proteins are often found in association with particular types of cancers; breast, leukemia, adenocarcinoma, etc.[36,177-178] Gaining the knowledge and ability to regulate specific proteins found in the SET-domain family has the potential to be a game changer in drug discovery. This is especially true if the Zn^{2+} finger binding motif of the Rubisco-LSMT or I-SET could be utilized in synergy with other inorganic metals. Even greater potential lies in understanding how to regulate the functions of SYMD3, utilizing its catalytic domain and designing drug inhibitors to combat invasive metastatic cancers.

5.7.2 *Cell-based Assays*

The colony formation assays represented in figures 5.9A and 5.9B demonstrate the short-term effects of the SMYD3 inhibitor on lung (A549) and colorectal (DLD-1) cancer cell lines at concentrations from 0.0 – 250.0µM. As indicated by the declining SMYD3 inhibitor line, as the concentration increases the ability for A549 and DLD-1 cells to form new colonies decreases. Meaning, the treatment of cells by SMYD3 inhibitor

successfully suppressed the clonogenic activity in both lung and colorectal cancers. The data graphed in figures 5.10A and 5.10B show the viability of the lung (A549) and colorectal (DLD-1) cancer cell lines after long-term treatment with the SMYD3 inhibitor at concentrations from 0.0 – 250.0μM. As indicated by the declining SMYD3 inhibitor line, as the concentration increases for both A549 and DLD-1 cells, viability decreases. Essentially meaning the SMYD3 inhibitor impacts the cellular viability of both cell lines at high concentrations.

5.8 Conclusion and Future Directions

The SET-domain protein can regulate gene expression and ultimately be controlled in unwanted cells, like malignant cancer cells. This protein domain encodes the enzymatic activity, known as methyltransferase activity, on specific lysine residues during posttranslational modification. Methyltransferases have recently been recognized as key players in regulating gene expression and protein activity in a wide range of physiologic processes. The SMYD family of methyltransferases have proved to be particularly important during embryogenesis, via histone methylation, and have also been shown to regulate the expression and activity of several known oncogenes. The localization of the enzymatic activity presents challenges to studying the mechanistic behavior of this SMYD family domain, yet also presents viable options for modifiable enzyme-substrate docking ports or active sites for future drug design and development in oncological therapeutics.

SMYD2 and SMYD3 have strong implications for wider use as potential targets in treating some cancers. SMYD2 is widely expressed during normal embryogenesis but also in several cancers. To further elucidate the role of SMYD2 in development and

carcinogenesis, future research studies should address (1) the purpose of the robust expression of SMYD2 in the heart during development, (2) the preferred pathway for SMYD2-WNT-β-catenin signaling, and (3) the specific mechanisms by which SMYD2 directs apoptosis in HSCs and downstream progenitor pools. Aside from the completion of a third trial of SMYD3 in the colony formation and viability assays, several options could serve as future directions, (1) assays targeted at deletion of SMYD3 for loss of function, (2) continued development of an inhibitor with a library indexed for potential small molecule cofactors, and (3) design clinical models for testing SMYD3 inhibition.

Due to the COVID-19 global pandemic, this project has not been classified as critical and therefore data from the completion of both the colony formation and the viability assays are lacking from this chapter. This leaves the data presented as preliminary; without the statistics necessary for quantitative analysis.

Contributions: The cell-based assay data was generated by Ilham Alshiraihi of the Brown Lab in Clinical Sciences at Colorado State University.

5.9 Figures and Tables

Table 5.1 Summary of SET-Domain Proteins. Table summarizes the characteristics of SET-domain proteins and their histone targets.

SET Domain Families:	Characteristics:	Histone Target:	Refs.:
ASH1L	Regulatory SET-domain catalytic loop	H3K4, H3K9me1 & H3K36,	3, 25-26
BAT8 or G9a	Transcription repression	H3K9me3	27-29
EHMT1, EHMT2, EZH1, EZH2	Regulates skeletal growth and proliferation	H3K27 & H3K9	30-32
MLL, MLL2, MLL3, MLL5	Modulates *HOX* genes, associates with Pax7, regulates the expression of p53 during DNA repair, indirectly regulates histone modification and promotes myogenic differentiation	H3K4	34-40
NSD1	Transcription corepressor and coactivator	H3K36 & H4K20	41-43
NSD3(WHSC1L1)	Upregulation in tumor cell proliferation and metastasis	H3K4, H3K27 & H3K36	44-46
SETD1A	Mitosis and proliferation regulation	H3K4	47-50
SETD2	Alternative splicing during tumorigenesis	H3K36me3	51-53
SETD3	Mediates the encoding for actin-specific histidine *N*-methyltransferase	H3K4 & H3K36	54-59
SETD4	Found in human ER-negative breast cancers	H3K9,H3K79, H3K27me & H4K20	8, 60 & 61
SETD5	Transcription regulation, heterochromatin formation and X-chromosome inactivation	H3K9	5,20,62
SETD6	Gene transcription repressor and cofactor in cellular processes; proliferation and signaling	H3K9	63 & 64
SETD7/9	Embryonic stem cell differentiation	H3K4	65-67
SETD8	Cellular processes; DNA replication & damage repair, cell cycle regulation & transcription	H4K20	68
SETDB1 & SETDB2	Cofactors; suppression of transcription	H3K9	74-77

SMYD1	Modulates chromatin formation; cardiac & skeletal muscle cell differentiation	H3K4 & H3K4me	82-85
SMYD2	Suppress cell proliferation	H3K4 & H3K36	86-90
SMYD3	Cell cycle signaling and proliferation	H3K4 & H3K5	91-100
SMYD4	Tumor suppressor	H3K4	15, 101 &102
SMYD5	Early stage developmental gene expression, embryogenesis and hematopoiesis	H3K20	103-105
SUV39H1	Regulatory component of NF-χB pathway, heterochromatin replication, DNA repair	H3K9	106-108
SUV39H2	Binding site modulation	H3K4 & H3K9	109-111
SUV420H1 & SUV420H2	Forms a complex with *S*-adenosyl-*L*-methionine (SAM)	H4K20	14,112
WBP7 (KMT2B)	Triggers the recruitment of nuclear factor erythroid-2 (NFE2)	H3K4	113-115
WHSC1	Peptide inhibitor, modulates modulator of cell cycle signaling & proliferation	H3K4 & H3K36	27,116-119

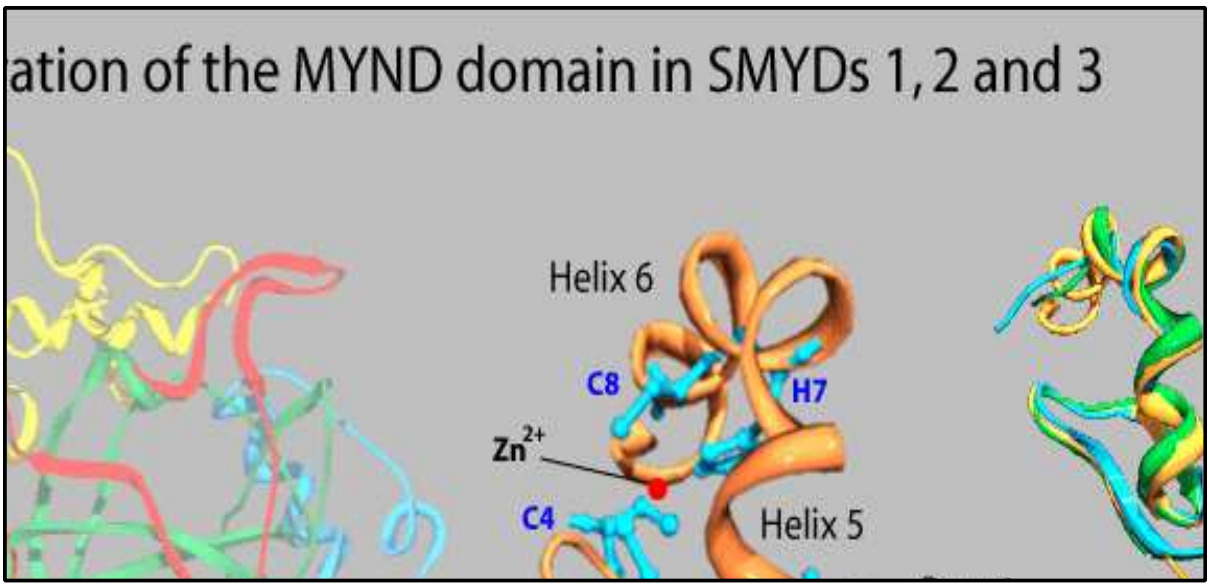

Figure 5.1 MYND domain protein sequence alignments. SMYD1-3 human, mouse, chicken, frog and fish protein sequences have been aligned. ETO (corepressor) and ZMYND10 (co-expressor) human protein sequences have been aligned as zinc finger activity references.

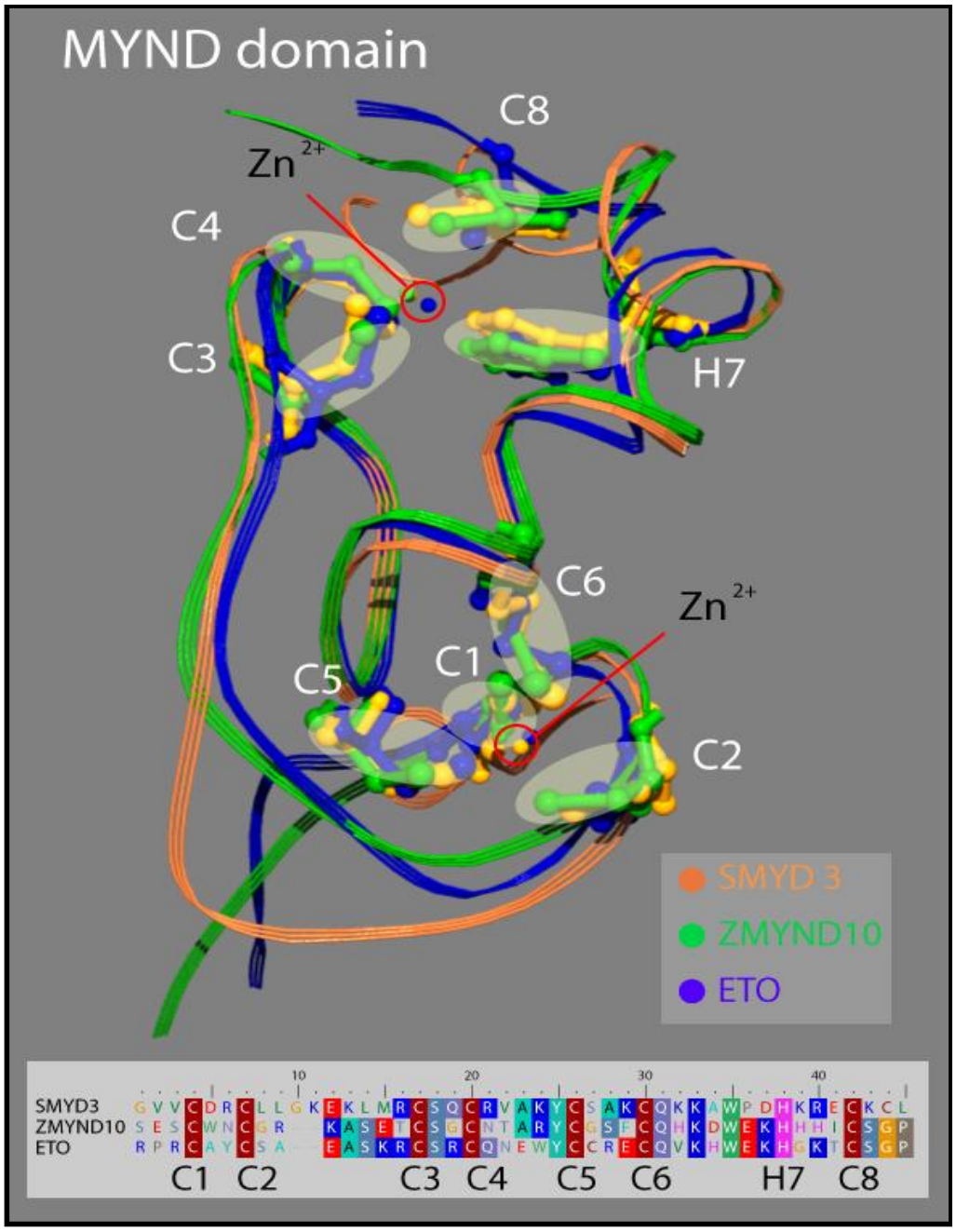

Figure 5.2 MYND domain 3D Ribbon Model of SMYD3, ZMYND10 and ETO protein sequence alignments. C1-6, and C8 represent cysteine residues. H7 identifies the histidine residue and the Zn^{2+} ions are circled in red.

Table 5.2 SMYD2 Summary. Modified from Ref. 179. Table summarizes the characteristics of SMYD2 targets and the cancers associated with their activities.

Targets:	Characteristics:	Associated Cancers:	Refs.:
AHNAK/2	Cell migration and invasion	Chronic myeloid leukemia (CML), Mixed lineage leukemia rearranged adult B-acute lymphoblastic leukemia (MLLr-B-ALL), adult B-acute lymphoblastic leukemia (B-ALL), and T-cell acute lymphoblastic leukemia (T-ALL)	143, 144
Bone Morphogenic Receptor Protein-2 (BMPR2)	Methylation upregulates BMP2 signaling, bone marrow development and MSC proliferation	Skin, colorectal, ovarian, embryonic kidney carcinomas	128
Estrogen receptor-α (ER-α)	At K266 represses ER-α transactivation activity, nuclear receptor for sex hormone estrogen	Breast	131
H3K36	Associated with gene bodies, defines exons, recruits HDACs, modulates transcription	Embryonic kidney, fibroblast carcinomas	120, 35, 37, 39
H3K4	Interacts with RNA Polymerase II, RNA helicase, drives gene transcription at promoter region	Lung, breast, glioblastomas	6, 22, 35
Heat shock protein 90 (HSP90)	Titin stability and sarcomere assembly in muscle tissue, drives the handling of oncoproteins	Lung, breast, urothelial, colorectal, bladder carcinomas	18, 21, 35, 36
p53	Regulation through methylation at K370, of which represses p53-mediated transcriptional regulation, cell cycle arrest	Carcinoma; non-small cell lung cancer	120, 121, 125, 131, 133, 130
PARP1	At K528, enhances the poly (ADP-ribose) activity	Esophageal squamous cell & bladder	130

		carcinoma, pediatric acute lymphoblastic leukemia	
Phosphatase & tensin homologue (PTEN)	At K313, deregulates tumor suppressor & activates the phosphatidylinositol 3-kinase-AKT pathway	Prostate, small cell lung	129
Retinoblastoma tumor suppressor protein (RB1)	At K810, with phosphorylation promotes cell cycle progression; G1/S transition	Bladder carcinomas	124, 125
STAT3	Becomes activated in complex with SMYD2, p56, NF-kB. Transcription activator, feed-forward SMYD2 expression, increased proliferation, stem cell self-renewal	Breast carcinomas, leukemias	145
β-catenin	Promotes its nuclear entry and activation of WNT signaling at K133	B-cell precursor acute lymphoblastic leukemia(ALL), colon & breast cancers and hepatocellular carcinomas	120, 124, 35, 137, 144

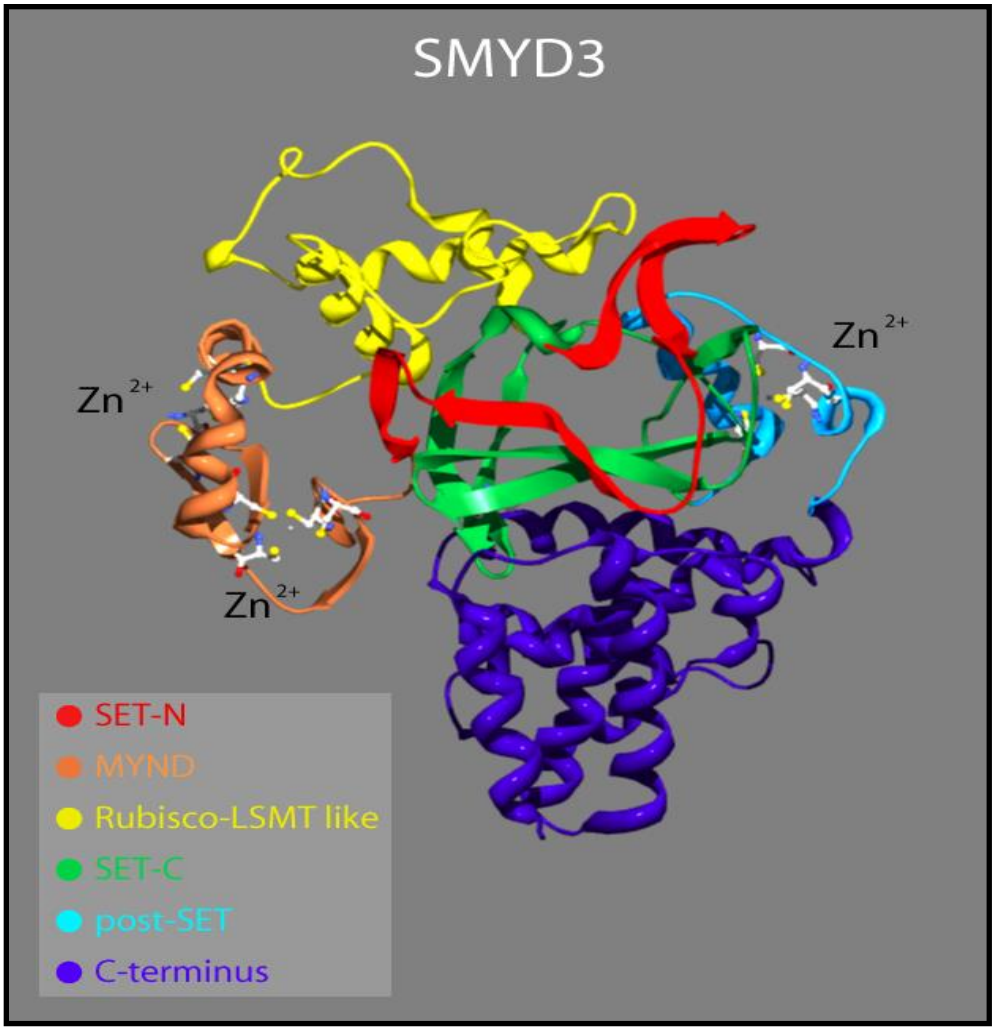

Figure 5.3 SMYD3 3D Ribbon Model. Full-length SMYD3 protein structure illustrated using SWISS-DOCK software. SMYD3 consists of Su(var)3–9, Enhancer of Zeste and Trithorax also known as N-terminal portion of SET domain (N-SET) that encodes for histone lysine methyltransferase activity. Nervy, Deaf (MYND) domain; a cofactor is responsible for recruiting other proteins for various interactions. The N-SET is connected to the intermediate or linker sequence (I-SET) domain that has been identified as the Rubisco-large subunit methyltransferase (LSMT)- like region; highly conserved in multiple divergent species. The C-SET domain incudes the catalytic SET-dependent folded segments for enzymatic activity. The post-SET functions as a critical component of the active site by supplying an aromatic residue that anchors against the conserved SET core to form a hydrophobic channel. The C-terminus has a knot-like structure blocking its enzymatic active sites.

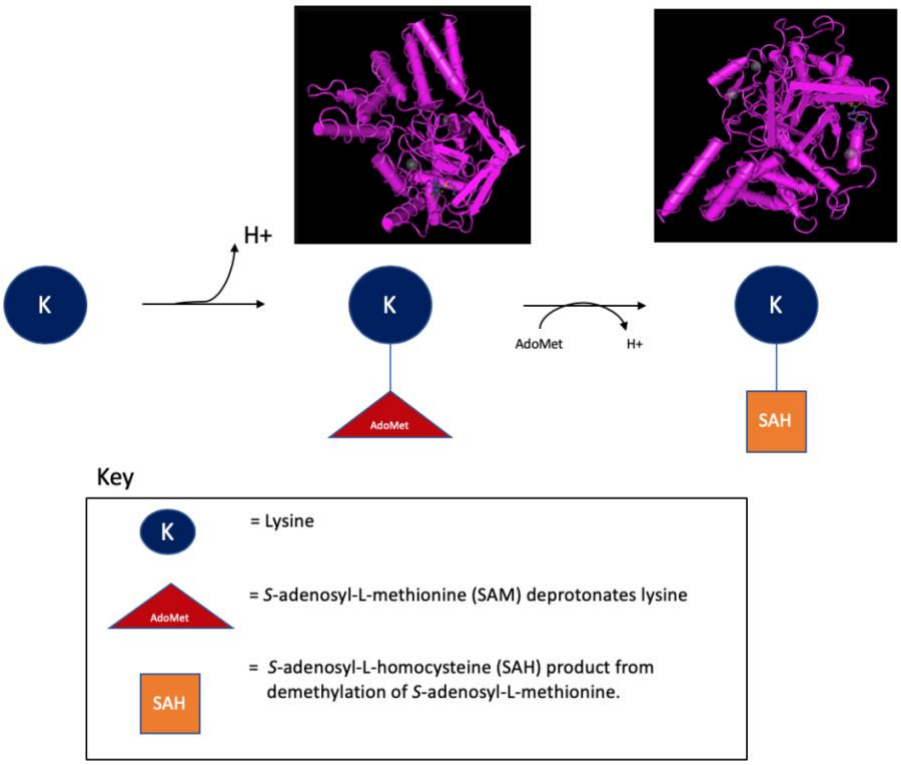

Figure 5.4 Histone (lysine) methyltransferase activity; Mechanism of Action in SMYD3 Lysine becomes deprotonated, allowing for methyltransferase activity to change the structural conformation of lysine; converting from SAM to SAH complex with the deprotonation. Trimethylation would result in additional lysine-SAH complex formations from three lysine residue reactions. Modified from Ref. 160

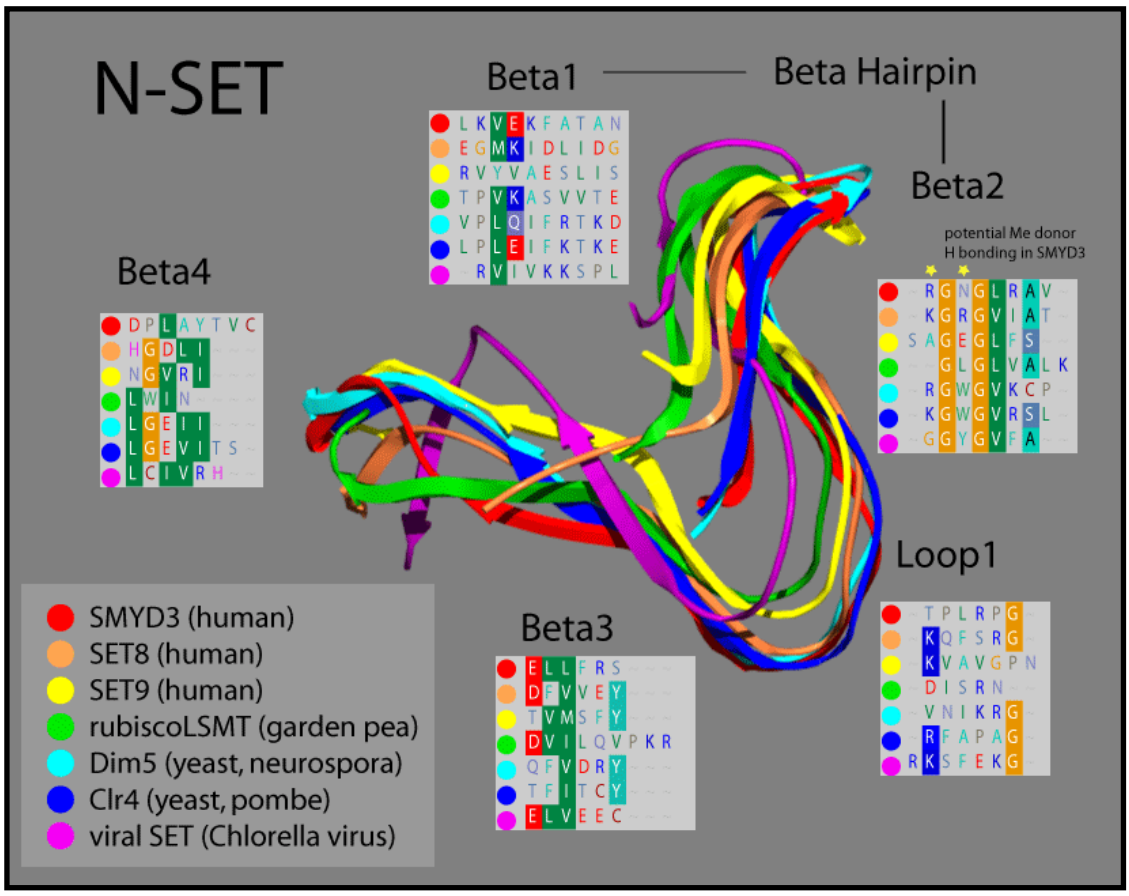

Figure 5.5 Ribbon Model of Conserved N-SET Region of SMYD3. Colors correspond to individual ribbons from different sources sharing the SET-domain protein motifs. β1-4 panels correspond the ribbons to the specific residues and like Loop 1, the protein sequence highlights shared homology in this region. Yellow stars indicate areas for AdoMet interaction on lysine residue.

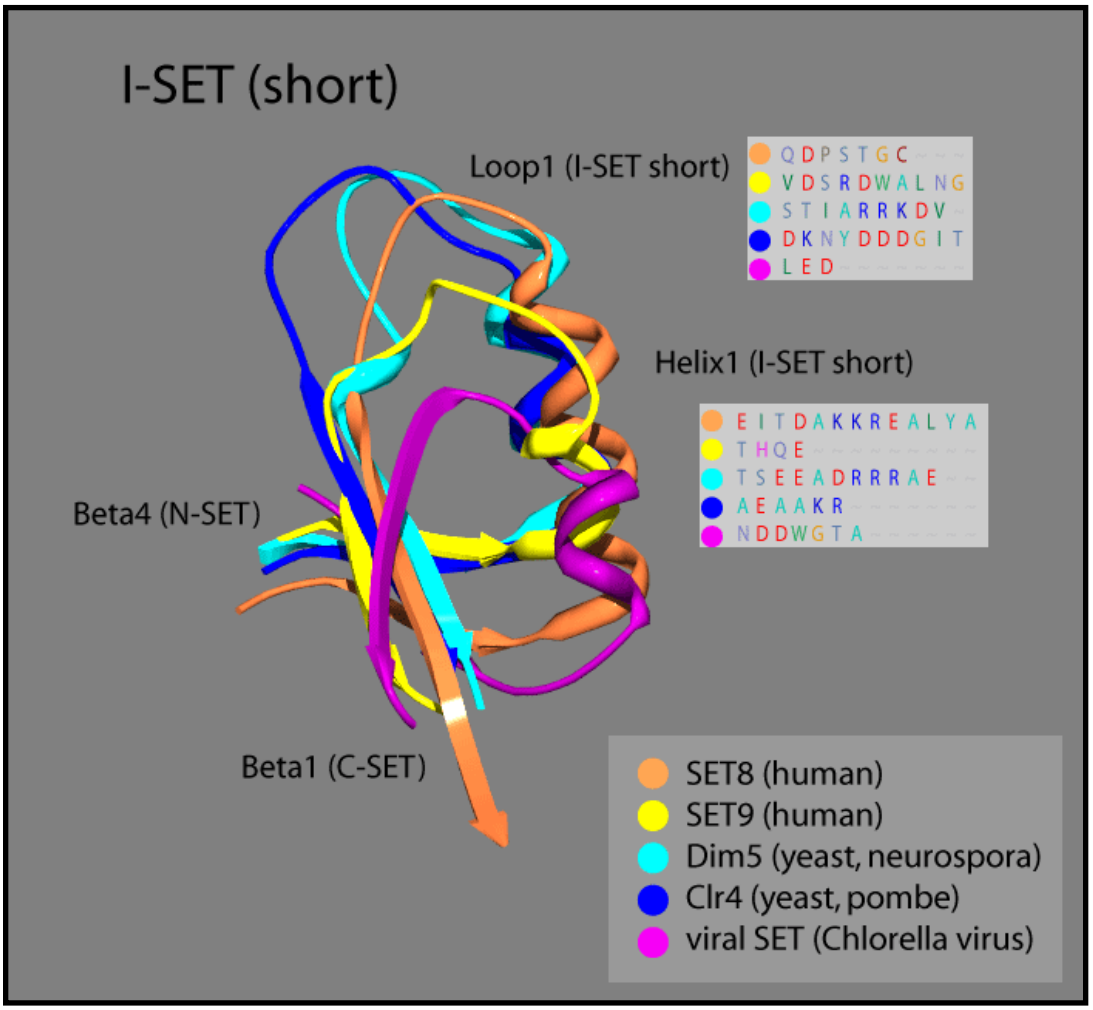

Figure 5.6 3D Ribbon Model of (Short) I-SET. Colors correspond to labels in key for each ribbon strand. Loop 1 and Helix 1 boxes are predicted protein sequences corresponding to the location of Loop 1 and Helix 1 of I-SET.

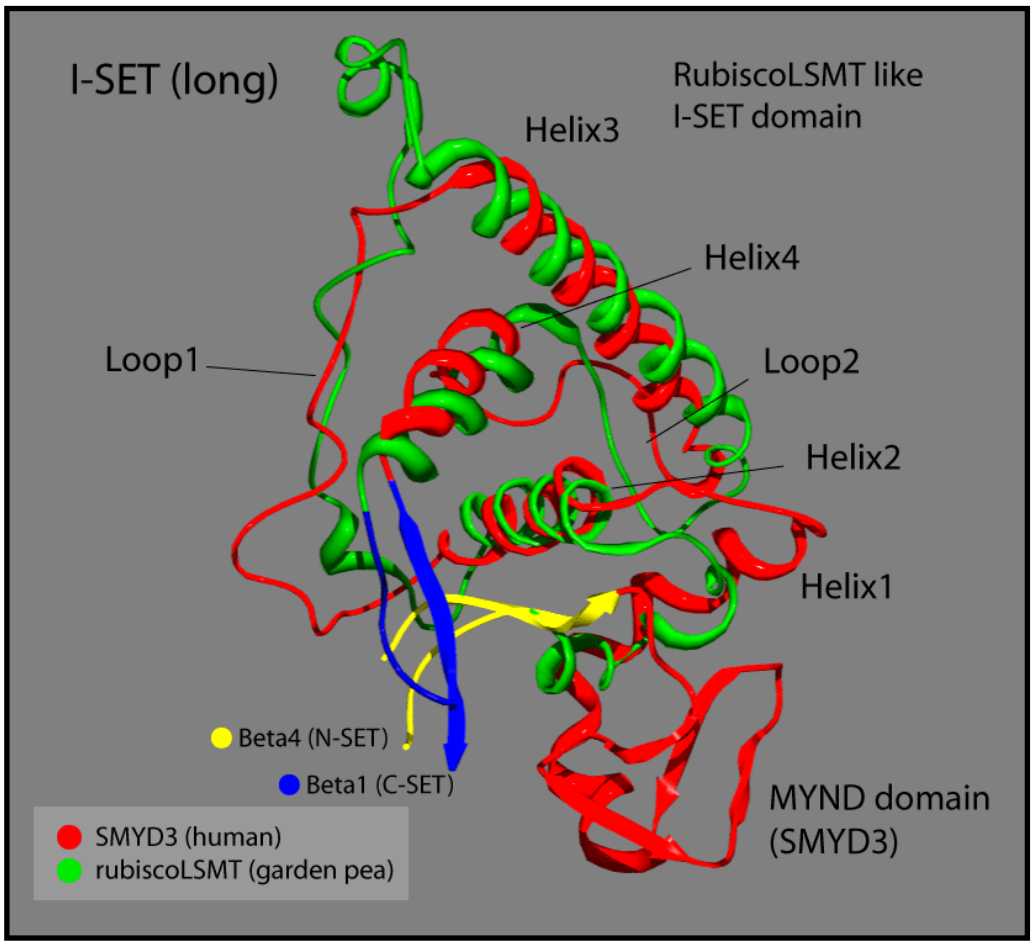

Figure 5.7 3D Ribbon Model of (Long) I-SET. Plant and animal comparison with corresponding colors. Overlay of human and garden pea I-SET. Distinctive homology illustrated in the helix 1-4 and loop 1 and 2 patterns.

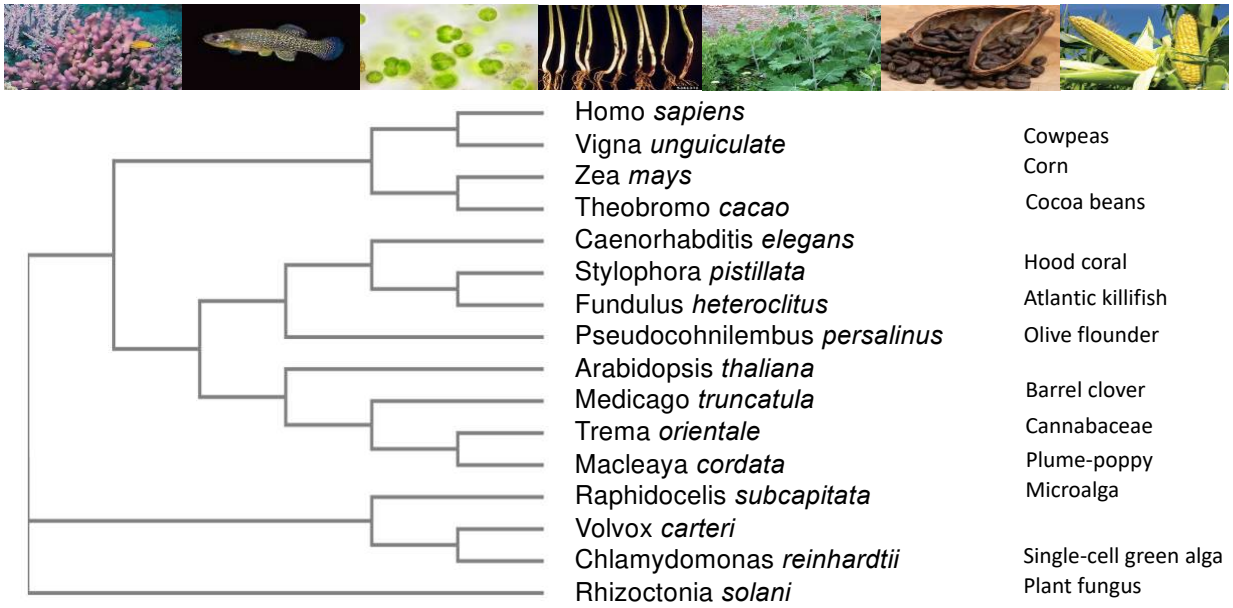

Figure 5.8 Phylogenetic Tree Analysis. Phylogenetic tree data analysis of Rubisco-LSMT protein domain illustrating the evolutionary lineage in various divergent species.

A)

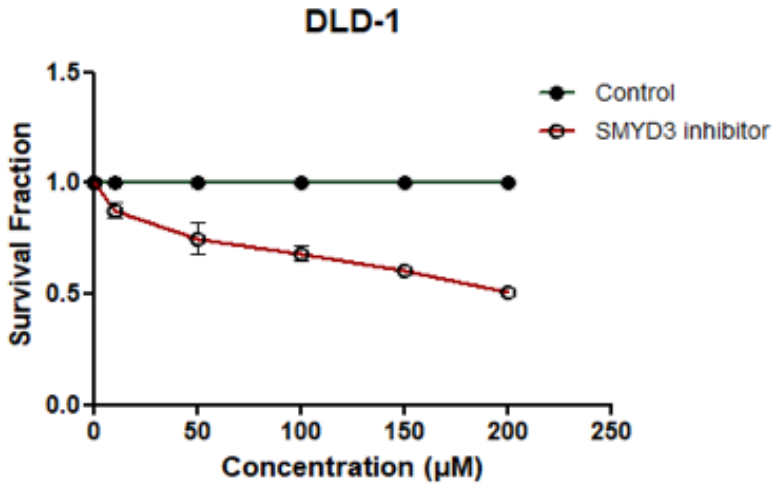

B)

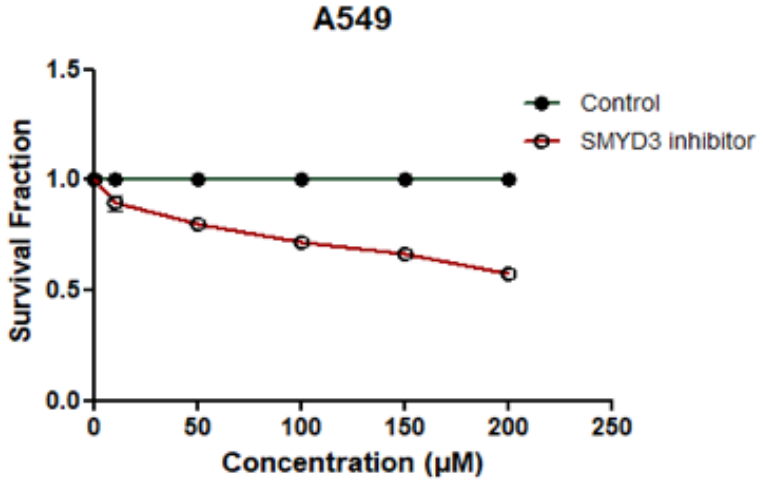

Figures 5.9A & 5.9B DLD-1 (colorectal) and A545 (lung) Colony Formation Assay**.** X-axis represents SMYD3 inhibitor [0.0 – 250.0μM], Y-axis represents survival fraction. Control in green, SMYD3 inhibitor in red.

A)

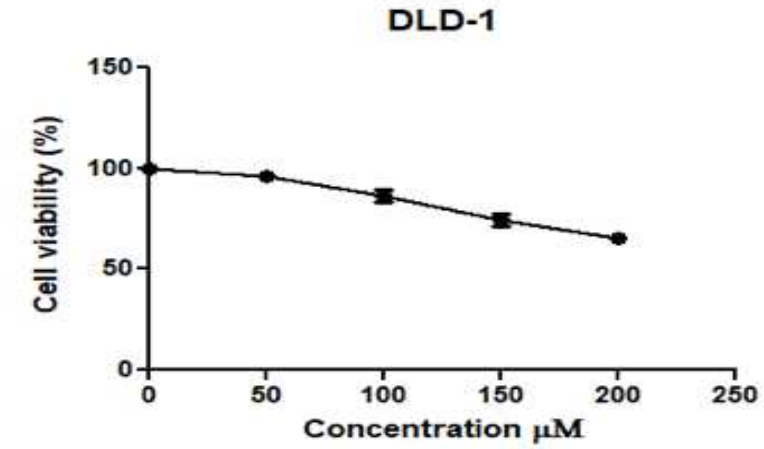

B)

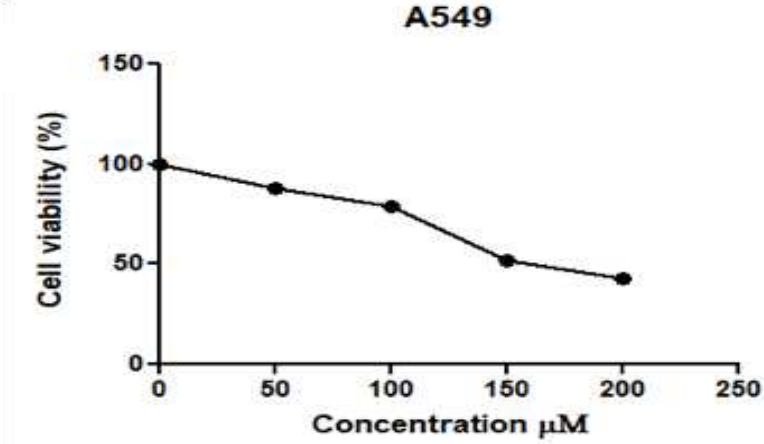

Figures 5.10A & 5.10B DLD-1 (colorectal) and A545 (lung) Viability Assay. X-axis represents SMYD3 inhibitor [0.0 – 250.0µM], Y-axis represents % cell viability. Control in green, SMYD3 inhibitor in red.

REFERENCES

(1) Herz, H.-M.; Garruss, A.; Shilatifard, A. SET for Life: Biochemical Activities and Biological Functions of SET Domain-Containing Proteins. *Trends in Biochemical Sciences* **2013**, *38* (12), 621–639. https://doi.org/10.1016/j.tibs.2013.09.004.

(2) Jaskelioff, M.; Peterson, C. L. Chromatin and Transcription: Histones Continue to Make Their Marks. *Nature Cell Biology* **2003**, *5* (5), 395–399. https://doi.org/10.1038/ncb0503-395.

(3) Fischle, W.; Wang, Y.; Allis, C. D. Histone and Chromatin Cross-Talk. *Current Opinion in Cell Biology* **2003**, *15* (2), 172–183. https://doi.org/10.1016/S0955-0674(03)00013-9.

(4) Margueron, R.; Trojer, P.; Reinberg, D. The Key to Development: Interpreting the Histone Code? *Current Opinion in Genetics & Development* **2005**, *15* (2), 163–176. https://doi.org/10.1016/j.gde.2005.01.005.

(5) Martin, C.; Zhang, Y. The Diverse Functions of Histone Lysine Methylation. *Nature Reviews Molecular Cell Biology* **2005**, *6* (11), 838–849. https://doi.org/10.1038/nrm1761.

(6) Lachner, M.; Jenuwein, T. The Many Faces of Histone Lysine Methylation. *Current Opinion in Cell Biology* **2002**, *14* (3), 286–298. https://doi.org/10.1016/S0955-0674(02)00335-6.

(7) Helin, K.; Dhanak, D. Chromatin Proteins and Modifications as Drug Targets. *Nature* **2013**, *502* (7472), 480–488. https://doi.org/10.1038/nature12751.

(8) Feng, Q.; Wang, H.; Ng, H. H.; Erdjument-Bromage, H.; Tempst, P.; Struhl, K.; Zhang, Y. Methylation of H3-Lysine 79 Is Mediated by a New Family of HMTases without a SET Domain. *Curr. Biol.* **2002**, *12* (12), 1052–1058. https://doi.org/10.1016/s0960-9822(02)00901-6.

(9) Strahl, B. D.; Ohba, R.; Cook, R. G.; Allis, C. D. Methylation of Histone H3 at Lysine 4 Is Highly Conserved and Correlates with Transcriptionally Active Nuclei in Tetrahymena. *Proceedings of the National Academy of Sciences* **1999**, *96* (26), 14967–14972. https://doi.org/10.1073/pnas.96.26.14967.

(10) Couture, J.F.; Hauk, G.; Thompson, M. J.; Blackburn, G. M.; Trievel, R. C. Catalytic Roles for Carbon-Oxygen Hydrogen Bonding in SET Domain Lysine Methyltransferases. *Journal of Biological Chemistry* **2006**, *281* (28), 19280–19287. https://doi.org/10.1074/jbc.M602257200.

(11) Dillon, S. C.; Zhang, X.; Trievel, R. C.; Cheng, X. The SET-Domain Protein Superfamily: Protein Lysine Methyltransferases. *Genome Biol.* **2005**, *6* (8), 227. https://doi.org/10.1186/gb-2005-6-8-227.

(12) Kouzarides, T. Histone Methylation in Transcriptional Control. *Current Opinion in Genetics & Development* **2002**, *12* (2), 198–209. https://doi.org/10.1016/S0959-437X(02)00287-3.

(13) Zhang, X.; Yang, Z.; Khan, S. I.; Horton, J. R.; Tamaru, H.; Selker, E. U.; Cheng, X. Structural Basis for the Product Specificity of Histone Lysine Methyltransferases. *Mol. Cell* **2003**, *12* (1), 177–185. https://doi.org/10.1016/s1097-2765(03)00224-7.

(14) Schapira, M. Structural Chemistry of Human SET Domain Protein Methyltransferases. *Current Chemical Genomics* **2011**, *5* (Suppl 1), 85–94. https://doi.org/10.2174/1875397301005010085.

(15) Rea, S.; Eisenhaber, F.; O'Carroll, D.; Strahl, B. D.; Sun, Z.-W.; Schmid, M.; Opravil, S.; Mechtler, K.; Ponting, C. P.; Allis, C. D.; Jenuwein, T. Regulation of Chromatin Structure by Site-Specific Histone H3 Methyltransferases. *Nature* **2000**, *406* (6796), 593–599. https://doi.org/10.1038/35020506.

(16) Trievel, R. C.; Flynn, E. M.; Houtz, R. L.; Hurley, J. H. Mechanism of Multiple Lysine Methylation by the SET Domain Enzyme Rubisco LSMT. *Nature Structural & Molecular Biology* **2003**, *10* (7), 545–552. https://doi.org/10.1038/nsb946.

(17) Baumbusch, L. O.; Thorstensen, T.; Krauss, V.; Fischer, A.; Naumann, K.; Assalkhou, R.; Schulz, I.; Reuter, G.; Aalen, R. B. The Arabidopsis Thaliana Genome Contains at Least 29 Active Genes Encoding SET Domain Proteins That Can Be Assigned to Four Evolutionarily Conserved Classes. *Nucleic Acids Res.* **2001**, *29* (21), 4319–4333. https://doi.org/10.1093/nar/29.21.4319.

(18) Schneider, G.; Lindqvist, Y.; Branden, C. I. Rubisco: Structure and Mechanism. *Annual Review of Biophysics and Biomolecular Structure* **1992**, *21* (1), 119–143. https://doi.org/10.1146/annurev.bb.21.060192.001003.

(19) Ma, S.; Martin-Laffon, J.; Mininno, M.; Gigarel, O.; Brugière, S.; Bastien, O.; Tardif, M.; Ravanel, S.; Alban, C. Molecular Evolution of the Substrate Specificity of Chloroplastic Aldolases/Rubisco Lysine Methyltransferases in Plants. *Molecular Plant* **2016**, *9* (4), 569–581. https://doi.org/10.1016/j.molp.2016.01.003.

(20) Qian, C.; Zhou, M.M. SET Domain Protein Lysine Methyltransferases: Structure, Specificity and Catalysis. *Cellular and Molecular Life Sciences* **2006**, *63* (23), 2755–2763. https://doi.org/10.1007/s00018-006-6274-5.

(21) Trievel, R. C.; Beach, B. M.; Dirk, L. M. A.; Houtz, R. L.; Hurley, J. H. Structure and Catalytic Mechanism of a SET Domain Protein Methyltransferase. *Cell* **2002**, *111* (1), 91–103. https://doi.org/10.1016/S0092-8674(02)01000-0.

(22) Spellmon, N.; Holcomb, J.; Trescott, L.; Sirinupong, N.; Yang, Z. Structure and Function of SET and MYND Domain-Containing Proteins. *International Journal of Molecular Sciences* **2015**, *16* (1), 1406–1428. https://doi.org/10.3390/ijms16011406.

(23) Saloura, V.; Vougiouklakis, T.; Sievers, C.; Burkitt, K.; Nakamura, Y.; Hager, G.; van Waes, C. The Role of Protein Methyltransferases as Potential Novel Therapeutic Targets in Squamous Cell Carcinoma of the Head and Neck. *Oral Oncology* **2018**, *81*, 100–108. https://doi.org/10.1016/j.oraloncology.2018.04.014.

(24) Hung, M.H.; Chen, K.F. Reprogramming the Oncogenic Response: SET Protein as a Potential Therapeutic Target in Cancer. *Expert Opinion on Therapeutic Targets* **2017**, *21* (7), 685–694. https://doi.org/10.1080/14728222.2017.1336226.

(25) An, S.; Yeo, K. J.; Jeon, Y. H.; Song, J.J. Crystal Structure of the Human Histone Methyltransferase ASH1L Catalytic Domain and Its Implications for the Regulatory Mechanism. *Journal of Biological Chemistry* **2011**, *286* (10), 8369–8374. https://doi.org/10.1074/jbc.M110.203380.

(26) Strahl, B. D.; Allis, C. D. The Language of Covalent Histone Modifications. *Nature* **2000**, *403* (6765), 41–45. https://doi.org/10.1038/47412.

(27) Liu, L.; Kimball, S.; Liu, H.; Holowatyj, A.; Yang, Z.Q. Genetic Alterations of Histone Lysine Methyltransferases and Their Significance in Breast Cancer. *Oncotarget* **2015**, *6* (4), 2466–2482. https://doi.org/10.18632/oncotarget.2967.

(28) Shankar, S. R.; Bahirvani, A. G.; Rao, V. K.; Bharathy, N.; Ow, J. R.; Taneja, R. G9a, a Multipotent Regulator of Gene Expression. *Epigenetics* **2013**, *8* (1), 16–22. https://doi.org/10.4161/epi.23331.

(29) Tachibana, M.; Sugimoto, K.; Fukushima, T.; Shinkai, Y. Set Domain-Containing Protein, G9a, Is a Novel Lysine-Preferring Mammalian Histone Methyltransferase with Hyperactivity and Specific Selectivity to Lysines 9 and 27 of Histone H3. *J. Biol. Chem.* **2001**, *276* (27), 25309–25317. https://doi.org/10.1074/jbc.M101914200.

(30) Lui, J. C.; Garrison, P.; Nguyen, Q.; Ad, M.; Keembiyehetty, C.; Chen, W.; Jee, Y. H.; Landman, E.; Nilsson, O.; Barnes, K. M.; Baron, J. EZH1 and EZH2 Promote Skeletal Growth by Repressing Inhibitors of Chondrocyte Proliferation and Hypertrophy. *Nat Commun* **2016**, *7*, 13685. https://doi.org/10.1038/ncomms13685.

(31) Ezhkova, E.; Lien, W.H.; Stokes, N.; Pasolli, H. A.; Silva, J. M.; Fuchs, E. EZH1 and EZH2 Cogovern Histone H3K27 Trimethylation and Are Essential for Hair Follicle Homeostasis and Wound Repair. *Genes Dev.* **2011**, *25* (5), 485–498. https://doi.org/10.1101/gad.2019811.

(32) Shen, X.; Liu, Y.; Hsu, Y.J.; Fujiwara, Y.; Kim, J.; Mao, X.; Yuan, G.C.; Orkin, S. H. EZH1 Mediates Methylation on Histone H3 Lysine 27 and Complements EZH2 in Maintaining Stem Cell Identity and Executing Pluripotency. *Mol. Cell* **2008**, *32* (4), 491–502. https://doi.org/10.1016/j.molcel.2008.10.016.

(33) Mavaddat, N.; Dunning, A. M.; Ponder, B. A. J.; Easton, D. F.; Pharoah, P. D. Common Genetic Variation in Candidate Genes and Susceptibility to Subtypes of Breast Cancer. *Cancer Epidemiology Biomarkers & Prevention* **2009**, *18* (1), 255–259. https://doi.org/10.1158/1055-9965.EPI-08-0704.

(34) Rabello, D. D. A.; De Moura, C. A.; De Andrade, R. V.; Motoyama, A. B.; Silva, F. P. Altered Expression of MLL Methyltransferase Family Genes in Breast Cancer. *International Journal of Oncology* **2013**, *43* (2), 653–660. https://doi.org/10.3892/ijo.2013.1981.

(35) Deng, H.; Lei, Z. Preparation and Characterization of Hollow Fe3O4/SiO2PEG–PLA Nanoparticles for Drug Delivery. *Composites Part B: Engineering* **2013**, *54*, 194–199. https://doi.org/10.1016/j.compositesb.2013.05.010.

(36) Ayton, P. M.; Cleary, M. L. Molecular Mechanisms of Leukemogenesis Mediated by MLL Fusion Proteins. *Oncogene* **2001**, *20* (40), 5695–5707. https://doi.org/10.1038/sj.onc.1204639.

(37) McKinnell, I. W.; Ishibashi, J.; Le Grand, F.; Punch, V. G. J.; Addicks, G. C.; Greenblatt, J. F.; Dilworth, F. J.; Rudnicki, M. A. Pax7 Activates Myogenic Genes by Recruitment of a Histone Methyltransferase Complex. *Nature Cell Biology* **2008**, *10* (1), 77–84. https://doi.org/10.1038/ncb1671.

(38) Lee, J.; Kim, D.H.; Lee, S.; Yang, Q.H.; Lee, D. K.; Lee, S.K.; Roeder, R. G.; Lee, J. W. A Tumor Suppressive Coactivator Complex of P53 Containing ASC-2 and Histone H3-Lysine-4 Methyltransferase MLL3 or Its Paralogue MLL4. *Proceedings of the National Academy of Sciences* **2009**, *106* (21), 8513–8518. https://doi.org/10.1073/pnas.0902873106.

(39) Emerling, B. M.; Bonifas, J.; Kratz, C. P.; Donovan, S.; Taylor, B. R.; Green, E. D.; Le Beau, M. M.; Shannon, K. M. MLL5, a Homolog of Drosophila Trithorax Located within a Segment of Chromosome Band 7q22 Implicated in Myeloid Leukemia. *Oncogene* **2002**, *21* (31), 4849–4854. https://doi.org/10.1038/sj.onc.1205615.

(40) Sebastian, S.; Sreenivas, P.; Sambasivan, R.; Cheedipudi, S.; Kandalla, P.; Pavlath, G. K.; Dhawan, J. MLL5, a Trithorax Homolog, Indirectly Regulates H3K4 Methylation, Represses Cyclin A2 Expression, and Promotes Myogenic

Differentiation. *Proceedings of the National Academy of Sciences* **2009**, *106* (12), 4719–4724. https://doi.org/10.1073/pnas.0807136106.

(41) Tatton-Brown, K.; Rahman, N. The NSD1 and EZH2 Overgrowth Genes, Similarities and Differences. *Am J Med Genet C Semin Med Genet* **2013**, *163C* (2), 86–91. https://doi.org/10.1002/ajmg.c.31359.

(42) Huang, N. Two Distinct Nuclear Receptor Interaction Domains in NSD1, a Novel SET Protein That Exhibits Characteristics of Both Corepressors and Coactivators. *The EMBO Journal* **1998**, *17* (12), 3398–3412. https://doi.org/10.1093/emboj/17.12.3398.

(43) Wagner, E. J.; Carpenter, P. B. Understanding the Language of Lys36 Methylation at Histone H3. *Nature Reviews Molecular Cell Biology* **2012**, *13* (2), 115–126. https://doi.org/10.1038/nrm3274.

(44) Yi, L.; Yi, L.; Liu, Q.; Li, C. Downregulation of NSD3 (WHSC1L1) Inhibits Cell Proliferation and Migration via ERK1/2 Deactivation and Decreasing CAPG Expression in Colorectal Cancer Cells. *OncoTargets and Therapy* **2019**, *Volume 12*, 3933–3943. https://doi.org/10.2147/OTT.S191732.

(45) Kang, D.; Cho, H.S.; Toyokawa, G.; Kogure, M.; Yamane, Y.; Iwai, Y.; Hayami, S.; Tsunoda, T.; Field, H. I.; Matsuda, K.; Neal, D. E.; Ponder, B. A. J.; Maehara, Y.; Nakamura, Y.; Hamamoto, R. The Histone Methyltransferase Wolf-Hirschhorn Syndrome Candidate 1-like 1 (WHSC1L1) Is Involved in Human Carcinogenesis. *Genes, Chromosomes and Cancer* **2013**, *52* (2), 126–139. https://doi.org/10.1002/gcc.22012.

(46) Rona, G. B.; Almeida, D. S. G.; Pinheiro, A. S.; Eleutherio, E. C. A. The PWWP Domain of the Human Oncogene WHSC1L1/NSD3 Induces a Metabolic Shift toward Fermentation. *Oncotarget* **2017**, *8* (33). https://doi.org/10.18632/oncotarget.11253.

(47) Tajima, K.; Matsuda, S.; Yae, T.; Drapkin, B. J.; Morris, R.; Boukhali, M.; Niederhoffer, K.; Comaills, V.; Dubash, T.; Nieman, L.; Guo, H.; Magnus, N. K. C.; Dyson, N.; Shioda, T.; Haas, W.; Haber, D. A.; Maheswaran, S. SETD1A Protects from Senescence through Regulation of the Mitotic Gene Expression Program.

Nature Communications **2019**, *10* (1). https://doi.org/10.1038/s41467-019-10786-w.

(48) Shilatifard, A. The COMPASS Family of Histone H3K4 Methylases: Mechanisms of Regulation in Development and Disease Pathogenesis. *Annual Review of Biochemistry* **2012**, *81* (1), 65–95. https://doi.org/10.1146/annurev-biochem-051710-134100.

(49) Tajima, K.; Yae, T.; Javaid, S.; Tam, O.; Comaills, V.; Morris, R.; Wittner, B. S.; Liu, M.; Engstrom, A.; Takahashi, F.; Black, J. C.; Ramaswamy, S.; Shioda, T.; Hammell, M.; Haber, D. A.; Whetstine, J. R.; Maheswaran, S. SETD1A Modulates Cell Cycle Progression through a MiRNA Network That Regulates P53 Target Genes. *Nature Communications* **2015**, *6* (1). https://doi.org/10.1038/ncomms9257.

(50) Jin, M. L.; Kim, Y. W.; Jin, H. L.; Kang, H.; Lee, E. K.; Stallcup, M. R.; Jeong, K. W. Aberrant Expression of SETD1A Promotes Survival and Migration of Estrogen Receptor α-Positive Breast Cancer Cells: SETD1A in ERα-Positive Breast Cancer Cells. *International Journal of Cancer* **2018**, *143* (11), 2871–2883. https://doi.org/10.1002/ijc.31853.

(51) Yuan, H.; Li, N.; Fu, D.; Ren, J.; Hui, J.; Peng, J.; Liu, Y.; Qiu, T.; Jiang, M.; Pan, Q.; Han, Y.; Wang, X.; Li, Q.; Qin, J. Histone Methyltransferase SETD2 Modulates Alternative Splicing to Inhibit Intestinal Tumorigenesis. *Journal of Clinical Investigation* **2017**, *127* (9), 3375–3391. https://doi.org/10.1172/JCI94292.

(52) Park, I. Y.; Powell, R. T.; Tripathi, D. N.; Dere, R.; Ho, T. H.; Blasius, T. L.; Chiang, Y.-C.; Davis, I. J.; Fahey, C. C.; Hacker, K. E.; Verhey, K. J.; Bedford, M. T.; Jonasch, E.; Rathmell, W. K.; Walker, C. L. Dual Chromatin and Cytoskeletal Remodeling by SETD2. *Cell* **2016**, *166* (4), 950–962. https://doi.org/10.1016/j.cell.2016.07.005.

(53) Simon, J. M.; Hacker, K. E.; Singh, D.; Brannon, A. R.; Parker, J. S.; Weiser, M.; Ho, T. H.; Kuan, P. F.; Jonasch, E.; Furey, T. S.; Prins, J. F.; Lieb, J. D.; Rathmell, W. K.; Davis, I. J. Variation in Chromatin Accessibility in Human Kidney Cancer Links H3K36 Methyltransferase Loss with Widespread RNA Processing Defects. *Genome Research* **2014**, *24* (2), 241–250. https://doi.org/10.1101/gr.158253.113.

(54) Kwiatkowski, S.; Seliga, A. K.; Vertommen, D.; Terreri, M.; Ishikawa, T.; Grabowska, I.; Tiebe, M.; Teleman, A. A.; Jagielski, A. K.; Veiga-da-Cunha, M.; Drozak, J. SETD3 Protein Is the Actin-Specific Histidine N-Methyltransferase. *eLife* **2018**, *7*. https://doi.org/10.7554/eLife.37921.

(55) Chen, Z.; Yan, C. T.; Dou, Y.; Viboolsittiseri, S. S.; Wang, J. H. The Role of a Newly Identified SET Domain-Containing Protein, SETD3, in Oncogenesis. *Haematologica* **2013**, *98* (5), 739–743. https://doi.org/10.3324/haematol.2012.066977.

(56) Eom, G. H.; Kim, K. B.; Kim, J. H.; Kim, J. Y.; Kim, J. R.; Kee, H. J.; Kim, D. W.; Choe, N.; Park, H. J.; Son, H. J.; Choi, S. Y.; Kook, H.; Seo, S. B. Histone Methyltransferase SETD3 Regulates Muscle Differentiation. *Journal of Biological Chemistry* **2011**, *286* (40), 34733–34742. https://doi.org/10.1074/jbc.M110.203307.

(57) Guo, Q.; Liao, S.; Kwiatkowski, S.; Tomaka, W.; Yu, H.; Wu, G.; Tu, X.; Min, J.; Drozak, J.; Xu, C. Structural Insights into SETD3-Mediated Histidine Methylation on β-Actin. *eLife* **2019**, *8*. https://doi.org/10.7554/eLife.43676.

(58) Abaev-Schneiderman, E.; Admoni-Elisha, L.; Levy, D. SETD3 Is a Positive Regulator of DNA-Damage-Induced Apoptosis. *Cell Death & Disease* **2019**, *10* (2). https://doi.org/10.1038/s41419-019-1328-4.

(59) Dai, S.; Horton, J. R.; Woodcock, C. B.; Wilkinson, A. W.; Zhang, X.; Gozani, O.; Cheng, X. Structural Basis for the Target Specificity of Actin Histidine Methyltransferase SETD3. *Nature Communications* **2019**, *10* (1). https://doi.org/10.1038/s41467-019-11554-6.

(60) Faria, J. A. Q. A.; Corrêa, N. C. R.; de Andrade, C.; de Angelis Campos, A. C.; Dos Santos Samuel de Almeida, R.; Rodrigues, T. S.; de Goes, A. M.; Gomes, D. A.; Silva, F. P. SET Domain-Containing Protein 4 (SETD4) Is a Newly Identified Cytosolic and Nuclear Lysine Methyltransferase Involved in Breast Cancer Cell Proliferation. *J Cancer Sci Ther* **2013**, *5* (2), 58–65.

(61) Zhong, Y.; Ye, P.; Mei, Z.; Huang, S.; Huang, M.; Li, Y.; Niu, S.; Zhao, S.; Cai, J.; Wang, J.; Zou, H.; Jiang, Y.; Liu, J. The Novel Methyltransferase SETD4 Regulates TLR Agonist-Induced Expression of Cytokines through Methylation of

Lysine 4 at Histone 3 in Macrophages. *Molecular Immunology* **2019**, *114*, 179–188. https://doi.org/10.1016/j.molimm.2019.07.011.

(62) Yu, H.; Sun, J.; Zhao, C.; Wang, H.; Liu, Y.; Xiong, J.; Chang, J.; Wang, M.; Wang, W.; Ye, D.; Zhou, H.; Yu, T. SET Domain Containing Protein 5 (SETD5) Enhances Tumor Cell Invasion and Is Associated with a Poor Prognosis in Non-Small Cell Lung Cancer Patients. *BMC Cancer* **2019**, *19* (1), 736. https://doi.org/10.1186/s12885-019-5944-2.

(63) O'Neill, D. J.; Williamson, S. C.; Alkharaif, D.; Monteiro, I. C. M.; Goudreault, M.; Gaughan, L.; Robson, C. N.; Gingras, A. C.; Binda, O. SETD6 Controls the Expression of Estrogen-Responsive Genes and Proliferation of Breast Carcinoma Cells. *Epigenetics* **2014**, *9* (7), 942–950. https://doi.org/10.4161/epi.28864.

(64) Levy, D.; Kuo, A. J.; Chang, Y.; Schaefer, U.; Kitson, C.; Cheung, P.; Espejo, A.; Zee, B. M.; Liu, C. L.; Tangsombatvisit, S.; Tennen, R. I.; Kuo, A. Y.; Tanjing, S.; Cheung, R.; Chua, K. F.; Utz, P. J.; Shi, X.; Prinjha, R. K.; Lee, K.; Garcia, B. A.; Bedford, M. T.; Tarakhovsky, A.; Cheng, X.; Gozani, O. Lysine Methylation of the NF-KB Subunit RelA by SETD6 Couples Activity of the Histone Methyltransferase GLP at Chromatin to Tonic Repression of NF-KB Signaling. *Nature Immunology* **2011**, *12* (1), 29–36. https://doi.org/10.1038/ni.1968.

(65) Castaño, J.; Morera, C.; Sesé, B.; Boue, S.; Bonet-Costa, C.; Martí, M.; Roque, A.; Jordan, A.; Barrero, M. J. SETD7 Regulates the Differentiation of Human Embryonic Stem Cells. *PLoS ONE* **2016**, *11* (2), e0149502. https://doi.org/10.1371/journal.pone.0149502.

(66) Luo, M. Chemical and Biochemical Perspectives of Protein Lysine Methylation. *Chem. Rev.* **2018**, *118* (14), 6656–6705. https://doi.org/10.1021/acs.chemrev.8b00008.

(67) Wilson, J. R.; Jing, C.; Walker, P. A.; Martin, S. R.; Howell, S. A.; Blackburn, G. M.; Gamblin, S. J.; Xiao, B. Crystal Structure and Functional Analysis of the Histone Methyltransferase SET7/9. *Cell* **2002**, *111* (1), 105–115. https://doi.org/10.1016/S0092-8674(02)00964-9.

(68) Blum, G.; Ibáñez, G.; Rao, X.; Shum, D.; Radu, C.; Djaballah, H.; Rice, J. C.; Luo, M. Small-Molecule Inhibitors of SETD8 with Cellular Activity. *ACS Chemical Biology* **2014**, *9* (11), 2471–2478. https://doi.org/10.1021/cb500515r.

(69) Goodman, R. H.; Smolik, S. CBP/P300 in Cell Growth, Transformation, and Development. *Genes Dev.* **2000**, *14* (13), 1553–1577.

(70) Chakravarti, D.; Ogryzko, V.; Kao, H. Y.; Nash, A.; Chen, H.; Nakatani, Y.; Evans, R. M. A Viral Mechanism for Inhibition of P300 and PCAF Acetyltransferase Activity. *Cell* **1999**, *96* (3), 393–403. https://doi.org/10.1016/S0092-8674(00)80552-8.

(71) Pagans, S.; Kauder, S. E.; Kaehlcke, K.; Sakane, N.; Schroeder, S.; Dormeyer, W.; Trievel, R. C.; Verdin, E.; Schnolzer, M.; Ott, M. The Cellular Lysine Methyltransferase Set7/9-KMT7 Binds HIV-1 TAR RNA, Monomethylates the Viral Transactivator Tat, and Enhances HIV Transcription. *Cell Host & Microbe* **2010**, *7* (3), 234–244. https://doi.org/10.1016/j.chom.2010.02.005.

(72) Pradhan, S.; Chin, H. G.; Estève, P. O.; Jacobsen, S. E. SET7/9 Mediated Methylation of Non-Histone Proteins in Mammalian Cells. *Epigenetics* **2009**, *4* (6), 383–387. https://doi.org/10.4161/epi.4.6.9450.

(73) Dhayalan, A.; Kudithipudi, S.; Rathert, P.; Jeltsch, A. Specificity Analysis-Based Identification of New Methylation Targets of the SET7/9 Protein Lysine Methyltransferase. *Chemistry & Biology* **2011**, *18* (1), 111–120. https://doi.org/10.1016/j.chembiol.2010.11.014.

(74) Cruz-Tapias; Robin; Pontis; Maestro; Ait-Si-Ali. The H3K9 Methylation Writer SETDB1 and Its Reader MPP8 Cooperate to Silence Satellite DNA Repeats in Mouse Embryonic Stem Cells. *Genes* **2019**, *10* (10), 750. https://doi.org/10.3390/genes10100750.

(75) Ropa, J.; Saha, N.; Hu, H.; Peterson, L. F.; Talpaz, M.; Muntean, A. G. SETDB1 Mediated Histone H3 Lysine 9 Methylation Suppresses MLL-Fusion Target Expression and Leukemic Transformation. *Haematologica* **2019**. https://doi.org/10.3324/haematol.2019.223883.

(76) Tsusaka, T.; Shimura, C.; Shinkai, Y. ATF7IP Regulates SETDB1 Nuclear Localization and Increases Its Ubiquitination. *EMBO Rep.* **2019**, *20* (12), e48297. https://doi.org/10.15252/embr.201948297.

(77) Torrano, J.; Al Emran, A.; Hammerlindl, H.; Schaider, H. Emerging Roles of H3K9me3, SETDB1 and SETDB2 in Therapy-Induced Cellular Reprogramming. *Clin Epigenetics* **2019**, *11* (1), 43. https://doi.org/10.1186/s13148-019-0644-y.

(78) Jaiswal, D.; Turniansky, R.; Moresco, J. J.; Ikram, S.; Ramaprasad, G.; Akinwole, A.; Wolf, J.; Yates, J. R.; Green, Erin. M. Function of the MYND Domain and C-Terminal Region in Regulating the Subcellular Localization and Catalytic Activity of the SMYD Family Lysine Methyltransferase Set5. *Molecular and Cellular Biology* **2019**. https://doi.org/10.1128/MCB.00341-19.

(79) Tracy, C. M.; Warren, J. S.; Szulik, M.; Wang, L.; Garcia, J.; Makaju, A.; Russell, K.; Miller, M.; Franklin, S. The Smyd Family of Methyltransferases: Role in Cardiac and Skeletal Muscle Physiology and Pathology. *Current Opinion in Physiology* **2018**, *1*, 140–152. https://doi.org/10.1016/j.cophys.2017.10.001.

(80) Leinhart, K.; Brown, M. SET/MYND Lysine Methyltransferases Regulate Gene Transcription and Protein Activity. *Genes* **2011**, *2* (1), 210–218. https://doi.org/10.3390/genes2010210.

(81) Doughan, M.; Spellmon, N.; Li, C.; Yang, Z.; 1 Department of Biochemistry and Molecular Biology, Wayne State University School of Medicine, Detroit, MI, USA. SMYD Proteins in Immunity: Dawning of a New Era. *AIMS Biophysics* **2016**, *3* (4), 450–455. https://doi.org/10.3934/biophy.2016.4.450.

(82) Rasmussen, T. L.; Tucker, H. O. Loss of SMYD1 Results in Perinatal Lethality via Selective Defects within Myotonic Muscle Descendants. *Diseases* **2018**, *7* (1). https://doi.org/10.3390/diseases7010001.

(83) Chow, M. Z.-Y.; Sadrian, S. N.; Keung, W.; Geng, L.; Ren, L.; Kong, C.-W.; Wong, A. O.-T.; Hulot, J.-S.; Chen, C. S.; Costa, K. D.; Hajjar, R. J.; Li, R. A. Modulation of Chromatin Remodeling Proteins SMYD1 and SMARCD1 Promotes Contractile Function of Human Pluripotent Stem Cell-Derived Ventricular Cardiomyocyte in 3D-Engineered Cardiac Tissues. *Sci Rep* **2019**, *9* (1), 7502. https://doi.org/10.1038/s41598-019-42953-w.

(84) Du, S. J.; Tan, X.; Zhang, J. SMYD Proteins: Key Regulators in Skeletal and Cardiac Muscle Development and Function. *Anat Rec (Hoboken)* **2014**, *297* (9), 1650–1662. https://doi.org/10.1002/ar.22972.

(85) Warren, J. S.; Tracy, C. M.; Miller, M. R.; Makaju, A.; Szulik, M. W.; Oka, S.; Yuzyuk, T. N.; Cox, J. E.; Kumar, A.; Lozier, B. K.; Wang, L.; Llana, J. G.; Sabry, A. D.; Cawley, K. M.; Barton, D. W.; Han, Y. H.; Boudina, S.; Fiehn, O.; Tucker, H. O.; Zaitsev, A. V.; Franklin, S. Histone Methyltransferase Smyd1 Regulates Mitochondrial Energetics in the Heart. *Proceedings of the National Academy of Sciences* **2018**, *115* (33), E7871–E7880. https://doi.org/10.1073/pnas.1800680115.

(86) Brown, M. A.; Sims, R. J.; Gottlieb, P. D.; Tucker, P. W. Identification and Characterization of Smyd2: A Split SET/MYND Domain-Containing Histone H3 Lysine 36-Specific Methyltransferase That Interacts with the Sin3 Histone Deacetylase Complex. *Mol. Cancer* **2006**, *5*, 26. https://doi.org/10.1186/1476-4598-5-26.

(87) Yi, X.; Jiang, X. J.; Fang, Z. M. Histone Methyltransferase SMYD2: Ubiquitous Regulator of Disease. *Clin Epigenetics* **2019**, *11* (1), 112. https://doi.org/10.1186/s13148-019-0711-4.

(88) Sun, J. J.; Li, H. L.; Ma, H.; Shi, Y.; Yin, L. R.; Guo, S. J. SMYD2 Promotes Cervical Cancer Growth by Stimulating Cell Proliferation. *Cell & Bioscience* **2019**, *9* (1). https://doi.org/10.1186/s13578-019-0340-9.

(89) Abu-Farha, M.; Lambert, J.-P.; Al-Madhoun, A. S.; Elisma, F.; Skerjanc, I. S.; Figeys, D. The Tale of Two Domains: Proteomics and Genomics Analysis of SMYD2, A New Histone Methyltransferase. *Molecular & Cellular Proteomics* **2008**, *7* (3), 560–572. https://doi.org/10.1074/mcp.M700271-MCP200.

(90) Sesé, B.; Barrero, M. J.; Fabregat, M. C.; Sander, V.; Izpisua Belmonte, J. C. SMYD2 Is Induced during Cell Differentiation and Participates in Early Development. *The International Journal of Developmental Biology* **2013**, *57* (5), 357–364. https://doi.org/10.1387/ijdb.130051ji.

(91) Chandramouli, B.; Silvestri, V.; Scarno, M.; Ottini, L.; Chillemi, G. Smyd3 Open & Closed Lock Mechanism for Substrate Recruitment: The Hinge Motion of C-Terminal Domain Inferred from μ-Second Molecular Dynamics Simulations. *Biochimica et Biophysica Acta (BBA) - General Subjects* **2016**, *1860* (7), 1466–1474. https://doi.org/10.1016/j.bbagen.2016.04.006.

(92) Codato, R.; Perichon, M.; Divol, A.; Fung, E.; Sotiropoulos, A.; Bigot, A.; Weitzman, J. B.; Medjkane, S. The SMYD3 Methyltransferase Promotes Myogenesis by Activating the Myogenin Regulatory Network. *Scientific Reports* **2019**, *9* (1). https://doi.org/10.1038/s41598-019-53577-5.

(93) Foreman, K. W.; Brown, M.; Park, F.; Emtage, S.; Harriss, J.; Das, C.; Zhu, L.; Crew, A.; Arnold, L.; Shaaban, S.; Tucker, P. Structural and Functional Profiling of the Human Histone Methyltransferase SMYD3. *PLoS ONE* **2011**, *6* (7), e22290. https://doi.org/10.1371/journal.pone.0022290.

(94) Fu, W.; Liu, N.; Qiao, Q.; Wang, M.; Min, J.; Zhu, B.; Xu, R. M.; Yang, N. Structural Basis for Substrate Preference of SMYD3, a SET Domain-Containing Protein Lysine Methyltransferase. *Journal of Biological Chemistry* **2016**, *291* (17), 9173–9180. https://doi.org/10.1074/jbc.M115.709832.

(95) Giakountis, A.; Moulos, P.; Sarris, M. E.; Hatzis, P.; Talianidis, I. Smyd3-Associated Regulatory Pathways in Cancer. *Seminars in Cancer Biology* **2017**, *42*, 70–80. https://doi.org/10.1016/j.semcancer.2016.08.008.

(96) Lyu, T.; Jiang, Y.; Jia, N.; Che, X.; Li, Q.; Yu, Y.; Hua, K.; Bast, R. C.; Feng, W. SMYD3 Promotes Implant Metastasis of Ovarian Cancer *via* H3K4 Trimethylation of Integrin Promoters. *International Journal of Cancer* **2019**. https://doi.org/10.1002/ijc.32673.

(97) Van Aller, G. S.; Graves, A. P.; Elkins, P. A.; Bonnette, W. G.; McDevitt, P. J.; Zappacosta, F.; Annan, R. S.; Dean, T. W.; Su, D. S.; Carpenter, C. L.; Mohammad, H. P.; Kruger, R. G. Structure-Based Design of a Novel SMYD3 Inhibitor That Bridges the SAM-and MEKK2-Binding Pockets. *Structure* **2016**, *24* (5), 774–781. https://doi.org/10.1016/j.str.2016.03.010.

(98) Wu, X.; Xu, Q.; Chen, P.; Yu, C.; Ye, L.; Huang, C.; Li, T. Effect of SMYD3 on Biological Behavior and H3K4 Methylation in Bladder Cancer. *Cancer*

Management and Research **2019**, *Volume 11*, 8125–8133. https://doi.org/10.2147/CMAR.S213885.

(99) Huang, L.; Xu, A. M. SET and MYND Domain Containing Protein 3 in Cancer. *Am J Transl Res* **2017**, *9* (1), 1–14.

(100) Peserico, A.; Germani, A.; Sanese, P.; Barbosa, A. J.; Di Virgilio, V.; Fittipaldi, R.; Fabini, E.; Bertucci, C.; Varchi, G.; Moyer, M. P.; Caretti, G.; Del Rio, A.; Simone, C. A SMYD3 Small-Molecule Inhibitor Impairing Cancer Cell Growth: INHIBITING SMYD3 FOR CANCER THERAPY. *Journal of Cellular Physiology* **2015**, *230* (10), 2447–2460. https://doi.org/10.1002/jcp.24975.

(101) Hu, L.; Zhu, Y. T.; Qi, C.; Zhu, Y. J. Identification of Smyd4 as a Potential Tumor Suppressor Gene Involved in Breast Cancer Development. *Cancer Research* **2009**, *69* (9), 4067–4072. https://doi.org/10.1158/0008-5472.CAN-08-4097.

(102) Xiao, D.; Wang, H.; Hao, L.; Guo, X.; Ma, X.; Qian, Y.; Chen, H.; Ma, J.; Zhang, J.; Sheng, W.; Shou, W.; Huang, G.; Ma, D. The Roles of SMYD4 in Epigenetic Regulation of Cardiac Development in Zebrafish. *PLOS Genetics* **2018**, *14* (8), e1007578. https://doi.org/10.1371/journal.pgen.1007578.

(103) Fujii, T.; Tsunesumi, S.; Sagara, H.; Munakata, M.; Hisaki, Y.; Sekiya, T.; Furukawa, Y.; Sakamoto, K.; Watanabe, S. Smyd5 Plays Pivotal Roles in Both Primitive and Definitive Hematopoiesis during Zebrafish Embryogenesis. *Scientific Reports* **2016**, *6* (1). https://doi.org/10.1038/srep29157.

(104) Kidder, B. L.; He, R.; Wangsa, D.; Padilla-Nash, H. M.; Bernardo, M. M.; Sheng, S.; Ried, T.; Zhao, K. SMYD5 Controls Heterochromatin and Chromosome Integrity during Embryonic Stem Cell Differentiation. *Cancer Research* **2017**, *77* (23), 6729–6745. https://doi.org/10.1158/0008-5472.CAN-17-0828.

(105) Kidder, B. L.; Hu, G.; Cui, K.; Zhao, K. SMYD5 Regulates H4K20me3-Marked Heterochromatin to Safeguard ES Cell Self-Renewal and Prevent Spurious Differentiation. *Epigenetics & Chromatin* **2017**, *10* (1). https://doi.org/10.1186/s13072-017-0115-7.

(106) Santos-Barriopedro, I.; Bosch-Presegué, L.; Marazuela-Duque, A.; de la Torre, C.; Colomer, C.; Vazquez, B. N.; Fuhrmann, T.; Martínez-Pastor, B.; Lu, W.; Braun, T.; Bober, E.; Jenuwein, T.; Serrano, L.; Esteller, M.; Chen, Z.; Barceló-Batllori, S.; Mostoslavsky, R.; Espinosa, L.; Vaquero, A. SIRT6-Dependent Cysteine Monoubiquitination in the PRE-SET Domain of Suv39h1 Regulates the NF-KB Pathway. *Nat Commun* **2018**, *9* (1), 101. https://doi.org/10.1038/s41467-017-02586-x.

(107) Wang, D.; Zhou, J.; Liu, X.; Lu, D.; Shen, C.; Du, Y.; Wei, F.-Z.; Song, B.; Lu, X.; Yu, Y.; Wang, L.; Zhao, Y.; Wang, H.; Yang, Y.; Akiyama, Y.; Zhang, H.; Zhu, W. G. Methylation of SUV39H1 by SET7/9 Results in Heterochromatin Relaxation and Genome Instability. *Proceedings of the National Academy of Sciences* **2013**, *110* (14), 5516–5521. https://doi.org/10.1073/pnas.1216596110.

(108) Park, S. H.; Yu, S. E.; Chai, Y. G.; Jang, Y. K. CDK2-Dependent Phosphorylation of Suv39H1 Is Involved in Control of Heterochromatin Replication during Cell Cycle Progression. *Nucleic Acids Research* **2014**, *42* (10), 6196–6207. https://doi.org/10.1093/nar/gku263.

(109) Zheng, Y.; Li, B.; Wang, J.; Xiong, Y.; Wang, K.; Qi, Y.; Sun, H.; Wu, L.; Yang, L. Identification of SUV39H2 as a Potential Oncogene in Lung Adenocarcinoma. *Clin Epigenetics* **2018**, *10* (1), 129. https://doi.org/10.1186/s13148-018-0562-4.

(110) O'Carroll, D.; Scherthan, H.; Peters, A. H. F. M.; Opravil, S.; Haynes, A. R.; Laible, G.; Rea, S.; Schmid, M.; Lebersorger, A.; Jerratsch, M.; Sattler, L.; Mattei, M. G.; Denny, P.; Brown, S. D. M.; Schweizer, D.; Jenuwein, T. Isolation and Characterization of Suv39h2, a Second Histone H3 Methyltransferase Gene That Displays Testis-Specific Expression. *Molecular and Cellular Biology* **2000**, *20* (24), 9423–9433. https://doi.org/10.1128/MCB.20.24.9423-9433.2000.

(111) Schuhmacher, M. K.; Kudithipudi, S.; Kusevic, D.; Weirich, S.; Jeltsch, A. Activity and Specificity of the Human SUV39H2 Protein Lysine Methyltransferase. *Biochimica et Biophysica Acta (BBA) - Gene Regulatory Mechanisms* **2015**, *1849* (1), 55–63. https://doi.org/10.1016/j.bbagrm.2014.11.005.

(112) Wu, H.; Siarheyeva, A.; Zeng, H.; Lam, R.; Dong, A.; Wu, X. H.; Li, Y.; Schapira, M.; Vedadi, M.; Min, J. Crystal Structures of the Human Histone H4K20 Methyltransferases SUV420H1 and SUV420H2. *FEBS Letters* **2013**, *587* (23), 3859–3868. https://doi.org/10.1016/j.febslet.2013.10.020.

(113) Austenaa, L.; Barozzi, I.; Chronowska, A.; Termanini, A.; Ostuni, R.; Prosperini, E.; Stewart, A. F.; Testa, G.; Natoli, G. The Histone Methyltransferase Wbp7 Controls Macrophage Function through GPI Glycolipid Anchor Synthesis. *Immunity* **2012**, *36* (4), 572–585. https://doi.org/10.1016/j.immuni.2012.02.016.

(114) Li, J.; Ivansson, E.; Klevebring, D.; Tobin, N. P.; Lindström, L. S.; Holm, J.; Prochazka, G.; Cristando, C.; Palmgren, J.; Törnberg, S.; Humphreys, K.; Hartman, J.; Frisell, J.; Rantalainen, M.; Lindberg, J.; Hall, P.; Bergh, J.; Grönberg, H.; Czene, K. Molecular Differences between Screen-Detected and Interval Breast Cancers Are Largely Explained by PAM50 Subtypes. *Clinical Cancer Research* **2017**, *23* (10), 2584–2592. https://doi.org/10.1158/1078-0432.CCR-16-0967.

(115) Shinsky, S. A.; Monteith, K. E.; Viggiano, S.; Cosgrove, M. S. Biochemical Reconstitution and Phylogenetic Comparison of Human SET1 Family Core Complexes Involved in Histone Methylation. *Journal of Biological Chemistry* **2015**, *290* (10), 6361–6375. https://doi.org/10.1074/jbc.M114.627646.

(116) Wu, J.; Luo, M.; Duan, Z.; Jia, Y.; Linghu, H.; Tian, P.; Qi, H. WHSC1 Acts as a Prognostic Indicator and Functions as an Oncogene in Cervical Cancer. *OncoTargets and Therapy* **2019**, *Volume 12*, 4683–4690. https://doi.org/10.2147/OTT.S204701.

(117) Morrison, M. J.; Boriack-Sjodin, P. A.; Swinger, K. K.; Wigle, T. J.; Sadalge, D.; Kuntz, K. W.; Scott, M. P.; Janzen, W. P.; Chesworth, R.; Duncan, K. W.; Harvey, D. M.; Lampe, J. W.; Mitchell, L. H.; Copeland, R. A. Identification of a Peptide Inhibitor for the Histone Methyltransferase WHSC1. *PLOS ONE* **2018**, *13* (5), e0197082. https://doi.org/10.1371/journal.pone.0197082.

(118) Liu, C.; Jiang, Y. H.; Zhao, Z. L.; Wu, H. W.; Zhang, L.; Yang, Z.; Hoffman, R. M.; Zheng, J. W. Knockdown of Histone Methyltransferase WHSC1 Induces Apoptosis and Inhibits Cell Proliferation and Tumorigenesis in Salivary Adenoid Cystic Carcinoma. *Anticancer Research* **2019**, *39* (6), 2729–2737. https://doi.org/10.21873/anticanres.13399.

(119) Kojima, M.; Sone, K.; Oda, K.; Hamamoto, R.; Kaneko, S.; Oki, S.; Kukita, A.; Machino, H.; Honjoh, H.; Kawata, Y.; Kashiyama, T.; Asada, K.; Tanikawa, M.; Mori-Uchino, M.; Tsuruga, T.; Nagasaka, K.; Matsumoto, Y.; Wada-Hiraike, O.;

Osuga, Y.; Fujii, T. The Histone Methyltransferase WHSC1 Is Regulated by EZH2 and Is Important for Ovarian Clear Cell Carcinoma Cell Proliferation. *BMC Cancer* **2019**, *19* (1). https://doi.org/10.1186/s12885-019-5638-9.

(120) *Biochemical Pathways: An Atlas of Biochemistry and Molecular Biology*, 2nd ed.; Schomburg, D., Michal, G., Eds.; John Wiley & Sons: Hoboken, N.J, **2012.**

(121) Wang, Q.; Parrish, A. R.; Wang, L. Expanding the Genetic Code for Biological Studies. *Chemistry & Biology* **2009**, *16* (3), 323–336. https://doi.org/10.1016/j.chembiol.2009.03.001.

(122) Anfinsen, C. B. *Advances in Protein Chemistry, 26.*; Elsevier: Burlington, **1972**.

(123) Brown, M. A.; Sims, R. J.; Gottlieb, P. D.; Tucker, P. W. Identification and Characterization of Smyd2: A Split SET/MYND Domain-Containing Histone H3 Lysine 36-Specific Methyltransferase That Interacts with the Sin3 Histone Deacetylase Complex. *Molecular Cancer* **2006**, *5* (1). https://doi.org/10.1186/1476-4598-5-26.

(124) Diehl, F.; Brown, M. A.; van Amerongen, M. J.; Novoyatleva, T.; Wietelmann, A.; Harriss, J.; Ferrazzi, F.; Böttger, T.; Harvey, R. P.; Tucker, P. W.; Engel, F. B. Cardiac Deletion of Smyd2 Is Dispensable for Mouse Heart Development. *PLoS ONE* **2010**, *5* (3), e9748. https://doi.org/10.1371/journal.pone.0009748.

(125) Huang, J.; Perez-Burgos, L.; Placek, B. J.; Sengupta, R.; Richter, M.; Dorsey, J. A.; Kubicek, S.; Opravil, S.; Jenuwein, T.; Berger, S. L. Repression of P53 Activity by Smyd2-Mediated Methylation. *Nature* **2006**, *444* (7119), 629–632. https://doi.org/10.1038/nature05287.

(126) Clappier, E.; Gerby, B.; Sigaux, F.; Delord, M.; Touzri, F.; Hernandez, L.; Ballerini, P.; Baruchel, A.; Pflumio, F.; Soulier, J. Clonal Selection in Xenografted Human T Cell Acute Lymphoblastic Leukemia Recapitulates Gain of Malignancy at Relapse. *The Journal of Experimental Medicine* **2011**, *208* (4), 653–661. https://doi.org/10.1084/jem.20110105.

(127) Cho, H.-S.; Hayami, S.; Toyokawa, G.; Maejima, K.; Yamane, Y.; Suzuki, T.; Dohmae, N.; Kogure, M.; Kang, D.; Neal, D. E.; Ponder, B. A. J.; Yamaue, H.;

Nakamura, Y.; Hamamoto, R. RB1 Methylation by SMYD2 Enhances Cell Cycle Progression through an Increase of RB1 Phosphorylation. *Neoplasia* **2012**, *14* (6), 476-IN8. https://doi.org/10.1593/neo.12656.

(128) Saddic, L. A.; West, L. E.; Aslanian, A.; Yates, J. R.; Rubin, S. M.; Gozani, O.; Sage, J. Methylation of the Retinoblastoma Tumor Suppressor by SMYD2. *Journal of Biological Chemistry* **2010**, *285* (48), 37733–37740. https://doi.org/10.1074/jbc.M110.137612.

(129) Olsen, J. B.; Cao, X. J.; Han, B.; Chen, L. H.; Horvath, A.; Richardson, T. I.; Campbell, R. M.; Garcia, B. A.; Nguyen, H. Quantitative Profiling of the Activity of Protein Lysine Methyltransferase SMYD2 Using SILAC-Based Proteomics. *Molecular & Cellular Proteomics* **2016**, *15* (3), 892–905. https://doi.org/10.1074/mcp.M115.053280.

(130) Deng, X.; Hamamoto, R.; Vougiouklakis, T.; Wang, R.; Yoshioka, Y.; Suzuki, T.; Dohmae, N.; Matsuo, Y.; Park, J. H.; Nakamura, Y. Critical Roles of SMYD2-Mediated Beta-Catenin Methylation for Nuclear Translocation and Activation of Wnt Signaling. *Oncotarget* **2017**, *8* (34). https://doi.org/10.18632/oncotarget.19646.

(131) Gao, S.; Wang, Z.; Wang, W.; Hu, X.; Chen, P.; Li, J.; Feng, X.; Wong, J.; Du, J. X. The Lysine Methyltransferase SMYD2 Methylates the Kinase Domain of Type II Receptor BMPR2 and Stimulates Bone Morphogenetic Protein Signaling. *Journal of Biological Chemistry* **2017**, *292* (30), 12702–12712. https://doi.org/10.1074/jbc.M117.776278.

(132) Nakakido, M.; Deng, Z.; Suzuki, T.; Dohmae, N.; Nakamura, Y.; Hamamoto, R. Dysregulation of AKT Pathway by SMYD2-Mediated Lysine Methylation on PTEN. *Neoplasia* **2015**, *17* (4), 367–373. https://doi.org/10.1016/j.neo.2015.03.002.

(133) Piao, L.; Kang, D.; Suzuki, T.; Masuda, A.; Dohmae, N.; Nakamura, Y.; Hamamoto, R. The Histone Methyltransferase SMYD2 Methylates PARP1 and Promotes Poly(ADP-Ribosyl)Ation Activity in Cancer Cells. *Neoplasia* **2014**, *16* (3), 257-264.e2. https://doi.org/10.1016/j.neo.2014.03.002.

(134) Zhang, X.; Tanaka, K.; Yan, J.; Li, J.; Peng, D.; Jiang, Y.; Yang, Z.; Barton, M. C.; Wen, H.; Shi, X. Regulation of Estrogen Receptor by Histone Methyltransferase

SMYD2-Mediated Protein Methylation. *Proceedings of the National Academy of Sciences* **2013**, *110* (43), 17284–17289. https://doi.org/10.1073/pnas.1307959110.

(135) Fabini, E.; Manoni, E.; Ferroni, C.; Rio, A. D.; Bartolini, M. Small-Molecule Inhibitors of Lysine Methyltransferases SMYD2 and SMYD3: Current Trends. *Future Medicinal Chemistry* **2019**, *11* (8), 901–921. https://doi.org/10.4155/fmc-2018-0380.

(136) Donlin, L. T.; Andresen, C.; Just, S.; Rudensky, E.; Pappas, C. T.; Kruger, M.; Jacobs, E. Y.; Unger, A.; Zieseniss, A.; Dobenecker, M. W.; Voelkel, T.; Chait, B. T.; Gregorio, C. C.; Rottbauer, W.; Tarakhovsky, A.; Linke, W. A. Smyd2 Controls Cytoplasmic Lysine Methylation of Hsp90 and Myofilament Organization. *Genes & Development* **2012**, *26* (2), 114–119. https://doi.org/10.1101/gad.177758.111.

(137) Burridge, P. W.; Matsa, E.; Shukla, P.; Lin, Z. C.; Churko, J. M.; Ebert, A. D.; Lan, F.; Diecke, S.; Huber, B.; Mordwinkin, N. M.; Plews, J. R.; Abilez, O. J.; Cui, B.; Gold, J. D.; Wu, J. C. Chemically Defined Generation of Human Cardiomyocytes. *Nature Methods* **2014**, *11* (8), 855–860. https://doi.org/10.1038/nmeth.2999.

(138) Lian, X.; Hsiao, C.; Wilson, G.; Zhu, K.; Hazeltine, L. B.; Azarin, S. M.; Raval, K. K.; Zhang, J.; Kamp, T. J.; Palecek, S. P. Cozzarelli Prize Winner: Robust Cardiomyocyte Differentiation from Human Pluripotent Stem Cells via Temporal Modulation of Canonical Wnt Signaling. *Proceedings of the National Academy of Sciences* **2012**, *109* (27), E1848–E1857. https://doi.org/10.1073/pnas.1200250109.

(139) Bai, H. J.; Zhang, P.; Ma, L.; Liang, H.; Wei, G.; Yang, H. T. SMYD2 Drives Mesendodermal Differentiation of Human Embryonic Stem Cells Through Mediating the Transcriptional Activation of Key Mesendodermal Genes: Roles of SMYD2 in Mesendoderm Commitment of HESCs. *STEM CELLS* **2019**, *37* (11), 1401–1415. https://doi.org/10.1002/stem.3068.

(140) Zhang, J. Z.; Termglinchan, V.; Shao, N.-Y.; Itzhaki, I.; Liu, C.; Ma, N.; Tian, L.; Wang, V. Y.; Chang, A. C. Y.; Guo, H.; Kitani, T.; Wu, H.; Lam, C. K.; Kodo, K.; Sayed, N.; Blau, H. M.; Wu, J. C. A Human IPSC Double-Reporter System Enables Purification of Cardiac Lineage Subpopulations with Distinct Function and Drug Response Profiles. *Cell Stem Cell* **2019**, *24* (5), 802-811.e5. https://doi.org/10.1016/j.stem.2019.02.015.

(141) Krishnamurthy, N.; Kurzrock, R. Targeting the Wnt/Beta-Catenin Pathway in Cancer: Update on Effectors and Inhibitors. *Cancer Treatment Reviews* **2018**, *62*, 50–60. https://doi.org/10.1016/j.ctrv.2017.11.002.

(142) Nusse, R.; Clevers, H. Wnt/β-Catenin Signaling, Disease, and Emerging Therapeutic Modalities. *Cell* **2017**, *169* (6), 985–999. https://doi.org/10.1016/j.cell.2017.05.016.

(143) Taciak, B. Wnt Signaling Pathway in Development and Cancer. *Journal of Physiology and Pharmacology* **2018**. https://doi.org/10.26402/jpp.2018.2.07.

(144) Bagger, F. O.; Sasivarevic, D.; Sohi, S. H.; Laursen, L. G.; Pundhir, S.; Sønderby, C. K.; Winther, O.; Rapin, N.; Porse, B. T. BloodSpot: A Database of Gene Expression Profiles and Transcriptional Programs for Healthy and Malignant Haematopoiesis. *Nucleic Acids Research* **2016**, *44* (D1), D917–D924. https://doi.org/10.1093/nar/gkv1101.

(145) Barrett, T.; Troup, D. B.; Wilhite, S. E.; Ledoux, P.; Rudnev, D.; Evangelista, C.; Kim, I. F.; Soboleva, A.; Tomashevsky, M.; Edgar, R. NCBI GEO: Mining Tens of Millions of Expression Profiles--Database and Tools Update. *Nucleic Acids Research* **2007**, *35* (Database), D760–D765. https://doi.org/10.1093/nar/gkl887.

(146) Geng, H.; Brennan, S.; Milne, T. A.; Chen, W. Y.; Li, Y.; Hurtz, C.; Kweon, S.-M.; Zickl, L.; Shojaee, S.; Neuberg, D.; Huang, C.; Biswas, D.; Xin, Y.; Racevskis, J.; Ketterling, R. P.; Luger, S. M.; Lazarus, H.; Tallman, M. S.; Rowe, J. M.; Litzow, M. R.; Guzman, M. L.; Allis, C. D.; Roeder, R. G.; Müschen, M.; Paietta, E.; Elemento, O.; Melnick, A. M. Integrative Epigenomic Analysis Identifies Biomarkers and Therapeutic Targets in Adult B-Acute Lymphoblastic Leukemia. *Cancer Discovery* **2012**, *2* (11), 1004–1023. https://doi.org/10.1158/2159-8290.CD-12-0208.

(147) Brown, M. A.; Edwards, M. A.; Alshiraihi, I.; Geng, H.; Dekker, J. D.; Tucker, H. O. The Lysine Methyltransferase SMYD2 Is Required for Normal Lymphocyte Development and Survival of Hematopoietic Leukemias. *Genes & Immunity* **2020**. https://doi.org/10.1038/s41435-020-0094-8.

(148) Li, L. X.; Fan, L. X.; Zhou, J. X.; Grantham, J. J.; Calvet, J. P.; Sage, J.; Li, X. Lysine Methyltransferase SMYD2 Promotes Cyst Growth in Autosomal Dominant Polycystic Kidney Disease. *Journal of Clinical Investigation* **2017**, *127* (7), 2751–2764. https://doi.org/10.1172/JCI90921.

(149) Tobet, S. A.; Chickering, T. W.; Sower, S. A. Relationship of Gonadotropin-Releasing Hormone (GnRH) Neurons to the Olfactory System in Developing Lamprey (Petromyzon Marinus). *The Journal of Comparative Neurology* **1996**, *376* (1), 97–111. https://doi.org/10.1002/(SICI)1096-9861(19961202)376:1<97::AID-CNE6>3.0.CO;2-J.

(150) Tobet, S. A.; Schwarting, G. A. Minireview: Recent Progress in Gonadotropin-Releasing Hormone Neuronal Migration. *Endocrinology* **2006**, *147* (3), 1159–1165. https://doi.org/10.1210/en.2005-1275.

(151) Wierman, M.; Pawlowski, J.; Allen, M.; Xu, M.; Linseman, D.; Nielsenpreiss, S. Molecular Mechanisms of Gonadotropin-Releasing Hormone Neuronal Migration. *Trends in Endocrinology and Metabolism* **2004**, *15* (3), 96–102. https://doi.org/10.1016/j.tem.2004.02.003.

(152) Tobet, S. A.; Bless, E. P.; Schwarting, G. A. Developmental Aspect of the Gonadotropin-Releasing Hormone System. *Molecular and Cellular Endocrinology* **2001**, *185* (1–2), 173–184. https://doi.org/10.1016/S0303-7207(01)00616-5.

(153) Wierman, M. E.; Kiseljak-Vassiliades, K.; Tobet, S. Gonadotropin-Releasing Hormone (GnRH) Neuron Migration: Initiation, Maintenance and Cessation as Critical Steps to Ensure Normal Reproductive Function. *Frontiers in Neuroendocrinology* **2011**, *32* (1), 43–52. https://doi.org/10.1016/j.yfrne.2010.07.005.

(154) Cui, L.; Fan, Q.; Cui, L.; Miao, J. Histone Lysine Methyltransferases and Demethylases in Plasmodium Falciparum. *International Journal for Parasitology* **2008**, *38* (10), 1083–1097. https://doi.org/10.1016/j.ijpara.2008.01.002.

(155) Brown, M. A.; Foreman, K.; Harriss, J.; Das, C.; Zhu, L.; Edwards, M.; Shaaban, S.; Tucker, H. C-Terminal Domain of SMYD3 Serves as a Unique HSP90-Regulated Motif in Oncogenesis. *Oncotarget* **2015**, *6* (6). https://doi.org/10.18632/oncotarget.2970.

(156) Hamamoto, R.; Furukawa, Y.; Morita, M.; Iimura, Y.; Silva, F. P.; Li, M.; Yagyu, R.; Nakamura, Y. SMYD3 Encodes a Histone Methyltransferase Involved in the Proliferation of Cancer Cells. *Nature Cell Biology* **2004**, *6* (8), 731–740. https://doi.org/10.1038/ncb1151.

(157) Hamamoto, R.; Silva, F. P.; Tsuge, M.; Nishidate, T.; Katagiri, T.; Nakamura, Y.; Furukawa, Y. Enhanced SMYD3 Expression Is Essential for the Growth of Breast Cancer Cells. *Cancer Sci.* **2006**, *97* (2), 113–118. https://doi.org/10.1111/j.1349-7006.2006.00146.x.

(158) Calpena, E.; Palau, F.; Espinós, C.; Galindo, M. I. Evolutionary History of the Smyd Gene Family in Metazoans: A Framework to Identify the Orthologs of Human Smyd Genes in Drosophila and Other Animal Species. *PLoS ONE* **2015**, *10* (7), e0134106. https://doi.org/10.1371/journal.pone.0134106.

(159) Kwon, T. Mechanism of Histone Lysine Methyl Transfer Revealed by the Structure of SET7/9-AdoMet. *The EMBO Journal* **2003**, *22* (2), 292–303. https://doi.org/10.1093/emboj/cdg025.

(160) Madej, T.; Lanczycki, C. J.; Zhang, D.; Thiessen, P. A.; Geer, R. C.; Marchler-Bauer, A.; Bryant, S. H. MMDB and VAST+: Tracking Structural Similarities between Macromolecular Complexes. *Nucleic Acids Research* **2014**, *42* (D1), D297–D303. https://doi.org/10.1093/nar/gkt1208.

(161) Valegård, K.; Andralojc, P. J.; Haslam, R. P.; Pearce, F. G.; Eriksen, G. K.; Madgwick, P. J.; Kristoffersen, A. K.; van Lun, M.; Klein, U.; Eilertsen, H. C.; Parry, M. A. J.; Andersson, I. Structural and Functional Analyses of Rubisco from Arctic Diatom Species Reveal Unusual Posttranslational Modifications. *Journal of Biological Chemistry* **2018**, *293* (34), 13033–13043. https://doi.org/10.1074/jbc.RA118.003518.

(162) Takahashi, T.; Sutherland, S. C.; Sweeney, C.; Poisson, A.; Metzl, N.; Tilbrook, B.; Bates, N.; Wanninkhof, R.; Feely, R. A.; Sabine, C.; Olafsson, J.; Nojiri, Y. Global Sea–Air CO2 Flux Based on Climatological Surface Ocean PCO2, and Seasonal Biological and Temperature Effects. *Deep Sea Research Part II: Topical Studies in Oceanography* **2002**, *49* (9–10), 1601–1622. https://doi.org/10.1016/S0967-0645(02)00003-6.

(163) Falkowski, P. Ocean Science: The Power of Plankton. *Nature* **2012**, *483* (7387), S17–S20. https://doi.org/10.1038/483S17a.

(164) Galmés, J.; Kapralov, M. V.; Andralojc, P. J.; Conesa, M. À.; Keys, A. J.; Parry, M. A. J.; Flexas, J. Expanding Knowledge of the Rubisco Kinetics Variability in Plant Species: Environmental and Evolutionary Trends: Variability of Rubisco Kinetics in Plants. *Plant, Cell & Environment* **2014**, *37* (9), 1989–2001. https://doi.org/10.1111/pce.12335.

(165) Badger, M. R.; Andrews, T. J. CO-Evolution of Rubisco and CO2 Concentrating Mechanisms. In *Progress in Photosynthesis Research*; Biggins, J., Ed.; Springer Netherlands: Dordrecht, **1987**; pp 601–609. https://doi.org/10.1007/978-94-017-0516-5_128.

(166) Nisbet, E. G.; Grassineau, N. V.; Howe, C. J.; Abell, P. I.; Regelous, M.; Nisbet, R. E. R. The Age of Rubisco: The Evolution of Oxygenic Photosynthesis. *Geobiology* **2007**, *5* (4), 311–335. https://doi.org/10.1111/j.1472-4669.2007.00127.x.

(167) Whitney, S. M.; Houtz, R. L.; Alonso, H. Advancing Our Understanding and Capacity to Engineer Nature's CO_2- Sequestering Enzyme, Rubisco. *Plant Physiology* **2011**, *155* (1), 27–35. https://doi.org/10.1104/pp.110.164814.

(168) Li, G.; Campbell, D. A. Interactive Effects of Nitrogen and Light on Growth Rates and RUBISCO Content of Small and Large Centric Diatoms. *Photosynthesis Research* **2017**, *131* (1), 93–103. https://doi.org/10.1007/s11120-016-0301-7.

(169) Stec, B. Structural Mechanism of RuBisCO Activation by Carbamylation of the Active Site Lysine. *Proc. Natl. Acad. Sci. U.S.A.* **2012**, *109* (46), 18785–18790. https://doi.org/10.1073/pnas.1210754109.

(170) Andersson, I. Catalysis and Regulation in Rubisco. *Journal of Experimental Botany* **2007**, *59* (7), 1555–1568. https://doi.org/10.1093/jxb/ern091.

(171) Andersson, I.; Backlund, A. Structure and Function of Rubisco. *Plant Physiology and Biochemistry* **2008**, *46* (3), 275–291. https://doi.org/10.1016/j.plaphy.2008.01.001.

(172) Ashida, H.; Saito, Y.; Nakano, T.; Tandeau de Marsac, N.; Sekowska, A.; Danchin, A.; Yokota, A. RuBisCO-like Proteins as the Enolase Enzyme in the Methionine Salvage Pathway: Functional and Evolutionary Relationships between RuBisCO-like Proteins and Photosynthetic RuBisCO. *Journal of Experimental Botany* **2007**, *59* (7), 1543–1554. https://doi.org/10.1093/jxb/ern104.

(173) Lorimer, G. H.; Badger, M. R.; Andrews, T. J. The Activation of Ribulose-1,5-Bisphosphate Carboxylase by Carbon Dioxide and Magnesium Ions. Equilibria, Kinetics, a Suggested Mechanism, and Physiological Implications. *Biochemistry* **1976**, *15* (3), 529–536. https://doi.org/10.1021/bi00648a012.

(174) Lorimer, G. H.; Miziorko, H. M. Carbamate Formation on the .Epsilon.-Amino Group of a Lysyl Residue as the Basis for the Activation of Ribulosebisphosphate Carboxylase by Carbon Dioxide and Magnesium(2+). *Biochemistry* **1980**, *19* (23), 5321–5328. https://doi.org/10.1021/bi00564a027.

(175) Spreitzer, R. J.; Salvucci, M. E. Rubisco: Structure, Regulatory Interactions, and Possibilities for a Better Enzyme. *Annu Rev Plant Biol* **2002**, *53*, 449–475. https://doi.org/10.1146/annurev.arplant.53.100301.135233.

(176) Mueller-Cajar, O.; Badger, M. R. New Roads Lead to Rubisco in Archaebacteria. *BioEssays* **2007**, *29* (8), 722–724. https://doi.org/10.1002/bies.20616.

(177) Batista, I. de A. A.; Helguero, L. A. Biological Processes and Signal Transduction Pathways Regulated by the Protein Methyltransferase SETD7 and Their Significance in Cancer. *Signal Transduction and Targeted Therapy* **2018**, *3* (1). https://doi.org/10.1038/s41392-018-0017-6.

(178) Bennett, R. L.; Swaroop, A.; Troche, C.; Licht, J. D. The Role of Nuclear Receptor–Binding SET Domain Family Histone Lysine Methyltransferases in Cancer. *Cold Spring Harbor Perspectives in Medicine* **2017**, *7* (6), a026708. https://doi.org/10.1101/cshperspect.a026708.

(179) Jarrell, D. K.; Hassell, K. N.; Crans, D. C.; Lanning, S.; Brown, M. A. Characterizing the Role of SMYD2 in Mammalian Embryogenesis—Future Directions. *Veterinary Sciences* **2020**, *7* (2), 63. https://doi.org/10.3390/vetsci7020063.

CHAPTER 6 – CONCLUDING REMARKS

6.1 Introduction

The research that contributed to this dissertation was intended to explore the vast possibilities of utilizing small molecules and proteins in developing safer, targeted cancer therapeutics. Thus, this document contains methodology and techniques that have great potential for applications in the drug discovery and clinical oncology. The overarching research questions answered in the first three chapters of this dissertation emphasized the toxicity of Cisplatin upon intravenous delivery in humans and the exploration of alternative methods. The second part of this dissertation utilized epigenetics to ask and answer questions about the ability to regulate cellular activity to target specific types of cancers.

6.2 Empirical Findings

Despite the preliminary data presented in this dissertation, clear interpretations and strong conclusions can be extrapolated from chapters two and three in regard to the repackaging small molecules like cisplatin. The data found in both chapters provided significant evidence to support alternative drug delivery vehicles as models, both with the potential mimics the cellular activities of mammalian cells. The hydrolysis of the Schiff-bases studied in chapter two are dependent on their molecular environments of which contribute the regulation of the water pool and interfacial space. Similarly, the hydrolysis of compound cisplatin is also dependent on its environment; increasing it toxicity from Pt(II) to Pt (IV). The preliminary data in chapter three supports

utilizing metallocages but more targeted construct would be needed to ensure encapsulation of cisplatin molecules for drug delivery. Palladium metallocages are slightly toxic to HeLa cells without the encapsulated cisplatin molecules. The flow cytometry methods used in chapter three have potential for broaden application in clinical oncology. Switching perspectives to a more intercellular exploration, the preliminary data in chapter 5 supports the manipulating the enzymatic characteristics of the SET-domain proteins; SMYD3. While more experimentation is clearly needed, the data presented in the drug inhibition assays show the decrease in colony formation for both A549 and DLD-1 cell lines were a result of increased SMYD3 dosage concentrations. Similarly, in the viability assays, both A549 and DLD-1 cell lines showed sensitivity to the SMYD3 inhibitor.

6.3 Theoretical Findings

The theoretical findings presented in this dissertation span the disciplines of biology; molecular and structural, chemistry; inorganic and synthetic as well as biochemistry and clinical sciences. The combinatory effects of utilizing the disciplines has resulted in the posing and answering of impactful scientific questions that been supported by methodology, techniques and analytical rationalization to justify the necessity of change to our current methodologies and drug applications. This dissertation is an example of the possibilities that could be achieved if multiple scientific disciplines are approached equally. Only have the knowledge of one discipline could prove to be a rate limiting factor in synthesizing the content needed to solve the vastly mounting scientific questions of today. Questions that require the fast acquisition of

new skills, excellent verbal and written communication skills to apply to innovative answers while utilizing bio- and cheminformatics skills. This dissertation is a representation of a finely crafted mosaic with multiple patterns, patches and shiny ornate décor. This document provides significant evidence in support of the impacts made and potential alterations to best practices in their respective disciplines.

6.4 Future Implications

It is my expectation that this dissertation serves as a springboard for the enhanced development of micelles and metallocages for encapsulated drug delivery, as well as support the argument for including epigenetics in drug discovery. More importantly, to continue to further the answering of the questions posed by the research in this dissertation, incorporating informatics in the 21st century has simply become mandatory. Chem- and bioinformatic simulations can be used to determine the speciation of metals and could be used to design various transitional metal-like capsules or metallocages for toxic drug delivery in humans. One of the next lines of questions for the inhibition of SMYD3 compound would require next generation sequencing (NGS) to truly isolate and investigate the specifics of its gene transcriptional activity in various types of cancer cells.

6.5 Limitations of Study

While there were several limitations to continuing the research present in this dissertation, lack of funding made the most detrimental to my progress and intellectual development. In the Schiff-base experimentation of chapter 2, having proper funding would have given me the opportunity to synthesize new compounds or investigate how

cisplatin molecules compare for analysis. Chapter 3, was the mini-project I designed and developed with less than two hundred dollars by asking my fellow graduate students and campus connections to utilize a biosafety hood for cell culturing, dyes and stains for flow cytometry applications and the countless time needed to run, collect and analyze my data was donated by the Directors of Flow Core at Colorado State University. If this project would have been awarded funding after my F31 submission, this research could have concluded with a ground- breaking data to support a completely new path to targeting cancerous tumors. As mentioned in chapter 3, the fine tuning to data collection warrants repeating, as well as the need to increase the sample population number (n). After data collection is become very difficult to back track and create segmented sample groups that would have been used for the necessary statistical analysis essential for a top-tier publication. The experimental data collection in chapter 5 was limited by lab space, and time.

Appendix

Supplemental Data

Data 5.1 Fasta format protein sequences from NCBI

>AAI07726.1 SMYD3 protein [Homo *sapiens*]
MEPLKVEKFATANRGNGLRAVTPLRPGELLFRSDPLAYTVCKGSRGVVCDRCLLGKE
KLMRCSQCRVAKYCSAKCQKKAWPDHKRECKCLKSCKPRYPPDSVRLLGRVVFKLM
DGAPSESEKLYSFYDLESNINKLTDKKEGLRQLVMTFQHFMREEIQDASQLPPAFDLFE
AFAKPIGMK

>QCD80391.1 [Vigna *unguiculata*]
MFVGLSLLSWGLSSGAAAPSCEGKGSNWLYFVLRYCHQLVLIFCRSNSSYSLCWRLQ
LEENEEASIVLFSDARAISFGSFRVVAAVMDTDEECSIVLELPESDPFFDKKKKLLQSKG
FSPKERIYLRSSSKPGWMSATVQVLVQIARIIQLNELELYFAEEDVCTAKEFYSPRNELE
ALNSIVLLTDISLSSCTHLHTNILQGLRQTVLDLITDLGDKNSVKGVVEKDHSCDQEERLI
EWGESNGVKTQLKIAYTERAGRGAIARKDLNVGDIALEIPVSIIISEELIHETQMYGVLKEI
DGISSETILLLWSMKEKYNSDSKFKIYFDTLPEKFNTGLSFSIEAITVLDGTLLLEEIMQAR
QHLHAQYDELFPALCNTFPDIFPPELYTWEKFLWACELWYSNSMKIMYSDGKIKTCLIPI
AGFLNHSLCPHVMHYGQVDSANNSLKFCLSRPCKSGEECCLSYGNFSSSHLITFYGFL
PQGDNPYDVIPLDIDGADVDSNEDIPESNWTSHMVRGTWLSRDHKMFYYGLPSPLLR
RSRSPMLRPKTFLQENLENELGVLENLKDIFDDMIENMGEMDLDDRENCCRDEKLAM
DFKNTQRRIARSVSTSCLAGMDMLKKELCKCMAEDIQG

>KRX00204.1 [Pseudocohnilembus *persalinus*]
MLEYLQSQPRYNGKVKKLKEYLENLFLTNQEKMQIINYLETDEMNLSLFVKDEEINLGA
TKFLKESEDRVRFCKWVQENGLLLKNVDYPVGFGLLGVPGIAASDEIPENTILAAVPNK
MIINVKKALESELIEVYKSSPKNFNMKINEDAEFNILTLFLIREYIKGTDSFWYPYISSIGKS
YTLYDWTKYDTEKTEDPEMIEESRYYADEIDQVYWQLGQVMKKFPQYFPPDQINRRIF
VEFYQAIMTRCFGYSVPSTCLIPFADLLNHNNNSATHYTVQTKYEQNPEQKPANYVIKQ
EKIDMDIFQIKEIQKADKTKFKQHGLRIKHVYEQKAFLEDTLYQNLESLEEFENLGLEDK
EIKDLTYVVNYNYYKQMGDCEKNQVDVKKINEIQFITSSNTEDNDTSEDDENQNFFKY
QIKQASDIEQDKIKFKNMLKNKQENDKQLENKEIKVVQNLIKPAELDKCEQPQIKKDQN
ALKSKQQAEQEYRTKLEEKIKRIKAQEAEEREEKRLRKERLKAQKKELKEEYKQNGEID
LNQQIQDKLNPINKNINMKQNDKNNDIIQNDNNSSDSENSYSEKSNNENEDEDSEQED
DTDDNQSSLSEESIFDWYETNDQDTYFIITSQDKIKKGEQIFNCYGRRTNKFLLMWYGF
CFQNNKYDSFTFRMNMSVKYDKLDDNFIERVLFRGSTNNEEMQMGTYNLNGENISIKD
LTKEFRLKKDNINIDVIIYLRALLVKIYEGQEKKDIFVTLPVSLDFEIFVLKFYKKIINYFQSQ
YSTSIEKDEELLKDHLLSYKKRFAIVLRVEQKKILQQQSVMIEDLLNFINMFKRQQNLHK
SVIQFCEQEEYAERFNQFKKVHRIKSYLIQIQESQDKYTILDFE

>KEP52673.1 [Rhizoctonia *solani* 123E]
MDSTLLQWFKSHDGIVDEEHMRLGEIDGCGFGAIAVKDIPKDHVLFEIPRHILLSTRTCIL
KFKLTSSEWEGLGKGWTPLILCMMWEAAKGSESSWDGYLATMPTRFDTPMFWPIPEL
EELRGTSIAEKIGRDDAEKEYNERVIPLLKSRPDLFLPSHLDTYYTLEQFHIMGSRILSRS
FHVEEDEVDKEENPDVSMESSKSMDVDRSREEANPPDQVNEDEHQDDGDSDSEDE
ENVEDVAMVPMADMLNARYGGENAKLFYEPRVLKMITTKSIAAGEQIWNTYGDPPNS
DLLRRYGYVDVPGQGLDIVELRGSLLVECASSYAPLSSDQQKERVDWWLEMGGDDT
FTLDMSSLLPPELLSFTQLLLLSDTEWEKTQEKEKPPKPKLDEVKKCVRDALVKRMELY
PTSLEEDENQLASGHNTLNKRHALIIRIGEKKVLKAALASVSEPAPKKRKAESQGGTRK
KGARQK

>PON48260.1 [Trema *orientale*]
MEVGSLHDRCMWSPIPSSSSPNRPPLLLHSRVSISPRKKNPSLLTSSSCRSFRRRNFC
SASSSSSSSNSDTLVAAGSRKEEEEEEGGFVDLKSWMHNNGLPPCKVVLRERPSHD
EKHRPIHYVAASQDLQVGDVAFSVPNSLVVTLERVLGNETIAELLTTNKLSELACLALYL
MYEKKQGKKSFWYPYIRELDRQRGRGQLAVESPLLWSEAELHYLTGSPTKAEVRERA
EGIKREYNELDTVWFMAGSLFQQYPYDIPTEAFPFEIFKQAFVAVQSCVVHLQKVSLAR
RFALVPLGPPLLAYRSNCKAMLTAVDDAVQLLVDRPYKAGESIVVWCGPQPNSKLLIN
YGFVDEDNSYDRLVVEAALNTEDPQYQDKRMVAQRNGKLSVQVYVGKEKEAVADML
PYIRLGYVSDPSEMQSVISSQGPICPVSPCMERAVLDQLADYFRARLAGYPTTLKEDE
SLLAGRNLNPKKRVATQLVRLEKKILHACLQVTVDLINQLPDHTVSPCPAPYAPLLK

>EFJ49228.1 [Volvox carteri f. *nagariensis*]
MQQALKAHASNWQAGLRRASSKRPTRLYCRAASAVLSSIPADAAVSWATSKGAKLER
ASLSNDLQTDRPVLIASTDAQQGDVLFSVPDSAWLSAESVKKAAVGKLAAAAGLEPWL
QIALQLVADRFGSTKSELSAYAASIPEDLDTPLLWSEDELQELQGTQVLQTLGGYLTFF
RSTFQQLQSGLFTSNPAAFPPSIFTLPRFLWAVAAVRSRSHPPLDGPKIALAPLTELVS
HRRAANSKLSVRSAGLFGRGQVLVLEATRAIRKGEPLSMDYGPGKLDGPVLVDYGVM
DVTSPKPGYSLTLKMPDSDRFIDDKLDILESNDLPQSVVYNLTPDEQPTIEMLAFLRLM
QLKGSDAFLLESIFRNDVWGFMQEPVSEGNEEAVCNTLSEGARAALGGYGTTIDQDL
AELRAQGSRAKGSRREAALLIRLGEKEALDAVARFFEDRRATQLKRLVYYQERRLRRL
GLVDDEGRTTYDSFFKDGIA

>GBF89663.1[Raphidocelis *subcapitata*]
MPPHEGLAARARRNAADALQGLLDWAASAKVATDKLAAAPSLATGAPLLVAARDIAAG
EAVLTVPDAHWITPAAVAKSPIGPSVSGLEPWLQLALLLVSERAAGAAAGALPGAFLAA
LPQALDAPLFWGDDEIDMLQGTQALQQLYGYRQFFQETFAELEATLFASDRALFPAEA
FTYEAFLWAAATVRGRAHAPLDGAAIALVPLADGLPHRRGGNCAWKAKSSGLFGQGR
VLTVEAARAIRKGEELTMDYGPGKLDSSLLVDYGVMDSSWPQGGYSLSLSVPDSDRY
RDDKLDVLERNGLAGAGAFAIKKGEEPSREMLGFLRLTQLSGSDCFLLESIFEAEVWS
FMCDPISPQNEAAVCSSCTEGVRAALAGYATAIEDDLAALRSGKLEPGSRQERAVQVR
LGEKEALDSFLGWLETRVGQLPRLEYYQERRLKRLGLIDDNGDTTYSSFFKDGIA

>XP_001697868.1 [Chlamydomonas *reinhardtii*]
MQQAFRAHAPRRAGGIRGSGSRLKPSVACRAASSVASKAAVESAIAWATKQGAKLEK
ANLSTDILTDKPILVASADVQPGESLIVVPDAAWVSVPNVAKTTVGKLASSAGLEPWLQ
LALVLVAERFGSAKSELAGYASSLPEDLGTPLLWSEEETRALAGTQVAGTLNSYLTFFR
STFAQLQAGLFTANPAAFPPAVFTLPNFVWAVAAVRSRSHPPLEGDKIALAPLVDLVSH
RRAANTKLSVRSSGLFGRGQVAVVEATRAIRKGEALGMDYAPGKLDGPVLLDYGVMD
TASPKPGYSLTLTLDESDKFVDDKADIVEGAGLRPSMTYSITPDQQPGEEMMAFLRLM
NIKAMDAFLLESIFRNEVSEGNEEAVCAMLAEGARAALAGYPTTLDQDLAALRSNSTPL
GSRAEAALLVRLGEKESLDAVARFFEDRRATQLKRLVYYQERRLRRLGLVDDEGRTTY
DNFFKDGIA

>OVA15388.1 [Macleaya *cordata*]
MDVAYLQSRCISSPIRLPSRPLSVFPRVSSHSILQKSNVFRAIRHRNFCLASGADTLIAG
SRKEDGKSHASGNKKADEFEDLKSWLHSKGLPPCKVVLNEKPSHDQKHRPIHYVAAS
EDLEEGDVAFSVPISLVVTLERVLGNETIAELLTTNKLSELACLALYLMYEKKQGKKSFW
YPFIRELDRQRGRGQLAVESPLLWSEDELAYLTGSPTKAAVLERAEGIKKEYNELDTV
WFMSGSLFQQYPYDIPTEAFPFEIFKQAFVAVQSCVVHLQKVSLARRFALVPLGPPLLA
YKSNCKAMLTAVEGVVQLIVDRPYKAGESIVIWCGPQPNSRLLINYGFVDEDNPYDRIL
VEASLNTEDPQYHDKRMVVQRNGKLAVQVFQVYAGKEKEAVSDMLPYLRLGYVSDP
SEMQSVISSEGPICPVSPCMERAVLDQLSDYFKGRLAAYPTTLHEDETLLADSRLDPKK
RVATQLVKLEKKMLNACLQATIELMNQLPDDTISPCPAPYAPHLK

>AQK54830.1 [Zea *mays*]
MATSSTTALHSQFRPPLRAPRHLRPLPHSYSSSSRTRGCAPVRASAASASAPAQREIA
AGVPWGCEIESLESAASLERWLIDSGLPEQRLAIQRVDIGERGLVALKNIRKGEKLLFVP
PSLVITADSEWGRPEVGDVMKRNSVPDWPLIATYLISEASLEGSSRWISYIAALPRQPY
SLLYWTRAELDAYLVASPIRKRAIQRITDVIGTYNDLRDRIFSRHPDLFPEEVYNIETFLW
SFGILFSRLVRLPSMDGRVALVPWADMLNHSPEVETFLDFDKSSRGIVFTTDRSYQPG
EQVFISYGKKSSGELLLSYGFVPKEGTNPNDSVELLVSLDKSDNCYKEKLQALKRNGL
SESESFPLRVTGWPVELMAYAFLVVSPPDMSQCFEEMAAAASNKTSSKPGLNYPDLE
EQALQFILDCCESNIEKYTKYLEGGAGSPEVPMNAKQANRTLLLKQLARDLCISERRILY
RTQYVSQCFDLAAKASDTCMPNQTAVQALGRKFHLDARNK

>EOX93543.1 [Theobroma *cacao*]
MDEKVALVPWADMLNHSCEVETFLDYDRSSHGVVFTTDRAYQPGEQVFISYGKKSNG
ELLLSYGFVPKEGTNPSDSVELSLSLKKSDKCYKEKLEALRKHGFSQCYPIQITGWPLE
LMAYAYLAVSPPSMSPQFEEMAAAASNKSTTKKDLRYPEIEEKALQFILDSCESSISKY
SKFLQASGSMDLDVTSPKQLNRGVFLKQLAVDLCTSEQRILFRAQHSEAISPKRGEEE
DALKVKEWEVGMFQNEVAASQGIRIRRRPPSGPPMHYVGPFEFRLQNEDNTPRNILE
EIIWHKDVEVSQVANDSGVWQMKEKKPLASLKKFIENAAPTRDFVGALKAAHSRTGLP
GLIAEVKKASPTRGILREDFDPVEIARAYEKGGAACLSVLTDEKYFKGSFENLEAIRSAG
VKCPLLCKEFVIDAWQIYYARIKGADGIRLIAAVLPDLDIRYMVKICKMLGLAALVEVLVG
ESIVTQRDLGKGITRLFGKDISLKIMSHFGDDNSSVEEVSSAEESYNTEFRSYPDDAWY
SVRVSLEGERGDKLRVKYENFPEEHDNVFLAEGFKSEDELYDFIGRFRKVSAQLQDRD
CYQIVRGMRVCASDSLGDDDNLFYDAIVDEVVHKKHSNVNGQEECECTFLLFWLHGP

NVGNVVEKGVANICLLQSAELEPKLATFMEIATQKIEKALCKLGSDTIDDVAFNPVFRHE
ANGSPIVKQKLSSIGRSRQGKCSQRSLSKVWPSEAVIGGAKIRSENRQDTDIGGDKKY
HMILVQNLEKELSSSTVLEFILKQTSIASQVYIFPSLPWELYTNGVIVLDCRKDLEQLFGF
LDNPNHFVVSSNGRPWVAAEKMSMNDHWTVMLESPKKLRNRSGGGFSNELKLVCFG
SEEYKRAKELRDLFLQFIAHQQGLYKKLCMEERSIAFSSNQLVQLPDKS

>AES75034.1 [Medicago *truncatula*]
MELSHLSLSENHFFFSTPTSPSSLSHRLPSFLSLSTNHRRRRRSFCSASNSDTLVAAT
GKKKRDEDDGDLKTWMHKNGLPPCKVVLKDKPSLDDSVKPIHYVAASEDLQKGDIAF
SVPNSLVVTLERVLGNETIAELLTTNKFSELACLALYLMYEKKQGKKSFWYPYIRELDR
QRGRGQLAVESPLLWSESELAYLEGSPLKDEIVKRIEGIRKEYNELDTVWFMSGSLFQ
QYPYDLPTEAFPFEIFKQAFAAVQSCVVHLQNVSLARRFALVPLGPPLLAYCSNCKAML
TAVDGAVQLVVDRPYKAGDPIVVWCGPQPNTKLLTNYGFVDEDNSNDRLIVEVALSTE
DPQYQDKRIVAQRNGKLSIQTFYVYTGKEREAVSDMIPYMRLGYVSDPSEMQSVISSQ
GPVCPVSPCMERAVLDQLADYFNTRLAAYPTTLAEDESMLTDGSLNPKRRVATQLVRL
EKKMLHACLQAIMDLISQLPDHSVSPCPAPYAPSLK

>PFX18006.1 [Stylophora *pistillata*]
MEHMRTVPISGLKFNFWITNPSDTPVLPVKQWEEHVKLREMVEKIRKRQAGQSLFEM
SDQYRRDHISSFTQWFNENGGVAKQVVIDDFGHQGLGLKAVSEIKEGQHFITIPRKLM
MSAESARNSDLGPLIEKDNILKVCPETAKLPLRRHFTFDDHRWAVSTVTTRQNKIPSTT
GEPTLALIPMWDMCNHCNGTITTGYDLAEDSCKSMSVRDFHAGEEVCIFYGERSNGD
LLVHNGFVFEENAHDKVSIQLGVSKSDPLFQMKERLLASMGMTASSHSFPVSHGERP
FDSELVTFLRIFSMTEDELKEWLKKASEDTNELKKLSGVQTFVKEETENKGWQFLETR
LTLLLKQYNTADSEDCELLENPEFPPHKKLCIRLKRAEKKVLQNALKHAAATRSKIKDSY
EERDLDCDDQNTNGHNDKSCTEENTSNMVDATISAVDQLCVQ

>JAR85826.1[Fundulus *heteroclitus*]
MGKKSRVKTQKSGSGASTVVSPKEMMNLISELLQKCSSAAPSAGKEWEEYVQIRGLV
EKIRKKQKGLSTVFEGNREDYFPDLMAWAQENGASCDGFTLADFGTEGYGLRASRDI
KAEELFLWIPRKMLMTVESAQNSLLGPLYGQDRIMQAMGNVTLALHLLCERASPSSFW
LPYIRSLPQAYDTPLYYQQDDVQLLLGTQAVQDVLSQYKNTARQYAYFYKLLQTHPAA
SKLPLKDGFTFDDYRWAVSSVMTRQNQIPTEDGSRVTLALIPLWDMCNHTNGLITTGY
NLEDDRCECVALKDYKENEQIYIFYGTRSNAEFVIHNGFFFQDNAHDRVKIKLGVSKSE
RLYAMKAEVLARAGIPASCVFALHCNEPPISAQLLAFLRVFCMTEEELKDYLLGDGAIN
KIFTLGNSEFPVSWENEIKLWTFLENRAALLLKTYKTTSEDDLAVLEKPDLSLHSRLAVL
LRLAEKQILEKVSASGRDKRLYFQTKLEEGAPLPHFEESDIALLENSDTDAKLPIILHKLE
EVEERDGLQVEEPLLNGEKVGLGAEESREVGRDVASDRTGQTEASEQSANRTEDDP
EENSK

>AEE79338.1 [Arabidopsis *thaliana*]
MLAAVLIREKKMGQKSRWVPYISRLPQPAEMHSSIFWGEDELSMIRCSAVHQETVKQK
AQIEKDFSFVAQAFKQHCPIVTERPDLEDFMYAYALVGSRAWENSKRISLIPFADFMNH
DGLSASIVLRDEDNQLSEFSTLQVTADRNYSPGDEVFIKYGEFSNATLMLDFGFTFPYN
IHDEVQIQMDVPNDDPLRNMKLGLLQTHHTRTVKDINIFHSSCDTFTIKEVKSAIGKGKG
IPQSLRAFARVLCCIIPQELNDLSKEAAQNDGRLARLPFKDGNRELEAHKILLSHINRLIE
DHSVCIKEMEECYFVSQRFAVRRQMARDLLYGELRVLRSAAEWLNHYCTTLLSETM

>CCD73865.1[Caenorhabditis *elegans*]
MAPSPTAELEDQILGKIATLFEETLSKQPPSNIVELWKEHVEIRRILNDVISIQAKLGDTD
ERLANSKRDADSIKTFLAWADGVGIARNNVTIGSTKTAGLSLQATGPIPKSHIVARVPRH
AMITLDLAKKSSLLKKAFEKDPIVGGMDNVGLALFLACQWIQNEKSKWKSYISILPTTFP
TPLFYSEEQLLQLKPSPIFEEAILFYRTISRQFCYFLLAIAKNKIYEAAQRRKDARNAMET
PIFYNVPFNVANFTPKLYFWAVGVVTTRVNMVPSENQVGEDGNPVIIPALIPVLDMANH
ENVLTDVLTEPIEDLVCYSPEEECAVITSHCDVKAGNEVTIFYGCRSKGEHLLHNGFVPI
YHGKFDVLKLKIGIPKTDKTLDAKKKLIQKFVKKVYCAGNIFHVDLYNYHEQPFPLDLLM
FAAIFVSTTPTEEAVSAPENRKKGLEFLKTRFSLLKRSYESSFDASKLKEIGIDGDSARL
KSAELDILQLALNYCETLEKQ